



Karlsruher Institut für Technologie
Botanisches Institut – Pflanzen-Mikroben Interaktion

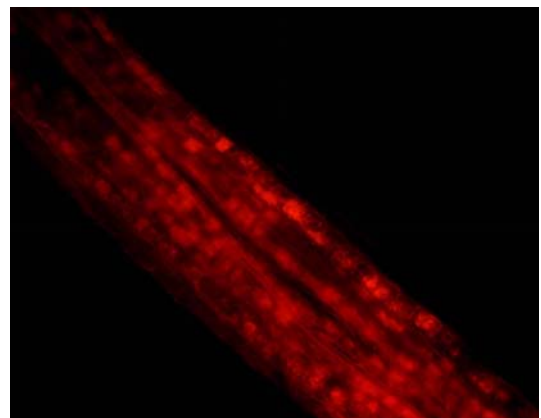
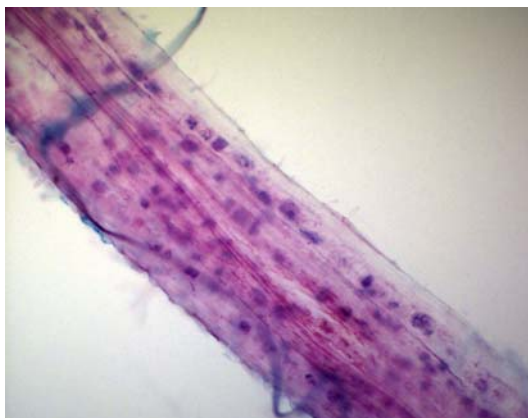
Analysis of the Sugar Transport and Metabolism in the Arbuscular Mycorrhizal Symbiosis

Zur Erlangung des akademischen Grades eines
DOKTORS DER NATURWISSENSCHAFTEN (Dr. rer. nat.)
der Fakultät für Chemie und Biowissenschaften
des Karlsruher Institut für Technologie (KIT)

vorgelegte
DISSERTATION

von Dipl.-Biol. Nicole Helber
aus Vaihingen an der Enz

8. September 2010



Dekan: Prof. Dr. Stefan Bräse
Referent: Prof. Dr. Natalia Requena
Korreferent: Prof. Dr. Peter Nick
Tag der mündl. Prüfung: 19. October 2010

To my parents.

Abstract

For more than 400 million years plants have maintained a mutualistic symbiosis with arbuscular mycorrhizal (AM) fungi. The evolutionary success of this symbiosis which is formed by more than 80 % of all terrestrial plants can be traced to the reciprocal exchange of nutrients. The plant receives mineral nutrients, mainly phosphate, from the fungus which profits from the plants photosynthates. Thus, a significant amount of photosynthetically fixed carbon is transferred over the hyphal network of the fungus into the soil. Studying this carbon flux is of great interest, as the AM symbiosis plays a significant role in the global carbon cycle. Besides, AM fungi are used in agricultural systems as biofertilisers. However, studies showed that certain soil management conditions, for example over-fertilisation, can increase the costs to outweigh the benefits for the plant, resulting in reduced plant growth compared to non-mycorrhized plants. Although several studies have been made, the molecular mechanism of carbon transfer in the AM symbiosis is not known.

This study reports the isolation and characterisation of the first symbiotic sugar transporter, GiMST1, of an AM fungus. GiMST1 was identified by Blast searches together with four other sugar transporters in the genome database of *Glomus intraradices*. Of these transporters, *GiMST1* was the only that was significantly expressed *in planta*. *In situ* hybridisation showed the location of GiMST1 in arbuscules and the intraradical mycelium. GiMST1 functions as a high-affinity transporter for glucose but transports also other sugars including xylose. Thus, it is suggested that xylose is an alternative carbon source for AM fungi. This was verified by the identification of genes of the xylose catabolism pathway. First experiments were performed to investigate the regulation of *GiMST1*, indicating that xylose is a possible inducer of *GiMST1* expression. Furthermore, it could be shown that *GiMST1* expression depends on the phosphate homeostasis of the host root. An unexpected finding was the expression of sugar transporters in the extraradical mycelium, a tissue so far believed with no sugar uptake capacity.

In addition, two new monosaccharide transporters from *S. tuberosum*, StHT2 and StHT6, were isolated from a cDNA library of arbuscule containing root cells. Expression analyses showed that *StHT6* is up-regulated in mycorrhized roots whereas *StHT2* is not differentially regulated. The promoter of StHT6 and a second known mycorrhiza-induced monosaccharide transporter from *M. truncatula*, MtST1, were analysed *in vivo* and *in silico* to investigate their possible regulation in mycorrhizas.

With the results presented in this work, the existing model for carbon flux in the AM symbiosis could be improved.

Zusammenfassung

Seit mehr als 400 Millionen Jahren bilden Pflanzen eine mutualistische Symbiose mit arbuskulären Mykorrhiza (AM) Pilzen aus. Der evolutionäre Erfolg dieser Symbiose, die mehr als 80 % aller Landpflanzen eingehen, lässt sich vor allem auf den gegenseitigen Nährstoffaustausch zurückführen. Dabei profitiert die Pflanze im Besonderen von einer verbesserten Phosphatversorgung durch den Pilz, dieser hingegen von den Photosynthesen der Pflanze. Ein beträchtlicher Teil des von der Pflanze fixierten Kohlenstoffes gelangt somit über das Hyphennetzwerk des Pilzes in den Boden. Die Untersuchung des Kohlenstoffflusses in der arbuskulären Mykorrhiza ist aus zweierlei Hinsicht von Bedeutung. Erstens, spielt die arbuskuläre Mykorrhiza eine nicht zu vernachlässigende Rolle im globalen Kohlenstoffzyklus. Zweitens, werden AM Pilze aufgrund ihrer positiven Eigenschaften zunehmend in der Landwirtschaft eingesetzt. Studien zeigten allerdings, dass unter bestimmten Bedingungen wie Überdüngung, die Kosten der Symbiose ihren Nutzen für die Pflanze übersteigen können. Mögliche Folgen sind ein reduziertes Pflanzenwachstum im Vergleich zu nicht-mykorrhizierten Pflanzen. Trotz vieler Studien auf diesem Gebiet, sind die grundlegenden Mechanismen des Kohlenstoffaustausches in der AM Symbiose nicht bekannt.

Die hier vorliegende Arbeit beschreibt die Isolierung und Charakterisierung des ersten symbiontischen Zuckertransporters, GiMST1, eines AM Pilzes. GiMST1 wurde zusammen mit vier weiteren Zuckertransportern mittels Sequenzanalysen in der Genomdatenbank von *Glomus intraradices* gefunden. Von diesen Zuckertransportern war GiMST1 der einzige, der *in planta* signifikant expremiert war. *In situ* Hybridisierung zeigte die Lokalisation von *GiMST1* in Arbuskeln und dem intraradikulärem Myzel. GiMST1 zeigt höchste Affinität für Glukose, transportiert aber auch andere Zucker wie Xylose. Demzufolge wird angenommen, dass Xylose als alternative Kohlenstoffquelle von AM Pilzen genutzt werden kann. Dies wurde durch die Identifizierung von Genen, die für die Verstoffwechslung von Xylose notwendig sind, bestätigt. Erste Experimente um die Regulation von GiMST1 zu untersuchen zeigten, dass Xylose die GiMST1 Expression induziert. Außerdem konnte gezeigt werden, dass die Expression von GiMST1 von dem Phosphathashalt der Wirtswurzel abhängt. Des weiteren wurde die Expression von Zuckertransportern im extraradikulärem Myzel beobachtet. Dies weist auf eine mögliche Aufnahme von Zuckern über das extraradikuläres Myzel hin, was bisher ausgeschlossen wurde.

Zusätzlich konnten zwei neue Monosaccharidtransporter von *S. tuberosum* isoliert werden, StHT2 und StHT6. Expressionsstudien zeigten, dass StHT6 in mykorrhizierten Wurzeln hochreguliert wird, während StHT2 nicht differenziell reguliert wird. Außerdem wurden *in vivo* und *in silico* Promoterstudien durchgeführt um die Regulation von StHT6 und eines weiteren bekannten Myorrhiza-induzierbaren Monosaccharidtransporters von *Medicago truncatula*, MtST1, zu untersuchen.

Anhand der Ergebnisse dieser Arbeit konnte das bestehende Modell des Kohlenstoffflusses in der AM Symbiose ergänzt werden.

Contents

1	Introduction	3
1.1	No Plant Is an Island	3
1.2	The Arbuscular Mycorrhizal Symbiosis	4
1.3	The Arbuscular Mycorrhizal Life Cycle	5
1.4	Uptake and Transfer of Nutrients in the AM Symbiosis	6
1.4.1	The Fungal-Soil Interface	6
1.4.2	The Plant-Fungal Interface	8
1.5	Carbon Fluxes in the AM Symbiosis	10
1.6	Motivation for this Thesis	12
2	Materials and Methods	15
2.1	Organisms and Culture Conditions	15
2.1.1	Organisms	15
2.1.2	Cultivation of <i>Escherichia coli</i> and <i>Agrobacterium rhizogenes</i>	15
2.1.3	Cultivation of <i>Saccharomyces cerevisiae</i> (Baker's Yeast)	18
2.1.4	Cultivation of <i>Aspergillus nidulans</i>	19
2.1.5	Cultivation of <i>Agrobacterium rhizogenes</i> Transformed Roots	21
2.1.6	<i>In vitro</i> Cultivation of <i>Glomus intraradices</i>	21
2.1.7	Isolation of <i>G. intraradices</i> Spores	23
2.2	Experimental Design	24
2.2.1	<i>In vitro</i> Mycorrhization Assay of Hairy Roots	24
2.2.2	<i>In vitro</i> Mycorrhization of <i>Medicago</i> Plants	25
2.2.3	Phosphate Treatment of Mycorrhized Roots	25
2.2.4	Root Exudate Synthesis	26
2.2.5	Treatments of Extraradical Mycelium in Liquid Cultures	26
2.3	Transformation Systems	26
2.3.1	Plasmids	26
2.3.2	Transformation of Bacteria	29
2.3.3	Transformation of Yeast	29
2.3.4	Transformation of <i>Aspergillus nidulans</i>	29
2.3.5	Generation of Hairy Roots from <i>S. lycopersicum</i> and <i>M. truncatula</i>	30
2.4	Preparation and Analysis of DNA	30
2.4.1	Preparation of Genomic DNA	30
2.4.2	Preparation of Plasmid DNA from <i>E. coli</i>	30
2.4.3	Agarose Gel Electrophoresis	31
2.4.4	Isolation and Purification of DNA from Agarose Gels	31

Contents

2.4.5	Concentration and Precipitation of DNA	31
2.4.6	Southern Blotting	31
2.4.7	Sequencing of Plasmid DNA	32
2.5	Enzymatic Modification of DNA	32
2.5.1	Restriction Endonuclease Digestion of DNA	32
2.5.2	Ligation of DNA	33
2.6	Preparation and Analysis of RNA	33
2.6.1	Preparation of Total RNA	33
2.6.2	Denaturing Agarose Gel Electrophoresis of RNA	34
2.6.3	DNase Digestion and cDNA Synthesis	34
2.6.4	Northern Blotting and Dot Blot	35
2.7	Polymerase Chain Reaction (PCR)	35
2.7.1	Oligonucleotides	35
2.7.2	Standard PCR	35
2.7.3	Cloning of PCR Fragments	36
2.7.4	Gateway Cloning	36
2.7.5	Colony PCR for the Selection of <i>Agrobacterium</i> Transformants	37
2.7.6	Rapid Amplification of cDNA Ends (RACE)	38
2.7.7	Isolation of Unknown Genomic Sequences by Genome Walking	40
2.8	Isolation of Arbusculated Cells for RNA Extraction	41
2.9	Screening of cDNA Libraries	43
2.9.1	SMART cDNA Synthesis and LD PCR Amplification	43
2.9.2	cDNA Size-Fractionation	44
2.9.3	Construction of cDNA Expression Libraries	44
2.9.4	Construction of the Yeast Expression Vector pNH196	45
2.9.5	Functional Complementation Assay in Yeast	46
2.9.6	Plasmid Preparation from Yeast and Retransformation in <i>E. coli</i>	48
2.10	Heterologous Expression of GiMST1 in Yeast	49
2.11	Spotting Test	49
2.12	Uptake Experiments with Radioactive Labelled Sugars	49
2.13	Transcription Analysis	50
2.13.1	Quantitative Real-Time PCR (qPCR)	50
2.13.2	In situ Hybridisation of Mycorrhized Roots	51
2.14	Histochemical Analysis	53
2.15	Imaging Techniques	55
2.16	Software and Webservices	55
3	Results	57
3.1	Characterisation of Sugar Transporters from Potato	57
3.1.1	Enrichment of Arbusculated Cells by Microdissection	57
3.1.2	Screening of cDNA Libraries for Sugar Transporters	57
3.1.3	Functional Analysis of StHT6 and StHT2 in Yeast	61
3.1.4	Phylogenetic Analysis of StHT6 and StHT2	62
3.1.5	Expression of Plant Sugar Transporters During Mycorrhization	65

3.1.6	Promoter Studies of <i>StHT6</i> and <i>MtST1</i>	65
3.2	Characterisation of AM Fungal Sugar Transporters	70
3.2.1	Screening for MFS Transporters in the Genome Database	71
3.2.2	Putative Sugar Transporters of <i>G. intraradices</i>	72
3.2.3	Isolation of <i>GiMST1</i> and <i>GiMST2</i>	74
3.2.4	<i>GiMST1</i> Expression and Transcript Localisation <i>in planta</i>	75
3.2.5	Functional Analysis of <i>GiMST1</i> in Yeast	79
3.3	Xylose as Putative Carbon Source for AM Fungi	82
3.3.1	Xylose Utilisation Pathway Genes of <i>G. intraradices</i>	82
3.3.2	Activity of Xyloglucan Modifying Enzymes During Mycorrhiza- tion	84
3.3.3	Orthologues of the XlnR Regulator in <i>G. intraradices</i>	86
3.3.4	<i>GiMST1</i> Promoter Analysis	87
3.4	Expression of Sugar Transporters in the ERM	89
3.5	<i>GiMST1</i> and <i>GiMST2</i> Expression in the Vicinity of Roots	92
3.6	Functional Relevance for <i>GiMST1</i> in the AM Symbiosis	92
4	Discussion	95
4.1	Cloning of Two New Sugar Transporters of Potato	95
4.1.1	<i>StHT6</i> : a Mycorrhiza-inducible Plant Hexose Transporter	95
4.1.2	Putative Regulatory Mechanisms for <i>StHT6</i> and <i>MtST1</i> Expression	96
4.2	Isolation of Fungal Sugar Transporters	97
4.3	First Description of AM Fungal Sugar Transporters	97
4.4	<i>GiMST1</i> : a Symbiotic Sugar Transporter of <i>G. intraradices</i>	98
4.4.1	<i>GiMST1</i> Is Active at Different Plant/Fungal Interfaces	98
4.4.2	<i>GiMST1</i> Supports the Biotrophic Lifestyle of AM Fungi	99
4.4.3	Xylose as Alternative Carbon Source for AM Fungi	101
4.4.4	<i>GiMST1</i> Expression Depends on the Root Phosphate Status	102
4.5	Sugar Uptake as Possible New Function of the ERM	104
4.6	Possible Regulation of <i>GiMST1</i>	105
5	Conclusion and Outlook	107
	Appendix	111
A	Oligos	111
B	Sequences and Alignments	115
C	Expression Data	127
D	Uptake Studies	133
	Bibliography	135

Contents

List of Abbreviations	151
List of Figures	153
List of Tables	161

Chapter 1

Introduction

1.1 No Plant Is an Island

No man is an island, entire of itself; every man is a piece of the continent,
a part of the main.

–J. DONNE

In its very simplest and most prosaic sense the poem of John Donne reminds us that human beings are interdependent. In a broader sense, this refers to all organisms, from a single celled organism in the ocean to the mountain lion in the Andes of South America. Also plants grown under natural conditions, are not isolated. They live and interact with members of their kind, but also with herbivorous animals, insects and microbes colonising different parts of the plant body. Especially the root surface and its surrounding, the rhizosphere, are densely populated with bacteria, fungi and oomycetes. The kind of interaction between the plant and its microbial subtenant can range thereby from parasitism to mutualism.

Parasitic plant-microbe interactions are one of the main subjects in plant research. Plants are the major source of food and biomaterial worldwide and infections of crop plants with plant pathogenic microbes cause tremendous harvest losses every year. One of the most prominent examples in history is the Great Irish Famine (1846/47) in which the complete potato harvest from North Europe was destroyed in a few weeks by the pathogenic oomycete *Phytophthora infestans* (Reader, 2009).

On the other side, mutualistic plant-microbe interactions come more and more into the focus of research. Studies on mutualistic plant-microbe interactions can also improve our knowledge of parasitic microbes, as the mechanisms to colonise the plant and to circumvent plant defense responses are often similar. Of particular importance are the benefits for the plant arising from these associations i.e., improved growth, yield and health. The rhizobial symbiosis, a relationship between leguminous plants like beans and nitrogen-fixing bacteria, is a classical example. The bacteria supply nitrogen to the plant and in return receive organic compounds as carbon source. Another example is the arbuscular mycorrhizal symbiosis which is one of the most curious cooperations between fungi and plants in the world. This symbiosis is the subject of this thesis.

1.2 The Arbuscular Mycorrhizal Symbiosis

Arbuscular mycorrhiza are the rule, not the exception.

–S.E. SMITH AND F.A. SMITH

The name mycorrhiza (from the Greek 'mykes', meaning fungus and 'rhiza' meaning root) was introduced by the German botanist Albert Bernhard Frank (original publication 1885; English translation 2005 in *Mycorrhiza*). During his scientific studies on truffles he observed, that roots of some trees are enclosed by a 'mantle' of fungal hyphae. His interpretation of this phenomenon was that some trees are nourished by fungi. This idea contrasted the common opinion at the beginning of the 19th century that fungi colonising plants were exclusively pathogens. Today, the mycorrhizal symbiosis is commonly regarded as a mutualistic symbiosis in which the plant is supplied over the hyphal network of mycorrhizal fungus with nutrients from the soil and in return provides the fungus with organic carbon.

There are two major forms of mycorrhiza, the ectomycorrhiza and the endomycorrhiza. The 'fungal-roots', which were described by Albert Frank, are an example for ectomycorrhiza, a symbiosis between trees and fungi which are belonging to different fungal phyla but with uniform structural features. These are a hyphal sheath around the root, a system of fungal hyphae growing between epidermal and cortical cells (the Hartig net) where nutrients are exchanged between the symbiotic partners, and an expanding hyphal network in the soil. Typically the hyphae in ectomycorrhiza remain extracellular whereas in endomycorrhiza the fungus penetrates into single cells of the root cortex to form specialised hyphal structures for nutrient exchange.

The most common type of an endomycorrhiza is the arbuscular mycorrhiza (AM). Arbuscular mycorrhizal fungi belong to the phylum Glomeromycota (Schüßler, 2001) and live in permanent association with roots of more than 80% of terrestrial plants including angiosperms, gymnosperms, some pteridophytes, or gametophytes (Read et al., 2000). Consequently, AM can be regarded as the normal state of plants in nature. Nevertheless, there are a few plant families which are characteristically non-mycorrhizal like *Brassicaceae* (Glenn et al., 1985), *Chenopodiaceae* (Hirrel et al., 1978) and *Urticaceae* (Vierheilig et al., 1996). AM fungi have a high impact on plant nutrition, mainly on phosphate supply which is described in detail in Chap. 1.4. Additionally, there is evidence that AM fungal colonisation improves the general fitness of a plant by increasing resistance to pathogens (Dehne and Schoenbeck, 1979; Cordier et al., 1998) and drought tolerance (Davies et al., 1993; Subramanian et al., 1995; Auge, 2001). In a broader context, AM have a strong influence on carbon and phosphate cycles, biodiversity and productivity of ecosystems (Bever, 1999; van der Heijden et al., 1998; Maherali, 2007). For the AM fungus itself, the symbiosis is obligate which means that the fungus is incapable to complete its life cycle in the absence of a plant partner. This might be due to the biotrophic life style of AM fungi, as they depend on the photosynthetic carbon of their green partner.

1.3 The Arbuscular Mycorrhizal Life Cycle

So test therefore who join forever if heart to heart be found together.

–F. SCHILLER

Roots in soil are colonised by AM fungi either by a pre-existing AM hyphal network growing from living or dead root fragments, or by germinating spores. Asexual spores are the only developmental stage of an AM fungus which is plant-independent. Characteristically, AM fungal spores are 40 to 100 µm in length and filled with a huge number of nuclei and storage lipids. The germination occurs spontaneously, independent of plant-derived signals (Mosse, 1959) while forming a small pre-symbiotic mycelium with limited growth (Mosse, 1988). During this pre-symbiotic phase the spore maintains hyphal growth by degrading its lipid reserves as carbon source (Bago et al., 1999). Nevertheless, a slight capacity to utilise exogenous sugars and acetate was measured (Shachar-Hill et al., 1995; Bago et al., 1999).

In the absence of a host, hyphal growth ceases after 2 to 4 weeks (Mosse, 1988). Cytoplasm and nuclei are relocated to the spore accompanied by the formation of septa starting at the hyphal tip (Logi et al., 1998; Dickson et al., 2001). With this programmed growth arrest the spore retains enough carbon to allow repeated germination until it encounters a new host.

In the vicinity of roots and triggered by host-derived signals, growth and branching of the fungus are intensified to increase the probability of direct hyphal-root contact (Giovanetti et al., 1993). Strigolactons have been characterised by Akiyama et al. (2005) as one of the crucial plant signals involved in this first crosstalk event between the symbiotic partners. Strigolactons are carotenoid derived plant compounds which are highly distributed in the plant kingdom and produced in larger quantities by AM hosts under phosphate limited conditions. The perception of strigolactons by the AM fungus triggers changes in hyphal architecture and increases mitochondrial activity as well as mitosis (Akiyama et al., 2005; Besserer et al., 2006). Interestingly also parasitic weeds like *Striga* and *Orobancha*, which are also obligate biotrophs, respond to strigolactons (Matusova et al., 2005). Analogue to plant-derived signals, the fungus must emit signals to initiate the symbiotic program of the plant before physical contact (Requena et al., 2007), like it is reported from the root nodulation symbiosis (Long, 1996). Here, lipochito-oligosaccharides referred to as Nod-factors are produced by the bacteria. The Nod-factors are recognised by a specific class of plant receptor kinases which further activate the genetic program necessary for nodule formation (Long, 1996). Recently, the chemical structure of the corresponding Myc-factor was determined also as a lipochito-oligosaccharide compound (Denarie et al., 2010). It is assumed that the Myc-factor is perceived by so far unknown plant receptors and transmitted over a signal transduction cascade to trigger expression of symbiosis related genes. Many of the plant genes involved in the following signal transduction cascade which is partially conserved in both the mycorrhizal and the root nodulation symbiosis were already identified by screening of AM or rhizobial symbiosis defective mutants (for review see Parniske, 2008).

After root attachment the fungus forms an appressorium from which it penetrates into the rhizodermis. Therefore the fungus follows two ways either through the cleft between two adjacent cells, which might involve the localised production of wall degrading enzymes as well as hydrostatic pressure (Garcia-Romera, 1991), or directly through the rhizodermal cell (Genre et al., 2005). By the direct passage the plant cell forms a prepenetration apparatus (PPA) that guides the invading hypha through the cell. After the successful colonisation, the fungus grows extensively inter- and intracellularly through the root cortex. The growth pattern describes two different morphological types, named after the plant species in which they were first observed (Gallaud, 1905). The Paris-type AM symbiosis (from *Paris quadrifolia*) is characterised by extensive development of intracellular coiled hyphae and little intercellular growth. The Arum-type (from *Arum maculatum*) is distinguished by the formation of arbuscules. Arbuscules (Latin for 'little tree') are highly branched hyphal structures which develop by invagination in the root cortical cell. Often the fungus forms also intraradical vesicles which might be used as lipid storage. The life cycle of an AM fungus is completed with the development of a widespread hyphal network in the soil, the extraradical mycelium (ERM), which absorbs phosphate and other soil-derived nutrients, initiates the colonisation of other roots, and is also the site of sporulation.

1.4 Uptake and Transfer of Nutrients in the AM Symbiosis

Plants do not have roots, they have mycorrhizas.

–S. WILLIAM

The AM symbiosis has a long history as predicted by fossil finds of arbuscules, preserved in the Devonian Rhynie chert which is approximately 400 million years old (Remy et al., 1994). However, Redecker et al. (2000) found fossil AM fungal spores from the mid-Ordovician (460 million years ago). Early land plants had just primitive roots and they were additionally confronted with nutrient-poor soils. Thus it is very likely, that the mutualistic symbiosis with AM fungi was particularly important for the nutrition of the first land plants. The highly absorptive extraradical mycelium of the fungus replaced the primitive roots and allowed the plants to conquer the terrestrial environment (Pirozynski et al., 1975). To this day, AM fungi contribute significantly to the plant nutrition, mainly by delivering phosphorus (Karandashov and Bucher, 2005) but also of nitrogen (Jin et al., 2005) and the micronutrients copper, zinc, manganese and iron (Liu et al., 2000).

1.4.1 The Fungal-Soil Interface

An essential role in the uptake of soil-derived nutrients is attributed to the extraradical mycelium (ERM). The fine hyphae can be compared with pipelines transporting nutrients to the plant and they outrange the plant roots by penetrating in soil pores and exploiting fresh nutrient pools. For the uploading of nutrients into the fungal

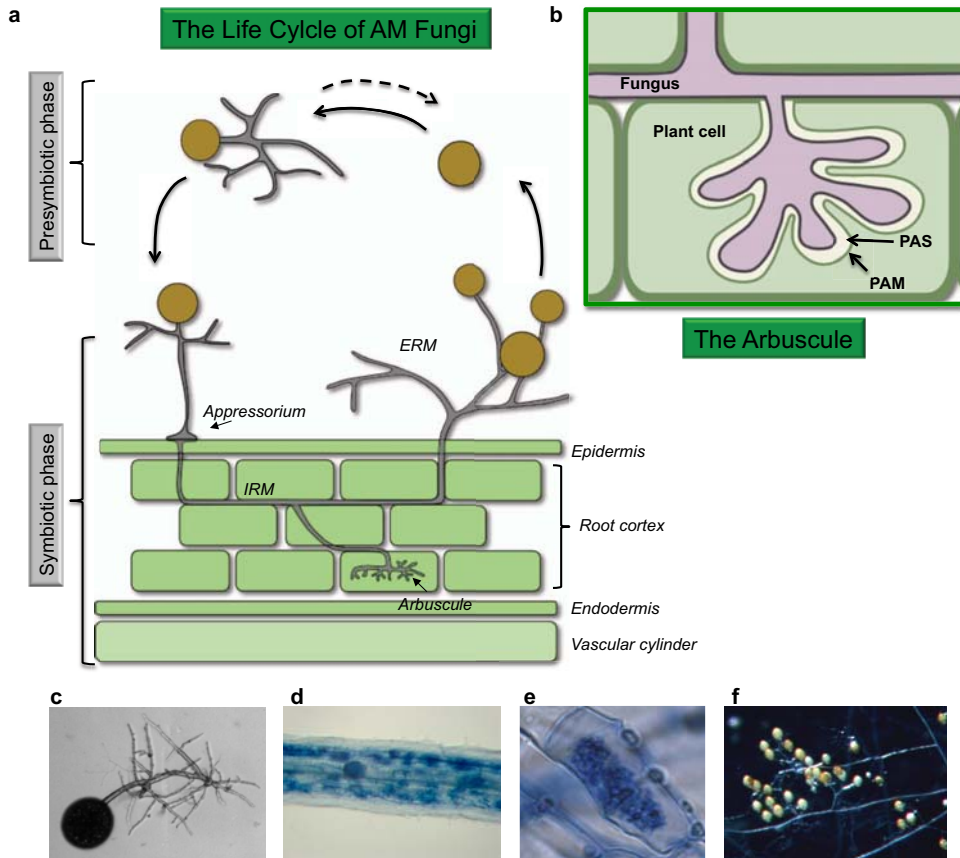


Figure 1.1. **a**, Life cycle of AM fungi. In the presymbiotic phase spores can germinate repeatedly in the absence of host roots. Colonisation of a root starts with the formation of an appressorium from which the fungus grows inter- and intracellularly through the root cortex forming arbuscules in the inner root cortex. The life cycle is fulfilled with the formation of an extraradical mycelium in the soil and the production of spores. **b**, Schema of an arbuscule. Plant and fungus are separated by the periarbuscular space. The periarbuscular membrane of the plant is involved in uptake of nutrients delivered by the fungus. **c**, Germinated spore. **d**, Colonised root (trypan blue stained). Fungal structures are shown in blue. **e**, Arbuscule stained with trypan blue. **f**, ERM with spores. (ERM: extraradical mycelium, IRM: intraradical mycelium, PAS: periarbuscular space, PAM: periarbuscular membrane)

system, transporter proteins are required. Only a few of these transporters have been identified so far, e.g. a zinc (González-Guerrero et al., 2005), an ammonium (Lopez-Pedrosa et al., 2006), an amino-acid transporter (Cappellazzo et al., 2008) from *G. intraradices* and three homologous high-affinity phosphate transporters isolated from three different AM fungi (Harrison and van Buuren, 1995; Maldonado-Mendoza et al., 2001; Benedetto et al., 2005). All of these transporters depend on the function of membrane H⁺-ATPases generating a proton gradient over the fungal membrane for active transport. H⁺-ATPases active in the ERM have been isolated from *G. mossae* and *G. intraradices* (Ferrol et al., 2000; Requena et al., 2003).

A central position in the AM symbiosis has the uptake and transfer of phosphate. Phosphate is an essential nutrient for plant growth and development. Total phosphate concentration in the soil is high, but orthophosphate (Pi), the inorganic form which is directly accessible for plants, is available only in minor concentrations due to its low solubility and slow diffusion rate (Schachtman et al., 1998). As a consequence, the rapid absorption of Pi by the plant results in the development of a depletion zone around the root (Schachtman et al., 1998). In general, roots use two pathways of phosphate absorption, the direct uptake through root epidermis and root hairs which depends on the extent of Pi depletion, and the mycorrhizal uptake via the extraradical mycelium which has access to Pi pools far beyond the depletion zone (Zhu et al., 2001). The significance of the mycorrhizal pathway has been demonstrated in experiments with radio-labelled Pi only accessible for the ERM (Smith et al., 2003). These studies confirmed that the AM pathway can dominate the total Pi uptake while decreasing the direct uptake pathway under low phosphate conditions.

In addition to phosphate, AM fungi assist the plant by providing a significant amount of nitrogen taken up either as ammonium or as nitrate. Furthermore there is evidence that AM fungi mineralise organic nitrogen sources (Hodge et al., 2001; Leigh et al., 2009) and absorb small peptides and amino acids (Cappellazzo et al., 2008).

For long distance transport towards the ERM, phosphate and nitrogen are converted into special forms. Pi is accumulated in the vacuoles as polyphosphate (Callow et al., 1978; Ezawa et al., 2003; Solaiman et al., 1999) whereas nitrogen is converted to arginin (Cruz et al., 2007). Together with other nutrients they are delivered to the intraradical fungal structures where they are taken by the plant cells at plant fungal interfaces.

1.4.2 The Plant-Fungal Interface

The main place for nutrient exchange between plant and AM fungus is the arbuscule. Arbuscules are specialised feeding structures, comparable with haustoria of biotrophic fungal pathogens, with the main difference that the nutrient transfer is bidirectional.

When the fungal hyphae penetrates the cortical cell to develop an arbuscule, the plant plasma membrane expands to surround the hyphae and forms the so called periarbuscular membrane (PAM) (Fig. 1.1).

1.4 Uptake and Transfer of Nutrients in the AM Symbiosis

The plant and the AM fungal cell stay separated by an apoplastic interface, the periarbuscular space (PAS) (Fig. 1.1). The PAS contains non-assembled primary plant cell wall components such as non-sterified polygalacturonans, xyloglucans, beta-1,4-glucans and arabinogalactan proteins (Bonfante and Perotto, 1995). Typically these cell wall components are not cross-linked maybe due to the activity of hydrolytic enzymes released by the fungus. Low levels of AM fungal polygalacturonases have been detected in the PAS (Peretto et al., 1995). Additionally, the activity of fungal or plant xyloglucanases (Rejon-Palomares et al., 1996) and plant xyloglucan endotransglucosylase/hydrolyase (Maldonado-Mendoza et al., 2005) is increased in colonised roots. The function of plant xyloglucan endotransglucosylase/hydrolyase in the AM is not known so far but they might be involved in the reorganisation of the plant cell wall around the forming arbuscule.

Plant gene expression studies show that some genes are specifically induced in cells containing arbuscules. The PAM shows for example a very high ATPase activity (Gianinazzi-Pearson et al., 1991, 2000). This and the increased surface structure are conform with the active transfer of fungal derived nutrients over this membrane. The evidence for the transfer of phosphate over the PAS correlates with the isolation of the first plant phosphate transporter (PT) from *S. tuberosum* (Rausch et al., 2001) specifically expressed in arbuscule containing cells. Until now, several phosphate transporters possibly involved in the uptake of AM fungal-derived Pi were isolated from various plants (Rausch et al., 2001; Harrison et al., 2002; Paszkowski et al., 2002; Glassop et al., 2005, 2007; Güimil et al., 2005; Nagy et al., 2005; Maeda et al., 2006). According their expression level these transporters can be subdivided in mycorrhiza up-regulated or specific transporters which were only located in the PAM. The mechanism for Pi release in the PAS is still in discussion. It is proposed that polyphosphate is hydrolysed and the released Pi follows passively a concentration gradient over the arbuscule membrane into the PAS where it is actively taken up by the plant cell (Javot et al., 2007).

Nitrogen is released from the fungus to the plant in inorganic form (Govindarajulu et al., 2005). Arginin arriving from the ERM is broken down in the intraradical fungal hyphae, liberating urea and ornithine which are further cleaved to ammonium (NH₄) (Jin et al., 2005; Cruz et al., 2007). NH₄ is released into the PAS by an unknown mechanism. The first plant ammonium transporter (AMT) mediating nitrogen uptake in arbuscules was isolated recently in a screen on mycorrhizal induced genes in *Lotus japonicus* by Güther et al. (2009).

Arbuscules are relatively short-living structures and degrade within seven days, whereas the affected plant cell recovers and can be re-colonised by the fungus (Smith and Read, 1997). The reason for the fast arbuscular collapse is not clear, particularly because their development demands complex cell rearrangements from both symbiotic partners. Host defense reactions against progressive fungal invasion as well as discrimination between efficient and inefficient arbuscules in term of phosphate delivery are considered (Smith and Read, 1997). Because of the short life span of arbuscules, the persistent intraradical mycelium of the fungus is also regarded to be

involved in nutrient transfer (Smith and Read, 1997). Also here, high ATPase activity indicating active transport processes was measured (Gianinazzi-Pearson et al., 1991, 2000).

1.5 Carbon Fluxes in the AM Symbiosis

Sweets for my sweet, sugar for my honey.

– THE SEARCHERS

In return to the absorbed nutrients, an estimated 20 % of photosynthetically fixed carbon is transferred to the fungus (Jakobsen and Rosendahl, 1990). An indirect evidence for the carbon transfer from the plant to the fungus is that AM fungi are only capable for ERM proliferation and spore production when the intraradical colonisation is established. Additionally, several authors have shown that a decrease of irradiance reduces fungal growth indicating that the fungus feeds on photosynthates (Hayman, 1974; Tester et al., 1985; Son and Smith, 1988; Smith and Gianinazzi-Pearson, 1990). Early studies with plants exposed to radio-labelled CO₂ proved a transfer of carbon to the fungus (Ho and Trappe, 1973; Hirrel and Gardemann, 1979; Francis and Read, 1984). Further experiments of Solaiman and Saito (1997) using radiorespirometric analysis demonstrated directly the sugar uptake capacity of isolated intraradical fungal structures.

Pfeffer et al. (1999) were not only able to confirmed the previous experiments, they were also able to determine in which form the carbon is transferred *in planta* using *in vitro* cultures of *G. intraradices* and *Daucus carota* hairy roots grown in dual compartment plates (for a detailed description of the system see Chap. 2.1.6). In their experimental assay they exposed the colonised carrot roots to radio-labelled sugars (glucose, fructose, mannitol or succinate) and measured the incorporation of ¹³C in fungal storage lipids by nuclear magnetic resonance spectroscopy (NMR). In summary, their results indicated that ¹³C-labelled glucose and to a lesser content fructose but not mannitol or succinate are taken up by the fungus within the roots. Pfeffer et al. (1999) confirmed also the findings of Sachar-Hill et al. (1995) which showed that the delivered hexoses are rapidly incorporated into glycogen and trehalose to buffer intracellular glucose concentrations. Furthermore, hexoses are either metabolised in the IRM via the pentose phosphate pathway (PPP) or are converted into lipids which are stored or transported to the ERM. Here hexoses can be released by gluconeogenesis and metabolised also via the PPP. Additionally, Pfeffer et al. (1999) were able to demonstrate that the ERM has no capacity to utilise exogenous sugars for catabolism, storage or transfer. This was tested by exposing only the separated ERM to ¹³C-glucose or ¹³C-fructose in the dual compartment system. Thus, they showed that the ¹³C-labelled sugars were not metabolised in the ERM by detecting the release of respired ¹³CO₂. Further they showed, that neither in the mycelium in the fungal compartment nor in colonised roots in the root compartment ¹³C was incorporated in fungal storage lipids using the NMR technique. The main conclusion of this ex-

periment was, that the fungus takes up sugars only in the plant but not by the ERM. Nevertheless, Bago et al. (2002, 2003) showed that other carbon sources than sugars are taken up by the ERM. When exposing the ERM to radioactive-labelled glycogen or acetate, they observed labelling of different fungal storage compounds like trehalose and triacylglycerol (TAG).

AM fungi increase the sink strength, alter the carbohydrate pools and influence expression of genes required for hexose uptake in the plant and allocation in roots. Sucrose is the main form in which photosynthetically fixed carbon is transported from photosynthetic leaves (sources) to non-photosynthetic organs like the roots (sinks). Thereby, sucrose is transferred in the phloem and delivered to the cells either via apoplastic or symplastic transport through plasmodesmata (Atwell et al., 1999). In sink tissues sucrose synthases or invertases cleave sucrose to glucose and fructose (Atwell et al., 1999). Such sucrose-cleaving enzymes of plant origin have been shown to be involved in carbon allocation in the AM symbiosis. Several studies revealed increased transcript accumulation of cytoplasmic sucrose synthases (Blee and Anderson, 2002; Ravnskov et al., 2003; Hohnjec et al., 2003), and cytoplasmic (Schubert et al., 2004) or apoplastic invertases (Schaarschmidt et al., 2006). Furthermore, Harrison et al. (1996) identified a hexose transporter of *M. truncatula* (MtST1) with increased transcript levels in roots colonised by the AM fungi *G. versiforme*. MtST1 is located in the phloem and the root tips in non-mycorrhized roots. However upon AM fungal colonisation transcripts could also be detected in arbusculated cells or cells close to the IRM. The increased activity of MtST1 in AM symbiosis might be a result of the higher metabolism of colonised cells or an attempt to restrict excessive hexose efflux to the fungus.

The place of carbon delivery is a matter of debate. It is often assumed that the arbuscule is the site of both phosphate and carbon transfer. The fact that hyphae can colonise roots effectively even when producing no arbuscules suggests, that intercellular hyphae might be at least in part of the location (Smith and Smith, 1996).

The mechanism of carbon uptake is also unclear. The uptake can be passive following a concentration gradient with high sugar concentrations at the plant-fungal interface and lower concentrations in the fungus because of the rapid conversion of the sugars to trehalose or glycogen (Bago et al., 2000), or it can be active by proton depending sugar transporters. H^+ -ATPase activity of arbuscules and the IRM (Gianinazzi-Pearson et al., 1991) as well as the isolation of a fungal ATPase active *in planta* indicate active transport processes. Additional evidence comes from the isolation and characterisation of active sugar transporters from other biotrophic fungi like ectomycorrhizal fungi or plant pathogens (Nehls et al., 1998; Voegelé et al., 2001; Nehls, 2004; Schüßler et al., 2006; Polidori et al., 2007; Wahl et al., 2010). Noteworthy is the description of the first Glomeromycotan monosaccharide transporter GpMST1 from *Geosiphon pyriformis*, a near relative of AM fungi that forms a symbioses with the cyanobacteria (*Nostoc punctiformis*) (Schüßler et al., 2001, 2006). GpMST1 was identified in a cDNA yeast-expression library from isolated 'bladders', symbiotic structures very similar to arbuscules, and therefore regarded as the relevant transporter in C-

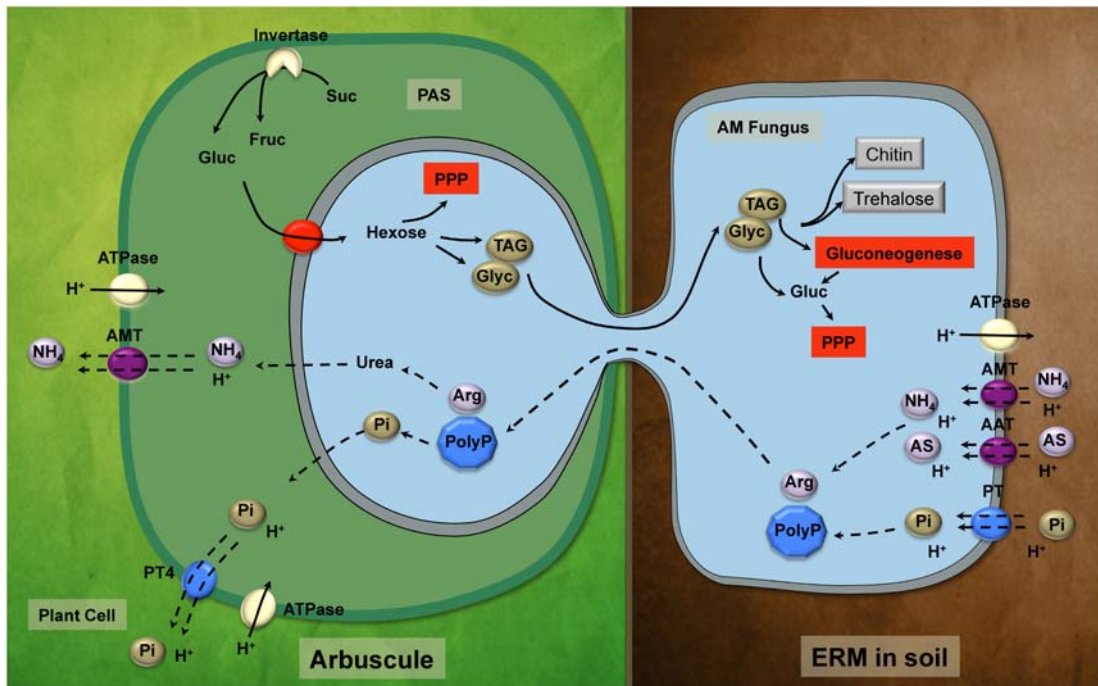


Figure 1.2. Metabolic fluxes in the AM symbiosis after Bago et al. (2000) and Parniske (2008). Plant hexoses are taken up by the fungus by an unknown mechanism. Hexoses are incorporated in triacylglyceral (TAG) and glycogen (Glyc) for long distance transporter or metabolised via the oxidative pentose phosphate pathway (PPP). In the ERM hexoses are synthesised from lipids by gluconeogenesis and metabolised in the PPP. TAG and Glyc are used for synthesis of trehalose and chitin. Inorganic phosphate is taken up by the fungus from the soil and transferred as polyphosphate (PolyP) to intraradicular structures. Nitrogen in form of amino acids or ammonium are transferred as arginine putatively bound on PolyP to the arbuscules. Phosphate is released in the periarbuscular space and taken up by the plant cell via plant specific phosphate transporters like PT4. Nitrogen is released as urea from arginine and transferred to the plant as ammonium.

flow from algae to fungus. By heterologous expression of GpMST1 in yeast, Schüßler et al. (2006) showed highest uptake rates for glucose and fructose, mannose, galactose and xylose. Because of the wide substrate specificity of GpMST1 they speculated that other monosaccharides than glucose liberated from the plant cell wall might be used as carbon source by AM fungi in general. Schüßler et al. (2007) states, that 'the GpMST1 sequence delivers valuable data for the isolation of orthologues from other AM fungi and may eventually lead to the understanding of C-flows in the AM'. However, a sugar transporter from an AM fungi has not been isolated so far and the key mechanisms in AM carbon transfer are not entirely known. The existing model for carbon, phosphate and nitrogen fluxes in the AM symbiosis is shown in Fig. 1.2.

1.6 Motivation for this Thesis

In order to satisfy the worldwide demand for nutrients, the majority of agricultural systems depend on the application of fertilisers. The total use of fertilisers increased from 14 million tons in the year 1950 to 145 million tons in the year 2003 (Earth Policy

Institute).

Phosphorous is one of the frequently limited nutrients in soil. The production of phosphorous fertilisers is highly energy-consuming and depends on non-renewable resources. It was estimated that the rock deposits, the main phosphorous sources, could be depleted in almost 50 years (Vance et al., 2003). To prevent a 'potential phosphate crisis' for the coming generations, sustainable management of phosphate in agricultural systems is indispensable (Abelson, 1999).

The application of arbuscular mycorrhizal fungi is one example for sustainable agriculture. Mycorrhizal associations can maximise the amount of phosphate available for the plant, and therefore improve the plant productivity. However, this is not always the case as the symbiosis can switch from mutualism to parasitism (Johnson et al., 1997), depending on the carbon fee the plant has to pay. Under laboratory conditions the plant invests around 17% of the photoassimilates in the fungus rather than in the development of roots (Bryla and Eisenstaat, 2005). Under phosphate limited conditions, the benefit (a surplus of phosphate) outranges the cost (a loss of carbon). However, the cost can also exceed the benefit for mycorrhizal plants under well-fertilised conditions. Here, the plant can supply itself with adequate amounts of phosphate from its surrounding, while still providing the fungus with carbon. For this reason, some plants inhibit mycorrhizal colonisation at high phosphate concentrations (Menge et al., 1978; Bruce et al., 1994). Other plants, maintain high colonisation rates (Peng et al., 1993). In this case, the fungus acts as a parasite which can result in growth depression relative to non-mycorrhized plants (Peng et al., 1993; Olsson et al., 2010). However, not only phosphate but also carbon limitation of the plant e.g. after shading can also minimise the beneficial effect of the AM symbiosis (Hayman, 1974; Olsson et al., 2010).

The aim of this work is the isolation and characterisation of sugar transporters mediating the carbon flow from the plant to the AM fungus. The identification of such transporters in the AM symbiosis has been elusive so far, despite many efforts in several laboratories. However, their characterisation opens the field for research on the key mechanisms involved in AM symbiotic carbon flow and its regulation.

Chapter 2

Materials and Methods

2.1 Organisms and Culture Conditions

2.1.1 Organisms

Tabs. 2.1 and 2.2 give a detailed list of all organisms which were used for this study considering genotype and origin of the strain or cultivar. The cultivation conditions and the generation of the genetically modified organisms are described in the following chapters.

2.1.2 Cultivation of *Escherichia coli* and *Agrobacterium rhizogenes*

E. coli and *A. rhizogenes* strains were grown in liquid cultures or on solid agar plates supplemented with the appropriate antibiotics (Tab. 2.3) under aerobic conditions. *E. coli* was cultivated at 37 °C on LB agar plates. Liquid cultures of *E. coli* were inoculated according the requirements in 3 to 20 ml of LB medium and incubated over night at 37 °C on a rotatory shaker at 180 rpm. *A. rhizogenes* was cultivated on TY plates. Liquid cultures of *A. rhizogenes* were grown in 3 ml TY medium at 28 °C on a rotatory shaker at 200 rpm.

All media and glass ware for bacterial cultivation were sterilised by autoclaving at 121 °C for 15 min. Heat sensitive reagents like antibiotics were filter sterilised and added after autoclaving.

For solid media 1.5 % Agar-Agar were added before autoclaving.

LB medium

- 10 g tryptone
- 5 g yeast extract
- 10 g NaCl
- add 1000 ml dH₂O
- pH 7.0

LB/X-gal/ITPG plates for 'blue-white' screening

- LB agar plates
- 40 $\frac{\mu\text{g}}{\text{ml}}$ X-gal (2 % stock solution in DMF)

Strain	Genotype	Reference
<i>Escherichia coli</i>		
DH5 α	<i>F- endA1 glnV44 thi-1 recA1 relA1 gyr A96 deoR nupG Φ80dlacZΔM15 Δ(lac ZY-argF) U169, hsdR17 (rK- mK+), λ-</i>	Invitrogen (USA)
TOP10	<i>F- mcrA Δ(mrr-hsdRMS-mcrBC) ϕ80lacZΔM15 ΔlacX74 recA1 araD139</i>	Invitrogen (USA)
XL1 Blue	<i>recA1 endA1 gyrA96 thi.1 hsdR17 supE44 ralA1 lac [F' proAB lacIqZΔM15 Tn10 (Tet^r)</i>	Stratagene (Germany)
<i>Agrobacterium rhizogenes</i>		
ARqua1	Sm ^r derivative of <i>A. rhizogenes</i> strain A4T (White et al. 1985)	Quandt et al., 1993
ARqua1-pMtPT4GFP-GUS-RR	ARqua1 transformed with the binary vector pMtPT4GFP-GUS-RR; Sm ^r , Spec ^r	Provided by H. Kuhn (KIT, Germany)
ARqua1-pHT6-GFP-GUS-RR	ARqua1 transformed with the binary vector pHT6-GFP-GUS-RR; Sm ^r , Spec ^r	This work
ARqua1-pST1-GFP-GUS-RR	ARqua1 transformed with the binary vector pST1-GFP-GUS-RR; Sm ^r , Spec ^r	This work
<i>Saccharomyces cerevisiae</i>		
EBYVW.4000	<i>MATa Δhxt1-17 Δgal2 Δstl1 Δagt1 Δmph2 Δmph3 leu2-3, 112 ura3-52 trp1-289 his3-Δ1 MAL2-8c SUC2</i>	Wieczorke et al., 1999
EBYVW.4000-pAOHX2	EBYVW.4000 transformed with pAOHX2; URA3	This work
EBYVW.4000-pNH196	EBYVW.4000 transformed with pNH196; URA3	This work
EBYVW.4000-pNH196-StHT6	EBYVW.4000 transformed with pNH196-StHT6; URA3	This work
EBYVW.4000-pNH196-StHT2	EBYVW.4000 transformed with pNH196-StHT2; URA3	This work
EBYVW.4000-pNEV-N	EBYVW.4000 transformed with pNEV-N; URA3	This work
EBYVW.4000-pNEV-N-GiMST1	EBYVW.4000 transformed with pNEV-N-GiMST1; URA3	This work
EBYVW.4000-pEX-TAG-GiMST1	EBYVW.4000 transformed with pEX-TAG-GiMST1; URA3	This work
EBYVW.4000-pEX-TAG-UmHXT1	EBYVW.4000 transformed with pEX-TAG-UmHXT1; URA3	Provided by K. Wippel (FAU Erlangen, Germany)
<i>Aspergillus nidulans</i>		
GR5	<i>pyrG89;wA3;pyroA4; veA1</i>	Waring et al., 1989
GR5-pMST1-DsRed-StuA	GR5 transformed with pPMST1-DsRed-StuA	This work
Arbuscular mycorrhizal fungi		
<i>Glomus intraradices</i>	DAOM 181602 (<i>wt</i>)	Schenk and Smith, 1982

Table 2.1. List of bacterial and fungal strains used for this work.

2.1 Organisms and Culture Conditions

Strain	Genotype	Reference
Plants		
<i>Solanum lycopersicum</i> Mill.cv Rio Grande	76R (<i>wt</i>)	Originally from Peto Seed Company, USA; seeds provided by E. Neumann (IGZ, Germany)
<i>S. lycopersicum</i> Mill.cv <i>rmc</i>	Tomato mutant line showing reduced mycorrhizal colonisation (<i>rmc</i>), parental line <i>S. lycopersicum</i> Mill.cv Rio Grande 76R	Barker <i>et al.</i> , 1998; seeds provided by E. Neumann (IGZ, Germany)
<i>Medicago truncatula</i> cv Jemalong	A17 (<i>wt</i>)	No data
Hairy roots		
<i>Daucus carota</i> -AR <i>qua1</i>	Transformed with AR <i>qua1</i>	No data
<i>S. tuberosum</i> -pStPT3-FT-GUS	Transformed with pBin19 carrying StPT3 promoter-Fluorescent Timer chimeric gene	Karandashov <i>et al.</i> , 2004
Rio Grande 76R-pMtPT4-GFP-GUS-RR	Transformed with AR <i>qua1</i> -pMtPT4-GFP-GUS-RR; RedRoot cassette, Km ^r	This work
Rio Grande 76R-pHT6-GFP-GUS-RR	Transformed with AR <i>qua1</i> -pHT6-GFP-GUS-RR; RedRoot cassette, Km ^r	This work
Rio Grande-pST1-GFP-GUS-RR	Transformed with AR <i>qua1</i> -pST1-GFP-GUS-RR; RedRoot cassette, Km ^r	This work
<i>rmc</i> -pMtPT4-GFP-GUS-RR	Transformed with AR <i>qua1</i> -pMtPT4-GFP-GUS-RR; RedRoot cassette, Km ^r	This work
<i>M. truncatula</i> -AR <i>qua1</i>	Transformed with AR <i>qua1</i>	Kuhn <i>et al.</i> , 2009
<i>M. truncatula</i> -pHT6-GFP-GUS-RR	Transformed with AR <i>qua1</i> -pHT6-GFP-GUS-RR; RedRoot cassette, Km ^r	This work
<i>M. truncatula</i> -pST1-GFP-GUS-RR	Transformed with AR <i>qua1</i> -pST1-GFP-GUS-RR; RedRoot cassette, Km ^r	This work

Table 2.2. List of plant cultivars and hairy roots used for this work.

Antibiotic	Provider	Final Conc. ($\mu\text{g/ml}$)	Stock Conc. (mg/ml)
Ampicillin Sodium (Amp)	Carl Roth GmbH & Co KG, Germany	100	100
Chloramphenicol (Cm)	Duchefa Biochemie, The Netherlands	34	34
Kanamycin Monosulfate (Km)	Carl Roth GmbH & Co KG, Germany	50	50
Streptomycin Sulfate (Sm)	Duchefa Biochemie, The Netherlands	60	100
Spectinomycin Dihydrochloride (Sp)	Duchefa Biochemie, The Netherlands	100 (<i>E.coli</i>) 600 (<i>A. rhizogenes</i>)	100
Tetracycline Hydrochlorid (Tet)	Carl Roth GmbH & Co KG, Germany	25	25

Table 2.3. Antibiotics and their working concentrations used for bacterial media. Antibiotics were dissolved in dH₂O, filter sterilised and stored at -20°C .

- $40 \frac{\mu\text{g}}{\text{ml}}$ ITPG (100 mM stock solution in sterile dH₂O)

TY medium

- 5 g tryptone
- 3 g yeast extract
- 0.9 g calcium chlorid dihydrate
- add 1000 ml dH₂O
- pH 7.0

2.1.3 Cultivation of *Saccharomyces cerevisiae* (Baker's Yeast)

S. cerevisiae strains were cultivated on solid plates at 30°C in a laboratory incubator. Liquid cultures were inoculated according the requirements in 3 to 100 ml medium and incubated at 30°C and 200 rpm on a rotatory shaker.

The autoclaving of media and glass ware for cultivation was usually carried out for 15 min at 120°C .

Amino acids and sugars were prepared separately as stock solutions, filter sterilised and added after autoclaving to the media in the appropriate concentrations (Tabs. 2.4 and 2.5). For solid media 2% Agar-Agar was added before autoclaving.

Rich medium:

YPD medium

- 1% (w/w) yeast extract
- 2% (w/w) peptone
- 2% (v/w) sugar

1X YPDA medium

Amino Acid	Provider	Final Conc. ($\mu\text{g/ml}$)	Stock Conc. (mg/100 ml)
Adenine (hemisulfate salt)	Sigma-Aldrich, Inc., USA	40	500
L-histidine	Biomol Feinchemikalien GmbH, Germany	20	240
L-leucine	Biomol Feinchemikalien GmbH, Germany	60	720
L-tryptophan	Applichem GmbH, Germany	40	480
Uracil	Applichem GmbH, Germany	20	240

Table 2.4. Amino acid concentrations used for YNB medium. The amino acids were prepared as stock solutions in dH_2O , filter sterilised and stored at 4°C .

- 1 % yeast extract
- 2 % sugar
- 0.003 % adenine
- pH 6.5

2X YPDA medium

- 2 % yeast extract
- 4 % peptone
- 4 % sugar
- 0.006 % adenine
- pH 6.5

Minimal medium:

YNB medium

- 0.17 % YNB -AA/AS (FormediumTM, UK)
- 0.5 % ammonium sulfate
- 0.1 or 2 % sugar
- pH 5.6

The YNB medium was supplemented with amino acids depending on the yeast genotype and the auxotrophic markers used for the selection of transformants.

2.1.4 Cultivation of *Aspergillus nidulans*

The *A. nidulans* strain GR5 (Waring et al., 1989) was cultivated on solid or in liquid minimal medium at 37°C under aerobic conditions. For solid media 1.5 % Agar-Agar was added before autoclaving.

The autoclaving of media and glass ware for cultivation was usually carried out for 15 min at 120°C .

Minimal Medium for *Aspergillus* Cultivation

Carbohydrate Source	Provider	Final Conc.	Stock Conc.
		%	%
D(+)-Maltose	Sigma-Aldrich, Inc., USA	2; 4	20 or 40
α -D(+)-Glucose	Carl Roth GmbH & Co KG, Germany	0.1; 2; 4	20 or 40
D(-)-Fructose	Carl Roth GmbH & Co KG, Germany	0.1; 2; 4	20 or 40
D(+)-Mannose	Carl Roth GmbH & Co KG, Germany	0.1; 2; 4	20 or 40
D(+)-Galactose	Merck KGaA, Germany	0.1; 2; 4	20 or 40
D(+)-Xylose	Carl Roth GmbH & Co KG, Germany	0.1; 2; 4	20 or 40
D(+)-Sucrose	Carl Roth GmbH & Co KG, Germany	0.1; 2; 4	20 or 40

Table 2.5. Carbohydrate sources and their concentrations used for different yeast media. The sugars were prepared as 20 or 40% stock solutions in dH₂O, filter sterilised and stored at 4 °C.

- 50 ml 20X salt solution
- 1 ml 1000X trace elements
- 100 mM glucose
- 1 g uridine
- 1 ml 500 mM uracil
- 1 ml 0.1 % (w/v) pyridoxine
- add 1000 ml dH₂O
- pH 6.5

20X Salt solution

- 120 g NaNO₃
- 10.4 g KCl
- 10.4 g MgSO₄x7H₂O
- 30.4 g KH₂PO₄
- add 1000 ml dH₂O

1000X Trace elements

- 22 g ZnSO₄x7H₂O
- 11 g H₃BO₃
- 5 g MnCl₂x4H₂O
- 5 g FeSO₄x7H₂O
- 1.6 g CoCl₂x5H₂O
- 1.6 g (NH₄)₆Mo₇O₂₄x4H₂O
- 1.1 g Na₄EDTA
- add 1000 ml dH₂O
- pH 6.5

2.1.5 Cultivation of *Agrobacterium rhizogenes* Transformed Roots

A. rhizogenes transformed roots ('hairy roots') were grown on modified minimal medium (M medium) with 1% saccharose (Bécard and Fortin, 1988; Tab. 2.6) on 9 cm petri dishes at 28 °C. The dishes were wrapped two times with PARAFILM® (American National Can Company, USA) to exclude contaminations. The medium was adjusted before autoclaving to a pH of 5.5 and solidified with 3% phyto-gel (Sigma-Aldrich, USA). For continuous cultures, pieces of the roots were transferred to fresh M medium.

2.1.6 *In vitro* Cultivation of *Glomus intraradices*

Many attempts have been made in the last decades to establish an *in vitro* system that enables the sterile and continuous cultivation of AM fungi under laboratory conditions. As the life cycle of the obligate biotrophic AM fungi depends fundamentally on the intimate symbiosis with a plant root, the long term cultivation without a host is not possible. One important step towards the *in vitro* cultivation was the application of excised roots which were grown on synthetic mineral medium supplemented with vitamins and a carbon source. Mosse and Hepper (1975) used such root-organ cultures for first mycorrhization experiments with *Glomus mosseae* spores. Later Mugnier and Mosse (1987) established the *in vitro* mycorrhization of *Agrobacterium rhizogenes* transformed roots which are in comparison to non-transformed roots much easier to handle on synthetic medium for long-term cultivations. However, it was the pioneering work of Bécard and Fortin (1988) that resulted in the first *in vitro* sporulation of an AM fungus demonstrating that AM fungi are able to fulfil their whole life cycle in this artificial system.

For this work, the AM fungus *G. intraradices* (Schenk and Smith, 1982) was cultivated with *A. rhizogenes* transformed carrot roots according Bécard and Fortin (1988) on modified M medium (Tab. 2.6). For continuous cultures mycorrhized roots were transferred to fresh M medium and cultivated at 27 °C allowing continued proliferation of the pre-existing root fungal association.

G. intraradices was also cultivated in a dual compartment system introduced by St. Arnaud et al. (1996) (Fig. 2.1) in which a 90 cm in diameter petri dish is subdivided by a plastic bridge into two compartments called the 'root compartment' and the 'fungal compartment'. In the 'root compartment' hairy roots of *Daucus carota* colonised by *G. intraradices* are cultivated on M medium supplemented with sucrose. From this site only the fungal hyphae are able to cross the border and to proliferate in the 'fungal compartment' on M medium without sucrose. The main advantages of this system are the physical separation of hyphae and mycorrhized roots, which facilitates the isolation of hyphae and spores in large quantities, a non-destructive monitoring of all symbiotic stages otherwise hidden by soil, and the sterile growth condition which is mandatory for physiological, molecular and biochemical studies.

Fungal hyphae were also cultivated in liquid medium. For that, the solid medium of the 'fungal compartment' was replaced with 8 ml of 2X M medium without sucrose.

Solution	Final Conc. (mg/l)	Stock Conc. (g/l)
Macroelements		
KNO ₃	80	3.2
MgSO ₄ × 7H ₂ O	731	29.24
KCl	65	2.6
Microelements		
MnCl ₂ × 4H ₂ O	6.0	6.0
H ₃ BO ₃	1.5	1.5
ZnSO ₄ × 7H ₂ O	2.65	2.65
Other Microelements		
Na ₂ MoO ₄ × 2H ₂ O	0.0024	0.02
CuSO ₄ × 5H ₂ O	0.13	1.3
KH ₂ PO ₄	4.8	48
Ca(NO ₃) ₂	288	115.2
NaFeEDTA	8	3.2
Vitamin solution		
Glycine	3	0.3
Myo-inositol	50	5
Nicotinic acid	0.5	50
Pyrodoxine HCl	0.1	10
Thiamine HCl	0.1	10
Sucrose	1 %	
Phytigel	3 %	
pH	5.5	

Table 2.6. M Medium composition after Bécard and Fortin (1988). All stock solutions were stored without autoclaving at 4 °C. The pH was adjusted to 5.5 and the media was solidified with 3 % phytigel.

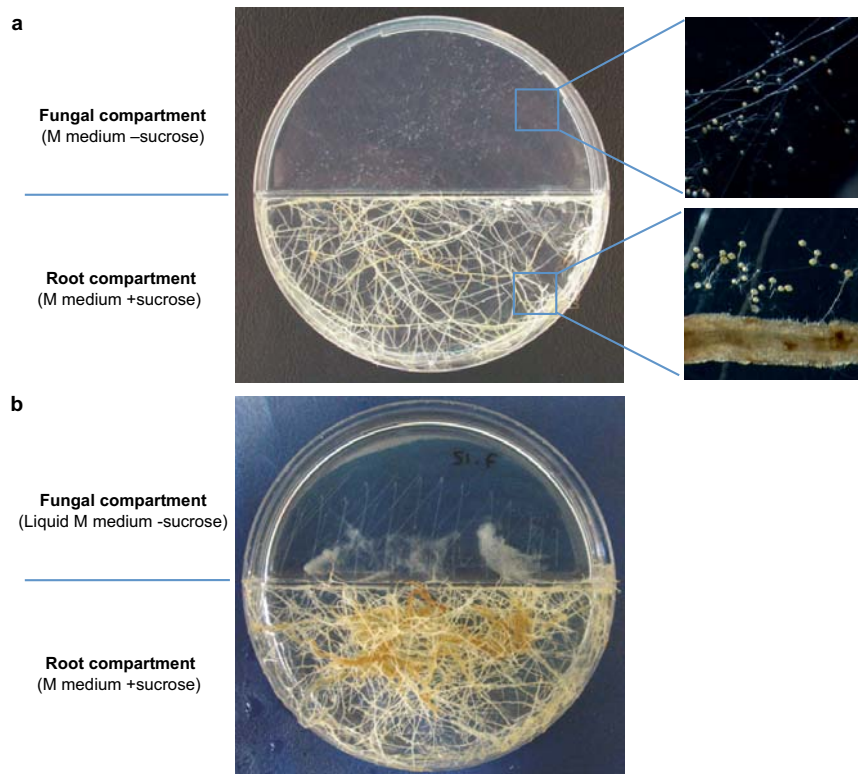


Figure 2.1. *In vitro* cultivation of *G. intraradices*. **a**, Cultivation of *G. intraradices* in a dual compartment system divided into a 'fungal compartment' (magnification showing hyphae and spores of *G. intraradices* grown on M medium without sucrose) and a 'root compartment' (magnification showing a *D. carota* root colonised with *G. intraradices* on M medium with sucrose). **b**, Dual compartment system for *G. intraradices* cultivation showing fungal hyphae grown in liquid M medium.

To facilitate the growth of the hyphae, a small grid like a trellis for creeping plants, was scratched on the bottom of the plate with a sterile scalpel.

M medium for the 'root compartment'

M medium described in Tab. 2.6 with 1 % sucrose.

M medium for the 'fungal compartment'

M medium described in Tab. 2.6 without sucrose.

2X M medium for hyphal proliferation in liquid cultures

M medium described in Tab. 2.6 but with the double concentration of all solutions except phosphate and without sucrose.

2.1.7 Isolation of *G. intraradices* Spores

AM fungal spores undergo a period of dormancy, a germination arrest which is often influenced by exogenous factors like moisture, pH or temperature. Several authors observed, that a cold period is essential to brake dormancy and synchronise germination of AM fungal spores (Tommerup, 1983; Juge et al., 2002), thus cold stratification of spores has become a common laboratory practice.

Prior spore isolation, four weeks old dual compartment plates of *D. carota* and *G. intraradices* were stored for at least two weeks in a cold room at 4 °C. The 'fungal compartment' sides were cut out from the cold treated plates and the phytigel was dissolved by stirring in an excess of citric acid buffer. The spores were finally collected using a sieve system with decreasing mesh width of 1 mm, 125 µm and 40 µm. Spores were surface sterilised overnight with antibiotics (100 $\frac{\mu\text{g}}{\text{ml}}$ gentamycin, 200 $\frac{\mu\text{g}}{\text{ml}}$ streptomycin) and further treated with a 2% (w/v) chloramin T solution (Carl Roth, Germany) for 15 min. Collected spores were placed directly on water agar (MES) plates onto 5 cm×5 cm sterile cellophane sheets. The spores were germinated at 27 °C for three days.

Citric acid buffer

- 1.7% (v/v) 0.1 M citric acid
- 8.3% (v/v) trisodium citrate
- pH 6.6

Water agar (MES)

- 1.9 g 10 mM 2-(N-morpholino)ethanesulfonic acid (MES)
- 8.8 ml 1 M NaOH
- 11.2 ml 1 M NaCl
- 0.8% Agar-Agar
- pH 5.5

2.2 Experimental Design

2.2.1 *In vitro* Mycorrhization Assay of Hairy Roots

Unlike in the rhizobial symbiosis are signals from the plant shoot not obligatory for the establishment of a functional AM symbiosis. Hence, hairy roots can be used as well as host for AM fungi with the advantage, that they can be genetically manipulated by *A. rhizogenes* to express or depress genes involved in the mycorrhization process. Further, the fungal colonisation of the roots can be performed under sterile conditions in the *in vitro* system (Chap. 2.1.6).

For mycorrhization experiments with hairy roots, the solidified medium on the 'fungal compartment' site from three weeks old plates was cut out with a sterile scalpel and replaced by new solid M medium with sucrose but with the half concentration of phosphate (17.5 µM KH₂PO₄). This reduction of phosphate should imitate phosphate limited conditions in the system, thereby stimulating the colonisation of the hairy roots by the fungus. The medium was poured diagonally to the compartment border like a gently sloping ramp to the other side to facilitate and to accelerate the passage of the new developing fungal hyphae (Fig. 2.2 c). A cellophane sheet was placed on top of the new medium on which the hyphae were allow to proliferate for

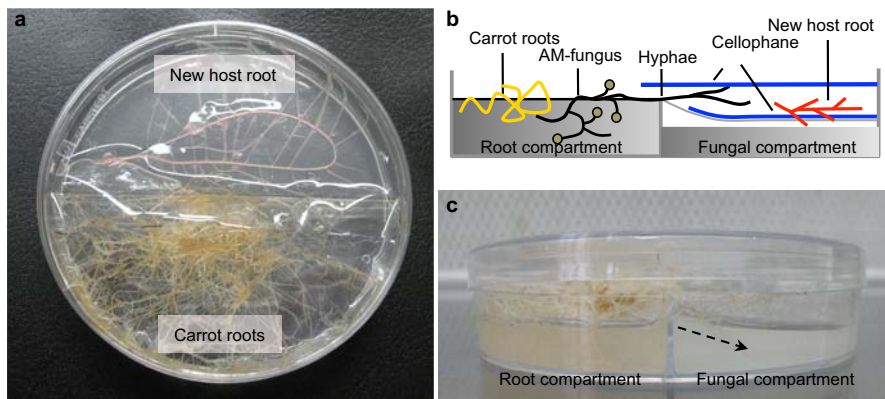


Figure 2.2. *In vitro* mycorrhization assay. **a**, Transgenic host root mycorrhized in the dual compartment *in vitro* system. **b**, Schema of a plate used for the mycorrhization assay. The new host root is placed between two cellophane sheets to increase contact sites with the fungal hyphae. **c**, Lateral view of a plate prepared for the mycorrhization assay. The medium in the 'fungal compartment' is poured diagonally to the compartment boarder (indicated by the dashed arrow).

three to five days in order to synchronise the following colonisation of a new host root. Hairy roots of tomato, potato or *Medicago* were placed into the 'fungal compartment' on the cellophane proximal to the hyphae. Roots and hyphae were covered with a second cellophane sheet to increase contact sides and to reduce contaminations (Fig. 2.2b). For time course experiments with potato, colonised roots were collected after 3, 11, 14 or 32 days. In general full mycorrhized roots were harvested after 14 to 21 days co-incubation of roots and fungal hyphae at 27 °C in dark.

2.2.2 *In vitro* Mycorrhization of *Medicago* Plants

Additionally whole *M. truncatula* plants were mycorrhized for a time course experiment in the dual compartment system but in liquid medium as described by Kuhn et al. (2010). In this case, the medium in the 'fungal compartment' side was replaced with liquid 2X M medium without sucrose and the plates were incubated 10 days at 27 °C for the development of extraradical hyphae (Chap. 2.1.6). Then three to five days old seedlings were planted into openings in the plate lid of the 'fungal compartment' side. The plants were incubated for 1, 12, 25 days in liquid medium together with the hyphae at 25 °C and with a photoperiod of 16 h of light.

2.2.3 Phosphate Treatment of Mycorrhized Roots

Hairy roots of potato (*S.tuberosum-pStPT3-FT-GUS*) were mycorrhized as described in Chap. 2.2.1 on M medium with sucrose and the half concentration of phosphate (17.5 μM KH_2PO_4). The plates were observed under the fluorescence stereo-microscope for arbuscule formation which could be seen as green fluorescence of colonised cells

because of the mycorrhiza-specific expression of the fluorescence timer gene (FT) (for detailed description of the pStPT3-FT-GUS hairy root line see Chap. 2.8). After one week, plates with an approximately equal colonisation status (estimated by the amount of fluorescent arbuscules) were cultured for an additional week with medium with a 200 fold increased phosphate concentration. Therefore, the mycorrhized potato roots were covered with 8 ml M medium containing sucrose and 3.5 mM KH_2PO_4 (200X). As control, the roots were covered with the same medium but with 17.5 μM KH_2PO_4 (0.5X). The roots were harvested after one week incubation at 27 °C in the dark.

2.2.4 Root Exudate Synthesis

Root exudates were isolated following the protocol of Bücking et al. (2008) with some modifications. Potato hairy roots (*S.tuberosum-pStPT3-FT-GUS*) were grown on solid M medium for three weeks. Then the roots were incubated in 50 ml liquid 2X M medium with sucrose in the dark by gentle shaking. After one week the medium containing the roots and root exudates was harvested. The root exudate solution was stored at -20 °C.

2.2.5 Treatments of Extraradical Mycelium in Liquid Cultures

To analyse the expression of fungal sugar transporters in the extraradical mycelium, plates were prepared as described in Chap. 2.1.6. After 10 days of hyphal growth the medium was replaced with 2X M medium supplemented with different sugars or sugar derivatives used in an end concentration of 2%. The hyphae were harvested after 5 days exposure to the sugars at 27 °C in dark. As control, ERM was cultivated in 2X M medium without sugar.

Extraradical mycelium was also co-incubated with hairy roots of the tomato cultivar *Rio Grande* or the *rmc* tomato mutant in liquid medium. Therefore, liquid 2X M medium with sucrose was added to the empty fungal side together with some hairy roots. Both, roots and the ERM were allowed to proliferate for 2 weeks at 27 °C in the dark before harvesting. In parallel, ERM was cultivated under the same conditions but without roots as control.

For the treatment with root exudates (Chap. 2.2.4), the medium of one week old ERM liquid cultures was replaced with 8 ml fresh medium (3 ml dH_2O and 5 ml 2X M medium without sucrose) or with 8 ml medium supplemented with root exudates (3 ml root exudate solution and 5 ml 2X M medium without sucrose). The hyphae were incubated for one week at 27 °C in dark before harvest.

2.3 Transformation Systems

2.3.1 Plasmids

Tabs. 2.7 and 2.8 list all plasmids used for this work.

Plasmid	Description	Reference
Bacterial Cloning Vectors		
pCR2.1-Topo	Cloning vector for Taq amplified PCR products; <i>LacZα</i> fragment, M13 reverse and forward priming site, multiple cloning site, T7 promoter, <i>fi</i> and pUC origin, Amp ^r , Km ^r	Invitrogen (USA)
pCRII-Topo	Dual promoter cloning vector for Taq amplified PCR products; <i>LacZα</i> fragment, M13 reverse and forward priming site, multiple cloning site, T7 promoter, Sp6 promoter, <i>fi</i> and pUC origin, Amp ^r , Km ^r	Invitrogen (USA)
pENTR/D-Topo	Vector for directional cloning of blunt end-PCR products in the Gateway system; attL1, attL2, M13 reverse and forward priming site, T7 promoter, pUC origin, Km ^r	Invitrogen (USA)
pCR2.1-GiMST1-NotI	Full CDS of <i>GiMST1</i> in pCR2.1-Topo with NotI restriction sites on 5' and 3' end Amp ^r , Km ^r	This work
pCR2.1-GiMST1-NcoI	Full CDS of <i>GiMST1</i> in pCR2.1-Topo with NcoI restriction sites on 5' and 3' end Amp ^r , Km ^r	This work
pCR2.1-DsRed-StuA	DsRed-StuA in pCR2.1-Topo	<i>Helber and Requena, 2008</i>
pCR2.1-pyr4	<i>pyr4</i> gene from <i>Neurospora crassa</i> in pCR2.1-Topo	AG Fischer (KIT, Germany)
pCRII-pMST1	1.7 kb of the putative promoter sequence of <i>GiMST1</i> in pCRII-Topo	This work
pCRII-GiMST1-148bp	148 bp CDS of <i>GiMST1</i> in pCRII-Topo (reverse orientation); Amp ^r , Km ^r	This work
pEntry-pHEX6	1.9 kb of the promoter region from <i>StHEX6</i> in pENTR/D-Topo; Km ^r	This work
pEntry-pST1	2.3 kb of the promoter region from <i>MtST1</i> in pENTR/D-Topo; Km ^r	This work
Plant Binary Vectors		
pPGFPGUS-RedRoot	Binary destination vector for Gateway cloning; LB and RB, attR1 and attR2, RedRoot cassette, <i>CmR-ccdB</i> , <i>gfp</i> , <i>gus</i> , Sm ^r , Sp ^r , Kan ^r	<i>Kuhn et al., 2010</i>
pHT6-GFP-GUS-RR	Binary vector pPGFPGUS-RedRoot with promoter sequence of <i>StHT6</i>	This work
pST1-GFP-GUS-RR	Binary vector pPGFPGUS-RedRoot with promoter sequence of <i>MtST1</i>	This work
pMtPT4-GFP-GUS-RR	Binary vector pPGFPGUS-RedRoot with promoter sequence of <i>MtPT4</i>	Provided by H. Kuhn (KIT, Germany)

Table 2.7. List of bacterial and plant binary vectors used for this thesis.

Plasmid	Description	Reference
Yeast Expression Vectors		
pDR196	High-level yeast expression vector containing the <i>S. cerevisiae</i> ATPase promoter (P_{MA1}) separated from the <i>ADH1</i> terminator (T_{ADH1}) by a multiple cloning site; Amp ^r , URA3, 2 μ origin	<i>Rentsch et al., 1995</i>
pGADT7-rec	For construction of Matchmaker libraries; P_{ADH1} and T_{ADH1} from <i>S. cerevisiae</i> , SMARTIII and CDSIII primer sequence, 5' and 3' PCR primer sequence, T7 promoter, HA tag, GAL4 AD polypeptide with SV40 NLS, <i>LEU2</i> , Amp ^r , pUC and 2 μ origin	Clontech (USA)
pNH196	Derivative of pDR196 with SMARTIII/CDSIII and 5' / 3' PCR sequences for homologue recombination of SMART cDNA libraries	This work
pNEV-N	High-level yeast expression vector containing the <i>S. cerevisiae</i> ATPase promoter (P_{MA1}) separated from the terminator (T_{MA1}) by a NotI restriction site; Amp ^r , URA3, 2 μ origin	<i>Sauer and Stolz, 1994</i>
pEXTAG-GFP	For gene localisation in yeast; URA3, Amp ^r , P_{MA1} promoter and <i>gfp</i> reporter gene	<i>Aluri and Büttner, 2007</i>
pDR196-HXT1	CDS of <i>HXT1</i> <i>S. cerevisiae</i> in pDR196	Doctorial Thesis A. Ocón
pNEVN-MST1	pNEVN with full CDS of <i>GiMST1</i> in NotI site	This work
pNH196-StHT2	CDS of <i>StHEX6</i> ligated via homologue recombination in pNH196	This work
pNH196-StHT6	CDS of <i>StHT2</i> ligated via homologue recombination in pNH196	This work
pEXTAG-MST1	CDS of <i>GiMST1</i> (without stop codon) in pEXTAG-GFP	This work
<i>Aspergillus</i> Vectors		
PpMST1-DsRed-StuA	Promoter of <i>GiMST1</i> fused to DsRed-StuA in pCRII-Topo	This work

Table 2.8. List of yeast expression and *Aspergillus* vectors used for this thesis.

2.3.2 Transformation of Bacteria

Plasmid-DNA was introduced either into commercially available chemically competent *E. coli* cells from Invitrogen (USA) following the provided manual or into competent cells treated with CaCl_2 prepared after the protocol of Ausubel et al. (1999). Alternatively, plasmid-DNA was introduced into electrocompetent *E. coli* cells prepared after Ausubel et al. (1999), using the Gene-Pulser II system from BioRad Laboratories (USA) and 2 mm cuvettes (Peqlab Biotechnology, Germany). Prior electroporation, salt was removed from the plasmid solution by the drop dialysis method (Silhavy et al., 1984) using 0.025 μm Millipore membrane filters.

A. rhizogenes electrocompetent cells were produced and transformed after Mersereau et al. (1990).

Transformed cells were selected on the appropriate medium and cultivated as described in Chap. 2.1.2.

2.3.3 Transformation of Yeast

Plasmid-DNA was introduced in yeast following the transformation protocol of Gietz and Woods (2001). Transformed yeast cells were selected according their auxotrophy markers and cultivated as described in Chap. 2.1.3. cDNA libraries were transformed as described in Chap. 2.9.5.

2.3.4 Transformation of *Aspergillus nidulans*

For studying the promoter of GiMST1 the *Aspergillus* expression vector PpMST1-DsRed-StuA was constructed. First, the 1.7 kb GiMST1 promoter sequence was amplified using the primers pMST1_F1 and pMST_R1 and cloned in the pCRII-Topo vector. The received plasmid was called pCRII-pMST1. The DsRed-StuA cassette was released from the pCR2.1-DsRed-StuA vector (Helber and Requena, 2008) by BamHI restriction-digestion and ligated in the respective sites of the BamHI linearised pCRII-pMST1 vector. In the received plasmid, the auxotrophic marker gene *pyr4* of *Neurospora crassa* released by NotI restriction digestion from the pCRII-pyr4 vector, was cloned in the NotI sites before the pMST1-DsRed-StuA fusion gene. The generated plasmid was named PpMST1-DsRed-StuA.

The PpMST1-DsRed-StuA vector was introduced in the *A. nidulans* GR5 strain by PEG/ CaCl_2 -mediated transformation as described by Yelton et al. (1984). The transformants were selected on KCl medium agar plates without pyridoxin but with uracil and uridine. Positive clones were grown overnight at room temperature in liquid minimal medium without pyridoxine either with 2 % xylose or 2 % glycerol as carbon source for microscopy.

KCl Medium for Protoplast Regeneration

Minimal medium for *Aspergillus* cultivation as described in Chap. 2.1.4 but with 0.6 M KCl, 1.5 % Agar-Agar and without pyridoxine.

2.3.5 Generation of Hairy Roots from *S. lycopersicum* and *M. truncatula*

For the generation of hairy roots, seeds of *S. lycopersicum* and *M. truncatula* were surface sterilised and germinated on water agar plates (4 g Agar-Agar in 500 ml dH₂O).

Tomato seeds were surface sterilised by incubation for 1 min in 70 % EtOH and 10 min in 5 % (w/v) calcium hypochloride solution (Carl Roth, Germany). The seeds were washed several times with sterile dH₂O and placed on water agar plates. After a cold treatment of 2 days, the seeds were germinated for at least 5 days at 27 °C.

M. truncatula seeds were treated for 10 min with sulfuric acid (Carl Rot), washed several times with sterile dH₂O and stored over night on water agar plates at 4 °C. The seeds were germinated over night at 27 °C.

The seedlings of *S. lycopersicum* and *M. truncatula* were transformed with the *A. rhizogenes* strain *ARqua1* (Quandt et al., 1993) carrying different binary vectors (see Tab. 2.1) according the protocol of Boisson-Dernier et al. (2001). All binary vectors used for plant transformation contain in the T-DNA region a kanamycin resistance gene and a constitutive expressed DsRed gene named RedRoot cassette for selection of transgenic roots. Hairy roots emerging from the root section were checked under the fluorescence binocular for DsRED expression. Red fluorescent transgenic roots were explanted on 1X M medium with sucrose supplemented with 25 $\frac{\mu\text{g}}{\text{ml}}$ kanamycin for root selection and 400 $\frac{\mu\text{g}}{\text{ml}}$ augmentin to eliminate *A. rhizogenes* contaminations. In weekly steps, the roots were propagated on new M medium with decreasing concentrations of augmentin (300, 200, 100, 0 $\frac{\mu\text{g}}{\text{ml}}$).

2.4 Preparation and Analysis of DNA

2.4.1 Preparation of Genomic DNA

Genomic DNA from plant and fungal tissue was isolated after homogenisation in liquid nitrogen with the DNeasy Plant Mini Kit (Quiagen, Germany).

2.4.2 Preparation of Plasmid DNA from *E. coli*

Plasmid DNA was prepared from *E. coli* in two different scales depending on the required amount and purity of the DNA. Mini preparations were isolated from 3 ml *E. coli* cultures with the alkaline lysis protocol described by Sambrook et al. (1989). When high quality and quantities of plasmid DNA were required, the NucleoBond PC 100 plasmid DNA purification kit (Macherey-Nagel, Germany) for midi preparations was used following the manual instructions.

The plasmid DNA concentration and the purity was determined by measuring spectrophotometrically the absorption at 260 and 280 nm with the NanoDrop device (Thermo Fisher Scientific, USA).

2.4.3 Agarose Gel Electrophoresis

To assess the quality of DNA preparations or to visualise DNA fragmentation after restriction endonuclease treatment, DNA samples were separated on agarose gels with the Mupid-ex U electrophoresis system (Eurogentec, Belgium). Depending on the DNA fragment size, agarose gels of 0.8 to 2.5% (w/v) agarose (Peqlab Biotechnology, Germany) in 0.5X TAE buffer were prepared. The DNA probes were mixed before loading with 6X loading buffer (30% glycerol, 0.25% bromophenol blue). As standard, the 2log marker from New England Biolabs (UK) was loaded in parallel.

The gel was afterwards stained in 0.5X TAE buffer with $0.5 \frac{\mu\text{g}}{\text{ml}}$ ethidium bromide (Carl Roth, Germany). To visualise the DNA bands, the gel was illuminated by UV light and photographed using a Quantum gel documentation station (Peqlab Biotechnology).

10X TAE buffer

- 48.4 g trisbase
- 11.42 ml glacial acetic acid
- 7.44 g $\text{Na}_2\text{EDTA} \times 2\text{H}_2\text{O}$
- add 1000 ml dH_2O
- pH 8.5

2.4.4 Isolation and Purification of DNA from Agarose Gels

Specific DNA fragments were excised with a scalpel from agarose gels under low-strength UV light to reduce UV damage. The DNA was then recovered from the gel following the freeze-squeeze procedure described by Thuring et al. (1975) or by using either the QIAquick® Gel Extraction Kit (QIAGEN, Germany) or the Zymoclean™ Gel DNA Recovery Kit (Zymo Research Corp., USA).

2.4.5 Concentration and Precipitation of DNA

DNA was concentrated by ethanol precipitation with $\frac{1}{10}$ volume of 3 M sodium acetate (pH 4.9) plus 2.5 volumes of absolute ethanol for 30 min at -80°C . After precipitation, the DNA was centrifuged for 30 min with 13,000 rpm at 4°C . The DNA pellet was washed with 70% ethanol, air-dried and finally dissolved in sterile ddH_2O .

2.4.6 Southern Blotting

All solutions for southern blotting and detection were prepared according to the DIG Application Manual for Filter Hybridization (Roche Diagnostics, Germany). The digoxigenin (DIG) labelled probes were generated by PCR with gene specific primers using the PCR DIG Probe Syntheses Kit from Roche Diagnostics following the provided protocol.

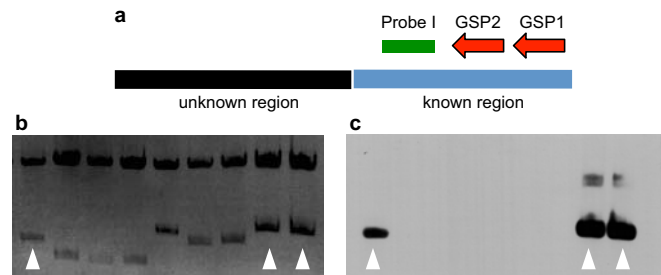


Figure 2.3. Isolation of the partial promoter sequence of StHT6. **a**, Location of the gene-specific primers GSP1, GSP2 and the DIG-labelled probe I in the known sequence downstream of the promoter. **b**, EcoRI digested pPCRII-Topo clones. **c**, Positive clones identified by binding of the sequence-specific probe I.

Southern Blotting was used as screening method for positive RACE PCR or GenomeWalker™ PCR clones (see also Chap. 2.7.6 and Chap. 2.7.7). First, the by RACE or genome walking amplified bands were transformed in the pCRII-Topo vector (Invitrogen, USA) and transformed in *E. coli*. Then the plasmids were recovered and cut with an appropriate restriction enzyme to release again the inserted DNA fragment. The DNA was separated by electrophoresis and transferred over night on a positively charged nylon membrane (GE Healthcare Life Sciences, UK) by capillary transfer as described in the DIG Application Manual for Filter Hybridization (Roche Diagnostics). After the transfer, the membrane was UV crosslinked to fix the DNA and prehybridised for at least 2 h with the DIG standard hybridisation buffer at 68 °C. Hybridisation was performed under high stringency conditions at 68 °C over night with a specific DIG-labelled DNA probe. The membrane was washed in several steps according the DIG Application Manual. The probe-DNA hybrids were detected by chemoluminescence using phosphatase-conjugated anti-DIG antibodies and CDP-Star as alkaline phosphatase substrate (both available from Roche Diagnostics). Positive clones were sequenced for the full nucleotide sequence information. Fig. 2.3 shows exemplary the identification of positive clones from the first GenomeWalker™ PCR for the isolation of the StHT6 promoter sequence.

2.4.7 Sequencing of Plasmid DNA

Plasmid DNA was sequenced by Eurofins MWG Operon (Germany).

2.5 Enzymatic Modification of DNA

2.5.1 Restriction Endonuclease Digestion of DNA

In general, 1 µg DNA was restriction digested with 1 unit of the restriction endonuclease in a reaction volume of 10 to 25 µl for 1 h at the required temperature. If necessary, the restriction endonuclease was heat-inactivated for 20 min at 68 °C. Restriction endonucleases were used from New England Biolabs (UK) or Fermentas (Canada).

2.5.2 Ligation of DNA

For ligation of an insert DNA fragment in a plasmid, the T4 ligase from New England Biolabs (UK) was used. When the plasmid was linearised with one restriction endonuclease producing cohesive ends, the DNA was treated right after restriction digestion with SAP (shrimp alkaline phosphatase; Fermentas, Canada) for 30 min at 37 °C in order to remove 5' phosphates and to prevent self-ligation. The linearised plasmid and insert DNA were purified by gel electrophoresis and recovered from the gel using the QIAquick® Gel Extraction Kit (Chap. 2.4.4). Following the recommendation of New England Biolabs, a plasmid:insert ratio of approximately 1:3 was used. The ligation products were introduced in *E. coli* and positive clones are selected on plate with the appropriate antibiotics.

In order to produce blunt-ends for ligation, the plasmid and/or insert DNA were treated for fill-in-reactions with 0.5 µl exo-Klenow fragment (Fermentas, Canada) in addition with 0.5 µl dNTPs (25 mM) for 15 min at 37 °C. The reaction was stopped by heating for 10 min at 72 °C and the ligation protocol was followed as described above.

2.6 Preparation and Analysis of RNA

2.6.1 Preparation of Total RNA

Total RNA was isolated from freshly harvested or RNAlater (Ambion, USA) preserved fungal or plant tissues with the TRIzol reagent (Invitrogen, USA) which based on the guanidine isothiocyanate method (Chomczynski and Sacchi, 1987).

Prior RNA preparation, Millipore water was stirred overnight with 0.1 % (v/v) of diethyl dicarbonate (DEPC) (Invitrogen, USA) to inactivate RNase enzymes. The DEPC water was autoclaved before use for 20 min to destroy DEPC traces which might interfere with downstream reactions. Mortars, pestles and spatulas were soaked 30 min with RNAase away solution (1 M NaOH, 2 mM EDTA in DEPC-treated water) to avoid RNase activity and then rinsed thoroughly with DEPC-treated water. RNase-free reaction tubes were prepared by autoclaving them two times for 20 min. Gloves and filter tips were always used while working with RNA.

AM fungal spores and roots were ground in liquid nitrogen and the fine powder was transferred with a spatula in 1 ml TRIzol. AM fungal hyphae were directly ground in 1 ml TRIzol. RNA from yeast cells was isolated from 10 ml overnight cultures with an OD₆₀₀ of 0.6 (approximately 6×10^6 cells). The cells were harvested by centrifugation for 3 min. The pellet was resuspended in 100 µl TRIzol and disrupted using Lysis Tubes S from Analytik Jena (Germany) in a speed mill for 5 min. Then, TRIzol was added to an end volume of 1 ml.

The homogenised samples were first shaken by vortexing for 15 s and then incubated for 5 min at room temperature. Remaining cell debris were removed from the homogenate by additional centrifugation for 10 min at 13,000 rpm and 4 °C. 200 µl chloroform was added to the samples, shaken vigorously for 15 sec and rested at room temperature for 3 min followed by a 10 min centrifugation step at 13,000 rpm

and 4 °C. The upper RNA containing aqueous phase was recovered and mixed with 500 µl isopropyl alcohol for RNA precipitation. The sample was incubated at room temperature for 10 min and centrifuged for 15 min at 13,000 rpm and 4 °C. Precipitated RNA was washed with 70 % EtOH (diluted in DEPC-treated water) by centrifugation for 5 min at 9,000 rpm. The pellet was air-dried, resolved in 30 µl of DEPC-treated water containing 1 % (v/v) RNase Out (Invitrogen, USA) at 80 °C for 2 min and finally stored at –80 °C.

Quantity and integrity of the isolated RNA was assessed using the NanoDrop spectrophotometer (Thermo Fisher Scientific, USA) measuring the absorption at 260 nm and 280 nm, by running a denaturing agarose gel, or by northern blotting (see following chapters).

2.6.2 Denaturing Agarose Gel Electrophoresis of RNA

The quality of total RNA was assessed by denaturing agarose gel electrophoresis and ethidium bromide staining. As mentioned in the section before, all plastic and glass ware was treated prior with RNase away solution for 30 min or autoclaved twice to inhibit RNase activity.

1 g agarose was dissolved by heating in 72 ml DEPC-treated water. When cooled to 60 °C, 10 ml 10X MOPS buffer and 18 ml 37 % (v/v) formaldehyde was added. The gel was poured in a gel tank and allowed to set. 5 µl of the RNA sample was mixed with an equal volume of 2X RNA loading dye (Fermentas, USA) and denatured for 10 min at 70 °C. The denatured RNA was loaded on the formaldehyde-agarose gel and separated in 1X MOPS buffer using the Mupid-ex U electrophoresis system (Eurogentec, Belgium).

For staining, the gel was first treated twice 20 min in 0.5 M ammonium acetate to remove the formaldehyde and then incubated in 0.5 M ammonium acetate containing 0.5 $\frac{\mu\text{g}}{\text{ml}}$ ethidium bromide for 30 min. To visualise the 28S and 18S ribosomal bands, the gel was first destaining in DEPC-treated water and then imaged with a Quantum gel documentation station (Peqlab Biotechnology, Germany).

10X MOPS buffer

- 200 mM 3-(N-morpholino)propanesulfonic acid (MOPS)
- 50 mM sodium acetate
- 10 mM EDTA
- dissolved in DEPC-treated water
- pH 7.0

2.6.3 DNase Digestion and cDNA Synthesis

Prior cDNA synthesis 1 µg of total RNA was treated with DNaseI, Amplification Grade (Invitrogen, USA) following the recommendations. Total digestion of genomic DNA was verified by PCR before cDNA synthesis. Therefore, 0.5 µl DNase digested RNA was used as template in a Taq PCR reaction (see Chap. 2.7.2) with primers for

the housekeeping genes used also in the quantitative real-time PCR (Chap. 2.13.1). When no positive band was visible the cDNA was finally generated according the Fermentas first-strand cDNA synthesis protocol using Oligo(dt)12-18 primers and the SuperScriptII™ Reverse transcriptase (both provided from Fermentas, Canada).

2.6.4 Northern Blotting and Dot Blot

Northern blotting was done after the DIG Application Manual for Filter Hybridization (Roche Diagnostics GmbH, Germany). For RNA detection a DIG labelled probe was used, which was constructed from a phage clone containing the complete 18S RNA gene, the ITS of the 5.8S RNA gene and a part of the 25S rRNA gene from *Glomus mossae* (Franken and Gianinazzi-Pearson, 1996). This probe was kindly provided by P. Franken (IGZ, Germany). The RNA was hybridised under non-stringency conditions and RNA-probe hybrids were visualised following the manual by chemoluminescent detection (see also Chap. 2.4.6). The DIG labelling of non-radioactive RNA probes for *in situ* hybridisation was tested in a Dot blot according the DIG Application Manual for Filter Hybridization (Roche Diagnostics, Germany). For RNA blotting all solutions were prepared with DEPC water. Plastic and glass ware were treated with RNase away solution (Chap. 2.6.1) for 20 min to eliminate RNase contaminations and rinsed several times with DEPC water.

2.7 Polymerase Chain Reaction (PCR)

2.7.1 Oligonucleotides

Tab. A.2, A.1, A.3 and A.2 contain all oligonucleotides used for this work subdivided in standard PCR primers, RACE and GenomeWalker™ PCR and quantitative real-time PCR primers. All oligonucleotides were synthesised by Eurofins MWG Operon (Germany).

2.7.2 Standard PCR

Standard PCR reactions were performed with Taq-DNA Polymerase from *Thermus aquaticus* and the following protocol in 0.5 ml reaction tubes.

For all PCR reactions the Tpersonal thermo cycler from Biometra (Germany) was used. Tab. 2.9 shows exemplary a standard PCR program for Taq-amplification of ≥ 1 kb PCR product. The primer annealing temperature (T_m or melting temperature) was set according the calculations of Eurofins MWG Operon (Germany). For PCR reactions with unspecific overhangs, the first four cycles were performed at a lower annealing temperature to ensure primer binding. In following steps the T_m was again risen to the recommended temperature.

Standard PCR setup for Taq DNA Polymerase

- 16 μ l sterile Water

Temp.	98°C	98°C	X°C	72°C	72°C
Time	3 min	30 sec	30 sec	30 sec	10 min
Cycles	1	30			1

Table 2.9. Cycling parameters for standard PCR reactions for Taq polymerase amplification of 1 kb PCR products. The annealing temperature of the primer pairs is variable.

- 2.5 µl 10X PCR Buffer (without MgCl₂)
- 2.0 µl dNTP Solution (25 mM)
- 1.0 µl MgCl₂ (50 mM)
- 1.0 µl forward Primer (F) (10 µM)
- 1.0 µl reverse Primer (R) (10 µM)
- 0.5 µl Taq DNA Polymerase
- 1 µl DNA Template

Proof-reading polymerases like the Phusion High-Fidelity DNA Polymerase (Finnzymes OY, Finland) and Pfu Polymerase (Fermentas, Canada) were used after the distributors protocol for the amplification of products used for further cloning reactions (Chap. 2.7.3).

2.7.3 Cloning of PCR Fragments

PCR products were cloned either using the TOPO T/A Cloning® Kit for PCR products with TA overhangs or the TOPO ENTR Cloning® system for blunt end PCR products (Invitrogen, USA).

TA overhangs of blunt-end PCR products used for TOPO T/A Cloning® were generated by additional incubation for 10 min at 72 °C with 0.5 µl Taq Polymerase. The PCR products were separated and purified via gel electrophoresis. The appropriate bands were recovered by 'freeze squeeze' or by the gel purification system from Zymoclean (Chap 2.4.4).

The TOPO ENTR Cloning® system was used for further sub-cloning of PCR amplified sequences (next chapter). For ENTR cloning, PCR products with 3'-CACC overhang were produced which were site-directed cloned over the complementary 3'-GTGG overhangs of the pENTR/D-Topo vector.

Against the provided protocol, TOPO reactions were set up in 6 µl end volume with 0.5 µl TOPO T/A Cloning® or TOPO ENTR Cloning® vector, 1 µl salt solution and 4.5 µl purified PCR product. The reaction was incubated for 20–30 min at 25 °C, stored afterwards at –20 °C or directly introduced in *E. coli*. Positive clones were selected on LB agar plates with the appropriate antibiotics. For TOPO T/A clones, LB/X-gal/ITPG plates with ampicillin or kanamycin were used for 'blue-white' screening.

2.7.4 Gateway Cloning

The Gateway cloning system is a commercialised technology invented by Invitrogen (USA). This system is based on the phage λ-based site-specific recombination instead

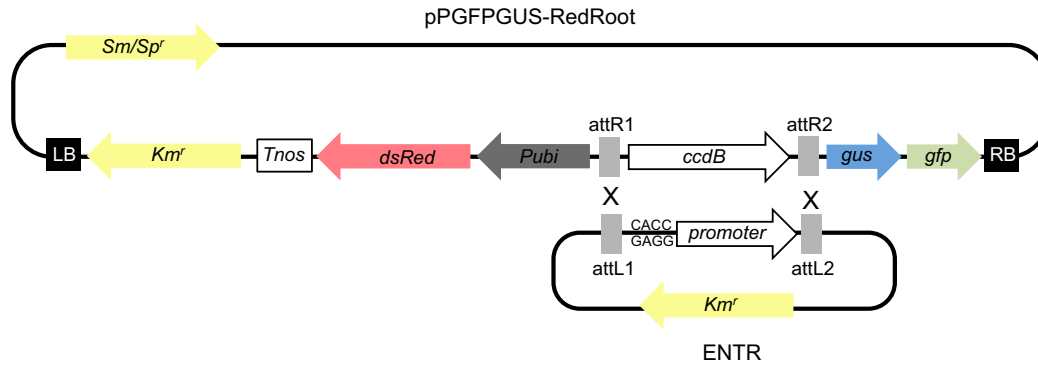


Figure 2.4. Homologous recombination of a promoter sequence into the pPGFPPGUS-RR binary vector (Kuhn et al., 2010) via Gateway cloning. LB: left border sequence; RB: right boarder sequence; Km^r: kanamycin resistance; Tnos: nopalyn synthase terminator; Pubi: ubiquitin promoter; gus: β glucuronidase gene; gfp: green fluorescence protein; Sm/Sp^r: streptomycin/spectinomycin resistance.

of restriction endonucleases digestion and ligation.

For Gateway cloning, the sequence of interest was first cloned in the pENTR/D-Topo vector where it is flanked by 'att'-recombination sites (Fig. 2.4). From the resulting pENTR/D-Topo clone the sequence was subcloned in a destination vector by homologous recombination on the att-sites which is presented on both vectors. This reaction is mediated by the Gateway LR Clonase II Enzyme Mix (Invitrogen). The recombination reaction was set up according the protocol provided from Invitrogen.

Positive clones were selected on LB medium with the appropriate antibiotics. Additionally, the growth of clones containing the empty destination vector is prevented due to the *ccdB* gene which is located between the att-sites and encodes for a bacterial gyrase inhibitor. For this work the destination vector pPGFPPGUS-RR (Kuhn et al., 2010) for plant transformation via *Agrobacterium* was used. This vector is optimised for promoter studies in plants. Promoter sequences can be shuttled by homologous recombination over the att-sites before a GFP-GUS reporter cassette. Transgenic roots can be selected on kanamycin containing medium or under green fluorescence light due to the DsRED reporter which is under control of the constitutive active Ubiquitin promoter (Pubi). In bacteria, pPGFPPGUS-RR can be selected via the streptomycin/spectinomycin resistance (Sm/Sp^r).

2.7.5 Colony PCR for the Selection of *Agrobacterium* Transformants

To select positive *Agrobacterium rhizogenes* clones after transformation, single colonies were heat treated for 10 min at 95 °C for cell break-down. 2 μ l of the cell suspension was used as template in a standard PCR reaction (Chap. 2.7.2) with primers amplifying a distinct region of the transformed plasmid. Clones with a positive amplification were used for the generation of hairy roots (Chap. 2.3.5).

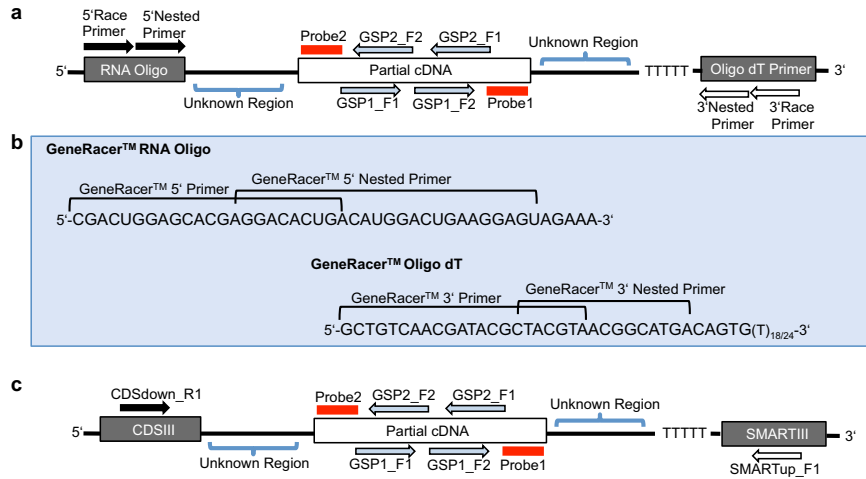


Figure 2.5. First strand cDNAs with primer binding sites and Digoxigenin labelled probe binding sites for RACE PCR of unknown 3' and 5' cDNA ends. **a**, cDNA created with the GeneRacer™ Kit (Invitrogen) and **c**, cDNA created with SMART cDNA library Kit (Clontech). **b**, Location of GeneRacer™ oligos in the GeneRacer™ RNA and Oligo dT sequence. GSP: gene specific primer.

2.7.6 Rapid Amplification of cDNA Ends (RACE)

Full-length 3' and 5' cDNA ends of partial cDNA sequences were obtained using the GeneRacer™ Kit from Invitrogen (USA). Following the instructions of the provider, 1 µg of total RNA was dephosphorylated in a first step with the calf intestinal phosphatase (CIP) to eliminate truncated RNA and non-mRNA molecules. In a second step the 5' cap structure of full length mRNAs was removed with the tobacco acid pyrophosphatase (TAP) and replaced using the T4 RNA ligase with the GeneRacer™ RNA oligo that serves as binding site for the GeneRacer™ 5' Primer and the GeneRacer™ 5' Nested Primer. Differing from the protocol, the SuperScript II Reverse Transcriptase (Invitrogen) was used in combination with the GeneRacer™ Oligo dT Primer to create a first-strand cDNA with known priming sites at both cDNA ends (Fig. 2.5).

5' RACE PCR was performed with the GeneRacer™ 5' Primer and a reverse oriented gene-specific primer in the known cDNA region in a Touchdown PCR using the Platinum Taq Polymerase (Invitrogen) in order to increase specificity and reduce background amplification (Tab. 2.10). Correspondingly, 3' ends were amplified using the GeneRacer™ 3' Primer and a forward oriented gene-specific primer. This primary PCR served then as template for a nested PCR after the standard PCR protocol (Chap. 2.7.2) with the GeneRacer™ 5' Nested Primer and a second reverse gene-specific primer or the GeneRacer™ 3' Nested Primer in combination with a second forward gene-specific primer.

Touchdown PCR setup

- 16 µl sterile Water
- 2.5 µl 10X High Fidelity PCR buffer)

Temp.	94°C	94°C	72°C	94°C	70°C	94°C	60-65°C*	68°C	68°C
Time	2 min	30 sec	1 min/ 1kb DNA	30 sec	1 min/ 1kb DNA	30 sec	30 sec	1 min/ 1 kb DNA	10 min
Cycles	1	5		5		25			1

Table 2.10. Cycling parameters for Touchdown PCR. PCR starts with a high annealing temperature to accumulate specifically gene-specific cDNAs. Successive decrease of the annealing temperature to the T_m of the used GSP1 primer (*) should increase PCR efficiency. 1 min extension was used per 1 kb DNA.

Temp.	95°C	95°C	68°C	68°C	70°C
Time	1 min	30 sec	1-3 min*	1 min	10 min
Cycles	1		25-35	1	1

Table 2.11. Cycling parameters for Advantage 2 PCR. Depending on target size the extension was performed for 1 (< 1 kb) to 3 min (1–5 kb) (*). An additional 10 min extension at 70 °C was added to increase TOPO T/A Cloning® efficiency.

- 2.0 µl dNTP Solution (25 mM)
- 1.0 µl MgCl₂ (50 mM)
- 1.5 µl GeneRacer™ 3'Primer/GeneRacer™ 5'Primer (10 µM)
- 0.5 µl gene-specific primer 1 (GSP1) (10 µM)
- 0.5 µl Platinum Taq DNA Polymerase (5 u/µl) (Invitrogen)
- 0.5 µl first strand cDNA

In analogy to the GeneRacer™ Kit, 3' and 5' cDNA ends were isolated using SMART amplified cDNA libraries (Chap. 2.9.1). As SMART generated cDNAs are also flanked by known priming sites (CDSIII at the 5' and SMARTIII at the 3' end), full length cDNA sequences can be provided in a similar way. In a primary PCR, unknown 5' end sequences were amplified with the CDSdownR1 primer binding in the CDSIII priming site and a forward gene-specific primer by using the Advantage 2 Polymerase Mix (Clontech, USA), 3' ends were amplified using the SMARTupF1 primer that binds in the SMART priming site and a gene-specific reverse primer, respectively.

RACE PCR setup for SMART amplified cDNAs

- 17 µl sterile Water
- 2.5 µl 10X Advantage 2 PCR buffer)
- 2.0 µl dNTP Solution (25 mM)
- 1.0 µl CDSdownR1/SMARTupF1 (10 µM)
- 0.5 µl gene-specific primer 1 (GSP1) (10 µM)
- 0.5 µl 50X Advantage 2 Polymerase mix (50X) (Clontech)
- 0.5 µl SMART cDNA

The RACE and SMART PCR products were separated by gel electrophoresis and single bands of the predicted sizes were cloned directly into the TOPO T/A Cloning® vector pCRII-Topo (Invitrogen). Positive clones were screened by southern blotting using a specific DIG labelled DNA probe complementary to the known region downstream of the second gene-specific primer and sequenced (see also Chap. 2.4.6).

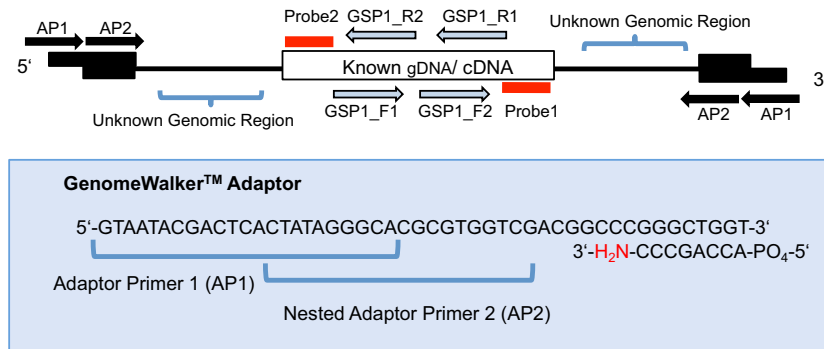


Figure 2.6. Example of an adaptor-ligated blunt end fragment for genome walking produced with the GenomeWalker™ kit from Clontech (USA) showing position of the adaptor-specific primer binding sites (AP1 and AP2) and the gene-specific primer binding sites (GSP1_F1 and the nested primer GSP1_F2 for downstream amplification of unknown regions; GSP1_R1 and the nested primer GSP1_R2 for upstream amplifications). DIG labelled DNA-probes for southern blot screening are shown in red. The design of the GenomeWalker™ Adaptor is shown more in detail (highlighted in blue). The amine group at the 3' end of the lower strand prevents the 3' extension by the polymerase.

2.7.7 Isolation of Unknown Genomic Sequences by Genome Walking

Genome walking is a method for the isolation of unknown genomic regions upstream or downstream of known genomic or cDNA sequences. In order to isolate putative promoter sequences, the GenomeWalker™ Universal Kit from Clontech Laboratories (USA) was used. According the manual, isolated genomic DNA was digested with four restriction enzymes (DraI, EcoRV, PvuII and StuI) to produce blunt-end fragments that were ligated at both ends to the GenomeWalker™ adaptor (Fig. 2.6) to create four respective GenomeWalker™ libraries.

In the following primary PCR with the Advantage 2 Polymerase mix (Clontech) unknown genomic regions were amplified using a gene-specific (GSP1) and adaptor-specific primer (AP1) (Fig. 2.6). Thereby, the amplification of unspecific PCR products is reduced by the special design of the GenomeWalker™ Adaptor (Fig. 2.6). Briefly, the GenomeWalker™ adaptor contains at the lower 3' strand an amine group, that prevents the 3' end extension through the polymerase and the formation of an AP1 binding site before the actual PCR cycle starts. With the first amplification round of the searched target sequence with the gene-specific primer (GSP1) the first AP1 priming site should appear which secures that only fragments containing the specific GSP1 binding site serve as template.

The preliminary PCR was then used as template for a secondary nested PCR with the nested gene-specific primer GSP2 and the second adaptor-specific primer AP2. The primary and secondary PCR products of all four libraries were analysed by gel electrophoresis, the major bands were purified from the gel by the 'freeze squeeze' method (Chap. 2.4.4) and cloned into the pCRII-Topo vector (Chap. 2.7.3). The screening of positive clones was done by southern blotting with a specific DIG labelled DNA-probe binding downstream of the GSP2 primer binding site, and by sequencing (Chap. 2.4.6).

2.8 Isolation of Arbusculated Cells for RNA Extraction

Temp.	94°C	72°C	94°C	67°C	67°C
Time	25 sec	3 min	25 sec	3 min	7 min
Cycles	7		32		1

Table 2.12. Cycling parameters for the primary GenomeWalker™ PCR with the AP1 and GSP1 primer pair.

Temp.	94°C	72°C	94°C	67°C	67°C	70°C
Time	25 sec	3 min	25 sec	3 min	7 min	10 min
Cycles	5		20		1	1

Table 2.13. Cycling parameters for the secondary GenomeWalker™ PCR with the AP2 and GSP2 primer pair.

PCR setup for primary GenomeWalker™ PCR

- 10 µl sterile Water
- 2.5 µl 10X Advantage 2 PCR buffer)
- 0.5 µl dNTP Solution (10 mM)
- 0.5 µl AP1 (10 µM)
- 0.5 µl gene-specific primer 1 (GSP1) (10 µM)
- 0.5 µl 50X Advantage 2 Polymerase mix (Clontech)
- 1 µl GenomeWalker™ library (1:10 diluted)

PCR setup for secondary GenomeWalker™ PCR

- 20 µl sterile Water
- 2.5 µl 10X Advantage 2 PCR buffer)
- 0.5 µl dNTP Solution (10 mM)
- 0.5 µl AP2 (10 µM)
- 0.5 µl gene-specific primer 2 (GSP2) (10 µM)
- 0.5 µl 50X Advantage 2 Polymerase mix (Clontech)
- 1 µl primary PCR (1:10 diluted)

2.8 Isolation of Arbusculated Cells for RNA Extraction

For the isolation of arbusculated plant cells, the *S.tuberosum-pStPT3-FT-GUS* potato hairy root carrying the StPT3 promoter - Fluorescent Timer fusion gene (Karandashov et al., 2004) were mycorrhized 2 to 3 weeks with *G. intraradices* in the dual compartment system as described in Chap. 2.2.1.

The phosphate transporter StPT3 from *S. tuberosum* belongs to a group of mycorrhiza-inducible plant phosphate transporters which are mediating the transfer of fungal-derived phosphate from the periarbuscular space into the plant cell (Rausch et al., 2001; Fig. 2.7 a). Mycorrhiza-inducible phosphate transporter genes are conserved

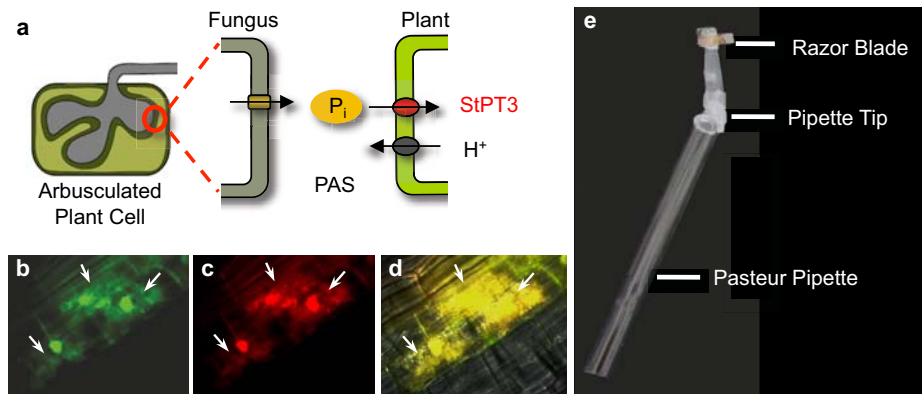


Figure 2.7. Localisation and promoter activity of StPT3 in mycorrhizal roots. **a**, The mycorrhiza-upregulated plant phosphate transporter StPT3 from *S. tuberosum* is involved in the ATP dependant phosphate uptake from the periarbuscular spaces (PAS) into the plant cell. The protein localises in the plant plasma membrane surrounding the arbuscule. **b-d**, Fluorescent Timer protein expression under control of the StPT3 promoter in potato hairy roots mycorrhizal with *G. intraradices*. Green fluorescence (**b**) indicates recent and red fluorescent (**c**) ceased promoter activity in arbusculated cells (arrows). **d**, Merged image of (**b**) and (**c**) shows yellow fluorescence indicating continuous promoter activity. **e**, Self-constructed micro-razor blade. Razor blade has a length of 3–5 mm.

among different plant species all showing an expression in arbuscule containing cells of the inner root cortex where the protein is located in the plant plasma membrane surrounding the arbuscule (Karandashov et al., 2004). Because of this specialised expression pattern, the promoters of mycorrhiza-inducible plant phosphate transporters fused to a fluorescent reporter gene can be used as markers to visualise *in vivo* arbuscule containing cells.

In this work a reporter system based on the Fluorescent Timer (Terskikh et al., 2000), a mutant form of the DsRed fluorescent protein from the coral *Discosoma sp.*, fused to the StPT3 promoter was used. Because of a delayed fluorophore maturation, the Fluorescent Timer gradually turns from bright green (500 nm emission) to bright red (580 nm emission) giving informations about the StPT3 promoter activity. Green indicates recent activity, yellow-to-orange (because of the overlap of green and red fluorescence) continuous promoter activity and red fluorescence declined promoter activity (Figs. 2.7b–d). As arbuscules are highly dynamic symbiotic structures with a quick turn over rate, the StPT3 dependant Fluorescent Timer expression helps to distinguish between young and highly metabolic active arbuscules or old arbuscules which are at the point of degradation correlating with a decrease in StPT3 promoter activity.

Green fluorescent root regions indicating highly arbusculated areas were cut out for RNA extraction under the fluorescent binocular (Zeiss, Germany) using micro-razor blades (Fig. 2.7e). The 2 to 7 mm long root pieces were transferred quickly in RNA later (Invitrogen, USA) to prevent RNA degradation and stored at -80°C until enough material (arbuscules of ca. 30 plates) was selected. RNA extraction was performed as described earlier (Chap. 2.6.1).

2.9 Screening of cDNA Libraries

2.9.1 SMART cDNA Synthesis and LD PCR Amplification

Prior cDNA synthesis for library construction, remaining DNA in RNA samples of arbusculated cells or *G. intraradices* spores was eliminated by desoxyribonuclease digestion. Therefore, up to 39.5 μl of total RNA (approximately 6 μg) was treated with 5 μl DNaseI, Amplification Grade (Invitrogen, USA), 5 μl of DNaseI buffer and 0.5 μl RNase Out (Invitrogen) for 15 min at room temperature in an end-volume of 50 μl . DNaseI was inactivated by the addition of 5 μl EDTA solution to the reaction mixture and heated for 10 min at 65 °C. DEPC water was added to an end-volume of 100 μl and the RNA sample was purified using the RNeasy Plant Mini Kit (Quiagen, Germany) according to the providers protocol. The purified RNA was eluted in 30 μl DEPC water and was directly used for first strand cDNA synthesis using the Matchmaker Library Construction and Screening Kits and user Manual (Clontech Laboratories, USA; Protocol No PT3955-1, Version No PR79376), which takes advantage of the 'SMART' technology (switching mechanism at the 5' end of RNA transcript) based on the intrinsic terminal transferase activity of the reverse transcriptase (Chenchik et al., 1998).

Differing from the protocol, the Superscript II Reverse Transcriptase (Invitrogen) was used to transcribe 3 μl RNA (approximately 200 ng) into single-stranded (ss) cDNA, which was initiated by the oligo (dt) primer CDSIII. Finally, the single-strand cDNA was treated with 1 μl RNase H at 37 °C for 20 min in order to remove remaining RNA from the sample. Generation of cDNA double-strands was performed by Long Distance PCR Amplification (LD PCR) using the Clontech 3' and 5' PCR primers corresponding to the CDSIII and SMARTIII adaptors. The LD PCR setup is listed below. The optimal cycle number for the LD PCR was determined a priori in a test PCR under the same conditions by taken 15 μl samples at cycle 18, 21, 24, 27, 30 and 33. After running an agarose gel, the optimal cycle number was defined as the cycle after which no further increase of the cDNA size was visible, which was in general after cycle 27 (Fig. 2.8 a).

PCR setup for Long Distance PCR

- 56 μl DEPC-treated water
- 10 μl 10X Advantage 2 PCR buffer)
- 8.0 μl dNTP Solution (25 mM)
- 2 μl 5' PCR Primer
- 2 μl 3' PCR Primer
- 10 μl 10X GC Melt Solution
- 2 μl 50X Advantage 2 Polymerase mix (Clontech)
- 10 μl SMART first strand cDNA (1:5 diluted)

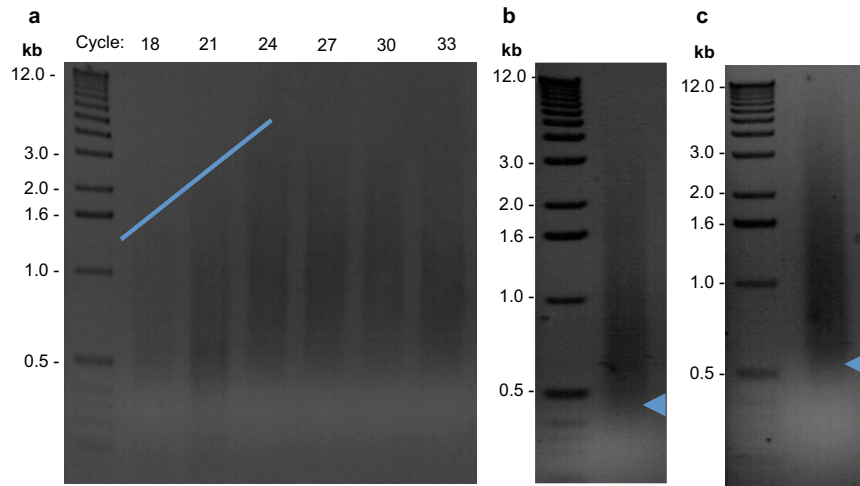


Figure 2.8. **a**, LD-PCR of cDNA from arbusculated plant cells. Samples from different cycles are shown. The blue line indicates the increase of the cDNA length from cycle 18 to cycle 27. **b**, Two pooled samples of LD-amplified cDNAs from arbusculated potato cells. **c**, Same LD-PCR as in **(b)** after size-fractionation using the CHROMA SPIN Columns -400 (Clontech, USA). Arrows in **(b)** and **(c)** indicating shift in cDNA size after the remove of smaller nucleotides in the size-fractionated sample **(c)** compared to the untreated sample **(b)**.

2.9.2 cDNA Size-Fractionation

CHROMA SPIN Columns -400 (Clontech, USA) were used to purify the synthesised cDNAs (Chap. 2.9.1) from smaller nucleotides which can interfere with the recombination of putative sugar transporter genes into the yeast vector pNH196 (Chap. 2.9.4).

As the open reading frame of sugar transporter genes has in general an average size of 1.6 kb, they can quickly move through the column matrix, whereas smaller molecules then 100 nucleotides are held back and can be removed from the sample. To size fractionise the LD-amplified cDNAs, two PCR samples were combined and loaded on a pretreated column as described in the manual (CHROMA SPIN Columns User Manual, Protocol No. PT1300-1, Version No. PR49719). The column was centrifuged at 2,240 rpm for 5 min and the flow out was recovered in a 2 ml reaction tube.

The now size-fractionated cDNAs were precipitated over night at -20°C with 100 % ethanol and 4 M potassium acetate (pH 4.9), centrifuged the next day for 20 min at room temperature at 13,300 rpm and air dried for 20 min. The dried pellet was finally resuspended in 23 μl RNase free water.

2.9.3 Construction of cDNA Expression Libraries

In principal, there are two different methods for cDNA expression library construction. The first method based on restriction enzyme cleavage and ligation of cDNAs into a cloning vector. This procedure bares the risk, that internal restriction sites in the cDNA molecules are also cleaved resulting finally in truncated or chimeric clones. An other disadvantage results from the ineffective ligation of large and rare cDNA se-

quences which can lead to under-representation of some clones in the library. A more efficient and simple method based on *in vivo* homologous recombination of cDNAs into a cloning vector in yeast which was the method of choice for this work.

All cDNA libraries were constructed *in vivo* by homologous recombination of SMART synthesised cDNAs directly into the yeast expression vector pNH196 (Fig. 2.10; see also next chapter). As described more in detail in the following chapter, the vector pNH196 contains homologous sites for the SMARTIII and CDSIII primers which are also flanking the cDNA molecules permitting the uni-directional incorporation of cDNAs with high efficiency. Additionally, the library was directly screened for sugar transporters by functional complementation of a hexose-uptake impaired yeast strain (Chap. 2.9.5).

Simultaneous construction and screening of cDNA libraries in yeast is much faster than the conventional method that provides as intermediate step the transfection of *E. coli* or the bacteriophage λ , but it implies that the genes of interest can complement an appropriate yeast mutant, which makes this method not suitable for all genes. An other disadvantage is, once the library is transformed in the yeast mutant, the screening is restricted for complementing genes (e.g. sugar transporters in a hexose-uptake impaired yeast strain) and the library is finally lost for screening of genes with differing functions.

2.9.4 Construction of the Yeast Expression Vector pNH196

The yeast expression vector pNH196 allows the construction of cDNA libraries *in vivo* via homologous recombination and their high-level expression in yeast. It was created by the ligation of the recombination-cassette from the commercial available pGADT7-Rec vector (Clontech, USA) (Fig. 2.9), which is homologous to the Clontech SMARTIII and CDSIII primers, into the backbone of the yeast expression vector pDR196 (Rentsch et al., 1997). Therefore, pGADT7-Rec was first digested with EcoRI which cuts the vector before the homologous SMARTIII primer site. The resulting EcoRI 5' overhangs were filled in using the exo-Klenow fragment in order to create blunt ends (see also Chap. 2.5.2). The recombination-cassette was finally released from pGADT7-Rec by cutting the linearised vector with XhoI. The 45bp blunt-end/XhoI fragment containing the full recombination-cassette was then ligated after gel purification into the SmaI and XhoI site of pDR196 using the T4 ligase from New England Biolabs (UK) (see also Chap. 2.5.2).

The new created pNH196 vector contains a fragment of the *S. cerevisiae* plasma membrane ATPase promoter (P_{PMAI}) separated from the alcohol dehydrogenase terminator (T_{ADH}) by the SMARTIII/CDSIII recombination cassette with a central SmaI restriction site for vector linearisation, a Amp^r gene for selection in *E. coli*, URA3 as auxotrophic marker for yeast selection, the 2 μ replicon origin and the unique cloning sites SpeI, XbaI, ClaI, SacI and XhoI.

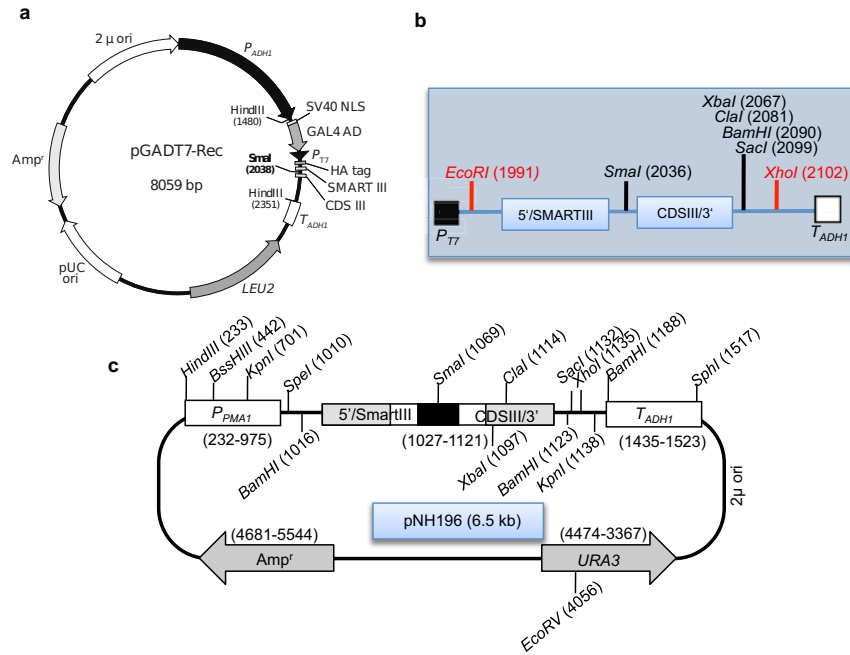


Figure 2.9. **a**, Plasmid card of the yeast expression vector pGADT7-Rec (Clontech, USA). **b**, Recombination cassette of pGADT7-Rec for homologous *in vivo* recombination of SMART created cDNA libraries in yeast. **c**, Plasmid card of the yeast expression vector pNH196.

2.9.5 Functional Complementation Assay in Yeast

The hexose transporter family of *S. cerevisiae* includes 20 genes which are important for efficient hexose uptake. As shown in the work of Wieczorke et al. (1999), the deletion of the hexose transporters *hxt1-17*, the galactose transporter *gal2* and additionally of three genes belonging to the maltose permease family (the α -glucoside-permeases *mph2*, *mph3* and *agt1*) in the CEN.PK2-1C wild type background results in a mutant (EBY.VW4000) which is incapable to grow on media with hexoses as the only carbon source, but on the disaccharide maltose which is transported via a different uptake system. Because of this, the EBY.VW4000 mutant (Mat α leu2-3, 112 ura3-52 trp1-289 his3- Δ 1 MAL2-8c SUC2 Δ hxt1-17 Δ gal2 Δ stl1 Δ agt1 Δ mph2 Δ mph3) is commonly used for the characterisation of sugar transporters from various organisms (Schüßler et al., 2006; Polidori et al., 2006; Hayes et al., 2007; Wang et al.; 2008).

Also for this work, the mutant EBY.VW4000 (kindly provided by Prof. E. Boles, J.W. Goethe University, Germany) was used for the screening of cDNA libraries for symbiosis-specific sugar transporters in mycorrhizas. As the construction of cDNA libraries (Chap. 2.9.4) and their screening for transporters were performed simultaneously, SMART synthesised cDNAs and the SmaI-linearised yeast expression vector pNH196 were co-transformed into the yeast mutant EBY.VW4000 following the Matchmaker Library Construction and Screening Kits User Manual (Clontech Laboratories, Protocol No PT3955-1, Version No PR79376) with same modifications.

Competent cells of the yeast mutant EBY.VW4000 were prepared according the LiAc method. One colony from a freshly streaked out YPDA agar plate was inocu-

lated into 3 ml of 2X YPDA with 2 % maltose in a sterile 15 ml tube and incubated for 8 h at 30 °C and 250 rpm. 5 µl of this pre-culture was further used to inoculate 50 ml 2X YPDA with 2 % maltose in a 250 ml sterile flask and incubated for at least 16 h at 30 °C and 250 rpm to an OD₆₀₀ of 0.15 to 0.3. The overnight culture was centrifuged at 700 × g for 5 min at room temperature and the cell pellet was resuspended in 100 ml of 2X YPDA with 2 % maltose for a final incubation for 3 to 5 h at 30 °C and 250 rpm to an OD₆₀₀ of 0.4 to 0.5. Then, the cells were centrifuged again at 700 × g for 5 min at room temperature, washed with 60 ml of sterile water and resuspended in 3 ml 1.1X TE/LiAc solution. The competent cells were divided in two 1.5 ml reaction tubes and centrifuged for 15 s at high speed. Each pellet was resuspended in 600 µl 1.1X TE/LiAc Solution and used immediately for transformation.

Therefore, 20 µl of the double-strained cDNA, 6 µl SmaI-linearised pNH196 (3 to 7 µg) and 20 µl carrier DNA (2 $\frac{\text{mg}}{\text{ml}}$ Salmon sperm, denatured in advance for 5 min at 100 °C) were mixed in a 15 ml tube. 600 µl of the competent yeast cells were added and mixed gently before the addition of 2.5 ml PEG/LiAc solution. Afterwards, the transformation suspension was incubated for 45 min at 30 °C and mixed every 15 min. At the end, the yeast cells were heat shocked after the addition of 160 µl DMSO for 20 min in a 42 °C water bath, then centrifuged at 700 × g for 5 min at room temperature, resuspended in 3 ml 2X YPDA with 2 % maltose and incubated for 90 min at 30 °C and 265 rpm.

The transformed cells were centrifuged at room temperature 700 × g for 5 min, resuspended in 6 ml 0.9 % NaCl solution and 150 µl of the co-transformation was plated onto YNB medium with 2 % of either glucose, fructose, galactose or mannose but without uracil.

After one week incubation at 30 °C, first colonies were streaked out for a second selection round on YNB medium plates with 2 % of either different hexoses glucose, fructose, galactose or mannose and without uracil. Positive clones were finally identified by growing them in liquid 2X YPDA medium with 2 % of glucose, fructose, galactose or mannose.

TE buffer

- 0.1 mM TrisHCl
- 10 mM EDTA
- pH 7.5

1.1X TE/LiAc solution

- 1.1 ml TE buffer
- 1.1 ml 1 M LiAc (Sigma-Aldrich), pH 7.5
- 7.8 ml ddH₂O

PEG/LiAc solution

- 8 ml 50 % (v/v) PEG 3350 (Sigma-Adrich)
- 1 ml 10X TE
- 1 ml 1 M LiAc

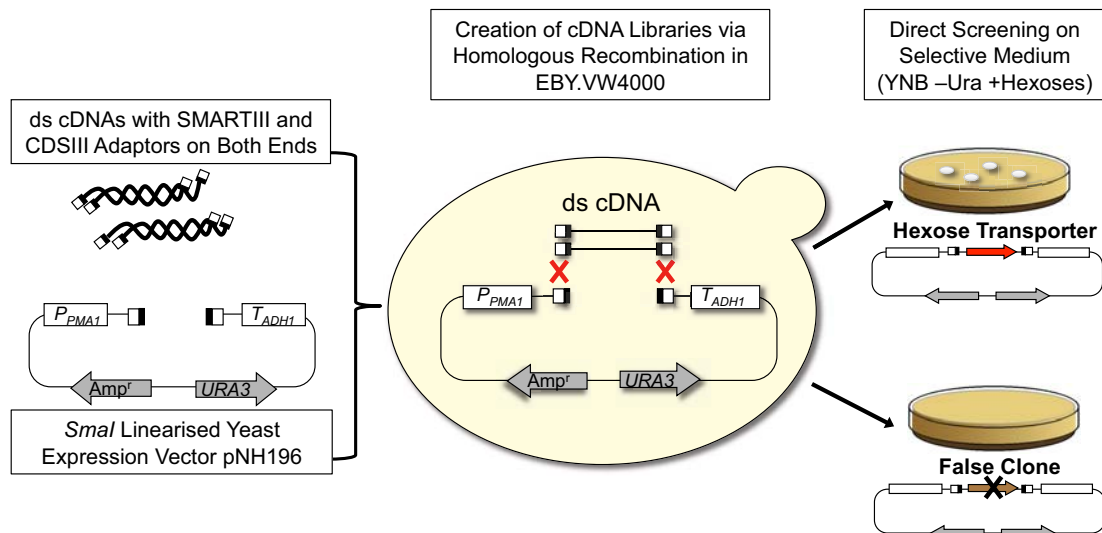


Figure 2.10. One-Step cDNA library construction and screening. SMART generated double-strained (ds) cDNAs were co-transformed with the SmaI linearised yeast expression vector pNH196 in the hexose-uptake impaired yeast mutant EB.YVW4000. *In vivo*, ds cDNAs were integrated by homologous recombination in pNH196 over SMARTIII/CDSIII recombination sites. Putative hexose transporters were isolated by functional complementation of EB.YVW4000 on selective medium without uracil and with hexoses as only carbon source.

2.9.6 Plasmid Preparation from Yeast and Retransformation in *E. coli*

To identify the cDNAs cloned into pNH196, the transformed plasmids were recovered from yeast. Therefore, 2 ml of two days old yeast cultures inoculated in 3 ml liquid 2X YNB medium with 2% maltose and without uracil were centrifuged for 3 min at 13,000 rpm. The cell pellet was resuspended in 500 μ l Glucanex solution (120 $\frac{\text{mg}}{\text{ml}}$ GlucanexTM(Novozyme, Denmark) and 60 $\frac{\text{mg}}{\text{ml}}$ BSA (Carl Roth, Germany)) and incubated at 30 °C for cell wall digestion. After 1 h, the cells were centrifuged for 1 min at 7,900 rpm, resuspended in 500 μ l resuspension buffer and incubated for 5 min at room temperature. 50 μ l 10% sodium dodecyl sulfate (SDS) was added, followed by an incubation step at 68 °C for 30 min. Proteins were precipitated by the addition of 200 μ l 5 M potassium acetate and a centrifugation step of 5 min and 13,000 rpm after a resting time on ice for 1 h. The supernatant was transferred in 750 μ l isopropanol. The plasmid DNA was precipitated by 10 min centrifugation at 13,000 rpm, washed with 800 μ l 70% ethanol and dried at 68 °C. The dried pellet was resolved in 50 μ l ddH₂O.

The isolated plasmids were transferred via electroporation in *E. coli* (Chap. 2.3.2) and transformants were selected on LB agar plates with 100 $\frac{\mu\text{g}}{\text{ml}}$ ampicillin. Plasmids of at least three *E. coli* clones, from each transformation, were isolated by mini preparation (Chap. 2.4.2) and analysed for cDNA insert size by restriction endonuclease digestion and agarose gel electrophoresis. Clones with an appropriate insert size of more than 1.5 kb were sequenced in forward direction using the primer NH196_F1 (5'-tccaccaagcagtgtatc-3') and in reverse direction with NH196_R1 (5'-agctcgtatgga-

tcccgtatc-3').

Resuspension buffer

- 1 M TrisHCl
- 0.5 M EDTA
- 0.1 $\frac{\text{mg}}{\text{ml}}$ RNaseA (Carl Roth)

2.10 Heterologous Expression of *GiMST1* in Yeast

For the heterologous expression of *GiMST1* in yeast, the 1.5 kb ORF of *GiMST1* was cloned in the yeast expression vector pNEV-N (kindly provided by K. Wippel, FAU, Germany) right before the constitutively active promoter of the *S. cerevisiae* ATPase PMA1. For this, *GiMST1* was first amplified with the primers MST1atgNot_F1 and MST1endNot_R1 containing NotI restriction sites on the 3' ends. The received amplification was cloned in the vector pCR2.1-Topo. The resulting plasmid was named pCR2.1-*GiMST1*-NotI. pCR2.1-*GiMST1*-NotI was digested with NotI and cloned in the NotI-linearised vector pNEV-N. The created vector pNEV-MST1 was then transformed in the EBY.VW4000 strain as described in Chap. 2.3.3.

In addition, a *GiMST1*-GFP fusion construct was generated to test the membrane location of *GiMST1* in yeast. Therefore, *GiMST1* was amplified without stop codon using the primers pEXTAGiMST1_F1 and pEXTAGiMST1_R1 containing NcoI restriction sites on the 3' ends and cloned in pCR2.1-Topo creating pCR2.1-*GiMST1*-NcoI. From there, *GiMST1* was released by NcoI digestion and cloned in the NcoI-linearised yeast vector pEXTAG-GFP (kindly provided by K. Wippel, FAU, Germany). The received plasmid pEXTAG-MST1-GFP was transformed in the yeast strain EBY.VW4000 as described in Chap. 2.3.3.

2.11 Spotting Test

The growth of the complemented yeast mutant strains on different sugars was determined in a spotting test. Therefore, the yeast strains were pre-grown in 3 ml liquid YNB medium with 2% maltose under selective conditions at 30 °C and 200 rpm overnight. The cells were centrifuged for 2 min at 10,000 rpm, washed twice with sterile distilled water and resuspended in sterile water to a final OD₆₀₀ of 1. A dilution series was prepared (10^{-1} to 10^{-4}), whereon 10 µl of each 10-fold dilution was spotted on YNB plates supplemented with 0.1 or 2% of different monosaccharides (maltose, glucose, fructose, mannose) and with a pH of 6.5 or 5.5. The plates were incubated at 30 °C up to one week.

2.12 Uptake Experiments with Radioactive Labelled Sugars

Yeast cells were grown overnight in selective medium to an OD₆₀₀ of 1.0, harvested by centrifugation, washed twice in 50 mM potassium-phosphate buffer pH 5.0 and

resuspended in the same buffer to an OD₆₀₀ of 40.

If not otherwise indicated, uptake was started by the addition of 1 mmol of radio-labelled sugar (¹⁴C glucose, ¹⁴C fructose, ¹⁴C xylose or ¹⁴C mannose) to 500 μl of potassium-phosphate buffered yeast suspension shaken in a water-bath at 28 °C. 50 μl samples were taken at given intervals, filtered onto glass microfibers filters and washed twice with Millipore water. The filters were transferred into scintillation vials containing 4 ml scintillation cocktail (LumaSafe PLUS; Lumac LSC, The Netherlands) and radioactivity was measured with a scintillation counter.

For inhibition studies, yeast cells were pre-incubated for 1 min with 50 μM of the protonophore CCCP (carbonylcyanide m-chlorophenylhydrazone), before the reaction was started by the addition of ¹⁴C glucose. pH dependency was determined by measuring ¹⁴C glucose uptake of yeast cells resuspended in 50 mM potassium-phosphate buffer with pH 5.0, 6.0, 7.0 or 8.0. Competition for glucose uptake was performed by adding 10 mM of the competitor to cells of an OD₆₀₀ of 10. The yeast cells were incubated 1 min with the competitor before 0.1 mM radio-labelled glucose was added. The K_m value was determined by measuring the uptake rates at different glucose concentrations.

All uptake experiments were repeated with independent samples at least three times.

2.13 Transcription Analysis

2.13.1 Quantitative Real-Time PCR (qPCR)

In order to compare the expression levels of genes in different samples a quantitative real-time PCR (qPCR) was performed. For real-time reactions the MESA GREEN qPCR MasterMix Plus (Eurogentec, Belgium) was used. Per reaction 12.5 μL MESA GREEN was mixed with 0.5 μl forward and reverse primer (each 0.2 $\frac{\text{pm}}{\mu\text{l}}$), 1 μl cDNA and 10.5 μl DEPC H₂O. The cDNA templates (1 μg of reverse transcribed total RNA) were used as a dilution of 1:5 in DEPC-treated H₂O. The primers for qPCR were designed using the Primer3 software program. Primers used for qPCR are listed in Tabs. A.1 and A.3. When possible, intron-spanning primers were used. Routinely three technical replicates were set per reaction and the appropriate water controls (containing water instead of template) were included to check for contaminations. For real-time PCR the Bio-Rad iCycler MyIQ (Bio-Rad, USA) was used. The cycling parameters were set as described in Tab. 2.14. At the end of the qPCR a meltcurve was run by rising the temperature slowly from 57 to 97 °C to check for unspecific PCR products or primer dimers formed during the reaction.

The relative expression was calculated by normalising the Ct values (threshold cycle) of the target gene against the Ct values of an housekeeping gene:

$$\text{Relative Expression} = 2^{\text{Ct}_{\text{Housekeeping Gene}} - \text{Ct}_{\text{Target Gene}}}$$

For *M. truncatula*, *S. tuberosum* and *G. intraradices* the elongation factor alpha 1 (TEF)

Temp.	95°C	95°C	56°C	72°C	95°C	57°C	57-97°C
Time	1 min	30 sec	30 sec	30 sec	1 min	1 min	10 sec
Cycles	1	40			1	1	77

Table 2.14. Cycle parameters for qPCR.

was used (TC106470; AJ536671; DQ282611), for *S. cerevisiae* specific primers against the actin gene Act1p (NP_116614) was used.

Fold change expression was calculated by the comparative Ct method according Livak et al. (2001):

$$\text{Fold change} = 2^{-\Delta\Delta Ct}$$

$$\Delta\Delta Ct = \Delta Ct_{\text{Target Gene I}} - \Delta Ct_{\text{Target Gene II}}$$

$$\Delta Ct_{\text{Target Gene}} = Ct_{\text{Target Gene}} - Ct_{\text{Housekeeping Gene}}$$

A minimum of a twofold change in expression was considered to be biologically relevant. Errors were calculated as standard deviation (s.d.).

2.13.2 In situ Hybridisation of Mycorrhized Roots

The procedure was carried out as described by Schaarschmidt et al. (2006) with some modifications. *Medicago truncatula* hairy roots, transformed with the *Agrobacterium rhizogenes* strain ARqua1, were mycorrhized for three weeks in dual compartment plates with *G. intraradices*, as described before in Chap. 2.2.1. Root pieces of 3 mm in length were vacuum infiltrated three times for 10 min with 4% (w/v) paraformaldehyde, 0.1% (v/v) Triton X-100 in phosphate buffered saline (PBS; pH 7.0) and fixed for 2 h at room temperature with gentle shaking in fresh para-formaldehyde solution. After a washing step with PBS (2x for 15 min) following by dehydration of the root pieces in a graded series of ethanol (30 min 10% EtOH at RT, 60 min 30% at RT, 60 min 50% at RT, overnight 70% at 4°C) the material was stored at 4°C. For embedding in Paraplast plus (Carl Roth, Germany) the roots were further dehydrated 30 min with 90%, 60 min with 100% EtOH and finally stained for 30 min at room temperature with 0.1 $\frac{\text{mg}}{\text{ml}}$ Eosin G (Merck, Germany) in 100% EtOH. EtOH was stepwise replaced by Rotihistol (Carl Roth) and the roots were slowly infiltrated with liquid paraplast by addition of small droplets at 60°C. Cross-sections of the embedded material were cut using a microtome (HM 355, Microm International, Germany) with a thickness of 8 μm and mounted on poly-L-Lysine slides (Sigma-Aldrich, Germany). Sections were deparaffinised with Roticlear (Carl Roth) and hydrated with an EtOH series from 96% to 10%. After 10 min in 10 mM TrisHCl (pH 8.0) the sections were treated with 5 $\frac{\mu\text{g}}{\text{ml}}$ Proteinase K in TrisHCl (pH 8.0) for 30 min at 37°C, washed with the same buffer and blocked for 30 min at room temperature with 1% (w/v) Albumin Fraction V (BSA) (Carl Roth) with 2 $\frac{\text{mg}}{\text{ml}}$ Glycin in 10 mM TrisHCl (pH 8.0).

Following an equilibration step in PBS, slides were treated for post-fixation with 4 % (w/v) paraformaldehyde for 10 min and equilibrated in 0.1 M triethanolamine (pH 8.0) (Sigma-Aldrich) before acetylation with 0.25 % (v/v) acetic anhydride in 0.1 M triethanolamine (pH 8.0) for 10 min. The sections were finally washed in TrisHCl (pH 8.0), dehydrated with EtOH and air dried. Prior hybridisation, the sections were pre-hybridised for 1 h at 45 °C in hybridisation solution consisted of 50 % (v/v) Formamid, 0.3 M NaCl, 10 mM TrisHCl (pH 7.5), 5 mM EDTA, 1X Denhardt's solution, 1 $\frac{\text{mg}}{\text{ml}}$ tRNA (Roche Diagnostics, Germany) and 0.5 % (w/v) BSA to avoid unspecific binding of the RNA probes. Finally, sections were incubated with hybridisation solution containing 10 $\frac{\text{mg}}{\text{ml}}$ RNase inhibitor and 1 μg digoxigenin (DIG) labelled sense or antisense probe overnight at 45 °C under humid conditions. Slides were washed with 0.2X SSC (2 times 30 min at 55 °C), equilised with STE for 3 min at room temperature, treated with 20 $\frac{\mu\text{g}}{\text{ml}}$ RNase A in STE (30 min at 37 °C) and washed again with STE (5 min, room temperature) and 0.2X SSC (30 min, 55 °C).

For the immunological detection of RNA-RNA hybrids, sections were incubated for 5 min in TBS, for 30 min in 1 % (w/v) blocking reagent (Roche Diagnostics) in TBS and for 120 min with 1:1000 diluted Anti-DIG fab fragment conjugated with alkaline phosphatase (Roche Diagnostics), 1 % Blocking reagent and 1 % acetylated BSA (Aurion, Netherlands) in TBS.

For the histochemical staining, sections were incubated in detection buffer with 0.4 M nitroblue-tetrazolium (NBT), 0.5 M 5-bromo-4-chloro-3-indolyl-phosphat (BCIP) and 10 mM Levamisol (Sigma Aldrich), over night at 37 °C in a humid chamber. Reaction was stopped with 10 mM TrisHCl and 1 mM EDTA and sections were preserved in Glycerol:PBS (1:1).

Sense and antisense cRNA probe of *GiMST1* were *in vitro* transcribed using the DIG RNA labelling Kit (Roche Diagnostics, Germany). A 148 bp specific region of *GiMST1* was amplified from a cDNA library of microdissected and arbusculated potato root cells using specific primers MST1situ_F1 and MST1situ_R1, ligated in the polylinker site of the dual promoter vector pCRII-Topo (Invitrogen, USA) which was afterwards named pCRII-GiMST1-148bp (Fig. 2.11 a). For sense probe synthesis the vector was cut with HindIII, purified by gel electrophoresis and 1 μg of the linearised vector was transcribed in cRNA via T7 RNA polymerase according the manual description. For antisense probe synthesis the vector was linearised with XbaI, purified and transcribed via Sp6 RNA polymerase. Sense and antisense probe were purified using the Miniolute PCR Kit from Peqlab Biotechnology (Germany). The RNA was eluted twice from the columns with 20 μl RNase free water. The efficiency of the labelling reaction was determined with a spot test following the DIG Application Manual for Filter Hybridization (Roche Diagnostics) and equal yields of sense and antisense probe were used for hybridisation (Fig. 2.11 b).

PBS

- 135 mM NaCl
- 3 mM KCl
- 8 mM Na₂HPO₄

- pH 7.0

STE

- 3 mM TrisHCl (pH 7.8)
- 1 mM EDTA
- 0.1 M NaCl

20X SSC

- 3 mM NaCl
- 300 mM trisodium citrate
- pH 7.0

TBS

- 0.1 M TrisHCl (pH 7.5)
- 0.15 M NaCl

50X Denhardt's Reagent

- 1 % (w/v) Ficoll 400
- 1 % (w/v) polyvinylpyrrolidone
- 1 % (w/v) BSA

Detection buffer

- 0.1 M TrisHCl (pH 9.5)
- 0.05 M MgCl₂
- 0.1 M NaCl

2.14 Histochemical Analysis

The β -glucuronidase gene (GUS) from *E. coli* was used in this work as reporter to visualise promoter activities in plant tissues. The GUS assay is based on the activity of the β -glucuronidase which catalyses the cleavage of X-Gluc (5-bromo-4-chloro-3-indolyl- β -D-glucuronid) to an indoxyl-derivative which forms after oxidation by potassium ferro/ferric cyanid a blue dye. Thus, blue tissue refers to promoter activity and β -glucuronidase expression.

For GUS assays, fresh root material was heated for 30 min at 53 °C in sterile dH₂O. Then the roots were incubated in GUS staining solution at 37 °C in dark over night. To visualise fungal hyphae of mycorrhized roots, the stained material was transferred directly to 10 % KOH at 45 °C to clear the tissues, acidified with 1 % HCl, and then counterstained for 45 min at 90 °C with acid fuchsin dissolved in lactoglycerol (lactic

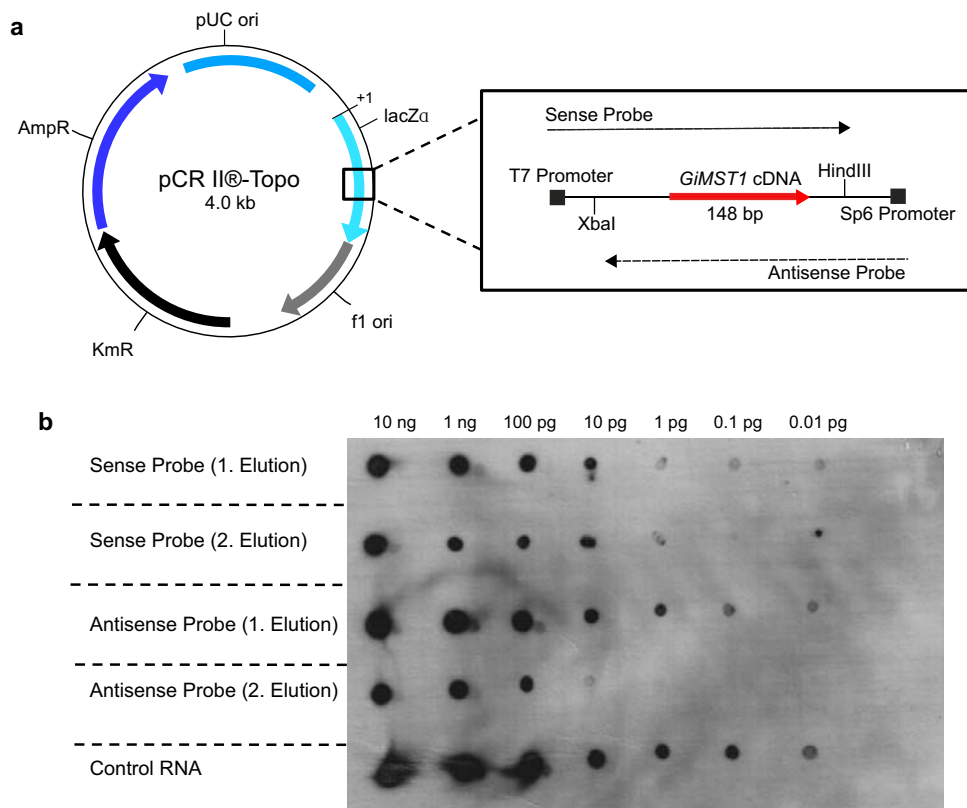


Figure 2.11. Preparation of sense and antisense probe for *GiMST1*. **a**, Cloning of the reverse transcribed *GiMST1* sequence in the pCRII-Topo vector. Location of T7 and Sp6 promoter sequences and XbaI and HindIII restriction sites are shown in the black box. **b**, Spot test of the first and second elution of the *GiMST1* sense and antisense probe. The RNA probes were spotted in a dilution series from 10 ng to 0.01 pg. The first elution of the probes showed a sufficient strength compared to the control RNA (Roche Diagnostics).

acid:glycerol:water, 1:1:1). The roots were destained over night in 50 % glycerol by gentle shaking and prepared the next day on microscope slides in 100 % glycerol and sealed. The stained material was analysed by light and fluorescent microscopy.

GUS staining solution

- 960 $\frac{\mu\text{l}}{\text{ml}}$ TrisHCl/NaCl buffer
- 20 $\frac{\mu\text{l}}{\text{ml}}$ 100 mM potassium ferro/ferri cyanide solution (1:1)
- 25 $\frac{\mu\text{l}}{\text{ml}}$ 20 % (w/v) X-Gluc in DMF

TrisHCl/NaCl buffer

- 100 mM TrisHCl (pH 7.0)
- 50 mM NaCl

2.15 Imaging Techniques

Microscopy was done with the SteREO Lumivar.V12 stereo-microscope (Carl Zeiss, Germany) or the AxioImager Z1 fluorescence microscope (Carl Zeiss) equipped with a 64X oil and water immersion objective. Images were captured using three different cameras from Carl Zeiss: the AxioCam MRm (for fluorescence imaging), the AxioCam ICc3 (for live color imaging), or the AxioCam HRc (for fluorescence or live color imaging with the stereo-microscope). The AxioVision V4.5 software was used for image analysis (Carl Zeiss).

2.16 Software and Webservices

The software and web pages used for data and sequence analysis are listed in Tab. 2.15.

Software or Webservice	Description	Reference
Ape-A plasmide Editor	Free plasmid analysis and editor software	M. Wayne Davis, University of Utha
Artemis	Free annotation software	Ruhterford et al. (2000). <i>Bioinformatics</i> 16(10): 944-5
DNA strider software	Free DNA and protein sequences analysis	Marck (1988). <i>Nucleic Acids Res.</i> , 16 (5), 1829-36
Jalview	Multiple alignment editor	Clamp et al. (2004). <i>Bioinformatics</i> 20 : 426-7
ClustalW	Multiple sequence alignment program for nucleotide and protein sequences	Thompson et al. (1994). <i>Nucleic Acids Res.</i> 22(22): 4673-80
MEGA4	Free software for molecular evolutionary genetics analysis	Tamura et al. (2007). <i>Molecular Biology and Evolution</i> 24:1596-99
THMM Server v. 2.0	Prediction of transmembrane helices in proteins	Krogh et al. (2001). <i>J Mol Biol.</i> 305(3): 567-80
TopPred	Topology prediction of membrane proteins	Claros and Heijne (1994). <i>CABIOS</i> 10: 685-86
PLACE Signal Scan	Database of Plant Cis-acting Regulatory DNA Elements	Higo et al. (1999). <i>Nucleic Acids Research</i> 27:297-300
TRANSFAC database	Database on eukaryotic cis-acting regulatory DNA elements and trans-acting factors	Ghosh (1991). <i>Trends in Biochemical Sciences</i> 16: 445-447
TFD database	Transcription factor database	Wingender et al. (1996). <i>Nucleic Acids Research</i> 16: 1879-1902
NCBI	Database for scientific publications; database for DNA, RNA and protein sequences; bioinformatic software tools	National Center for Biotechnology Information (USA)
INRA GlomusDB database	<i>G. intraradices</i> genome database	INRA (France)
Primer 3	Primer designing program	Rozwn and Skaletsky (2000). <i>Methods in Molecular Biology.</i> Humana Press, Totowa, NJ, 365-386

Table 2.15. Software and webservices used for sequence and data analysis.

Chapter 3

Results

3.1 Characterisation of Sugar Transporters from Potato

In order to identify sugar transporters featuring in the AM symbiosis, cDNA expression libraries were constructed from mycorrhized potato hairy roots and screened in a functional complementation assay in the yeast mutant strain EBY.VW4000 (Wieczorke et al., 1999). This method was already used successfully by Schüßler et al. (2006) to isolate a symbiosis relevant sugar transporter in the AM-like *Geosiphon*-symbiosis.

3.1.1 Enrichment of Arbusculated Cells by Microdissection

The material used for the construction of cDNA expression libraries consisted of potato roots colonised with *G. intraradices*. To enrich the material with RNA from arbuscule-containing cells, the potato hairy root line *S. tuberosum*-pStPT3-FT-GUS was microdissected under the fluorescent stereo-microscope using self-made micro-razor blades as described in Chap. 2.8. From this material moderate amounts (200 to 400 $\frac{\text{ng}}{\mu\text{l}}$) of high quality RNA could be isolated (Fig. 3.1 b).

To validate the enrichment of arbuscules, three different samples, non- (-myc), less- (+myc) or heavily-mycorrhized (++myc), were compared by quantitative real-time PCR (Figs. 3.1 a, c). As marker gene expressed exclusively in arbusculated plant cells, the transcript level of the mycorrhiza specific phosphate transporter 4 from potato (*StPT4*) was compared in all samples. Fig. 3.1 c shows the fold induction of *StPT4* in the -myc, +myc and ++myc samples. The increased expression of *StPT4* correlated positively with the arbuscule amount in each sample. A four-fold enrichment of arbuscule-containing cells in the ++myc sample was achieved.

3.1.2 Screening of cDNA Libraries for Sugar Transporters

Two independently collected arbuscule-enriched RNA samples were used for the construction of cDNA expression libraries in the yeast vector pNH196 (Chap. 2.9). The construction and screening of the cDNA libraries was performed simultaneously in the yeast mutant EBY.VW4000 (see also Fig. 2.10). Sample I was screened one time on glucose plates, Sample II repeatedly on selection medium with different hexoses in order to saturate the amount of clones which can be recovered from the cDNA pool (Tab. 3.1).

cDNA Library	Selection Conditions	Total of Clones	Positive Clones after 2. Selection in Liquid Medium			
			No	cDNA Size	GC Content	NCBI BLAST
cDNA arbuscules (RNA I)	YNB -Uracil +Glucose	42	1.	1.8 kb	40 %	XP_002510991 sugar transporter, putative [<i>Ricinus communis</i>]
			2.	1.8 kb	40 %	XP_002510991 sugar transporter, putative [<i>Ricinus communis</i>]
cDNA arbuscules (RNA II)	YNB -Uracil +Glucose	160	1.	1.8 kb	40 %	XP_002510991 sugar transporter, putative [<i>Ricinus communis</i>]
cDNA arbuscules (RNA II)	YNB -Uracil +Glucose	131	1.	1.8 kb	40 %	XP_002510991 sugar transporter, putative [<i>Ricinus communis</i>]
			2.	1.8 kb	40 %	XP_002510991 sugar transporter, putative [<i>Ricinus communis</i>]
			3.	1.8 kb	40 %	XP_002510991 sugar transporter, putative [<i>Ricinus communis</i>]
			4.	1.8 kb	40 %	XP_002510991 sugar transporter, putative [<i>Ricinus communis</i>]
			5.	1.8 kb	40 %	XP_002510991 sugar transporter, putative [<i>Ricinus communis</i>]
			6.	1.8 kb	40 %	XP_002510991 sugar transporter, putative [<i>Ricinus communis</i>]
cDNA arbuscules (RNA II)	YNB -Uracil +Glucose	162	1.	1.8 kb	40 %	XP_002510991 sugar transporter, putative [<i>Ricinus communis</i>]
			2.	1.8 kb	40 %	XP_002510991 sugar transporter, putative [<i>Ricinus communis</i>]
			3.	1.8 kb	40 %	XP_002510991 sugar transporter, putative [<i>Ricinus communis</i>]
cDNA arbuscules (RNA II)	YNB -Uracil +Galactose	25	1.	1.8 kb	40 %	XP_002510991 sugar transporter, putative [<i>Ricinus communis</i>]
			2.	1.8 kb	40 %	XP_002510991 sugar transporter, putative [<i>Ricinus communis</i>]
			3.	1.8 kb	40 %	XP_002510991 sugar transporter, putative [<i>Ricinus communis</i>]
			4.	1.8 kb	40 %	XP_002510991 sugar transporter, putative [<i>Ricinus communis</i>]
			5.	1.8 kb	40 %	XP_002510991 sugar transporter, putative [<i>Ricinus communis</i>]
cDNA arbuscules (RNA II)	YNB -Uracil +Fructose	165	1.	1.9 kb	40 %	CAB52689 hexose transporter [<i>Solanum lycopersicum</i>]
cDNA spores	YNB -Uracil +Glucose	132	-	-	-	-

Table 3.1. List of clones isolated from cDNA libraries of arbuscule-enriched and spore material by complementation of the yeast mutant strain EBY.VW4000.

3.1 Characterisation of Sugar Transporters from Potato

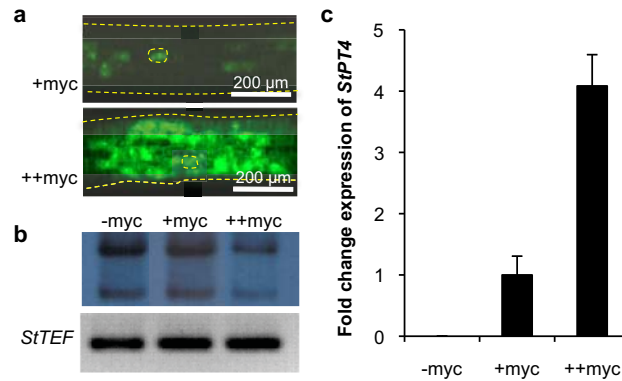


Figure 3.1. **a**, Example for less- (+myc) and heavily-mycorrhized (++) microdissected root regions observed under the fluorescent binocular. Arbuscule-containing cells are green fluorescent. The shape of the roots and of a single cell are indicated with a yellow dashed line. **b**, Integrity of the RNA isolated from microdissected potato roots proved by northern blotting. Quality of cDNA was tested by amplification of *StTEF* via qPCR. **c**, Fold change expression of *StPT4* in -myc, +myc and ++myc samples. *StPT4* expression was normalised to *StTEF*. (Bars represent s.d.)

The recovered plasmids from complemented yeast clones were checked for cDNA insert size by restriction endonuclease digestion. As the average cDNA size of monosaccharide transporters is around 1.5 kb (the average protein size for monosaccharide transporters was estimated around 515 amino acids (aa), see alignment in Figs. B.3 and B.4), only plasmids with the appropriate insert size were sequenced for further analyses. The obtained sequences were run against the NCBI database.

A frequently isolated false positive clone shared highest homology to the plant kinetochor protein SKP1. To exclude false positive clones in following screenings, a second selection step in liquid medium was introduced. Thus, it was possible to isolate two distinct plant monosaccharide transporters named StHT6 according to its homology to the monosaccharide transporter HEX6 which was identified in *Ricinus communis* (Weig et al., 1994), and StHT2, which is closely related to the transporter HT2 from tomato (Gear et al., 2000) (Fig. 3.2; Tab. 3.2). The here identified potato transporters code for two proteins of 509 aa (StHT6) and 522 aa (StHT2) with calculated molecular masses of 55.4 kDa and 57.4 kDa, respectively. The deduced amino acid sequences showed a 12 transmembrane domain (TMD) topology, typical for transporters of the major facilitator superfamily (MFS), with intracellular termini and a long central loop (between TMD6 and TMD7) shared by most hexose transporters (Fig. 3.3). Also conserved domains common in proteins of the MFS (cd06174) and for sugar transporters (pfam00083) were found by NCBI domain blast search. Both proteins shared high homology with other plant monosaccharide transporters (Fig. 3.6; Tab. 3.2; Figs. B.3 and B.4).

StHT6 was the dominant transporter isolated repeatedly on glucose and galactose, whereas *StHT2* was isolated once on fructose selection medium (Tab. 3.1). Sequences of fungal sugar transporters were not isolated from the cDNA libraries of arbuscule-enriched material which represent a mixture of fungal and plant expressed genes. Additionally, a cDNA library constructed from germinated spores was screened on

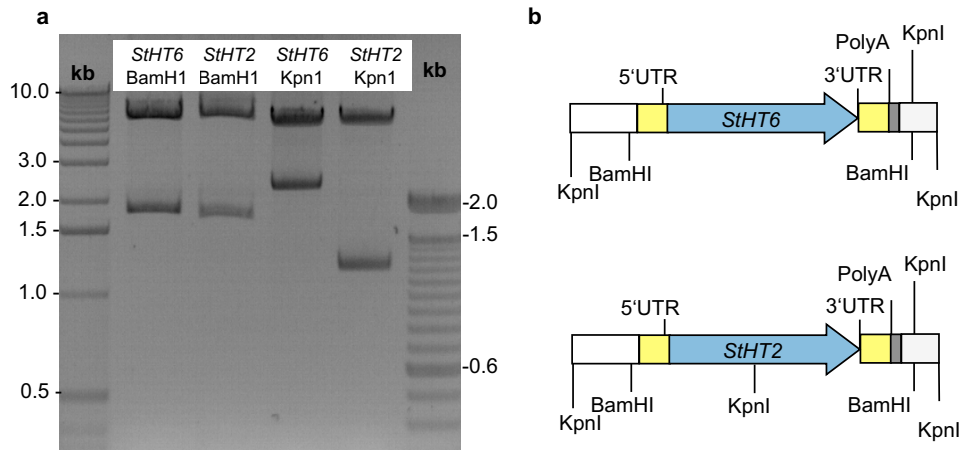


Figure 3.2. **a**, BamHI and KpnI endonuclease restriction digestion of the isolated potato sugar transporters StHT6 and StHT2 in the yeast vector pNH196. **b**, Position of KpnI and BamHI restriction sites in pNH196-StHT6 and pNH196-StHT2. (UTR: untranslated region; PolyA: polyadenylated tail)

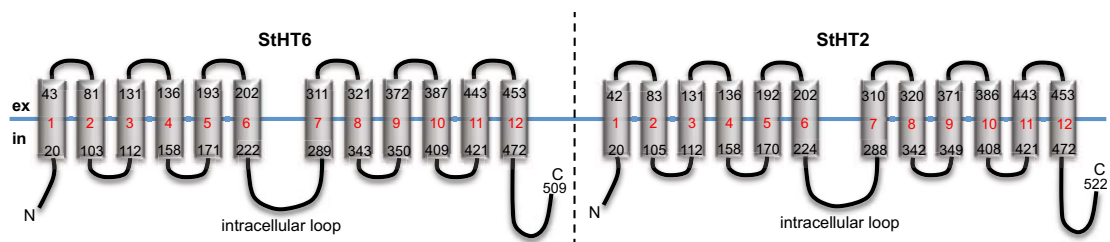


Figure 3.3. TMDs predicted by TMHMM program for the monosaccharide transporters StHT6 and StHT2.

3.1 Characterisation of Sugar Transporters from Potato

Accession Number	Organism	Description	Score	Evalue	Identity
StHT6					
AAA79857	<i>Ricinus communis</i>	Hexose carrier protein <i>HEX6</i>	741 (1912)	0.0	71 %
NP_001149551	<i>Zea mays</i>	Hexose carrier protein <i>HEX6</i>	642 (1655)	0.0	61 %
AAP55016	<i>Oryza sativa</i>	Hexose carrier protein <i>HEX6</i>	639 (1648)	0.0	59 %
ACF22763	<i>Brachypodium distachyon</i>	Sugar transport protein	633 (1633)	1e-179	62 %
NP_001105681	<i>Zea mays</i>	Monosaccharide transporter 1	632 (1630)	3e-179	60 %
StHT2					
CAB52689	<i>Solanum lycopersicum</i>	Hexose transporter (<i>LeHT2</i>)	992 (2565)	0.0	95 %
CAA09419	<i>Solanum lycopersicum</i>	Hexose transporter protein	964 (2491)	0.0	92 %
XP_002517216	<i>Ricinus communis</i>	Sugar transporter, putative	873 (2256)	0.0	80 %
Q94AZ2.2	<i>Arabidopsis thaliana</i>	Sugar transporter (<i>STP13</i>)	857 (2214)	0.0	79 %

Table 3.2. NCBI protein Blast results for the monosaccharide transporters StHT6 and StHT2.

glucose plates for fungal sugar transporters active in the presymbiotic phase. Also in this screen no fungal transporter was found.

3.1.3 Functional Analysis of StHT6 and StHT2 in Yeast

The EBY.VW4000 clones complemented with *StHT6* or *StHT2* were tested for their ability to take up different hexoses as carbon source. First tests in liquid medium showed no difference in growth between yeasts expressing heterologously *StHT6* or *StHT2*. Both transporters were able to complement the mutant which was able to grow with glucose, fructose or mannose as the carbon source (Fig. 3.4). More information about substrate specificity and affinity was gained by spotting a dilution series of the yeast mutants on solid medium with 0.1 % or 2 % of each sugar (Fig. 3.5; Chap. 2.11). *StHT6* expressing yeasts were able to grow efficiently on all sugars, whereas yeasts complemented with *StHT2* grew better on glucose and mannose but lesser on fructose. This was more obvious comparing growth of *StHT2* transformed yeasts on 0.1 % and 2 % sugar plates. Both transporters sustained growth of the mutant better on higher sugar concentrations. As control, all yeast clones were cultivated in liquid medium with maltose, which is the only monosaccharide that can be used by the EBY.VW4000 mutant without complementation. The high-affinity monosaccharide transporter HXT2 from *S. cerevisiae* (accession no. CAA88528) was used as positive control in all experiments.

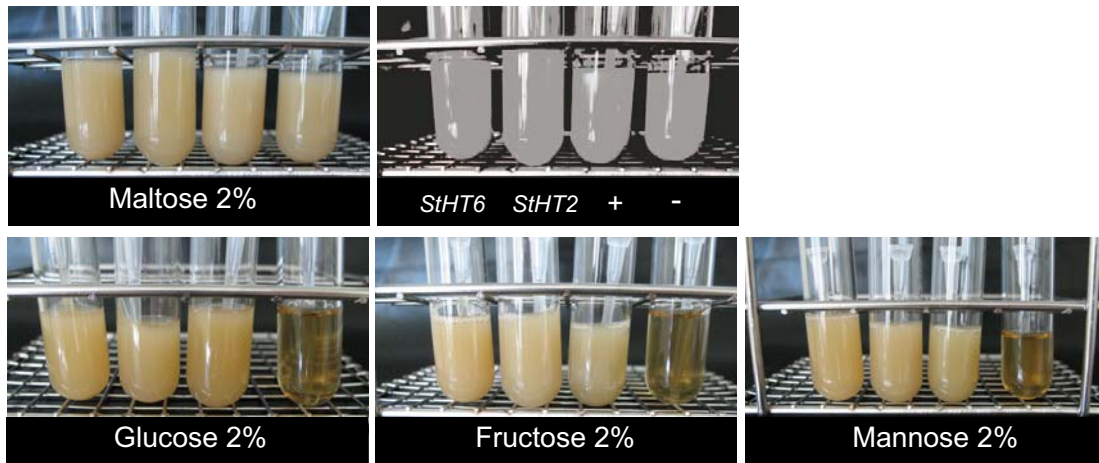


Figure 3.4. Growth test of the hexose-uptake impaired yeast mutant EB.Y.VW4000, complemented with StHT6 and StHT2, in liquid medium. Overnight cultures of EB.Y.VW4000 expressing heterologously StHT6 or StHT2, one negative control expressing the empty vector pNH196 and one positive control expressing the *S. cerevisiae* high-affinity sugar transporter HXT2 were diluted to an OD₆₀₀ of 1 and used as inoculum for 2X YPDA (pH 6.5) with 2% hexose content. Cultures were incubated for 2 days at 37 °C and 200 rpm.

3.1.4 Phylogenetic Analysis of StHT6 and StHT2

A phylogenetic tree was constructed based on the amino acid sequences of different plant monosaccharide transporters including the newly isolated potato transporters StHT6 and StHT2 (Fig. 3.6). According to this tree, four different groups of monosaccharide transporters could be distinguished which are highlighted with green, orange, or lilac boxes. It shows also, that StHT6 and StHT2 are only distantly related and belong to different groups. StHT6 clusters together with sugar transporters from several plants like rice, maize, sorghum, *Vitis vinifera* and *Arabidopsis thaliana* in the group highlighted in green, whereas StHT2 clusters together with transporters of tomato, maize and *A. thaliana* in the orange group.

In addition, the NCBI database was screened by BlastN for orthologues of StHT6 in *Solanum lycopersicum* and *Medicago truncatula*. Thus, the putative orthologue from *Medicago* could be identified on chromosome 3 (accession no. CU467812). The orthologue in tomato which was found in this Blast with the accession no. AK323115, is described as a cDNA clone isolated from leaf tissue by Aoika et al. (2010). The tomato (SIHT6) and the *Medicago* transporter (MtHT6) were named according to their homology to the potato hexose transporter 6.

None of the new identified potato sugar transporters appeared to be orthologous to the monosaccharide transporter 1 (MtST1) identified in the model legume *M. truncatula* (Harrison et al., 1996). MtST1 was also isolated from mycorrhizal roots and showed an enhanced expression during mycorrhization (Harrison et al., 1996).

3.1 Characterisation of Sugar Transporters from Potato

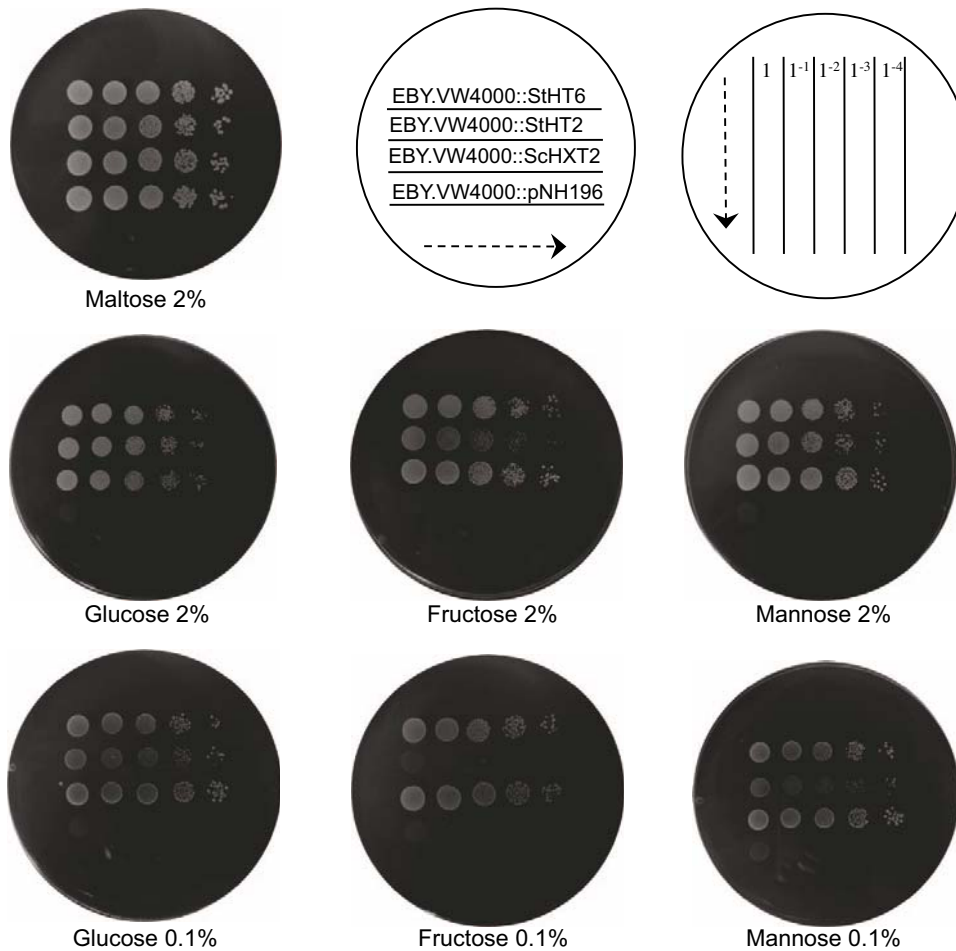


Figure 3.5. Growth test of the EB.Y.VW4000 yeast mutant complemented either with the *S. tuberosum* monosaccharide transporter *StHT6* and *StHT2* or the *S. cerevisiae* high-affinity sugar transporter *HXT2*. As negative control EB.Y.VW4000 was transformed with the empty vector pNH196. The yeast clones were spotted in a dilution series on YNB medium (pH 6.5) containing different hexoses as carbon source in two different concentrations (2% or 0.1%). The plates were incubated for 4 days at 37 °C. The sampling schema is shown in the upper right panel.

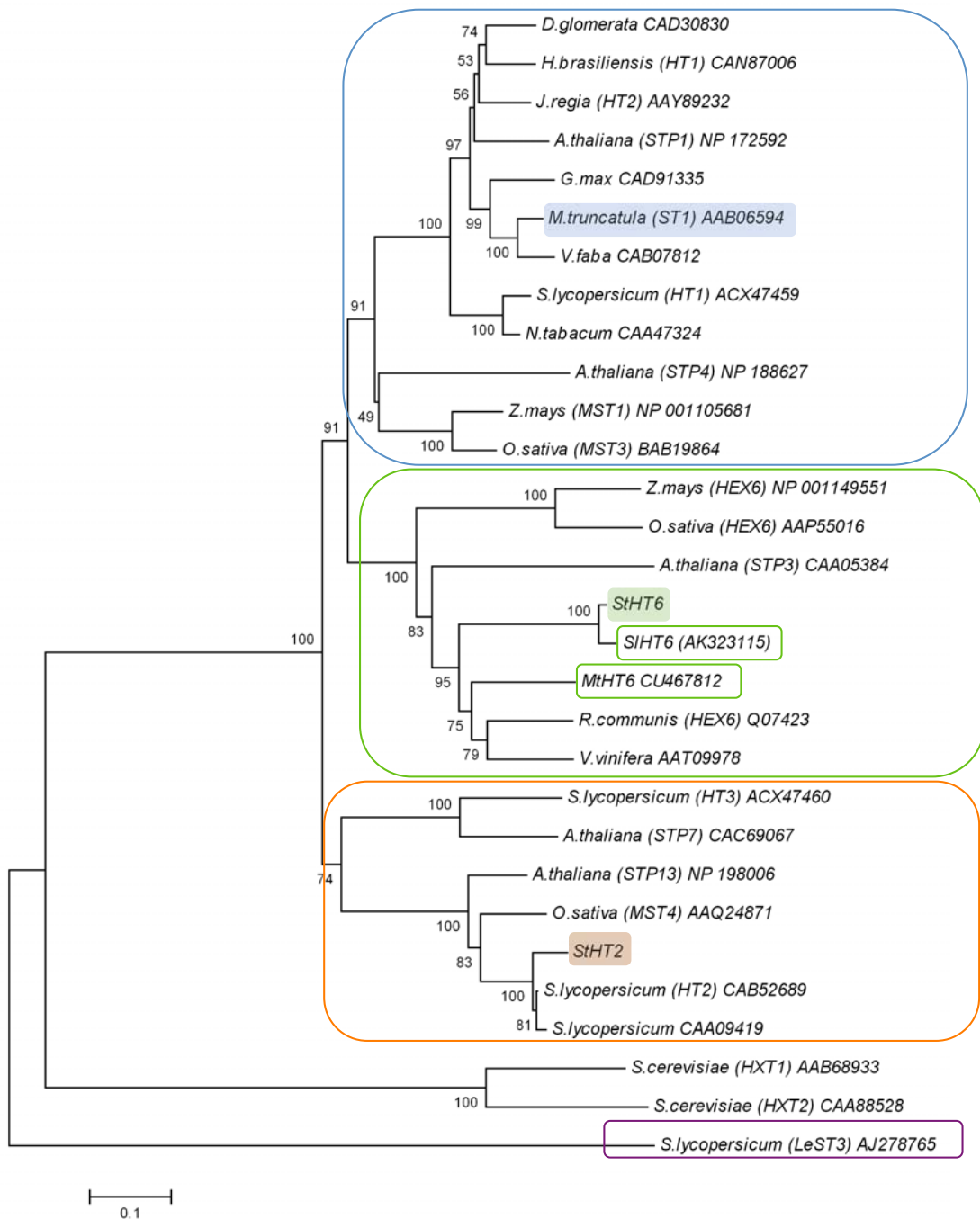


Figure 3.6. Phylogenetic tree of plant monosacchride transporters. The dendrogram was generated by MEGA 4.0 software using ClustalW for the alignment and the neighbour-joining method for the construction of the phylogeny. Bootstrap tests were performed using 1000 replicates. The branch lengths are proportional to the phylogenetic distance. The sequences of the yeast hexose transporters HXT1 and HXT2 were used as outgroup. Four groups were outlined with blue, green, orange and lilac boxes. StHT6 is marked in green. The putative orthologues of StHT6 and MtHT6 are outlined with green unfilled boxes. MtST1 is marked in blue, StHT2 in orange.

3.1.5 Expression of Plant Sugar Transporters During Mycorrhization

The transcript levels of *StHT6* and *StHT2* were determined in microdissected samples (non- (-), less- (+) and heavily- (++) mycorrhized) using quantitative real-time PCR (see also Chap. 3.1.1). Both transporters showed a basal expression level in non-mycorrhized root samples but *StHT6* had a higher overall expression. Interestingly, *StHT6* expression was upregulated with the increase of *StPT4* transcript levels, whereas *StHT2* was not affected by mycorrhization (Fig. 3.7 a). To determine the positive correlation of *StHT6* and *StPT4* expression, a time course experiment with the potato hairy root line *S.tuberosum*-p*StPT3*-FT-GUS was performed (Fig. 3.7b). The roots were mycorrhized with *G.intraradices* in the two-compartment *in vitro* system (Chap. 2.2.1). After contact with fungal hyphae, full roots were selected after 3, 11, 14 and 32 days for RNA extraction. The expression of *StPT4* was used to study the dynamic of mycorrhization on the gene level. After three days no transcript levels of *StPT4* were detectable indicating that at this time no arbuscule formation occurred. With the formation of functional arbuscules, represented by a significant increase of *StPT4* level between 11 and 14 days, the symbiosis was fully established. A decrease in *StPT4* transcripts after 32 days correlated with arbuscular collaps which is typically observed at this time. *StHT6* showed a similar dynamic with the highest expression after 14 days and a slight decrease after 32 days. In full roots the overall expression of *StHT6* was much higher than in the arbuscule-enriched samples (Fig. 3.7) indicating that *StHT6* is not exclusively expressed in arbuscule-containing cells but also in other root tissues.

In addition, the expression of the *M. truncatula* monosaccharide transporters *MtST1* and *HT6* was measured in non-mycorrhized (non-myc) and mycorrhized (myc) *M. truncatula* hairy roots (*M. truncatula*-AR*qua1*) 14 days after colonisation with *G. intraradices* (Fig. 3.8) . Expression levels were determined in three different root samples. *MtST1* was reported as a mycorrhiza-inducible sugar transporter showing increased transcription in colonised roots (Harrison et al., 1996) as it was observed for the potato transporter *HT6* (this work; Fig. 3.7). *MtHT6* was found by BlastN analysis as the most probable orthologue of *StHT6* (this work; Chap. 3.1.4). Fig. 3.8 shows that *MtST1* transcripts accumulated in mycorrhized roots, as it was demonstrated previously by Harrison et al. (1996). In contrast, *MtHT6* was not differential expressed between non-myc or myc samples. The expression pattern resembled that of the isolated potato transporter *StHT2* (Figs. 3.7 a and 3.8). The expression of *MtPT4* was measured to determine internal colonisation and formation of functional arbuscules. In non-mycorrhized roots no *MtPT4* transcripts were detectable (data not shown).

3.1.6 Promoter Studies of *StHT6* and *MtST1*

The promoter sequence of *StHT6* was isolated by genome walking from a genomic library. This library was constructed in this work from genomic DNA of the potato hairy root line *S.tuberosum*-p*StPT3*-FT-GUS (Chap. 2.7.7). With the gene-specific primers HT6_GSP1, HT6_GSP2 and HT6_GSP1a, HT6_GSP2a in combination with the adaptor-

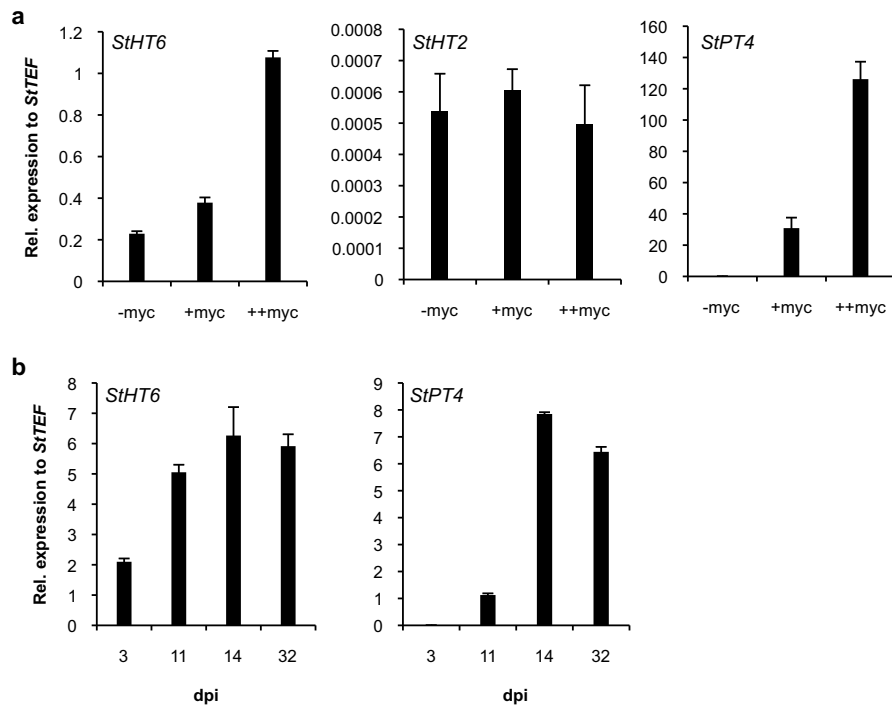


Figure 3.7. Effect of mycorrhization on *StHT6* and *StHT2* expression. **a**, Expression of *StHT6*, *StHT2* and *StPT4* in three microdissected root samples (non-mycorrhized, -myc; less-mycorrhized, +myc; full-mycorrhized, ++myc). **b**, Expression of *StHT6* and *StPT4* in a time course of potato hairy roots mycorrhized for 3, 11, 14 and 32 days post inoculation (dpi) with *G. intraradices*. (Bars represent s.d.)

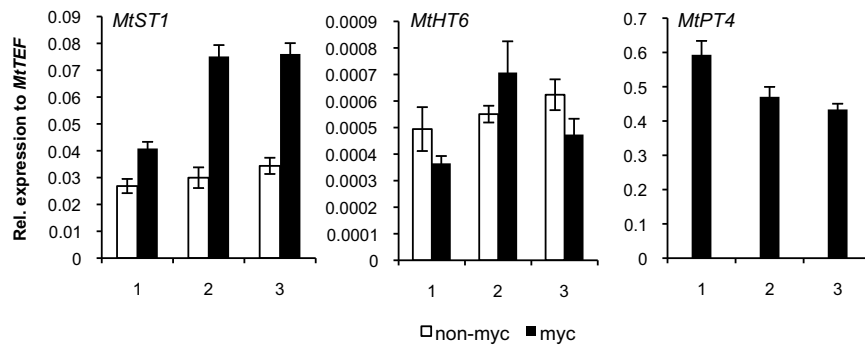


Figure 3.8. Expression analysis of *MtST1*, *MtHT6* and *MtPT4* in non-mycorrhized (non-myc) and mycorrhized (myc) *M. truncatula* hairy roots. The roots were colonised in the two-compartment system with *G. intraradices* for 14 days. Three independent root samples were used for quantitative real-time PCR analysis (1, 2, 3). (Bars represent s.d.)

3.1 Characterisation of Sugar Transporters from Potato

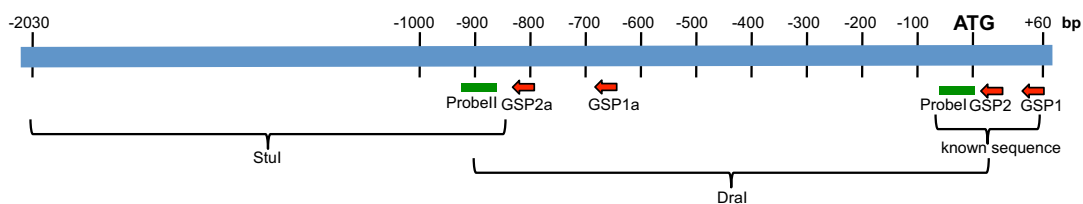


Figure 3.9. Schema of the promoter isolation of *StHT6* by genome walking. The first 900 bp were amplified from the *DraI* library using the primers HT6_GSP1 and GSP2. Additional ca. 1,200 bp were amplified from the *StuI* library with the primers HT6_GSP1a and GSP2a. The Probe I and Probe II were used for the identification of positive clones by southern blotting. The upper scale represents bp upstream or downstream of the ATG (+1).

specific primers ASP1, ASP2, it was possible to amplify a 2.0 kb fragment upstream of the ATG (Fig. 3.9). The full sequence was amplified and cloned in the pENTR/D-Topo vector using the primers pStHT6_F1 and pStHT6_R1. Additionally, 2.3 kb of the promoter sequence of the sugar transporter 1 from *Medicago truncatula* (MtST1) was isolated by PCR using the primers pMtST1_F1 and pMtST1_R1 and cloned in the pENTR/D-Topo vector.

Both promoter fragments (pHT6 and pST1) were fused by Gateway cloning to the GFP-GUS reporter cassette of the plant binary vector pPGFPGUS-RedRoot (see Chap. 2.7.4). The new plasmids pHT6-GFP-GUS-RR and pST1-GFP-GUS-RR were introduced in *Medicago* or tomato hairy roots via *A. rhizogenes* mediated transformation (Chap. 2.3.5). The fluorescence reporter GFP was not useful for promoter studies under the fluorescence microscope due to the high background fluorescence of the hairy roots. Nevertheless, the GUS reporter gave a precise picture of promoter activity before and after mycorrhization. Fig. 3.10 shows the promoter activity of StHT6 and MtST1 in non-mycorrhized tomato and *Medicago* roots. GUS was expressed for every combination (pStHT6 expressed in tomato, pStHT6 in *Medicago*, pMtST1 in tomato and pMtST1 in *Medicago*) in the vascular cylinder, in old root tips and young root tips of newly developing lateral roots. However, GUS expression was also detected in arbusculated cells (Fig. 3.11). While the activity of pHT6 in tomato, both solanaceous species, was not surprising, the activity of pHT6 in *Medicago*, belonging to a different plant family, as well as pST1 activity in tomato was quite interesting.

The fact that the promoters of *S. tuberosum* and of *M. truncatula* worked heterologously expressed in different plant species indicates that the promoter elements for the expression of both sugar transporters are conserved. Therefore, promoters of StHT6 and MtST1 were analysed *in silico* using the PLACE database. Thus, different cis-regulatory elements were identified in both promoter sequences commonly found in genes regulated by sugar. One representative element was SURE (sucrose responsive element) identified in genes up-regulated by sucrose (Grierson et al., 1994). The SURE1 element (AATAGAAAA) was found in pHT6 at position -1775 (+strand) and in pST1 at position -1349 (+strand). In addition, the SURE2 element (AATACTAAT) was found in pHT6 at position -1384 (-strand) and one putative Suc box 3 at position -137 (-strand) (AAAATCATAA) (Hattori et al., 1990; Tsukaya

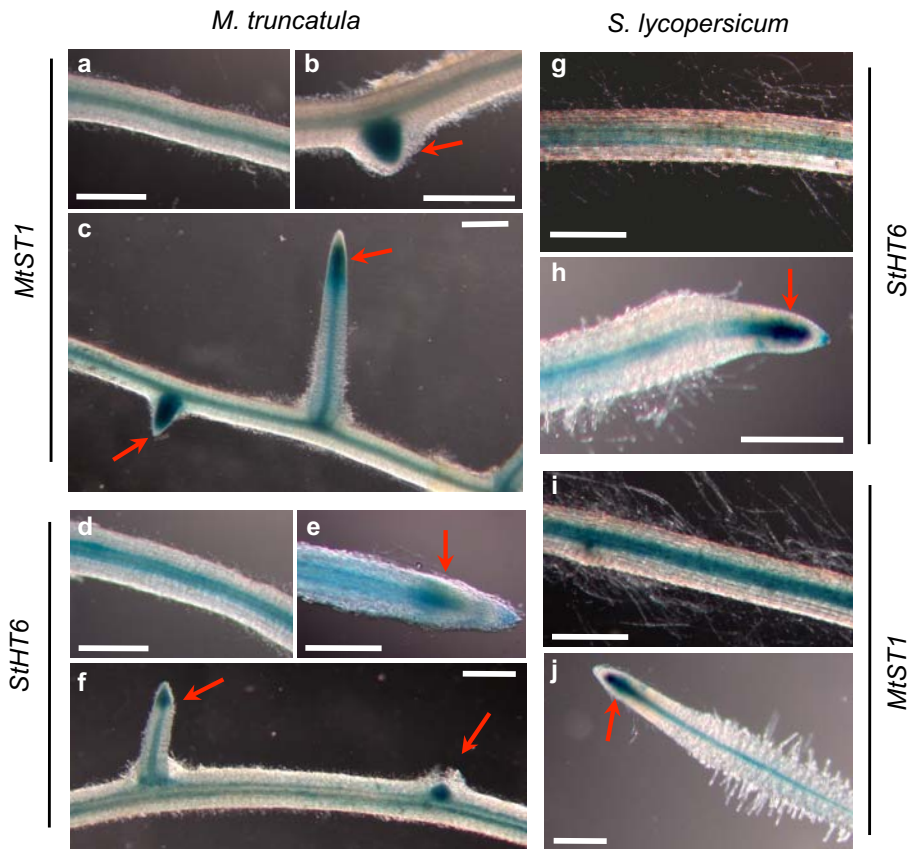


Figure 3.10. GUS staining of non-mycorrhized *M. truncatula* roots transformed with promoter-reporter constructs for StHT6 and MtST1. **a-c**, Homologous expression of the *gus* gene under control of the MtST1 promoter in *M. truncatula*. **d-f**, Heterologous expression the *gus* gene under control of the StHT6 promoter in *M. truncatula*. **d-f**, Homologous expression the *gus* gene under control of the StHT6 promoter in *S. lycopersicum*. **i, j**, Heterologous expression of the *gus* gene under control of the MtST1 promoter in *S. lycopersicum*. Red arrows indicate GUS expression in old and new root tips. (Bars indicate 200 μm)

3.1 Characterisation of Sugar Transporters from Potato

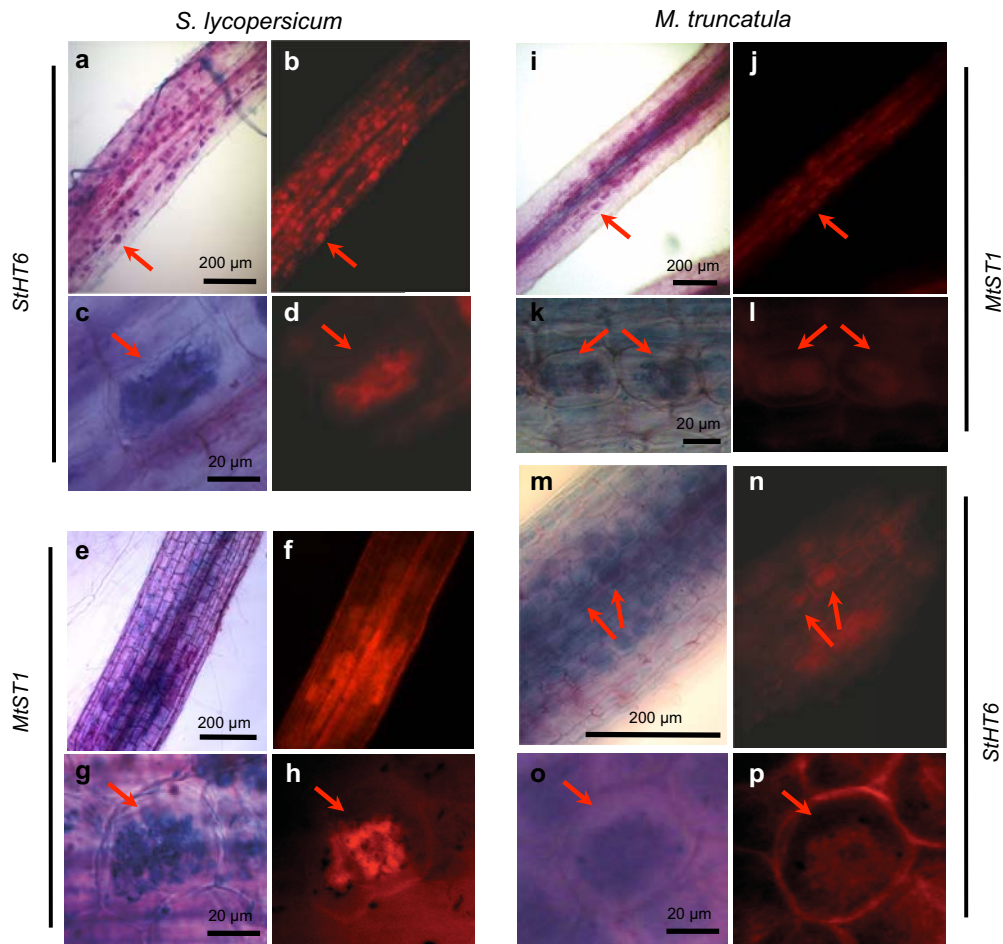


Figure 3.11. GUS and acid fuchsin counter staining of mycorrhizal *M. truncatula* transformed with promoter-reporter constructs for StHT6 and MtST1. **a, c, e, g, i, k, m, o,** Blue GUS staining indicates promoter activity in arbusculated cells. **b, d, f, h, j, l, n, p,** Fuchsin stained fungal structures within roots under the fluorescent light. GUS and fuchsin staining are overlapping. Red arrows indicate exemplary arbuscule-containing cells.

et al., 1991). A motif solely presented in pST1 at position -269, -1436 (+strand) and -1744 (-strand) is the AMYBOX1 (TAACAAA) conserved in α -amylase promoters of rice, wheat (*Triticum aestivum*), and barley (*Hordeum vulgare*) as an essential element of negative regulation by sugar (Huang et al., 1990). The AMYBOX2 (TATCCAT) (Huang et al., 1990) also known as sugar starvation enhancer element in α -amylase 5' region (Lu et al., 1998) was found in pST1 just at one position, -2231 (-strand). Another promoter element in common between both genes is the OSE1ROOTNODULE (AAAGAT) and OSE2ROOTNODULE element (CTCTT) described in genes expressed in root nodule infected cells as well as in arbuscule-containing cells (Vieweg et al., 2004; Fehlbeg et al., 2005). In pHT6 the OSE1ROOTNODULE element was found four times on location -935 (+strand) and on location -790 and -1115 (-strand), the OSE2ROOTNODULE (CTCTT) element seven times in minus-strand orientation on position -201, -358, -1029, -1077, -1708, -2038 and -1772. In pST1 the OSE1ROOTNODULE element was found on the positive strand at -159, -198, -729, -1113, -1266, -1570 and on the negative strand at -989, -1302, -1939. OSE2ROOTNODULE was found at position -25, -56, -111, -1589, -2190, -2198, -2342 (+strand) and at position -882, -896, -1931 (-strand). Putative cis-regulatory elements common in mycorrhizal specific phosphate transporters are the CTTC-motif (CTTCTTGTTCTA) presented in several AM inducible genes and the TAAT-motif (TAATATAT) specific for AM phosphate transporters (Karandashov et al., 2004). In the mycorrhiza-inducible sugar transporter StHT6 a modified CTTC-motif was found in the minus strand at position -845 with the sequence (AA)TCTTGTT(AAC) almost at the same position as in the promoter region of MtPT4 (-838) and in the AM induced *Medicago* gene MtGST1 (-864) (Karandashov et al., 2004). Also putative TAAT-motifs were located on the minus strand at -771 and on the positive strand at -514 presented with the sequence (C)AATATA. This motif was found in the StPT3 promoter (TAATATAT) at position -525, in MtPT4 (TAATATAT) at -90 and in LePT4 (GAATATAT) at -674 (Karandashov et al., 2004). In pST1 a modified CTTC-motif ((A)TT(A)TTGTTC(GTA)) could be found at position -671, whereas the full TAAT-motif was found at position -772 (-strand) and in modified form ((G)AATATAT) at -2168 (+strand). Fig. 3.12 shows the location of the most prominent motifs in both promoter sequences.

3.2 Characterisation of AM Fungal Sugar Transporters

The main purpose of the cDNA library screens described in the previous chapters was the identification of so far unknown sugar transporters from the AM fungus *G. intraradices*. Unfortunately, this method emerged to be not sensitive enough to isolate fungal transporters. However, with the release of the first draft of the *G. intraradices* genome sequencing putative sugar transporter sequences could be identified by Blast search in this work.

The United States Department of Energy's Joint Genome Institute (JGI) started with the sequencing of the *G. intraradices* isolate DAOM 197198 in 2004 using a whole genome shotgun approach. Four years later they were able to present a 4-fold cov-

3.2 Characterisation of AM Fungal Sugar Transporters

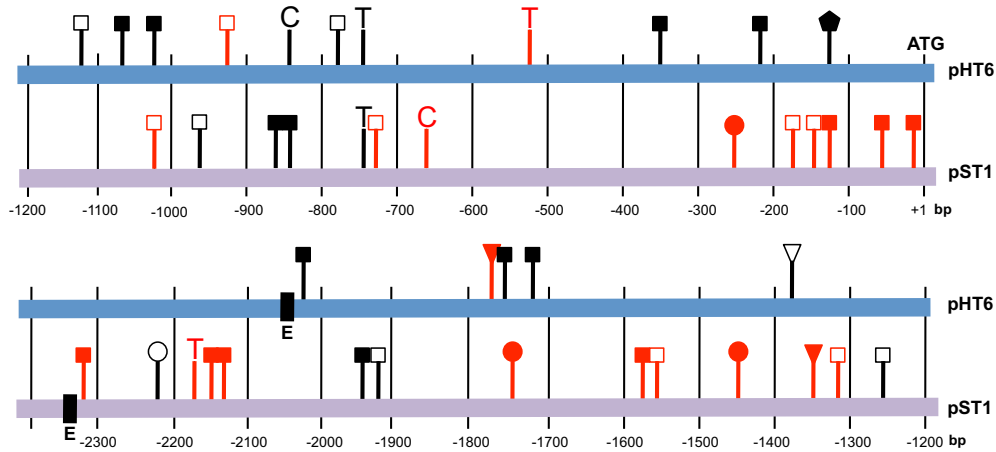


Figure 3.12. Putative cis-regulatory elements in the promoter sequences of the sugar transporters StHT6 (pHT6: blue) and MtST1 (pST1: lilac). The lower scale represents base pairs upstream of the transcriptional start codon ATG (+1). (closed triangle: SURE1; open triangle: SURE2; open box; pentagon: SUCBOX3; closed circle: AMYBOX1; open circle: AMYBOX2; open box: OSE1ROOTNODULE; closed box: OSE2ROOTNODULE; C: CTTC-motif; T: TAAT-motif; red: elements on the +strand; black: elements on the -strand; E means end-of-sequence)

erage of whole genome sequencing, but the assembly remained complicated due to the great abundance of repetitive and polymorphic sequences. The size of the *G.intraradices* genome is estimated at around 150 Mb (Peter Young and Francis Martin, personal communication). As expected for AM fungi, the genome of *G. intraradices* has a very low GC content (approximately 30%) (Hosny et al., 1997). In addition, ESTs derived from PCR amplified or normalised cDNA libraries of germinated spores or extraradical mycelium (ERM) were sequenced. Sequences of ESTs and contig reads are stored in the INRA GlomusDB database (<http://mycor.nancy.inra.fr/IMG/GlomusGenome/index.html>) available at the moment only for consortium members.

3.2.1 Screening for MFS Transporters in the Genome Database

The major facilitator superfamily (MFS) represents the largest family of secondary membrane transporters (Pao et al., 1998). Originally MFS were believed to function primarily in the uptake of sugars, but in the meanwhile they were expanded to 65 distinct families including transporters specific for phosphate, amino acids, drugs etc. (<http://www.tcdb.org/>). This superfamily is ubiquitous in all kingdoms of life acting as uniporters, symporters or antiporters (Law et al., 2008). Typically MFS transporters posse a uniform topology of 12 transmembrane helices forming two domains which surround a substrate-translocation pore (Law et al., 2008).

To get an overview of the MFS superfamily in *G. intraradices*, the database was screened in this work specifically for genes encoding MFS transporters. Fig. 3.13 gives an impression of MFS transporters in the *G. intraradices* genome.

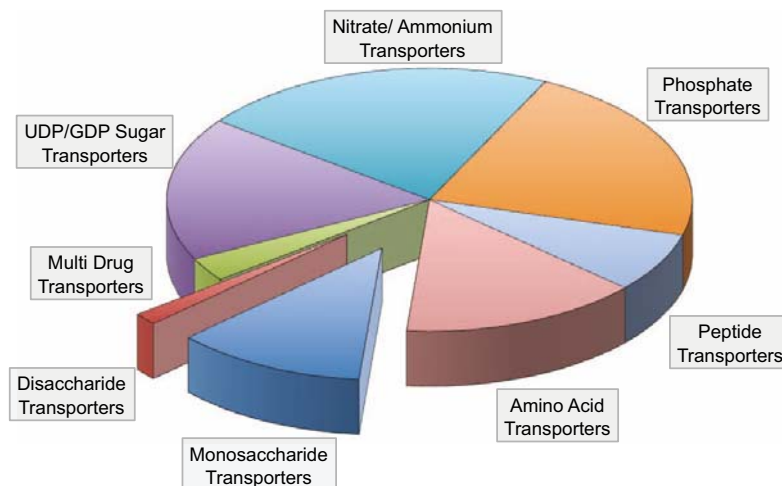


Figure 3.13. Putative MFS transporters found the *G. intraradices* genome database in this work. The outlined sections represent di- and monosaccharide transporters. (Disaccharide Transporters 1%; Monosaccharide Transporters 12%; Amino Acid Transporters 15%; Peptide Transporters 7%; Phosphate Transporters 22%; Nitrate/Ammonium Transporters 22%; UDP/GDP Sugar Transporters 18%; Multi Drug Transporters 3%)

3.2.2 Putative Sugar Transporters of *G. intraradices*

Among the identified MFS transporters, five partial genomic or EST sequences belonging to the sugar transporter superfamily were found in the *G. intraradices* genome by Blast search. Four of these transporters showed high similarity to genes encoding monosaccharide transporters (GiMST1–4) whilst one of them had higher similarity to a sucrose transporter (GiSUC1) (Tab. 3.3).

The Artemis annotation program was used to determine the partial open reading frame and the deduced amino acid sequence of those sugar transporters. The ClustalW program was used to generate a protein alignment in order to find out which part the protein is missing. Thus, the partial monosaccharide transporters sequences of *G. intraradices* were aligned against the sequence of the *Uromyces viciaefabae* sugar transporter HXT1 (CAC41332) as a typical fungal sugar transporter, whereas the GiSUC1 was aligned against the *Ajellomyces capsulatus* sucrose transporter EER44596. The results of these alignments are illustrated in Fig. 3.14. All partial sequences are located near the N-terminus.

Expression analyses using quantitative real-time PCR during different developmental stages of the life cycle of the fungus (spores, ERM, arbuscules) revealed that only *GiMST1* was highly induced during the *in planta* phase, and just detectable during the other stages (Fig. 3.15). Thus, it was proposed that *GiMST1* is involved in the symbiotic carbon transfer.

3.2 Characterisation of AM Fungal Sugar Transporters

Putative Sugar Transporters	NCBI Blastp Search Results					
EST or Contig Name	Accession Number	Organism	Description	Score	Evalue	Identity
Contig 22709 (<i>GiMST1</i>)	XP_001270693	<i>Aspergillus clavatus</i>	MFS sugar transporter, putative	115 (289)	1e-24	49 %
Contig 92861 (<i>GiMST2</i>)	XP_002487894	<i>Talaromyces stipitatus</i>	Sugar transporter, putative	187 (475)	7e-46	42 %
16504_0 (<i>GiMST3</i>)	EEH47391	<i>Paracoccidioides brassiliensis</i>	Glucose transporter	164 (416)	5e-39	40 %
11118_1 (<i>GiMST4</i>)	XP_002376006	<i>Aspergillus flavus</i>	MFS glucose transporter, putative	133 (335)	5e-30	70 %
7569_1 (<i>GiSUC1</i>)	EER44596	<i>Ajellomyces capsulatus</i>	Sucrose transporter	128 (544)	1e-53	57 %

Table 3.3. Putative sugar transporters found in the *G. intraradices* genome database by Blast searches in this work.

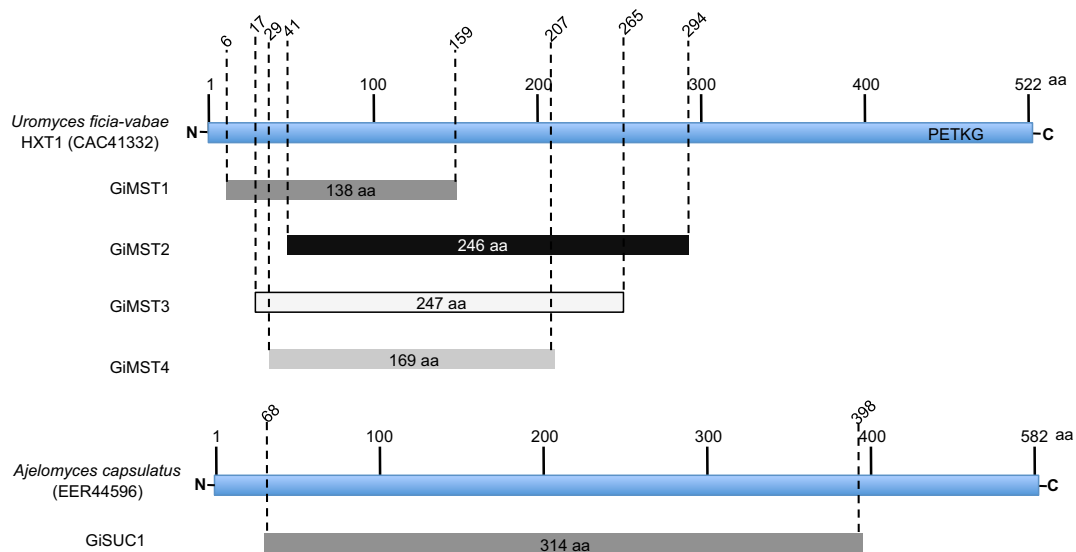


Figure 3.14. Location of the partial amino acid sequences of *G. intraradices* sugar transporters compared to the *Uromyces ficia-vabae* hexose transporter HXT1 (CAC41332) or the sucrose transporter of *Ajelomyces capsulatus* (EER44596). The location of the PETKG motif which is characteristic for hexose transporters is indicated at the C-terminus of HXT1.

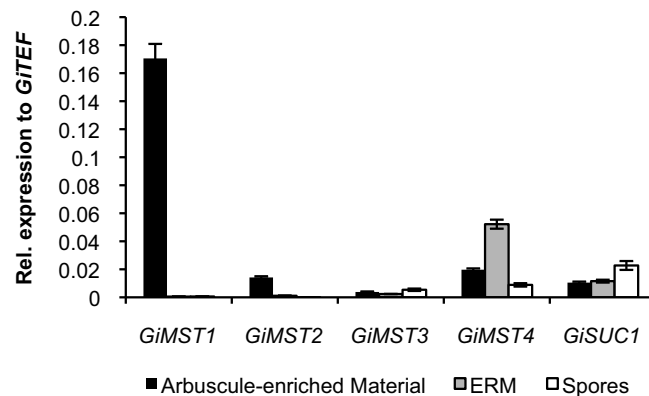


Figure 3.15. Expression analysis of putative sugar transporters of *G. intraradices* in different fungal tissues by qPCR. The arbuscule-enriched material originates from the microdissection of potato hairy roots colonised with *G. intraradices*. Results are presented as relative expression to the *G. intraradices* transcription elongation factor alpha 1 (*GiTEF*). (Bars represent s.d.)

3.2.3 Isolation of *GiMST1* and *GiMST2*

The original sequence of *GiMST1* (contig 922709) was found by a Blast search in the *Glomus* genome database using the amino acid sequences of the monosaccharide transporter HXT1 from *T. borchii* (AAY26391) and of a high-affinity glucose transporter from *P. tritrici-repentis* (XP001938670) as query. The intron/exon boundaries in the genomic sequence were defined using the Artemis annotation program to determine the predicted open reading frame (ORF) and the deduced amino acid sequence. A protein alignment with other fungal sugar transporters showed that 1.2 kb of the *GiMST1* 3' end were still missing. Thus, the full sequence of *GiMST1* was isolated by RACE PCR from an amplified SMART cDNA library of microdissected micorrhizal potato roots (see Chaps. 2.8, 2.9.1, and 3.1.1). Additionally, 1 kb of the *GiMST1* cDNA sequence was isolated using the CDSdown_R1 with the *GiMST1*-specific primer MST1down_F1 or the nested primer MST1down_F2. However, further sequence analyses showed that the 3' end was still absent which was isolated in a second RACE PCR using the primers CDSdown_R1 and MST1down_F3 as well the nested primer MSTdown_F4 (see Fig. 3.16). The 1.5 kb cDNA of *GiMST1* encodes for a 490 aa protein with 54 kDa. Protein analysis revealed that *GiMST1* is a MFS sugar transporter with the conserved motifs pfam00083 and cd06174 (characteristic for MFS proteins). Hydrophobicity analysis using the TMHMM and the ToPred program predicted 12 TMD with cytoplasmic N- and C-terminal ends and an intracellular loop between TMD6 and TMD7. The genomic sequence of *GiMST1* is 2.9 kb and contains 12 introns. *GiMST1* has a relative low GC content (37% for cDNA and 29% for genomic DNA) which is typical for AM fungal genes.

In Blast screens using the sequences of the sugar transporter HXT1 from *T. borchii* (AAY26391) and HEXT1 from *U. fabae* as query, a 1.2 kb genomic sequence of a second sugar transporter was found in the contig 92861. This transporter was named

3.2 Characterisation of AM Fungal Sugar Transporters

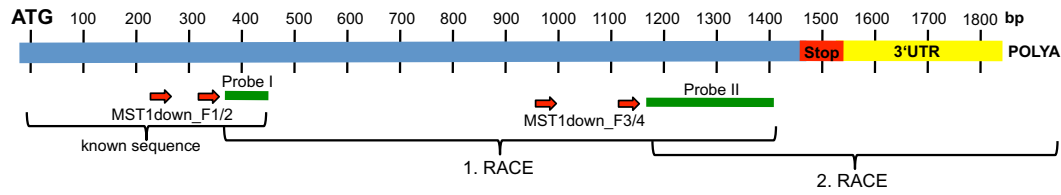


Figure 3.16. Schema of the RACE PCR for the isolation of *GiMST1*. In a first RACE PCR with the gene-specific primers MST1down_F1 and the nested primer MST1down_F2, 1 kb downstream of the ATG was isolated. The 3' end with 3'UTR (untranslated region) was amplified in a second RACE PCR with the gene-specific primers MST1down_F3 and the nested primer MST1down_F4. Specific probes in the known sequence regions were used for screening of the isolated clones. Scale bar represents base pairs downstream of the ATG (+1).

GiMST2. As for *GiMST1*, amino acid sequence comparison with other transporters demonstrated that 500 bp of the 5' and 400 bp of the 3' end were missing. Expression analysis of this transporter showed highest transcript levels for *GiMST2* in the ERM growing together with hairy roots of the tomato *rmc* mutant (see Chap. 3.5). Thus, both missing ends were isolated from a ERM/*rmc* cDNA library which was created in this work with the GeneRacer™ Kit by RACE PCR (Chapt. 2.7.6; Fig. 3.18). The 5' end was isolated using the GeneRacer™ 5' primer and the gene-specific primer MST2_GSP1 and the nested primers GeneRacer™ 5'Nested and MST2_GSP2. The 3' end was amplified with the primer GeneRacer™ 3' and MST2_GSP1a and the nested primers GeneRacer™ 3'Nested and MST2_GSP2a. The isolated 1.5 kb ORF of *GiMST2* has a GC content of 34 % and encodes a 512 aa protein of 57 kDa. The genomic sequence of *GiMST2* is 2.7 kb with a GC of 29 % and contains 14 introns. The amino acid sequences of *GiMST1* and *GiMST2* show highly homologous regions and have an identity of 63 %. *GiMST2* contains the same conserved domains as shown for *GiMST1*. Nevertheless, hydrophobicity analysis of *GiMST2* gave different predictions. Thus, while the THMM program predicts 11 TMDs for *GiMST2* in contrast to the 12 predicted for *GiMST1*. However, using the ToPred program 12 TMD are also found for *GiMST2*. Fig. 3.19 shows the protein alignment of both transporters and the predicted TMDs.

Phylogenetic analysis showed that *GiMST1* and *GiMST2* cluster with a group of fungal sugar transporters that includes several xylose transporters (Fig. 3.17). Surprisingly, *GiMST1* and *GiMST2* are only distantly related to the *G. pyriformis* monosaccharide transporter GpMST1 (24.6 % amino acid identity with *GiMST1* and 20.5 % with *GiMST2*). The protein alignment of the three glomeromycotan sugar transporters is shown in Fig. B.10. The full cDNA sequences of *GiMST1* and *GiMST2* are shown in Figs. B.7 and B.9.

3.2.4 *GiMST1* Expression and Transcript Localisation in planta

Further quantitative real-time PCR experiments were performed to investigate the function of *GiMST1* in carbon acquisition in the AM symbiosis. First, transcript levels of all sugar transporters in +myc and ++myc cDNA samples of microdissected myc-

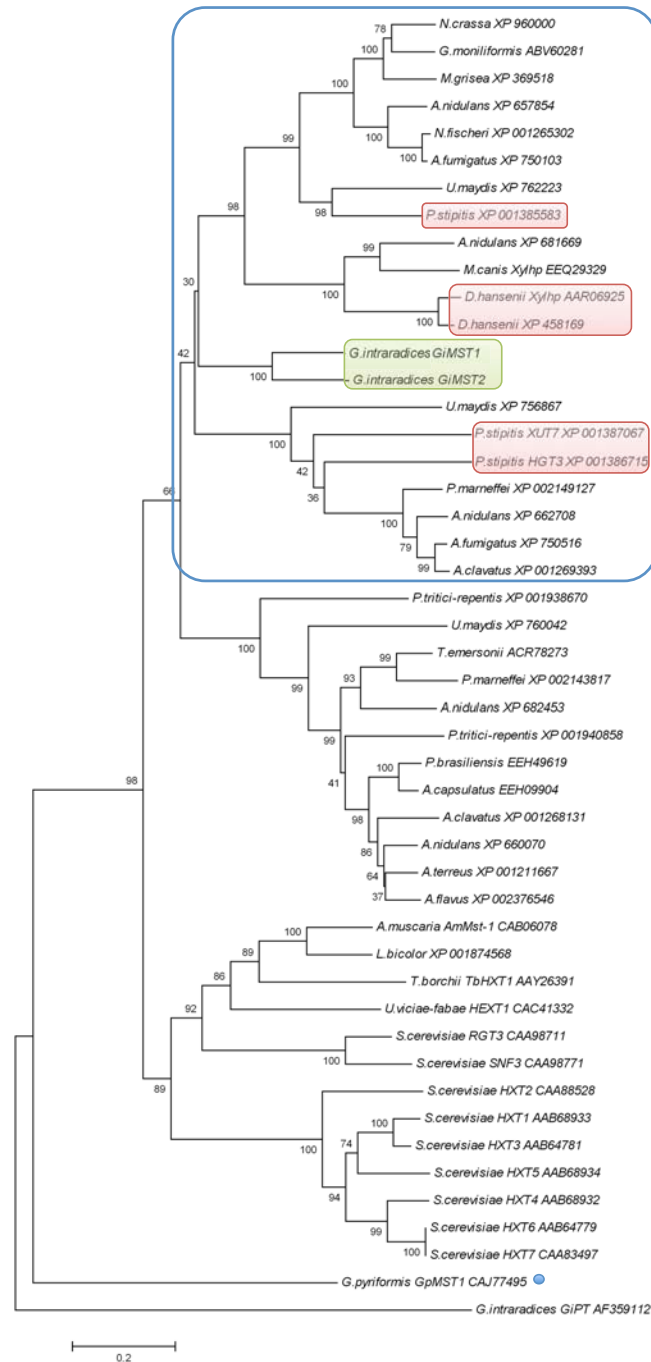


Figure 3.17. Phylogenetic tree of fungal monosaccharide transporter protein sequences. The dendrogram was generated by MEGA 4.0 software using ClustalW for the alignment and the neighbour-joining method for the construction of the phylogeny. Bootstrap tests were performed using 1000 replicates. The branch lengths are proportional to the phylogenetic distance. The sequence of the phosphate transporter GiPT from *G. intraradices* (AF359112) was used as outgroup. GiMST1 is highlighted in green, clusters together with fungal xylose transporters are shown in red. A square delimits a group of putative xylose transporters. The *G. pyriformis* monosaccharide transporter, GpMST1, is marked with a blue circle.

3.2 Characterisation of AM Fungal Sugar Transporters

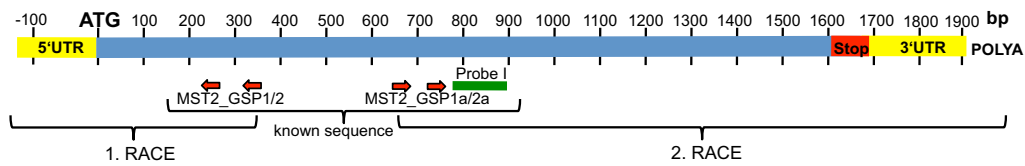


Figure 3.18. Schema RACE PCR *GiMST2*. The 5' end with the 5' UTR (untranslated region) was amplified using the gene-specific primers MST2_GSP1 and GSP2. The 3' end with 3'UTR was amplified with the gene-specific primers MST2_GSP1a and GSP2a. Probe I was used to identify positive clones in the 2nd RACE PCR. Upper scale represents bp upstream or downstream of the ATG (+1).

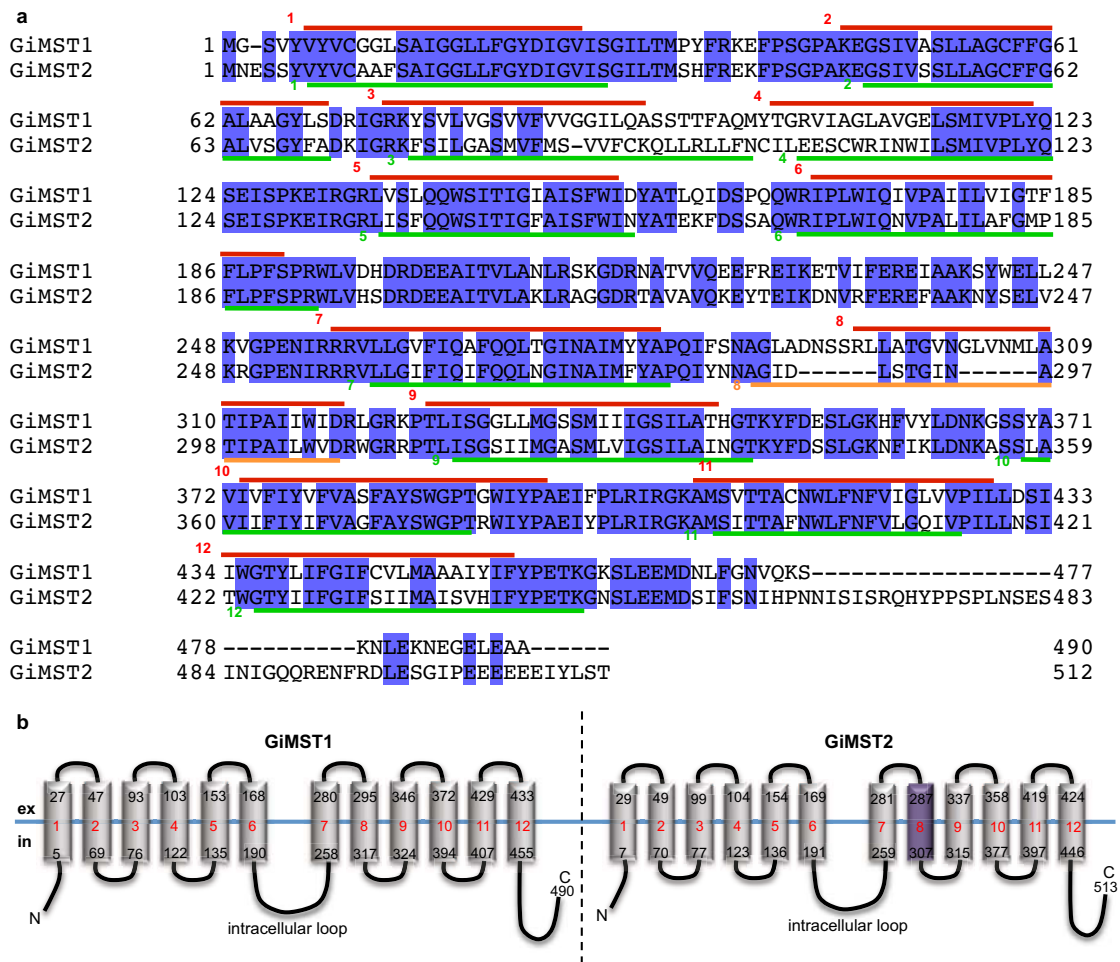


Figure 3.19. Transmembrane domains of *GiMST1* and *GiMST2*. **a**, Protein alignment of *GiMST1* and *GiMST2*. Sites of TMDs for *GiMST1* predicted by the THMM program are shown as red bars. Sites of TMDs for *GiMST2* predicted by the THMM program are shown as green bars. The additional TMD assessed by TopPred is indicated in orange. Blue indicates homologous regions. **b**, Schema of *GiMST1* and *GiMST2* TMD locations predicted by THMM. Purple TMD of *GiMST2* represents TMD predicted by TopPred.

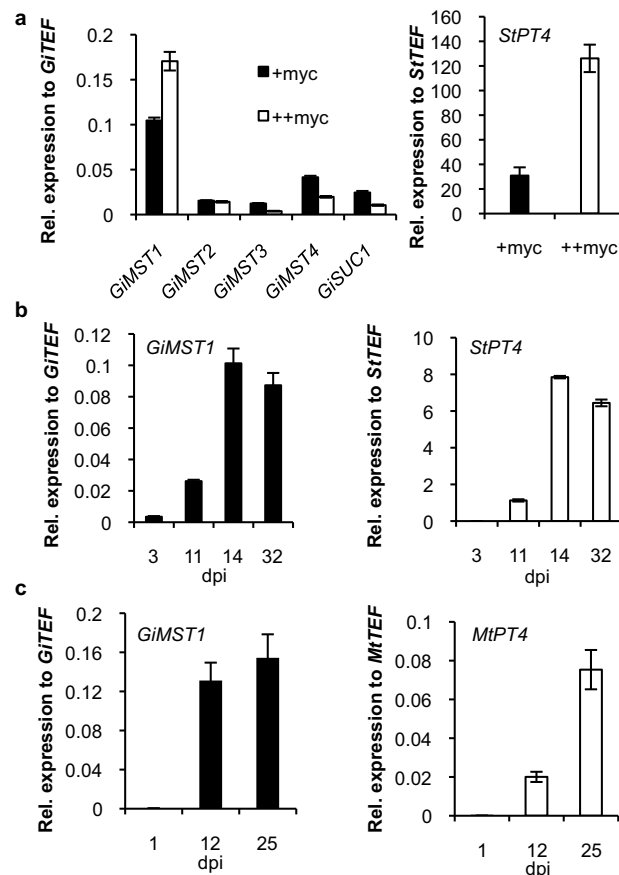


Figure 3.20. a, Relative Expression of the *G. intraradices* sugar transporters in +myc and ++myc samples of arbuscule-enriched material from mycorrhizal potato hairy roots and the corresponding expression of the *S. tuberosum* phosphate transporter *StPT4*. b, Time course analysis of expression of *StPT4* and *GiMST1* in mycorrhizal potato hairy roots after 3, 11, 14 and 32 days post inoculation (dpi). c, Time course analysis of expression of *MtPT4* and *GiMST1* in mycorrhizal *M. truncatula* roots after 1, 12 and 25 days post inoculation (dpi). (Bars indicate s.d.)

orrhizal potato roots were determined (Fig. 3.20 a). This experiment showed clearly that *GiMST1* is the most prominent transporter expressed in arbuscules. Additionally, comparing the +myc and ++myc samples, a positive correlation between *GiMST1* and *StPT4* expression could be observed. This dependency was further determined in two time course experiments with potato hairy roots and *M. truncatula* plants (Figs. 3.20 b–c). All three analyses revealed that *GiMST1* expression is linked to the expression of the symbiotic phosphate transporter *PT4*.

To identify the precise site of transcript localisation of *GiMST1*, *in situ* hybridisation was carried out on *M. truncatula* hairy roots colonised with *G. intraradices* (see also Chap. 2.13.2). Interestingly, *GiMST1* transcripts could be detected in the arbuscules but also in intraradical hyphae (Fig. 3.21). This indicates that not only arbuscules but also intraradical hyphae are sites of sugar uptake by the AM fungus.

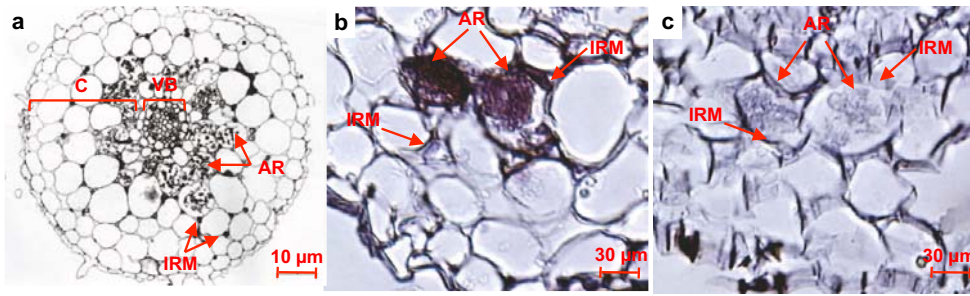


Figure 3.21. *In situ* hybridisation of *M. truncatula* hairy roots mycorrhized with *G. intraradices*. **a**, Overview of a cross-sectioned mycorrhized *M. truncatula* root. **b**, Detail of a cross-sectioned mycorrhized root hybridised with the antisense probe for *GiMST1*. Positive purple staining at arbuscules and IRM indicates *GiMST1* expression. **c**, No staining is visible in samples of the same root hybridised with the *GiMST1* sense probe. (C: cortex, VB: vascular bundle, AR: arbuscule, IRM: intraradical mycelium)

3.2.5 Functional Analysis of GiMST1 in Yeast

For biochemical studies, *GiMST1* was expressed in the hexose-uptake impaired *S. cerevisiae* mutant EBY.VW4000. This yeast mutant was already used for the characterisation of diverse fungal or plant sugar transporters (Schüßler et al., 2006; Polidori et al., 2006; Hayes et al., 2007; Wang et al., 2008). Nevertheless, it represents a heterologous expression system and instability of mRNA, mistargeting or subcellular localisation of the transporter might interfere with a successful yeast complementation. Thus, transcription and protein localisation of *GiMST1* in yeast was verified in a preliminary experiment.

Transcript accumulation of *GiMST1* was tested by quantitative real-time PCR in the EBY.VW4000 strain transformed with the yeast expression vector pNEV-MST1 (Chap. 2.10) The relative expression rates of *GiMST1* and *StHT6*, which was shown to be well expressed in yeast (this work, Chap. 3.1.3) are shown in Fig. 3.22 a. Both transporters were expressed at high levels in yeast.

The membrane localisation in yeast was tested using a *GiMST1*-GFP-tagged version. Therefore, the plasmid pEXTAG-MST1-GFP was transformed in the yeast strain EBY.VW4000 (Chap. 2.10). EBY.VW4000 expressing the *GiMST1*-GFP fusion protein and a positive control, expressing the *U. maydis* transporter HXT1 fused to GFP were compared for protein localisation under the fluorescent microscope. In both strains the GFP fusion proteins were localised at the plasma membrane (Fig. 3.22 b).

Sugar uptake of *GiMST1* was first investigated in a spotting test. Three clones expressing the pNEV-MST1 vector were tested for growth on medium with low or high sugar concentrations together with three negative controls and one positive control (Fig. 3.23). As the optimal pH for *GiMST1* was unknown to that time, a mean pH of 6.5 was used. The *GiMST1* expressing yeasts grew very poorly compared to the positive controls and growth was not visible until 11 days of incubation. The growth test showed that *GiMST1* is functional and able to restore the mutation in EBY.VW4000. Thereby, *GiMST1* complemented yeasts grew better on mannose and on plates with 2% than with 0.1% sugar concentration. Unfortunately, *S. cerevisiae* is unable to metabolise and thus to grow on pentoses like xylose or arabinose which

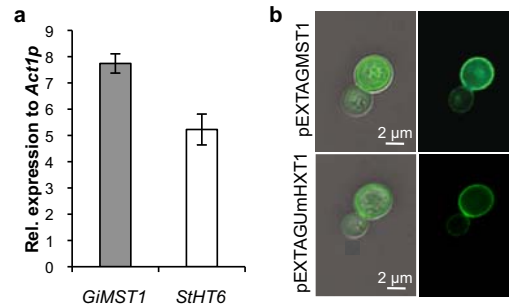


Figure 3.22. **a**, Relative expression of *GiMST1* and *StHT6* which are heterologously expressed in the yeast mutant EBY.VW4000. **b**, Localisation of the *GiMST1*-GFP fusion protein in the plasma membrane of the yeast mutant EBY.VW4000. The EBY.VW4000 strain expressing the *Ustilago maydis* sugar transporter HXT1 fused to GFP was used as positive control (kindly provided by K. Wippel, FAU, Germany).

could therefore not be tested in this assay. However, the phylogenetic tree showed a relation of *GiMST1* to fungal xylose transporters (Fig. 3.17). The transport of xylose by *GiMST1* was tested in following studies using radio-labelled ^{14}C sugars.

Quantitative uptake studies and affinity tests with radio-labelled ^{14}C sugars were also performed in the EBW.VW4000 strain expressing heterologously *GiMST1* as described in Chap. 2.12. The uptake was measured by the addition of radio-labelled sugars to a growing yeast suspension. The increase of radioactivity in the yeast cells with time was determined using a scintillation counter. Highest rates were thereby measured for glucose than for mannose, xylose and fructose (Fig. 3.24 a).

The substrate affinity of *GiMST1* for glucose was determined by measuring the Michaelis-Menten constant (K_m) which defines the substrate concentration at half of the maximal velocity. To determine the K_m value, uptake rates of *GiMST1* for different concentrations of ^{14}C glucose were measured. The Michaelis-Menten graph is shown in Fig. 3.24 b. The K_m of *GiMST1* for glucose is $33 \pm 12.5 \mu\text{M}$ (s.e.m.).

The pH optimum of *GiMST1* was defined by measuring the uptake of ^{14}C glucose by yeast cells resuspended in phosphate buffers with different pH values (pH 5, 6, 7 and 8). Fig. 3.24 c shows the mean uptake rates for glucose depending on the pH value. The highest uptake was found at pH 5 (Fig. 3.24 c).

Glucose transport was found to be sensitive to the presence of the protonophore CCCP (carbonylcyanide *m*-chlorophenylhydrazine). CCCP is a lipid soluble molecule that transports protons over the plasma membrane, thereby disturbing the proton gradient over the membrane which is important for active transport processes (Delrot und Bonnemain, 1981). The transport by *GiMST1* was significantly reduced by CCCP indicating a proton-dependent transport mechanism (Fig. 3.24 d). The uptake of glucose without CCCP was set as 100 %.

The versatility of *GiMST1* as a sugar transporter was shown in competition assays. Therefore, the reduction of ^{14}C glucose uptake was tested in the presence of non-labelled competing sugars (glucose, mannose, fructose, galactose, arabinose, xylose and ribose), sugar alcohols (mannitol, sorbitol, xylitol, myo-inositol), or carboxylic acids (glucuronic acid, galacturonic acid) which was added in 100-fold molar excess.

3.2 Characterisation of AM Fungal Sugar Transporters

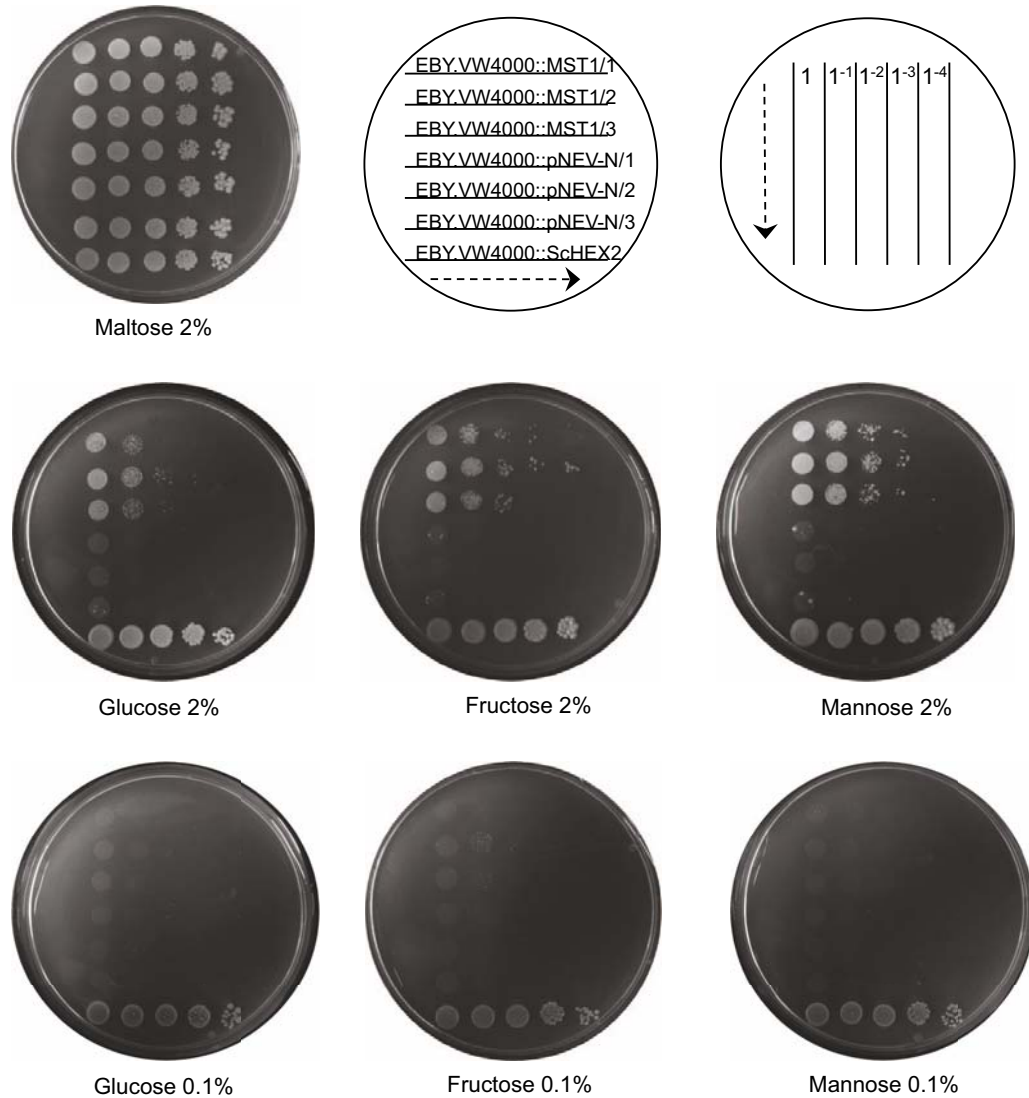


Figure 3.23. Growth test of the hexose-uptake impaired yeast mutant EB.Y.VW4000, complemented with the *G. intrardices* monosaccharide transporter GiMST1, on different sugars. Three clones expressing heterologously *GiMST1*, three yeast clones expressing the empty pNEV-N vector as negative controls and one positive control expressing the *S. cerevisiae* high-affinity sugar transporter HXT2 were spotted in a dilution series on YNB medium (pH 6.5) with different hexoses in two concentrations (2% or 0.1%). Plates were incubated for 11 days at 37 °C. Sampling schema is shown in the right upper panel.

The uptake of glucose without competitor was set as 100%. The uptake reduction of radio-labelled-glucose in the presence of an excess of non-labelled glucose was tested as control. Primary plant cell wall monosaccharides, such as galactose, mannose, glucuronic and galacturonic acid, and xylose were able to efficiently outcompete the uptake of glucose (Fig. 3.24 e). These substrates are able to interfere with the catalytic center of the transporter, which is not a clear evidence that they are transported by GiMST1. However, the transport and uptake of xylose was verified using ¹⁴C xylose (Fig. 3.24 a).

3.3 Xylose as Putative Carbon Source for AM Fungi

The in Chap. 3.2.5 presented uptake tests in yeast showed that GiMST1 has also the ability to transport xylose. Thus, it seems likely that AM fungi can use xylose as a carbon source. In the following sections results are presented assessing the hypothesis that not only glucose but also xylose might be catabolised by AM fungi.

3.3.1 Xylose Utilisation Pathway Genes of *G. intraradices*

In general, the use of xylose as carbon source requires its conversion to D-xylulose-5-phosphate via the xylose utilisation pathway before entering the pentose phosphate pathway (Fig. 3.25 a). In bacteria, xylose is directly converted in D-xylulose by a xylose isomerase (XI) and further activated to D-xylulose-5-phosphate by a xylulose kinase (XK). In contrast, fungi are not able to convert D-xylose directly into D-xylulose-5-phosphate. The conversion requires first the reduction of D-xylose to D-xylitol and a dehydrogenation to D-xylulose which can then be phosphorylated by the xylulose kinase. As previously noted, *S. cerevisiae* spp. are not able to metabolise directly xylose because they lack genes encoding for xylose reductases (XR) and xylose dehydrogenases (XDH).

In AM fungi it was found that intraradical hexoses are subject of significant pentose phosphate pathway activities (Saito, 1995; Pfeffer et al., 1999) but so far there was no hint for the direct utilisation of xylose. To see if *G. intraradices* is able to metabolise xylose, I screened for genes of the xylose utilisation pathway the genome and studied their expression during different stages of the fungal life cycle. Thus, two xylose reductases (GiXR1 and GiXR2), one xylitol dehydrogenase (GiXDH1) and one xylulose kinase (GiXK1) were identified (Tab. 3.4).

Gene expression analyses showed that the xylose reductase GiXR2 was highly induced *in planta* (Fig. 3.25 b). In contrast, the xylitol dehydrogenase and the xylulose kinase were not differentially regulated.

The missing 5' end of the xylose reductase GiXR2 was isolated from a cDNA library of arbuscule-enriched material (see Chaps. 2.8, 2.9.1, and 3.1.1) using the primers XR2_GSP1 and XR2_GSP2 by RACE PCR. The isolated 966 bp ORF encodes a 322 aa protein with 37 kDa and contains conserved domains cd06660 and cl00470 typical for the aldo-keto-reductase superfamily. Phylogenetic analysis showed that GiXR2

3.3 Xylose as Putative Carbon Source for AM Fungi

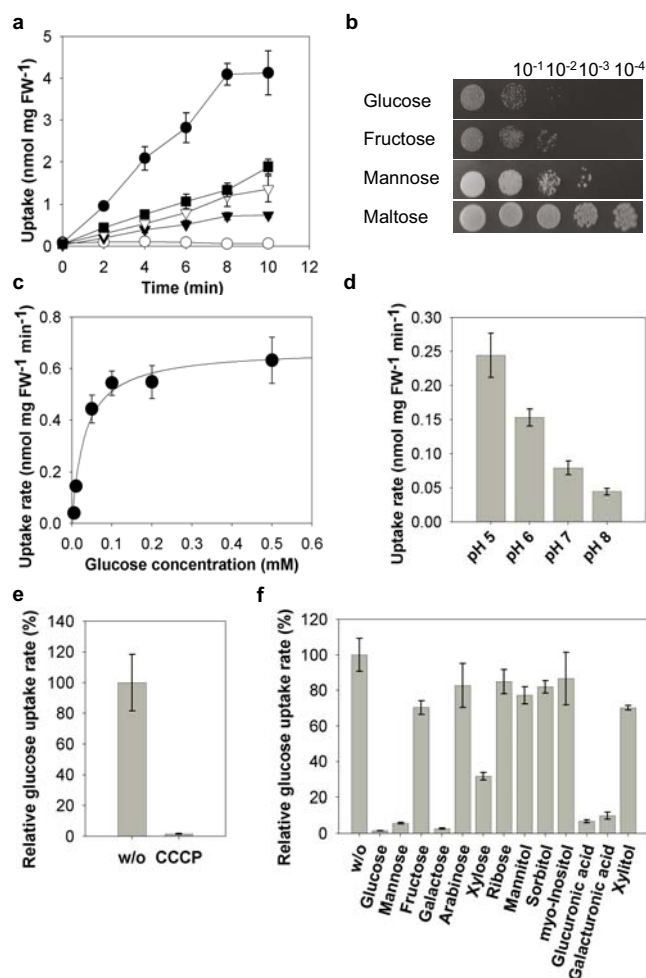


Figure 3.24. Sugar uptake experiments with the EBY.VW4000 mutant transformed with pNEV-MST1. **a**, Uptake of different radio-labelled substrates (1 mM). (open circles, vector control; closed circles, D-glucose; closed squares, D-xylose; open triangles, D-mannose; closed triangles, D-fructose) **b**, Growth test of GiMST1 expressing yeasts on different sugar plates with a pH of 5.5. **c**, Michaelis-Menten kinetics of glucose uptake at pH 5. **c**, Uptake of glucose is optimal at acidic pH-values. **e**, Glucose transport is sensitive to the protonophore CCCP. **f**, Uptake of ^{14}C -glucose (0.1 mM) without competitor (w/o) or with potential substrates of GiMST1 (100-fold molar excess). (Error bars represent s.e.m.)

Xylose Utilisation Pathway Genes		NCBI Blastx Search Results				
EST or Contig Name	Accession Number	Organism	Description	Score	Evalue	Identity
16366_0 (<i>GiXR1</i>)	XP_001269678.1	<i>Magnaporthe grisea</i>	D-xylose reductase	238 (607)	4e-61	55 %
6273_1 (<i>GiXR2</i>)	EEQ46327.1	<i>Candida albicans</i>	NAD(P)H-Dependent D-xylose reductase I,II	80.5 (197)	5e-14	62 %
5629_1 (<i>GiXDH1</i>)	XP_002153215.1	<i>Penicillium marneffei</i>	Xylitol dehydrogenase	305 (782)	5e-81	51 %
Contig 94763 (<i>GiXK1</i>)	EDV10064.1	<i>Saccharomyces cerevisiae</i>	Xylose kinase	168 (426)	7e-40	34 %

Table 3.4. Table of putative genes of the xylose utilisation pathway found in this work by Blast search in the *G. intraradices* genome database.

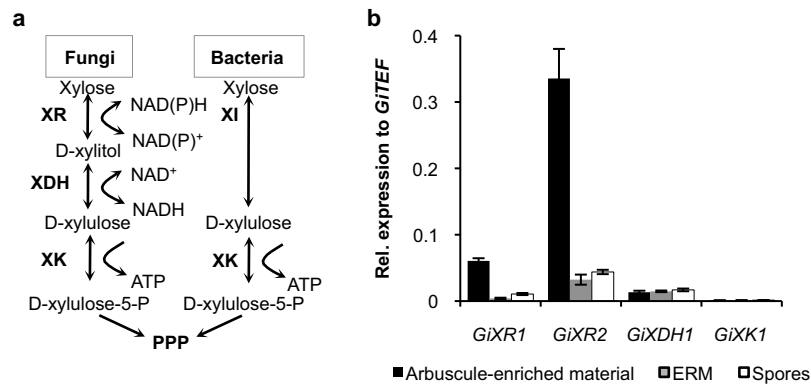


Figure 3.25. Evidence of the xylose utilisation pathway in *G. intraradices*. **a**, Schema of the xylose utilisation pathways in fungi and bacteria. (XR: xylose reductase, XDH: xylitol dehydrogenase, XK: xylulose kinase, XI: xylose isomerase, PPP: pentose phosphate pathway) **b**, Expression of genes involved in xylose utilisation in *G. intraradices* during different stages of the life cycle. (ERM: extraradical mycelium, error bars represent s.d.)

clusters together with yeast xylose reductases (Fig. 3.26).

3.3.2 Activity of Xyloglucan Modifying Enzymes During Mycorrhization

The primary cell wall of higher plants is composed mainly of the polysaccharides cellulose, hemicellulose, and pectin, but also of proteins and inorganic molecules (Carpita and McCann, 2000). Several models have been proposed to explain the organisation of these molecules in the primary cell wall (Cosgrove, 2001). However, these models have all in common that cellulose and the main hemicellulose xyloglucan form the basic network which accounts for the mechanical strength of the primary wall (Cosgrove, 2001). Xyloglucan, a heteropolymer of a β -(1 \rightarrow 4)-glucan backbone and α -(1 \rightarrow 6) xylose side chains which are often substituted with galactose or fucose residues, is thereby responsible for the cross-linking of the cellulose microfibrils (Eckardt, 2008). However, the primary cell wall is not a rigid framework but a highly dynamic structure that shows a balanced interaction of wall synthesis, disassembly, and reorganisation. Several cell wall modifying plant enzymes are involved in these processes like xyloglucan-specific endohydrolases (XEH) and xyloglucan endotransglycosylases (XET) both designated as xyloglucan endotransglucosylase/hydrolases (XTH) (Rose et al., 2002). Xyloglucan endohydrolases can break down the xyloglucan backbone whereas the xyloglucan endotransglycosylases reconnect the xyloglucan molecules. The combined action of both enzymes enables elongation and growth of the wall despite a high turgor pressure and without losing the mechanical strength of the cell wall (Rose et al., 2002).

Xyloglucan can also be the target of microbial hydrolytic enzymes (Pauly et al., 1999; Hasper et al., 2002; Yaoi and Mitsuishi, 2004). Soil microorganisms possess several xyloglucan hydrolytic enzymes to degrade dead plant material (Pauly et al., 1999; Yaoi and Mitsuishi, 2004). Plant pathogenic fungi secrete cell wall degrading enzymes to hydrolyse the plant cell wall and colonise the host plant (Judge, 2006). Because

3.3 Xylose as Putative Carbon Source for AM Fungi

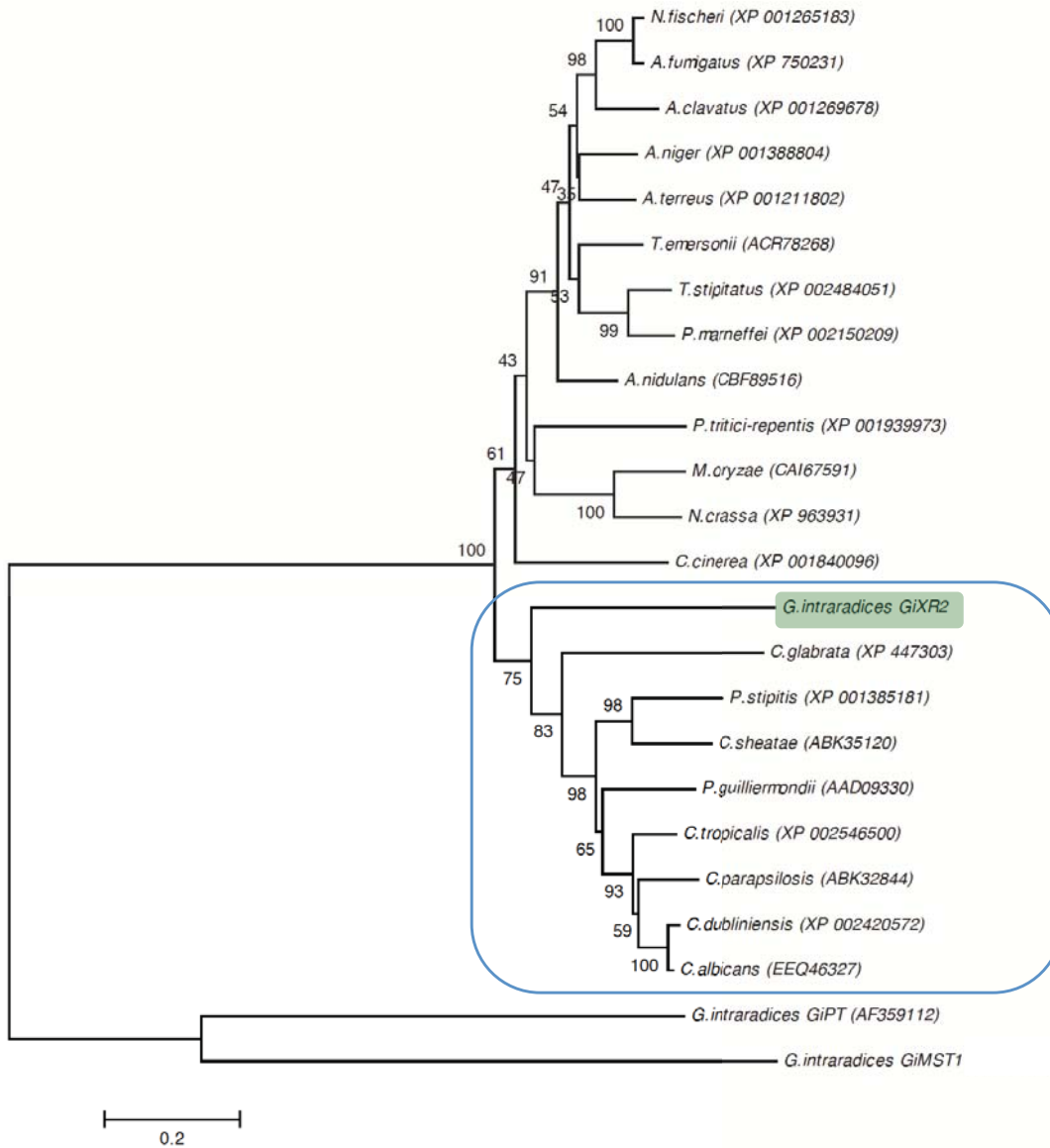


Figure 3.26. Phylogenetic tree of fungal xylose reductase protein sequences. The dendrogram was generated by MEGA 4.0 software using ClustalW for the alignment and the neighbour-joining method for the construction of the phylogeny (Tamura et al., 2007). Bootstrap tests were performed using 1000 replicates. The branch lengths are proportional to the phylogenetic distance. The sequences of the phosphate transporter GiPT from *G. intraradices* (AF359112) and of GiMST1 were used as outgroup. GiXR2, highlighted in green, clusters together with yeast xylose reductase (blue square). Full alignment of GiXR2 and other fungal xylose reductases is shown in Fig. B.12.

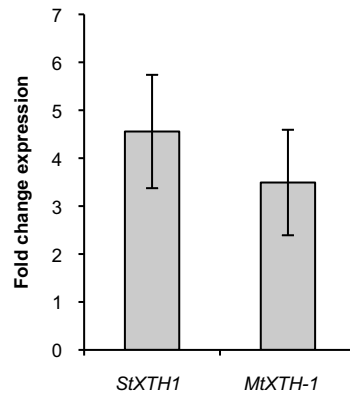


Figure 3.27. Increased expression of the xyloglucan endotransglucosylase/hydrolases *StXTH1* and *MtXTH-1* in mycorrhized potato and *Medicago* roots. Expression is represented as fold induction and normalised to StTEF or MtTEF, respectively. (Error bars represent s.d.)

of this, plants evolved protein inhibitors for those enzymes also for xyloglucanases to repel the pathogenic attack (Judge, 2006). Interestingly, xyloglucanase activity was also measured in AM fungal spores, the ERM, but also in mycorrhized roots (Rejón-Palomares et al., 1996) which probably facilitates the penetration and colonisation of the host root. The presence of non-crosslinked cell wall molecules in the periarbuscular space indicates also a weak and localised activity of AM fungal hydrolytic enzymes (Bonfante and Perotto, 1995; Balestrinin and Bonfante, 2005). Additionally, Maldonado-Mendoza et al. (2005) showed the increased activity of the plant xyloglucan endotransglucosylase/hydrolase MtXTH-1 in mycorrhized *M. truncatula* roots. It was proposed that MtXTH-1 is involved in plant cell wall rearrangements of colonised cells. However, the type of enzymatic activity is not confirmed for MtXTH-1. Thus, MtXTH-1 might act as endohydrolases which is involved in cell wall loosening or as xyloglucan endotransglycosylases which reinforces the cell wall.

Despite the measured activity of AM fungal xyloglucanases, Blast searches in the genome using protein sequences of different fungal xyloglucanases as query gave no positive hits. However in this work, an orthologue of MtXTH-1 was identified by Blast search in *S. tuberosum* with the annotation no. Caj77496. The *S. tuberosum* XTH named StXTH1 shares 44 % identity with MtXTH-1. Both genes showed elevated expression levels in hairy roots mycorrhized with *G. intraradices* (Fig. 3.27).

3.3.3 Orthologues of the XlnR Regulator in *G. intraradices*

The transcriptional regulator XlnR (xylanase regulator) belongs to the zinc binuclear cluster family of transcription factors, found exclusively in fungi. XlnR belongs to the GAL4 superfamily and regulates genes for cellulose- and hemicellulose-degradation like xylanases (van Peij et al., 1998; Gielkens et al., 1999; Hasper et al., 2000, 2002), the D-xylose reductase gene from *A. niger* (Hasper et al., 2000) and possibly sugar transporters in different *Aspergillus* species (Anderson et al., 2008).

Six putative orthologues of XlnR were identified in the genome of *G. intraradices* by

3.3 Xylose as Putative Carbon Source for AM Fungi

Putative <i>xInR</i> Orthologues	NCBI Blastx Search Results					
EST or Contig Name	Accession Number	Organism	Description	Score	Evalue	Identity
Contig 54787	CBF74531.1	<i>Aspergillus nidulans</i>	Putative Zn2Cys6 transcription factor	69 (229)	5e-17	30 %
Contig 19795	XP_710690.1	<i>Candida albicans</i>	Potential fungal zinc cluster transcription factor	59.3 (142)	5e-07	55 %
Contig 41282	CAY80378.1	<i>Saccharomyces cerevisiae</i>	<i>Asg1p</i> , <i>GAL4</i> like transcriptional regulator	56.6 (135)	8e-07	47 %
Contig 60527	EEU07433.1	<i>Saccharomyces cerevisiae</i>	<i>Rgt1p</i> , glucose-response transcriptional activator	42 (97)	0,022	31 %
Contig 57206	CAY81843.1	<i>Saccharomyces cerevisiae</i>	<i>Stb4p</i> , role in regulation of genes encoding transporters	53.1 (126)	1e-05	53 %
Contig 33952	CBF74715.1	<i>Aspergillus nidulans</i>	Putative Zn2Cys6 transcription factor	83.2 (204)	9e-15	37 %

Table 3.5. Putative orthologues of the transcriptional activator XInR which were found in this work by Blast search in the *G. intraradices* genome database.

Blast search using the XInR sequence of *A. niger* (XP_001397110) as query (Tab. 3.5). Only one orthologue, encoded in contig41, was highly expressed during the *in planta* phase (Fig. 3.28). Thus, it is supposed that this gene encodes the transcriptional regulator activating the expression of the xylose reductases and eventually fungal cell wall hydrolytic enzymes and transporters *in planta*. However, evidence for the regulatory function must first be provided.

3.3.4 GiMST1 Promoter Analysis

The promoter of GiMST1 was isolated by genome walking using different Genome-Walker™ libraries which were constructed in this work from germinated spores of *G. intraradices* (Chap. 2.7.7). In a first PCR a 840 bp sequence upstream of the ATG was isolated from the PvuII library using the gene-specific primers MST1_GSP1 and MST1_GSP2 binding in the known 3' region of *GiMST1* in combination with the adaptor-specific primers ASP1 and ASP2, respectively (Fig. 3.29). The full putative promoter sequence of 1.7kb was isolated in a second PCR from the EcoRV library which was constructed from the same material with the gene-specific primers MST1_GSP1a and MST1_GSP2a in combination with the adaptor-binding primers ASP1 and ASP2. The full sequence was amplified with the primers pMST1_F1 and

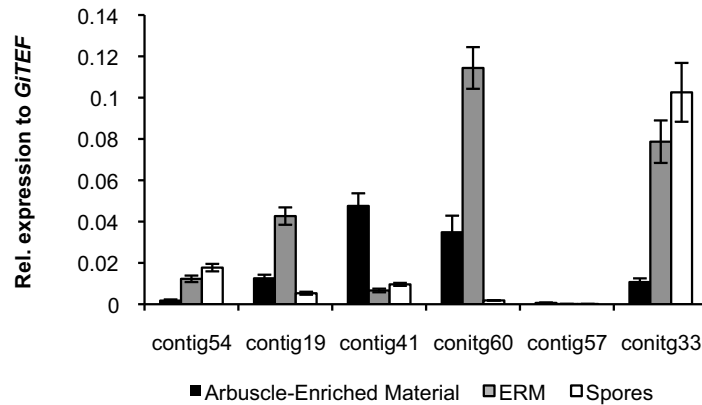


Figure 3.28. Expression of putative orthologues of the XlnR transcriptional activator in different developmental stages of *G. intraradices*. (Error bars represent s.d.)

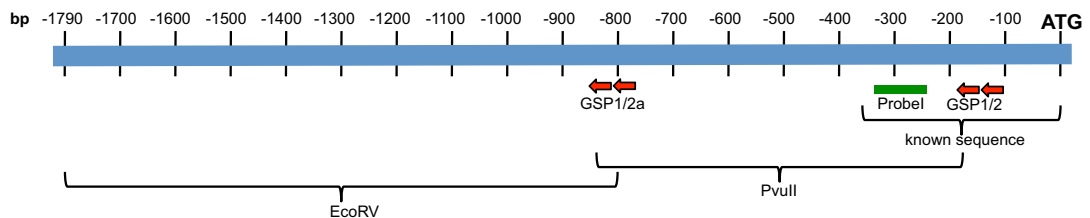


Figure 3.29. Isolation of the *GiMST1* promoter sequence by genome walking. 358 bp upstream of the ATG were known from the *GiMST1* sequence found in the genome database. In a first PCR 840 bp upstream of the ATG could be isolated using the gene-specific primers *MST1_GPS1* (-147 bp) and *MST1_GPS2* (-187 bp). In a second PCR using *MST1_GSP1a* (-790 bp) and *MST1_GSP2a* (-816 bp) primers located within the sequence of the *PvuII* library clone at least 1.79 kb upstream of the ATG were isolated from the *EcoRV* library. Probe I was used to identify positive clones by southern blotting. Upper scale represents base pairs upstream of the ATG (+1).

pMST_R1 and cloned in the pCRII-Topo vector for sequencing.

In silico analysis was performed to find cis-regulatory elements. Therefore the promoter sequence of GiMST1 was run against the TRANSFAC and TFD database. Several GAL4-like regulatory elements were found within the sequence (Fig. 3.30 a). GAL4 is a transcriptional activator in yeast regulating the expression of genes important for galactose and melobiose uptake, and metabolism. GAL4-like activators are found exclusively in fungi and regulate genes which are involved in metabolic processes.

One example for an GAL4-like activator is the XlnR transcriptional regulator which activates different genes for cellulose or hemicellulose degradation, and xylose catabolism (van Peij et al., 1998; Gielkens et al., 1999; Hasper et al., 2000, 2002). XlnR was found to interact with the 5'-GGCTAA-3' motif which is presented in xylanolytic genes of different *Aspergillus* species and *Penicillium chrysogenum* (van Peij et al., 1998). This motif was shown to be essential for the induction of genes in the presence of xylose by XlnR. Recently, Andersen et al. (2008) found this motif in promoter regions of xylose up-regulated sugar transporters in three different *Aspergillus* species. However, the regulation of sugar transporters through XlnR is not experimentally tested. The 5'-GGCTAA-3' cis-regulatory was also identified in the GiMST1 promoter sequence at position -781 (plus strand) (Fig. 3.30 a).

In a preliminary experiment it was tested if the promoter activity of GiMST1 can be triggered by xylose. This was studied in the *Aspergillus nidulans* strain GR5 as heterologous system. To visualise the promoter activity the 1.7 kb GiMST1 promoter sequence was fused to the DsRed reporter gene (Chap. 2.3.4). Additionally, the DsRed gene was fused to the nuclear localisation signal of the *A. nidulans* transcription factor StuA to target the fluorescence to the nuclei and thereby to exclude unspecific or profuse fluorescence signals within the cell (Chap. 2.3.4). *Aspergillus* clones expressing the pMST1-DsRed-StuA fusion gene were cultivated overnight at room temperature in liquid medium supplemented with 2 % xylose or 2 % glycerol as control. As shown in Fig. 3.30 b, xylose in the medium induced the expression of the DsRed reporter which accumulated the nuclei of the *Aspergillus* germling, whereas glycerol had no effect on DsRed expression. This points to a possible role of xylose and of GAL-like activators, for example XlnR, on the expression of *GiMST1*.

3.4 Expression of Sugar Transporters in the ERM

It was long proposed, that the extraradical mycelium of AM fungi has no sugar uptake function (Pfeffer et al., 1999). Unexpectedly, some of the identified sugar transporters from *G. intraradices* showed expression in the ERM (see Fig. 3.15). To test if the expression of these transporters could be triggered by the presence of sugar in the medium, the ERM of *G. intraradices* was exposed to different sugars or sugar derivatives for five days as described in Chap. 2.2.5. As control, the ERM was cultivated in the same medium but without sugars. Fig. 3.31 gives the relative expression levels of each transporter normalised to *GiTEF* in the different treatments.

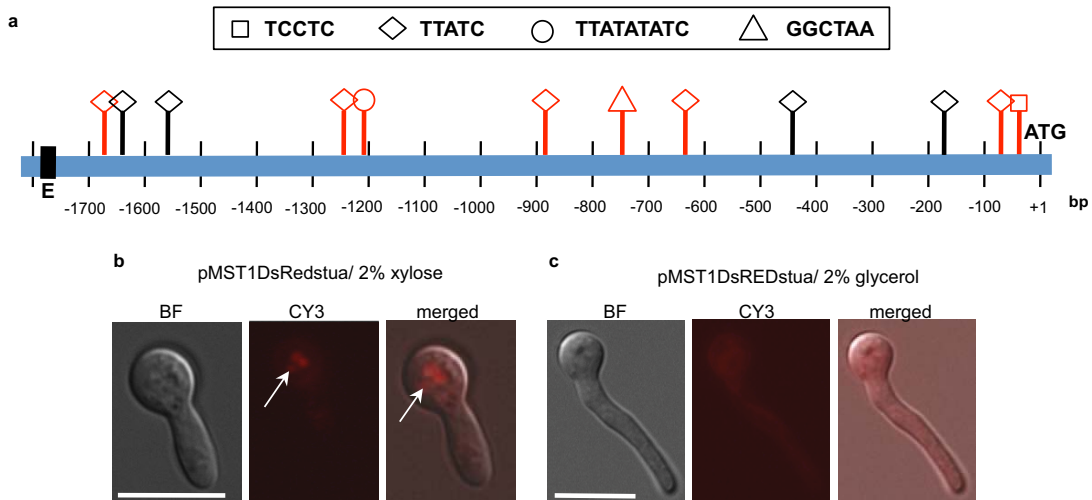


Figure 3.30. Promoter analysis of *GiMST1*. **a**, Putative cis-regulative motifs in the promoter sequence of *GiMST1*. GAL4-like consensus sequences (TCCTC; TTATC; TTATATATC) and XlnR-like motif (GGCTAA). Scale represents base pairs upstream of the ATG (+1). (Red colour: design motifs on the positive strand; black colour: design motifs on the negative strand; E means end-of-sequence). **b**, Expression of *PpMST1-DsRed-StuA* in the *Aspergillus* strain GR5 in minimal medium with 2% xylose. DsRed signal is visible in the nucleus of the germling. **c**, Expression of *pMST1-DsRed-StuA* in the *Aspergillus* strain GR5 in minimal medium with 2% glycerol. No signal is visible in the nuclei. Bars indicate 10 μ m.

Most transporters seemed to be specifically induced by one or more sugars. *GiMST1* which was expressed at very low levels under routine growing conditions without sugar was induced specifically in the ERM after the addition of xylose. None of the other analysed monosaccharides, including glucose, mannose, galactose, arabinose or glucuronic acid induced *GiMST1*. In contrast, the expression of the other sugar transporters was either non-modified or non-specifically induced by xylose. Glucuronic acid (*GlucA*) was tested because it could efficiently outcompete glucose in yeast (Fig. 3.24 f). *GlucA* had either no (for *GiMST4*) or a repressive (for *GiMST1*, 2, 3) effect on sugar transporter expression. *GiMST2* was inducible by both tested pentoses (xylose and arabinose) but repressed by *GlucA* and mannose. *GiMST3* was not induced by any of the tested sugars. Contrary, galactose and *GlucA* repressed *GiMST3* expression compared to the control treatment. Interestingly, glucose did only induce the expression *GiMST4* but not the expression of the other transporters. The relative expression *GiMST4* in the glucose treatment was the highest value reached for all transporters in the ERM.

Because of the induction of the monosaccharide transporter *GiMST1* by xylose, the influence of xylose on the expression of xylose utilisation pathway genes and of putative XlnR transcriptional regulators was tested in the same material. None of the tested xylose utilisation pathway genes were upregulated by the exposure to xylose. Only one putative XlnR orthologue (contig33) showed increased transcription in the ERM after the xylose treatment.

3.4 Expression of Sugar Transporters in the ERM

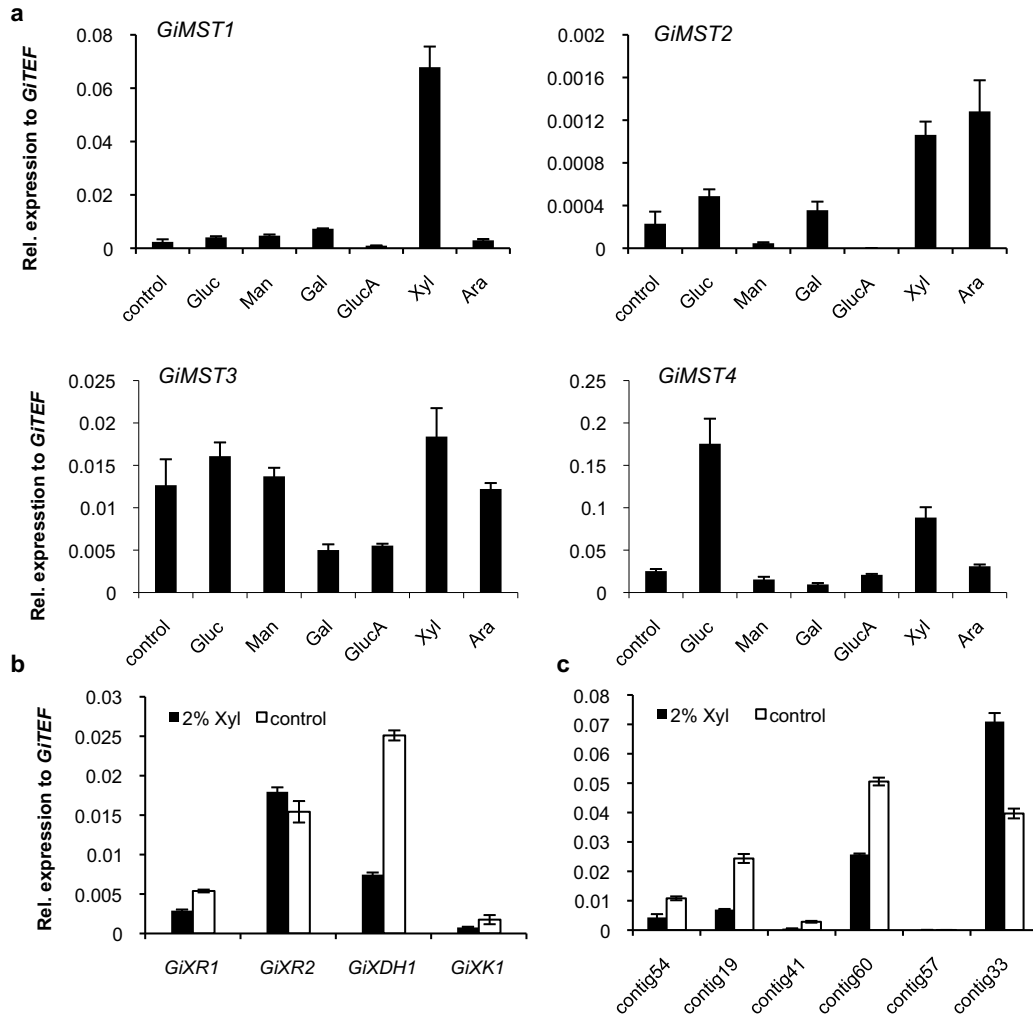


Figure 3.31. Expression analysis of sugar transporters and genes involved in xylose usage in the ERM. **a**, Expression of sugar transporters in the ERM exposed for five days with 2X M medium containing 2% sugar. As control, ERM was cultivated under standard conditions (2X M medium without sugar). (Gluc: glucose, Man: mannose, Gal: galactose, GlucA: glucuronic acid Xyl: xylose, Ara: arabinose) **b**, Expression of xylose utilisation genes in xylose and control treatment. (XR: xylose reductase, XDH: xylose dehydrogenase, XK: xylose kinase) **c**, Expression of XlnR orthologues in xylose and control treatment. (Error bars represent s.d.)

3.5 *GiMST1* and *GiMST2* Expression in the Vicinity of Roots

Because the ERM develops in the soil in the vicinity of other roots, it was tested whether the exposure of the mycelium to roots or their exudates could induce the expression of *GiMST1* and its homologue *GiMST2* (Chaps. 2.2.4 and 2.2.5). Root exudates represent an inhomogeneous mixture of different compounds including pentose sugars (Lugtenberg et al., 1999) which were shown to influence *GiMST1* or *GiMST2* expression. Also several authors described the influence of roots and their exudates on the AM fungal development (Graham, 1982; Elias and Safir, 1987; Bécard and Piché, 1989; Bücking et al., 2008).

The results presented in Fig. 3.32 showed that neither the vicinity of wild type (wt) tomato roots nor their root exudates have an comparable induction effect like it was observed for free xylose (Fig. 3.31). Contrary *GiMST1* expression was repressed in vicinity to wt roots and slightly increased in the presence of root exudates compared to the control. *GiMST2* expression was not altered by direct contact to wt tomato roots, whereas wt root exudates caused a clear repression of *GiMST2* in the ERM.

Interestingly, the vicinity of roots from the mycorrhiza-defective tomato mutant *rmc* (Barker et al., 1998) increased the expression of both transporters significantly whereas the *rmc* root exudates showed no effect.

The *rmc* mutant (reduced mycorrhizal colonisation) is a mycorrhiza-deficient tomato mutant, that is impaired in the colonisation by several AM fungi including *G. intraradices*, but allows the colonisation by *G. versiforme* (now *Glomus* sp. WFMAM23; Gao et al., 2001).

So far it is not known which gene is affected in the *rmc* mutant, but the defect was demonstrated to rely on a single mutation on chromosome 8 in the vicinity of R genes and R gene homologues, suggesting *rmc* could be involved in the perception or recognition of microbial ligands (Larkan et al., 2007). A defect in recognition processes would also explain the tolerance of the *rmc* mutant towards root knot nematodes and *Fusarium* wilt (Barker et al., 2005). However, due to the unknown function of the *rmc* locus, it is difficult to relate the genetic defect of the mutant to the increased *GiMST1* and *GiMST2* expression.

3.6 Functional Relevance for *GiMST1* in the AM Symbiosis

In the previous chapters it was shown that *GiMST1* transcripts accumulate *in planta* and that its expression correlates well with the increase of *PT4* expression. Additionally, *in situ* hybridisation revealed that transcripts localise in arbuscules and in intraradical hyphae. Furthermore, uptake studies in yeast demonstrated that *GiMST1* is well adapted to use sugars of primary cell wall components which were also found the periarbuscular space (Bonfante and Perotto, 1995). In summary, *GiMST1* appears as the perfect candidate for a transporter involved in symbiotic carbon transfer. The best method to validate this assumption would be the knock out or gene silencing of *GiMST1* to look for the symbiotic phenotype. This is a difficult task and due to the

3.6 Functional Relevance for *GiMST1* in the AM Symbiosis

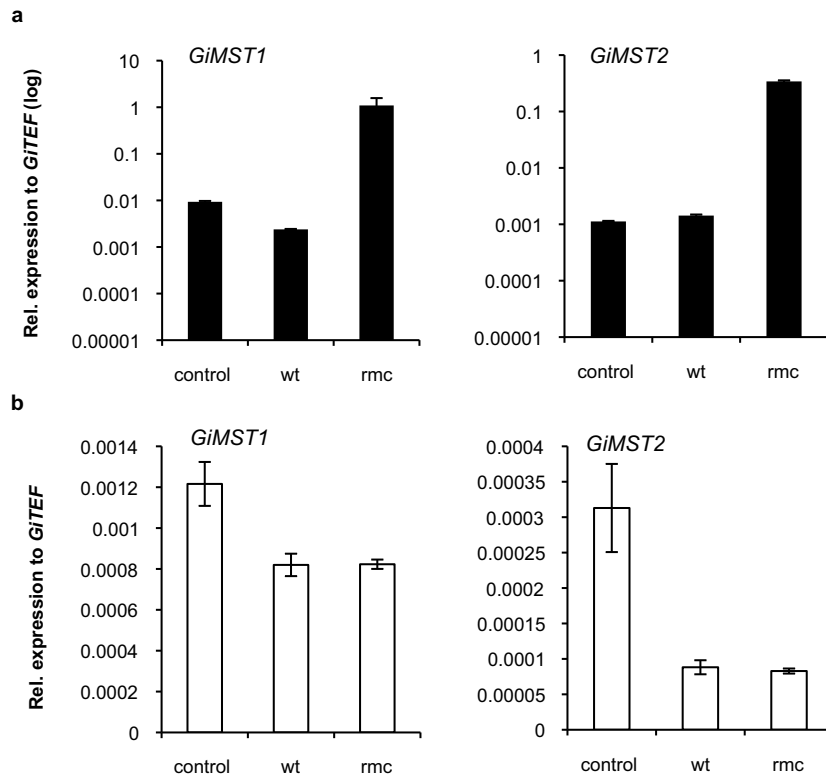


Figure 3.32. Expression of *GiMST1* and *GiMST2* in ERM **a**, in the vicinity of wild type (wt) tomato or *rmc* mutant hairy roots (ordinate is presented in logarithmic scale) or **b**, in the presence of their root exudates. The control was treated identical but was incubated either without roots or without root exudates. (Error bars represent s.d.)

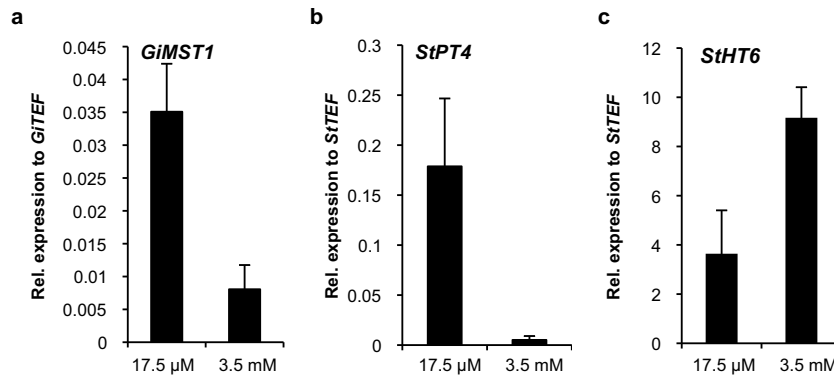


Figure 3.33. Effect of elevated phosphate levels on the expression of (a) *GiMST1*, (b) *StPT4*, (c) *StHT6*, in mycorrhizal potato hairy roots. The roots were treated after establishment of the AM symbiosis with a surplus of phosphate (3.5 mM P). Standard conditions are 17.5 μM of KH_2PO_4 . (Error bars represent s.d.)

lack of an efficient transformation system for AM fungi not possible.

To circumvent this problem and to show the physiological relevance of *GiMST1* in symbiotic carbon transfer, a physiological experiment was performed based on the long-standing hypothesis that carbon supply towards the fungus is connected with the phosphate status of the plant (reviewed in Fitter, 2006). Therefore, potato hairy roots were mycorrhized in the dual compartment system as described in Chap. 2.2.1. After the symbiosis was established, the amount of available phosphate from 17.5 μM to 3.5 mM KH_2PO_4 for the mycorrhizal potato roots were increased. As a consequence the roots shut-off the expression of the symbiotic phosphate transporter *PT4* to possibly rely on the non-symbiotic phosphate pathway (Fig. 3.33 b). Most interestingly, the expression of *GiMST1* was concomitantly down-regulated (Fig. 3.33 a). Also the expression of the mycorrhizal inducible plant sugar transporter *StHT6* was decreased after surplus of phosphate relative to the control treatment (Fig. 3.33 c).

Chapter 4

Discussion

4.1 Cloning of Two New Sugar Transporters of Potato

To identify sugar transporters expressed in the AM symbiosis, cDNA libraries were constructed by isolation of arbuscules from mycorrhized potato hairy roots using a new and low budget microdissection method (Chap. 3.1.1). Several clones were isolated by simultaneous cloning and screening of cDNA libraries from arbuscule-enriched material in the yeast hexose-uptake mutant EBY.VW4000 (Chap. 3.1.2). As the library contained plant and fungal sequences, the clones could be from both organisms. The high GC content of the isolated sequences attested clearly their plant origin (Chap. 3.1.2).

Two distinct plant sugar transporters named StHT6 and StHT2 were isolated in these screens. Phylogenetic analysis revealed that both transporters belong to distinct groups of plant monosaccharide transporters (Chap. 3.1.4). However, StHT6 and StHT2 are able to complement the yeast mutant EBY.VW4000. Thereby, the complemented yeasts showed the highest affinity for glucose (Chap. 3.1.3). Additionally, the direct uptake of radio-labelled fructose, mannose and glucose was determined for StHT6 showing highest uptake rates for glucose and very low rates for fructose (Fig. D.1). Nevertheless, the complete biochemical characterisation of StHT6 and StHT2 is still missing.

4.1.1 StHT6: a Mycorrhiza-inducible Plant Hexose Transporter

Expression analyses in this work demonstrated that both transporters StHT6 and StHT2 are active in roots (Chap. 3.1.5), but their expression in other plant tissues can not be excluded. While *StHT2* was not differentially expressed, *StHT6* showed increased transcript levels upon mycorrhization in roots (Chap. 3.1.5). In contrast, the expression of the putative orthologue of StHT6 in *M. truncatula* (MtHT6) which was identified in this work, was not increased in mycorrhized *Medicago* hairy roots (Chap. 3.1.4 and 3.1.5). To my knowledge StHT6 is the fourth described plant monosaccharide transporter regulated by AM fungal colonisation. Before, two mycorrhiza-inducible hexose transporters were isolated from *M. truncatula* (MtST1) (Harrison et al., 1996) and maize (ZmST1) (Wright et al., 2005) showing also an increased expression in AM roots as it was observed for StHT6. A third mycorrhiza-inducible sugar transporter was isolated from tomato with increased transcript levels in leaves of my-

corrhized plants (Garcia-Rodriguez et al., 2005). Interestingly, StHT6 is only distantly related to any of these transporters (Chap. 3.1.4). However, expression and promoter analyses which were performed in this work, showed that StHT6 and MtST1 are similarly regulated in roots in response to AM fungal colonisation. Using promoter-reporter constructs it was observed that StHT6 and MtST1 are constitutively active in cells of the vascular cylinder, in root tips, and in arbuscle-containing cells of mycorrhized roots (Chap. 3.1.6). This is in line with *in situ* hybridisation experiments done by Harrison et al. (1996) which showed transcripts of MtST1 in primary phloem cells of the vascular cylinder, in regions of cell elongation and cell division on the root tip, and in arbusculated root cells.

The role of MtST1 and StHT6 during mycorrhization is unclear. For MtST1, it was proposed that the expression is increased in mycorrhized roots, because the colonised cells need more hexoses to support their increased metabolism (Harrison et al., 1996). Besides the mutualistic AM symbioses, activation of plant sugar transporters was also reported in associations with pathogenic fungi. For example, Fotopoulos et al. (2003) reported an *A. thaliana* sugar transporter (AtSTP4) induced during infection with the fungal biotroph *Erysiphe cichoracearum*. Those authors suggested that induction of AtSTP4 in *Erysiphe*-infected leaves is a consequence of increase carbon need of the plant cells for repair and defense responses. Although AM fungi are able to induce defense responses, these reactions are transient, localised and weaker than those induced by pathogenic fungi (Pozo et al., 2002). Thus, a similar function of MtST1 or StHT6 is very unlikely. It is rather more likely, that MtST1 and StHT6 control the carbon flow towards the AM fungus. That plants actively regulate the carbon flow was recently demonstrated by Olsson et al. (2010). Those authors showed that less carbon is transferred to the fungus when the benefit of the symbiosis was decreased, e.g. by phosphate fertilisation.

4.1.2 Putative Regulatory Mechanisms for *StHT6* and *MtST1* Expression

The similar regulation of the *StHT6* and *MtST1* promoters in two distinct plant species indicates that conserved regulatory mechanisms are triggering the expression of both transporters. *In silico* studies of the *StHT6* and *MtST1* promoter sequences revealed motifs regulating the expression in the presence of sugars (Chap. 3.1.6). SURE elements in both promoters indicate the regulation of *StHT6* and *MtST1* in response to increased sucrose concentrations. Additionally, AMYBOX elements in the *MtST1* promoter sequence refer also to a sugar-dependant regulation. These findings are conform with the increased expression of both transporters in arbusculated cells where the fungus reinforce the sink strength of the root tissue.

Furthermore, putative motifs regulating the expression of *StHT6* and *MtST1* during mycorrhization were found. A common regulation of mycorrhiza-specific plant phosphate transporters was reported in different plant species by heterologous expression of promoter-reporter fusion constructs (Karandashov et al., 2004). With the expression of truncated promoter versions of the *S. tuberosum* phosphate transporters 3 (StPT3), those authors defined a minimal promoter of 125bp necessary for my-

corrhiza specific response. Within this promoter region they identified one motif, the CTTC motif, which was also presented in the promoters of the AM-regulated *M. truncatula* phosphate transporter 4 (MtPT4), and the AM-inducible *M. truncatula* glutathione S-transferase 1 (MtGst1). A second motif, the TAAT motif, was found only in the phosphate transporters STPT3 and MtPT4. Both motifs were found in the StHT6 and MtST1 promoter sequence together with OSE1ROOTNODULE and OSE2ROOTNODULE elements which were also described in genes expressed arbuscule-containing root cells (Vieweg et al., 2004; Fehlbeg et al., 2005).

These findings indicate that the systemic expression of *StHT6* and *MtST1* in mycorrhized roots might be triggered by increased sink strength, AM fungal colonisation, plant-fungal interactions in general, or a combination of all. Nevertheless, this has to be demonstrated experimentally. To verify the specific induction of *StHT6* and *MtST1* by AM fungi, it has to be shown first that their expression levels during infection with pathogenic fungi are not increased as well. Furthermore, promoter dissection studies and targeted mutations of the identified motifs are needed to define the regulatory domains mediating a possible mycorrhiza specific expression of *StHT6* and *MtST1*.

4.2 Isolation of Fungal Sugar Transporters

With the aim of isolating the fungal sugar transporters featuring during mycorrhiza, cDNA libraries were constructed for complementation in yeast. However, although the presence of these transporters in the libraries was proved later, the complementation approach was unsuccessful. One possible reason is that the arbuscule-enriched RNA used for the library construction contained much more mRNAs of plant than of fungal genes. Another reason is the used screening method. The transformed yeast strains were screened on plates with a pH value of 6.5, the pH optimum for the glomeromycotan monosaccharide transporter GpMST1 (Schüßler et al., 2006). However the characterisation of GiMST1 which was isolated in this work, revealed that in contrast to the *G. pyriformis* transporter, GiMST1 has an optimum at pH 5 (Chap. 3.2.5).

Fungal sugar transporters were also not isolated from spore material, although it was later shown that some transporter are expressed in the presymbiotic stage (see Chap. 3.2.2). However, the expression of these transporters was very low and the library was screened only one time on glucose medium (Chap. 3.1.2).

4.3 First Description of AM Fungal Sugar Transporters

The genome sequencing of *G. intraradices* enabled the identification of genes encoding proteins of the major facilitator superfamily including several partial sequences of potential sugar transporters. In total, four putative monosaccharide and one putative disaccharide transporters were found (Chaps. 3.2.1 and 3.2.2).

The number of hexose transporters in fungi can be quite variable. The largest number, with 48 potential sugar transporters, was found in the human pathogenic fungus

Cryptococcus neoformans (Loftus et al., 2005) followed by the fermentative yeast *S. cerevisiae* with 20 hexose transporters (Boles and Hollenberg, 1997), the plant pathogenic fungus *Ustilago maydis* with 19 (Kämper et al., 2006) and the saprotrophic living fungus *A. nidulans* with 17 putative hexose transporters (Wei et al., 2004). Genome sequencing of the ectomycorrhizal fungus *Laccaria bicolor* revealed the presence of 15 potential candidate genes (Fajardor Lopez et al., 2008). The actual number of sugar transporters which can be expected from strictly biotrophic living fungi is unknown. Only one sugar transporter was isolated so far from haustoria of the biotrophic plant pathogenic fungus *Uromyces fabae* (Voegelé et al., 2001). Also, just one hexose transporter is known from *Geosiphon pyriformis* forming an AM-like symbiosis with cyanobacteria (Schüßler et al., 2006). The identification of several sugar transporters in the *G. intraradices* genome in this work indicates that obligate biotrophic fungi could as well rely on more than one sugar transporter. Furthermore, the presence of not yet annotated sugar transporters in the *G. intraradices* genome is very likely.

Expression analysis in different developmental stages (spores, ERM and arbuscules) of the identified *G. intraradices* sugar transporters showed clearly that only one of them, named *GiMST1*, was almost exclusively expressed in the symbiotic stage. In contrast, other transporters seemed to be more expressed during the presymbiotic phase (germinated spores) like *GiMST2* or in the extraradical mycelium (ERM) like *GiMST4*.

The activity of sugar transporters in the presymbiotic phase is not surprising. Bago et al. (1999) showed using radio-labelled substrates a slight uptake of exogenous glucose by spores which possibly is carried out by one of the sugar transporters identified in this work. However, the expression of these sugar transporters was very low in spores germinated under standard conditions (water agar plates without sugar), but might be triggered by the presence of sugars in the medium. Future experiments has to focus on the identification of those sugar transporters and their transporting conditions. This might be interesting, as the long-term cultivation of AM fungi without a host root is not possible, although the germination of spores could be prolonged, e.g. by different sugar combinations (Azón-Aguilar and Bago, 1994), root exudates, or increased atmospheric CO₂ (Bécard and Piché, 1989).

Unexpected was the expression of sugar transporters in the ERM, a tissue so far believed to be incapable for sugar uptake (Pfeffer et al., 1999). A detailed discussion of these results is presented in Chap. 4.5.

4.4 *GiMST1*: a Symbiotic Sugar Transporter of *G. intraradices*

4.4.1 *GiMST1* Is Active at Different Plant/Fungal Interfaces

GiMST1 was the only hexose transporter significantly expressed *in planta* while the expression in other fungal tissues was negligible (Chap. 3.2.2). This indicates that *GiMST1* takes up plant-derived carbohydrates during mycorrhization. To investigate this assumption, the expression of *GiMST1* and the AM specific plant phos-

phate transporter *PT4* was studied in time course experiments with *S. tuberosum* or *M. truncatula* as plant partners (Chap. 3.2.4). *PT4* was used to quantify the amount of arbuscules in the root, because it is exclusively active in arbuscule-containing root cells and very tightly regulated at the transcriptional level. The observed correlation between *GiMST1* and *PT4* expression suggests that *GiMST1* is active in arbuscules (Chap. 3.2.4). However, several facts indicate that *GiMST1* is also active at other locations. On the one hand, *GiMST1* is expressed, albeit slightly, before *PT4* expression is even detectable (Chap. 3.2.4). On the other hand, an *in situ* localisation analysis showed transcripts of *GiMST1* not only in arbuscules but also in the IRM (Chap. 3.2.4). The uptake of sugars by the IRM is supported by the activities of H⁺-ATPases at the interface along the hyphae and the plant cells which indicates active transport processes (Gianinazzi-Pearson, 1991, 2000). Furthermore, the ERM is developed before the formation of arbuscules (Mosse and Hepper, 1975). The energy needed for the ERM development could come from sugars taken up by the IRM. Other authors described reduced growth of the ERM in plant mutants that prevent the fungus from forming arbuscules after internal colonisation. This suggests that carbon is taken up even when the fungus is unable to complete its life cycle (Gao et al., 2001).

4.4.2 *GiMST1 Supports the Biotrophic Lifestyle of AM Fungi*

Several monosaccharide transporters from plant pathogenic or mutualistic fungi involved in biotrophic carbon acquisition are characterised (Nehls et al., 1998; Voegelé et al., 2001; Nehls, 2004; Schüßler et al., 2006; Polidori et al., 2007). All of these proteins are localised on plant/fungal interfaces and catalyse the uptake mainly of glucose via a proton-symport mechanism. The K_m values for glucose of these transporters are reported in the range of high-affinity transporters, between 38 μ M to 1.2 mM. Sugar transporters from mutualistic plant/fungal systems are predominantly described in ectomycorrhizas. As mentioned above, only one transporter, *GpMST1*, was isolated and characterised from the glomeromycotan fungus *G. pyriiformis* (Schüßler et al., 2006). This fungus forms an interface for nutrient exchange similar to those of bonafide AM fungi.

The monosaccharide transporter *GiMST1* isolated and characterised in this work is only distantly related to any of these symbiotic sugar transporters, including *GpMST1* (Chap. 3.2.3). Nevertheless, the uptake studies in yeast showed that *GiMST1* is also a high-affinity transporter for glucose with a K_m of $33 \pm 12.5 \mu$ M (s.e.m.) (Chap. 3.2.5). These results confirm the transfer of glucose from the plant to the AM fungus previously observed using NMR and respirometric studies (Solaiman and Saito, 1997; Pfeffer et al., 1999). The low K_m of *GiMST1* is also in the range typical for high-affinity plant sugar transporters in roots (15 to 80 μ M for glucose, see Büttner and Sauer, 2000). This enables *GiMST1* to efficiently compete with these plant transporters for sugars in the apoplast. An additional hint for this competition is the observed up-regulation of the plant hexose transporters *StHT6* and *MtST1* in mycorrhizal roots (Harrison et al., 1996; this work).

It has to be emphasised that both glomeromycotan sugar transporters, *GpMST1*

and GiMST1, are different in two points. First of all, the measured K_m of GiMST1 is much lower than reported for the *G. pyriformis* transporter (1.2 mM) (Schüßler et al., 2006) showing that GiMST1 is much better adapted to low apoplastic sugar concentrations. Another difference between the two glomeromycotan transporters is their pH optimum. Whereas the *Geosiphon* transporter has an optimum at pH 7 (Schüßler et al., 2006), GiMST1 showed highest uptake rates at pH 5 (Chap. 3.2.5). The periarbuscular space has been shown to be very acidic due to increased proton-dependant transport processes (Guttenberger, 2000). Thus, the pH optimum of GiMST1 is consistent with its localisation in the apoplastic space, and particularly in the arbuscules. This is also comparable to other transporters located at the periarbuscular space. For example, the *M. truncatula* phosphate transporter MtPT4 and the ammonium transporter LjAMT2 of *Lotus japonicus* have acidic pH optima of 4.25 and 4.5, respectively (Harrison et al., 2002; Güther et al., 2009).

However, both glomeromycotan transporters are similar in their relatively broad substrate specificities for different monosaccharides as it was shown in competition studies in yeast (this work; Schüßler et al., 2006). These studies showed for GiMST1 that the glucose uptake can be efficiently outcompeted by sugars that are present in the primary cell walls of plants, like galactose, mannose, glucuronic acid, galacturonic acid and xylose (Chap. 3.2.5). Furthermore, a direct uptake could be demonstrated not only for radio-labelled glucose, but also for radio-labelled xylose, mannose and fructose (Chap. 3.2.5). This is in contrast to the reported narrow substrate specificities of pathogenic or ectomycorrhizal fungi (Nehls et al., 1998; Voegelé et al., 2001; Nehls, 2004; Schüßler et al., 2006; Polidori et al., 2007). It was shown that the transporters of those fungi are mainly restricted to the uptake of glucose and fructose which are produced by the hydrolysis of sucrose by fungal invertases. AM fungi produce no invertases to hydrolyse sucrose. However, an enhanced activity of plant invertases and sucrose synthase was measured in mycorrhizal roots possibly providing hexoses for the fungus (Blee and Anderson, 2002; Ravnkov et al., 2003; Hohnjec et al., 2003; Schubert et al., 2003; Schaarschmidt et al., 2006). The fact that artificially induced invertase activity in roots does not alter the AM fungal colonisation status suggests that either the amount of available free hexoses in roots is already optimised for the carbon demand of the fungus, or that the mycorrhizal induced invertases play more a role in providing the highly metabolic-active arbuscule-containing cells with an extra supply of sugars instead of the fungus. The last point is in line with the increased expression of the plant glucose transporters StHT6 and MtST1 in arbusculated cells (Harrison et al., 1996; this work). It is tempting to speculate that AM fungi, as 'perennial' biotrophs, might avoid the excessive induction of invertases and the use of glucose and fructose to keep plant defense responses low. It was reported by several authors that the invertase-derived monosaccharides in the apoplast act as signaling molecules that trigger plant defense response (Herbers et al., 1996; Ehness et al., 1997). One strategy to avoid this is the direct uptake and use of sucrose as it was reported for the maize pathogen *U. maydis* (Wahl et al., 2010). However, *G. intraradices* might circumvent this by the versatility of GiMST1 which takes up glucose

but also other plant cell wall sugars.

The ability of AM fungi to feed on cell wall components was proposed long time ago (Schwab et al., 1991) and fits well to the observed activity of cell wall weakening enzymes in mycorrhizal roots. This includes the systemic activation of plant xyloglucan endotransglucosylase/hydrolyases (Maldonado-Mendoza et al., 2005; this work), the measured activity of plant and AM fungal xyloglucanases (Rejon-Palomares et al., 1996) and the presence of fungal polygalacturonases at the periarbuscular space (Peretto et al., 1995). That AM fungi possibly feed on the plant wall material might explain also the observation of Bonfante and Peretto (1995). They described, that the primary cell wall material which fills the periarbuscular space is not crosslinked probably because of the localised activity of fungal hydrolytic enzymes.

4.4.3 Xylose as Alternative Carbon Source for AM Fungi

The uptake studies in yeast demonstrated that *GiMST1* transports not only glucose, but also other monosaccharides, for example xylose. Xylose is the main monomer of the hemicellulose xyloglucan which is predominantly found in primary plant cell walls. The measured activity of xyloglucanases in colonised roots lets assume that free xylose is available for AM fungi in the apoplast. In addition, plant xyloglucan endotransglucosylase/hydrolyases which can also play a role in cell wall loosening processes, were shown to be induced in mycorrhizal roots of *Medicago* and tomato (Maldonado-Mendoza et al., 2005; this work). Thus, xylose is suggested as an alternative carbon source for AM fungi. Of course, this proves not that xylose is really metabolised by the fungus. However, it was demonstrated that AM fungi metabolise hexoses mainly via the pentose phosphate pathway (PPP), which is active in all developmental stages, e.g. spores, intraradical structures, and the extraradical mycelium (for a review see Bago et al., 2000), and which is also the biochemical route for the metabolism of xylose. Before entering the PPP, xylose has to be first converted to xylulose-5-phosphate. This conversion is catalysed in fungi in a three step reaction involving a xylose reductase, a xylitol dehydrogenase and a xylulose kinase. Together, these enzymes form the xylose utilisation pathway. Quantitative real time analyses showed that only the xylose reductase *GiXR2* was significantly expressed *in planta* (Chap. 3.3.1). Thus, it is suggested that *GiXR2* initiates the conversion of xylose in the intraradical structures of the fungus which also proves the metabolism of xylose by AM fungi. The following reactions of the xylose utilisation pathway are then performed by a xylitol dehydrogenase and a xylulose kinase isozyme, which are not yet identified.

Additionally, orthologues of the transcriptional regulator *XlnR* were identified in *G. intraradices* (Chap. 3.3.3). This fungal regulator activates the expression of genes involved in xyloglucan or cellulose degradation, or of xylose reductase genes as reported for *A. niger* (Hasper et al., 2000). A possible *XlnR*-like regulator (*contig41*) which is highly active in the *in planta* phase is suggested as a possible regulator of *GiXR2* (Chap. 3.3.3). However, this has to be verified in further experiments.

To summarise, several genes involved in xylose metabolism were identified for the

AM fungus *G. intraradices*. The existence and activity of xylose utilisation pathway genes and the predominant metabolism of carbon through the PPP confirms that xylose taken up via GiMST1 can be used as carbon and energy source. Whether xylose is really taken up by the fungus *in planta* as a carbon source and how much in comparison to other sugars cannot be said at this moment. In addition, a possible regulator of the xylose reductase GiXR2 *in planta* was identified.

4.4.4 *GiMST1* Expression Depends on the Root Phosphate Status

A long standing hypothesis is that the exchange of carbon is coupled to the phosphate homeostasis of the root. The 'carbon-for-phosphate' model proposes that the local increase of symbiotically delivered phosphate at the arbuscular interface stimulates the flow of carbon at the sites of fungal colonisation where it can be taken up by the fungus (Fitter, 2006). Vice-versa, increased carbon availability stimulates the phosphate uptake by the fungal mycelium (Bücking et al., 2005). However, high overall phosphate concentrations in roots due to high external phosphate amounts reduce the flow of carbon towards the fungus, resulting in lower colonisation rates and in lesser amounts of functional arbuscules (Olsson et al., 2006).

Indeed, several studies indicate that high external phosphate reduces fungal colonisation (Menge et al., 1978; Bruce et al., 1994). A direct effect of high phosphate concentrations on the carbon flow towards the fungus was shown in the experiments of Olsson et al. (2006, 2010) using NMR techniques. The authors observed a decrease of carbon allocation and of fungal hyphal growth after increasing the amount phosphate which was available for the mycorrhizal roots.

To investigate the effect of increased phosphate concentrations on the expression of *GiMST1*, hairy roots of potato mycorrhized with *G. intraradices* were treated either with 17.5 μ M (low) or 3.5 mM (high) phosphate concentrations in the dual compartment system (Chap. 3.6). After one week, an almost complete shut-off of the symbiotic phosphate transporter *PT4* was observed in the treatment with 3.5 mM phosphate. Interestingly, *PT4* down-regulation was accompanied with a decrease of *GiMST1* expression *in planta*. The down-regulation of *GiMST1* possibly implies a reduced carbon flow towards the fungus under high phosphate conditions which is in line with the results of Olsson et al. (2006, 2010). Interestingly, *StHT6* expression levels were increased in the high phosphate treatment (3.5 mM) (Chap. 3.6) possibly to reduce the carbon flow towards the fungus. Fig. 4.1 summarises schematically the hypothesised regulation of *PT4* and *GiMST1* at low or high external phosphate concentrations.

The coupled regulation of the symbiotic phosphate-uptake pathway and the expression of *GiMST1* manifests the assumption that GiMST1 plays a role in the uptake of symbiotically delivered carbon. Nevertheless, it can not be excluded that other, yet unknown transporters might also contribute to the symbiotic carbon transfer. It is likely, that AM fungi might have different uptake systems for high and low glucose affinity as it is known for most fungi (Scarborough, 1970; Özcan and Johnston, 1999).

4.4 *GiMST1*: a Symbiotic Sugar Transporter of *G. intraradices*

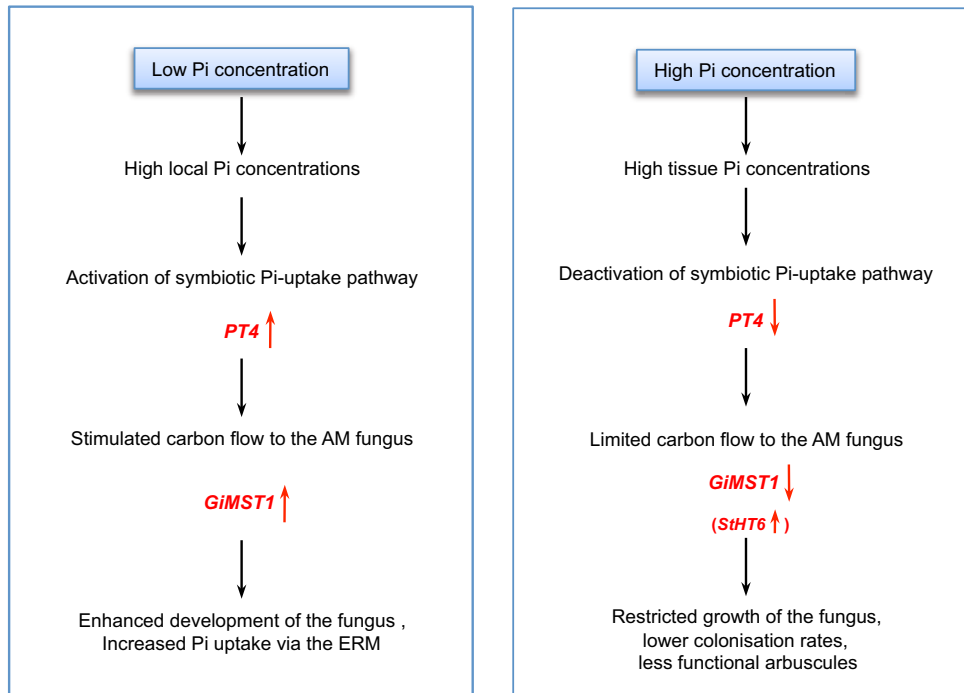


Figure 4.1. 'Carbon-for-phosphate' hypothesis. At low external phosphate (Pi) concentrations the fungus provides the plant with Pi which leads to a local increase of Pi concentrations in colonised root regions. This triggers the activation of the plant symbiotic phosphate transporter *PT4*. Furthermore, the carbon flow towards the fungus is stimulated which possibly triggers the expression of *GiMST1*. At high Pi concentrations in the surrounding, the plant can independently take up Pi from the soil. The symbiotic Pi-uptake pathway is shut-off leading to a decrease of *PT4* expression. The carbon flow towards the fungus is restricted possibly by increased uptake of glucose into the plant cells via plant sugar transporters like *StHT6*. This leads to the down-regulation of *GiMST1* and to reduced fungal growth and colonisation.

4.5 Sugar Uptake as Possible New Function of the ERM

An unexpected finding of this work was that sugar transporters are expressed in the ERM and that their expression is inducible by the addition of sugars to the medium (Chap. 3.4). This indicates that the ERM might be able to take up sugars from the soil. However, this is contradictory to the findings of Pfeffer et al. (1999). In their experiments, the ERM was exposed in the dual compartment *in vitro* system either to radio-labelled glucose or fructose, and tested the presence of radioactive carbon in fungal storage lipids or metabolites using the NMR technique. They showed that the ERM is not able to take up sugars from its surrounding. However, other authors observed the uptake of acetate and glycogen in small amounts by the ERM (Bago et al., 2002, 2003). Hence, the uptake of carbohydrates can not be excluded and the expression of sugar transporters in the ERM which is shown in this work supports this assumption.

Particularly, two of those sugar transporters, GiMST4 and GiMST1, showed interesting expression patterns in the ERM. *GiMST4* was the main transporter expressed in the ERM under standard culture conditions (without sugar) and it could be significantly induced by exposing the ERM to glucose. This suggests the possible uptake of glucose in the ERM by GiMST4 which is contrary to the results of Pfeffer et al. (1999) described above. However, it must be considered that the sugar concentrations used for the induction of *GiMST4* were approximately 4 times higher as those used by Pfeffer et al. (1999). In addition, four to eight weeks old ERM was used for their experiments. Observations in our laboratory showed that the ERM in *in vitro* cultures ages very fast, which leads to the formation of spores, the septation of the hyphae and finally to hyphal death after approximately three weeks. Thus, it is questionable whether the ERM in the experiments of Pfeffer et al. (1999) were still functional. Furthermore, GiMST4 was induced by glucose concentrations which presumably are seldomly reached in soils. Free sugars are generally presented in very small concentrations in the soil, because of their rapid turnover by microorganisms (Sparks et al., 1998). For example, glucose which is the predominant monosaccharide in different soils reaches minimal concentrations between 0.1 to 1.0 mM (Wainwright et al., 1996), whereas other sugars like xylose or arabinose are found in much lesser amounts (Sparks et al., 1998). The glucose concentration used for the induction of *GiMST4* was around 100 times higher than the soil concentration. Thus, it is very unlikely that *GiMST4* expression is induced under natural soil conditions. Whether GiMST4 is functional and transports sugars in the ERM cannot be said at this moment. To verify this, biochemical studies in yeast and in mycorrhiza cultures are needed.

Compared to the control treatment the expression of *GiMST1* in the ERM was increased by a factor of 30 at high xylose concentrations. However, the expression level was still two times lower than the maximum observed *in planta*. The uptake of xylose or other pentoses by the ERM was never tested before and could therefore not be excluded. The use of xylose as alternative carbon source was discussed in Chap. 4.4.3. Saito (1995) reported that the pentose phosphate pathway is highly active in the ERM, meaning that pentoses could be directly metabolised after uptake from

the soil. However, transcriptional induction of genes of the xylose utilisation pathway were not found in the ERM grown on xylose. The uptake of xylose by the ERM has to be investigated in future experiments using radio-labelled xylose.

An alternative source of pentoses in soil are root exudates. Root exudates represent a mixture of various components including pentoses (Lugtenberg et al., 1999). Because of this, the expression of the *GiMST1* and of a second presumably pentose-regulated transporter *GiMST2* was determined in the ERM in the presence of roots or their root exudates (Chap. 3.5; Fig. 3.32). The results showed no comparable induction of both transporters by wild type roots nor by their exudates as it was shown for free pentoses. On the contrary, *GiMST1* was down-regulated by both roots and root exudates in the ERM whereas only root exudates reduced *GiMST2* expression. Possibly sugar transporters are down-regulated in the ERM when they perceive signals from a root that can be newly colonised and/or when the mycelium begins to colonise a new host root. In parallel, the expression of *GiMST1* and *GiMST2* was tested in hyphae cultivated together with roots of the *rmc* mutant or only their exudates. The observed extreme induction of *GiMST1* and *GiMST2* expression in hyphae with contact to *rmc* mutant roots is surprising and difficult to explain, because the function of the defected *rmc* locus is not known. Whereas the root exudates showed no effect on both transporters, the direct contact with the roots must somehow trigger their expression. At the moment it can only be speculated that maybe a defect in the cell wall synthesis of the *rmc* mutant, which leads to the release of free xylose or xyloglucan components, induces the expression of *GiMST1* and *GiMST2*.

In summary, the induction of sugar transporters in the ERM reveals a new function, the possible uptake of exogenous sugars. So far, the uptake of hexoses by the ERM was excluded, and no direct evidence for the uptake of pentoses exists. It is hypothesised that sugar transporters in the ERM are less induced under natural soil conditions, but that their expression is inducible by extremely high concentrations of some sugars. Indeed, uptake of sugars from patches of organic matter in soil, where carbons are in higher quantities and much easier accessible for the fungus, was considered already (Hodge et al., 2001).

4.6 Possible Regulation of *GiMST1*

The transport processes in AM fungi are highly polarised. Whereas carbohydrates are taken up by intraradical fungal structures and transferred to the extraradical mycelium, phosphate and other nutrients are taken up by the ERM and transferred to the arbuscules. Consequently, genes involved in these processes must be regulated spatially and temporally. However, gene regulation mechanisms in AM fungi are not yet well understood.

The differential expression of genes within AM fungal hyphae was observed, for example, for the *G. versiforme* phosphate transporter GvPT. GvPT is mainly expressed in the ERM where phosphate is taken up by the fungus from the soil, whereas low expression levels were measured in intraradical structures within the root (Harrison

and van Buuren, 1995). The opposite was observed for GiMST1 which shows highest expression levels *in planta* and lower expression levels in the ERM. However, in this work it was also shown that the expression of *GiMST1* could be triggered in the ERM by the presence of xylose. Thus, xylose is suggested as a possible inducer of GiMST1. This is supported by the performed *in silico* analysis of the GiMST1 promoter sequence. In this study, the 5'-GGCTAA-3' cis-regulatory motif was identified. This motif was shown to be recognised by the fungal transcriptional regulator XlnR (van Peij et al., 1998). As mentioned above, XlnR activates several genes in the presence of xylose, for example genes for xyloglucan degradation, or the xylose reductases of the xylose utilisation pathway (van Peij et al., 1998; Gielkens et al., 1999; Hasper et al., 2000, 2002). However, XlnR cis-regulatory motifs were recently found in xylose-upregulated sugar transporters of *Aspergillus* ssp. suggesting their regulation by XlnR (Andersen et al., 2008). In addition, several orthologues of the XlnR activator were identified in the *G. intraradices* genome. One of these orthologues was highest expressed *in planta* and another in the ERM in the presence of xylose. The induction of the GiMST1 promoter by xylose was finally confirmed *in vivo* using a promoter-reporter construct expressed heterologously in *A. nidulans*.

In addition, several GAL4-like regulatory motifs were identified in the GiMST1 promoter. A GAL4-like protein is reported to be mediating the switch between the biotrophic and the necrotrophic lifestyle in the plant pathogen *Colletotrichum lindemuthianum* (Dufresne et al., 2000). Thus, it is possible that GAL4-like proteins play also a role in the AM symbiosis, for example as activator of biotrophic sugar transporters like GiMST1.

GiMST1 was also regulated by the phosphorous homeostasis of the plant root (Chap. 3.6). It was shown, that increased exogenous phosphate amounts decrease *PT4* and *GiMST1* expression. Hence, it is possible that the down-regulation of *GiMST1* is a consequence of the decreased symbiotic carbon flow sensed by the fungus. However, it might also be possible, that specific plant signals required for GiMST1 expression *in planta* are turned off when the delivery of symbiotic phosphate is no longer necessary.

In summary, xylose seems to be an important signal which might activate *GiMST1* expression through a XlnR orthologue, but also plant-derived signals seem to be involved in the regulation of GiMST1. Nevertheless, these results are preliminary and have to be verified by future experiments.

Chapter 5

Conclusion and Outlook

Although several studies have been undertaken to understand the carbon flux in the arbuscular mycorrhizal symbiosis, little is known about the molecular mechanism of the carbon transfer and its regulation. However, a better understanding of the carbon flow is crucial to calculate the costs of the symbiosis for the plant. This is mainly important for the application of AM fungi in agricultural systems. Furthermore, AM fungi play a significant role in the global carbon cycle, as large amounts of carbon are transferred over their hyphal network into the soil (Staddon et al., 2002).

The aim of this study was the isolation and characterisation of genes involved in the symbiotic carbon transfer in arbuscular mycorrhizas. Making use of the first draft of the *Glomus intraradices* genome sequencing it was possible to isolate the first symbiotic sugar transporter, GiMST1, from an AM fungus. The characterisation of GiMST1 helps to answer long standing questions, for example 'How is carbon taken up by the AM fungus?', 'Where is it taken up?', and 'Which carbohydrates are transferred?'. First, this study showed that AM fungi take up sugars actively over a proton dependent sugar transport mechanism. Furthermore, *in situ* hybridisation studies of GiMST1 showed that arbuscules and intraradical hyphae are the locations of carbon transfer. Finally, it could be shown that GiMST1 prefers mainly glucose, but transports also other monosaccharides, such as galactose, mannose and xylose. Whether other sugars besides glucose are taken up by AM fungi could not be directly tested. However, genes of the xylose catabolism were identified in this work and shown to be highly expressed *in planta* indicating that at least xylose is taken up and used as alternative carbon source.

The existing model for carbon uptake and metabolism in the AM symbiosis proposed by Bago et al. (2000) and Parniske et al. (2008) is presented in Fig. 5.1, while taking the results of this work into account. According to this model, GiMST1 and mycorrhiza-induced plant hexose transporters, for example MtST1 (Harrison et al., 1996) or StHT6 (identified in this work), compete for glucose in the apoplast. Glucose taken up via GiMST1 is rapidly converted into glycogen and triacylglycerol (TAG), which are used for carbon storage and long-distance transfer to the ERM (Pfeffer et al., 1999). Enzymatic and genetic studies provided evidence for different metabolic pathways which are active in AM fungi. These are the glycolysis (Franken et al., 1997; Harrier et al., 1998), the tricarboxylic acid cycle (MacDonald and Lewis, 1978; Saito, 1995), the glyoxylate cycle (Lammers et al., 2001), and the pentose phosphate pathway (Saito, 1995). The cytoplasmic glucose was shown to be metabolised mainly

via the oxidative part of the PPP *in planta* and in the ERM (Saito, 1995; Pfeffer et al., 1999). In the ERM, hexoses are synthesised from glycogen or TAG through gluconeogenesis. TAG and glycogen are also converted to trehalose and chitin (Pfeffer et al., 1999). In addition, GiMST1 takes up xylose from the periarbuscular space. There, free xylose molecules are released from primary cell wall components due to the activity of plant or fungal cell wall hydrolytic enzymes (Bonfante and Perotto, 1995; Perotto et al., 1995; Rejon-Palomares et al., 1996; Maldonado-Mendoza et al., 2005; this work). Xylose is taken up via GiMST1 and converted in the xylose utilisation pathway to xylulose-5-phosphate which is metabolised in the PPP.

So far it could not be answered whether GiMST1 is the only sugar transporter in the AM symbiosis or if there might be other yet unidentified transporters. The isolation and characterisation of GiMST1 can be seen as a first step for a better understanding of the carbon flow in the AM symbiosis. However, further work has to be done to explore the function of GiMST1 in symbiotic carbon uptake. All experiments in this study took advantage of the *in vitro* system for the cultivation of *G. intraradices*. Several studies revealed that this system is a useful tool to investigate nutrient transfer mechanisms in the AM symbiosis (Pfeffer et al., 1999; Olsson et al., 2006). Nevertheless, the next step is to study the regulation of GiMST1 in pot experiments with full plants. In these experiments it would be interesting to combine the tracing of the carbon flow in mycorrhizas using isotopic labelling with the expression analyses of GiMST1 under different phosphate and light conditions. First experiments in the *in vitro* system showed already that increased phosphate amounts supplied to the host root down-regulate GiMST1 *in planta* which is in line with results of Olsson et al. (2006, 2010) showing that the phosphate homeostates of the plant regulates the carbon flow towards the fungus. However, a correlation between carbon flow in mycorrhizas and the expression of GiMST1 has first to be demonstrated in pot experiments as described above. This would be a positive proof for the function of GiMST1 in symbiotic carbon uptake.

Future studies should also focus on the activity of sugar transporters in the ERM and in spores. The possibility to induce the activity of sugar transporters in the presymbiotic phase or the ERM might be important for the axenic cultivation of AM fungi which is not possible at the moment.

Besides, the results presented here show clearly how important the genome sequencing of *G. intraradices* is for the mycorrhizal symbiosis. At the moment the genome database is the most important tool to study the fungal site of the AM symbiosis.

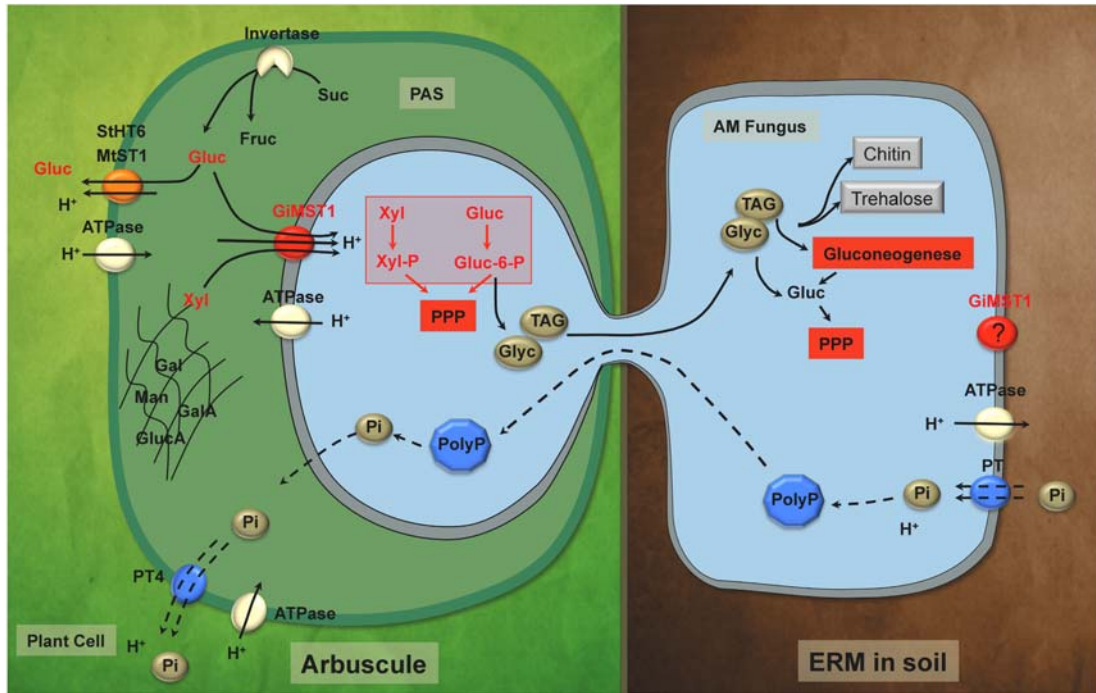


Figure 5.1. Carbon and phosphate flux in the AM symbiosis (after Bago et al., 2000; Parniske, 2008; this work). GiMST1 is involved in the symbiotic carbon uptake in arbuscules or intraradical hyphae. Mycorrhiza-inducible invertases cleave sucrose (Suc) into glucose (Gluc) and fructose (Fruc). Mainly glucose is taken up by the fungus via GiMST1 from the periarbuscular space (PAS). Cell wall sugars like xylose (Xyl) but possibly also mannose (Man), galactose (Gal), glucuronic and galacturonic acid (GlucA, GalA) can be taken up via GiMST1 and used as alternative carbon sources. Xylose and glucose are metabolised in the pentose phosphate pathway (PPP). Glucose is converted in triacylglycerol (TAG) or glycogen (Glyc) and transferred to the extraradical mycelium (ERM). There, glucose is synthesised via gluconeogenesis from TAG. TAG and Glyc are converted in chitin and trehalose. GiMST1 is also expressed in the ERM exposed to high levels of xylose, but its function there is not known. The plant sugar transporters StHT6 (*S. tuberosum*) and MtST1 (*M. truncatula*) compete with the fungus for glucose. In the opposite direction phosphate is transferred to the plant. Phosphate (Pi) is taken up by fungal phosphate transporters in the ERM, converted to polyphosphate (PolyP) and transported to the intraradical structures. *In planta*, Pi is released in the PAS and taken up by mycorrhiza-specific plant phosphate transporters like PT4.

Appendix A

Oligos

Primer Name	Sequence (5' ->3')	GC	Tm	Remarks
qPCR Primer for <i>S. tuberosum</i> and <i>M. truncatula</i>				
Stef1_F1	GAACATCCATTGCTTGCTTTC (21 bp)	42.9 %	56.0 °C	
Stef1_R1	CACAATTCATCGTACCTAGC (21 bp)	42.9 %	56.0 °C	Amplicon length 200 bp
StPT4_for	ATGAAGGGAAGCCATTGATG (21 bp)	42.9 %	56.0 °C	
StPT4_rev	TACCTTCCCATGTTAATCGC (21 bp)	42.9 %	56.0 °C	Amplicon length 200 bp
StHT6_F1	ATGTTTCAGTTTTGGGGGAATC (21 bp)	42.9 %	56.0 °C	
StHT6_R1	GAAC TAACCATCCTAATGGAC (21 bp)	42.9 %	56.0 °C	Amplicon length 181 bp
StHT2_F1	ACACGACAAGAAAACCTGGTC (21 bp)	42.9 %	56.0 °C	
StHT2_R1	CTGCCTGATTGGCGAAAC (18 bp)	55.6 %	56.0 °C	Amplicon length 156 bp
StXTH1_F1	CCTGTTTGGGCTGATAATTC (21 bp)	42.9 %	56.0 °C	
StXTH1_R1	ATTTCCAGGTACGAGTTTGAG (21 bp)	42.9 %	56.0 °C	Amplicon length 186 bp
MtTEF_F1	GATTGCCACACCTCTCACAT (18 bp)	50.0 %	57.3 °C	
MtTEF_R1	TCTTCTCCACAGCCTTGATG (18 bp)	50.0 %	57.3 °C	Amplicon length 197 bp
MtPT4_F1	GTGCGTTCGGGATAACAATACT (18 bp)	50.0 %	57.3 °C	
MtPT4_R1	GAGCCCTGTCAATTTGGTGTT (18 bp)	50.0 %	57.3 °C	Amplicon length 200 bp
MtHT6_F1	ATCAGGCAGTCCCATTATATC (21 bp)	42.9 %	56.0 °C	
MtHT6_R1	TGTTTTGAATTATGCTGTTTGGTG (24 bp)	42.9 %	56.0 °C	Amplicon length 246 bp
MtXTH1_F1	CAATCCATGGCCATATTTCC (21 bp)	42.9 %	56.0 °C	
MtXTH1_R1	TCTTCCCCAACAAAAACACA (21 bp)	42.9 %	56.0 °C	Amplicon length 96 bp

Table A.1. Primers used for quantitative real-time PCR (qPCR) of *S. tuberosum* and *M. truncatula* genes.

Appendix A Oligos

Primer Name	Sequence (5' ->3')	GC	Tm	Remarks
qPCR Primer for <i>G. intraradices</i>				
Gitef_for	TGTTGCTTTCGTCCCAATATC (21 bp)	42.9 %	56.0 °C	
Gitef_rev	GGTTTATCGGTAGGTCGAG (19 bp)	52.6 %	56.0 °C	Amplicon length 177 bp
GiMST1Real_F1	GGCAGGATATTTGTCTGATAG (21 bp)	42.9 %	56.0 °C	
GiMST1Real_R1	GCAATAACTCTTCCCGTATAC (21 bp)	42.9 %	56.0 °C	Amplicon length 100 bp
GiMST2Real_F1	ATTCTCGATTCTTGGTGCATC (21 bp)	42.9 %	56.0 °C	
GiMST2Real_R1	ATACGCCAGCAACGACTC (18 bp)	55.6 %	56.0 °C	Amplicon length 100 bp
GiMST3_F1	AAAATCTACCGGTCCAAATG (21 bp)	43.0 %	56.0 °C	
GiMST3_R1	AAAGTAATGATCCTATCAATCCAC (24 bp)	33.0 %	56.0 °C	Amplicon length 120 bp
GiMST4_F1	TAGCTACATTTGCTATTGGTTTAG (24 bp)	33.0 %	56.0 °C	
GiMST4_R1	CCCTAACTCCAAAATAATGAAC (24 bp)	33.0 %	56.0 °C	Amplicon length 153 bp
GiSuc1_F1	GGCAGGTATCGCGTATTC (18 bp)	55.6 %	56.0 °C	
GiSuc1_R1	TGCACGACATGACGCTTG (18 bp)	55.6 %	56.0 °C	Amplicon length 169 bp
Gixyr1_F1	TAAAATTAATCCAACCGGACAAC (24 bp)	33.0 %	56.0 °C	
Gixyr1_R1	TTAAGACCTATACCGATTCTTTC (24 bp)	33.0 %	56.0 °C	Amplicon length 169 bp
Gixyr2_F1	GGTGTGTACAACGTCAAATTG (21 bp)	42.9 %	56.0 °C	
Gixyr2_R1	CAAAGATTGGTAAATCGAAATCAG (24 bp)	33.3 %	56.0 °C	Amplicon length 174 bp
Gixyd1_F1	CATCACAAAACCAAACGAAG (21 bp)	43.0 %	56.0 °C	
Gixyd1_R1	CGCCAACCTCAAGATTTTAC (21 bp)	43.0 %	56.0 °C	Amplicon length 189 bp
Gixyk1_F1	TTCGACTTATCAACTCAACAATTG (24 bp)	33.0 %	56.0 °C	
Gixyk1_R1	ATGTGGCAATCTTTGTCAAAATG (24 bp)	33.0 %	56.0 °C	Amplicon length 105 bp
Contig60527_F1	AAGCGAGGTCCACGAAAC (18 bp)	55.6 %	56.0 °C	
Contig60527_R1	TGGGTACCAAATAAGCATATAATC (24 bp)	33.3 %	56.0 °C	Amplicon length 192 bp
Contig54787_F1	CTGTACGTTCCGATCCTG (18 bp)	55.6 %	56.0 °C	
Contig54787_R1	ATAAGGGCAGCTATTGTAGAC (21 bp)	42.9 %	56.0 °C	Amplicon length 118 bp
Contig41282_F1	ATGAGAAGGTACCAGAAAGTC (21 bp)	42.9 %	56.0 °C	
Contig41282_R1	TGCAGTTCCAATTACGATCAC (21 bp)	42.9 %	56.0 °C	Amplicon length 145 bp
Contig572026_F1	GGCAAAGGGTAACGGTAG (18 bp)	55.6 %	56.0 °C	
Contig572026_R1	ATCAAAAATGCATTCCTTGTCATG (24 bp)	33.3 %	56.0 °C	Amplicon length 110 bp
Contig33952_F1	CGAGTGAGGCTGAAACTC (18 bp)	55.6 %	56.0 °C	
Contig33952_R1	ACTAGGAAGGTATGTACAATTTAC (24 bp)	33.3 %	56.0 °C	Amplicon length 149 bp
qPCR Primer for <i>S. cerevisiae</i>				
Act1p_F1	AGGTTGCTGCTTTGGTTATTG (21 bp)	42.9 %	56.0 °C	
Act1_R1	TCTTGGATTGAGCTTCATCAC (21 bp)	42.9 %	56.0 °C	Amplicon length 177 bp

Table A.2. Primers used for quantitative real-time PCR (qPCR) of *G. intraradices* and *S. cerevisiae* genes.

Primer Name	Sequence (5' ->3')	GC	Tm	Remarks
Primers for RACE PCR and GenomeWalker™ DNA walking				
GeneRacer™5'Primer	CGACTGGAGCACGAGGACACTG A (23 bp)	61.0 %	74.0 °C	Invitrogen (USA)
GeneRacer™5'Nested	GGACTGACATGGACTGAAGG ACTA (26 bp)	50.0 %	78.0 °C	Invitrogen (USA)
GeneRacer™3'Primer	GCTGTCAACGATACGCTACGTAA CG (25 bp)	52.0 %	76.0 °C	Invitrogen (USA)
GeneRacer™3'Nested Primer	CGCTACGTAACGGCATGACAGTG (23 bp)	57.0 %	76.0 °C	Invitrogen (USA)
Adaptor Primer 1 (AP1)	GTAATACGACTCACTATAGGGC (21 bp)	45.0 %	59.0 °C	Clontech (Canada)
Nested Adaptor Primer (AP2)	ACTATAGGGCACGCGTGGT (19 bp)	58.0 %	71.0 °C	Clontech (Canada)
Smartup_F1	CACCCAAGCAGTGGTATCAACGC AGAG (27 bp)	55.6 %	68.0 °C	
CDSdown_R1	TAGAGGCCGAGGCGGCCGACAT G (23 bp)	69.6 %	69.6 °C	
MST1down_F1	CGCACTTGCGGCAGGATATTTGTC TGATAG (30 bp)	50.0 %	68.0 °C	
MST1 down_F2	CGGGAAGAGTTATTGCTGGCCTT GCAGTTG (31 bp)	53.3 %	69.6 °C	
MST1 down_F3	GGATAGATCGTTTGGGACGTAAA CCTACTC (30 bp)	46.7 %	66.8 °C	
MST1down_F4	GGGGCCCGACTGGATGGATTTAT CCTG (27 bp)	59.3 %	69.5 °C	
MST2_GSP1	CGTAGCAGTTGCTTGCAAACAC TACCGAC (30 bp)	50.0 %	68.1 °C	
MST2_GSP2	CCAGAGGGAAACTTTTCGCGGAA GTGAG (28 bp)	53.6 %	68.0 °C	
MST2_GSP1a	CCACGCTGGTTGGTACATCCGAT CGTG (28 bp)	57.1 %	69.5 °C	
MST2_GSP2a	GAGCCGGTGGCGATAGAACTGCA GTG (26 bp)	61.5 %	69.5 °C	
HT6_GSP1	GCAACGATGGATGATAACACCAC AAACACA (30 bp)	46.7 %	66.8 °C	
HT6_GSP2	ATCCCTCACTTGTTGGGACAATAC CAACTG (30 bp)	46.7 %	66.8 °C	
HT6_GSP1a	ACTTGTTACGCCAGTCACACCA CATATG (29 bp)	48.3 %	66.7 °C	
HT6_GSP2a	CAACTCCATAACCACTCACTATC ACCTAAC (31 bp)	45.2 %	66.8 °C	
MST1_GSP1	GTGGTCAGTCCCCTAGTACTATTG TTGATC (30 bp)	46.7 %	66.8 °C	
MST1_GSP2	CGTGCGAAAGAAAACCTTGCCGA ATTAGTCAC (30 bp)	46.7 %	66.8 °C	
MST1_GSP1a	ATGATCGACATTCCGATCATCAA GCGAGTC (30 bp)	46.7 %	66.8 °C	
MST1_GSP2a	AGTCAAATCCGCCAGATAACACA TG (25 bp)	44.0 %	61.3 °C	
XR2_GSP1	GCAAGACGATCATGATTATTAGAT TTTGGTAC (32 bp)	34.4 %	63.1	
XR2_GSP2	GGTACAATAGCAATTTGACGTTGT ACACAC (30 bp)	40.0 %	64.0	

Table A.3. Primers for RACE PCR and genome walking.

Appendix A Oligos

Primer Name	Sequence (5' ->3')	GC	Tm	Remarks
Primers for TOPO T/A and ENTR Cloning				
pStHT6_F1	<u>CACCATCCATCAA</u> AATACATAC	36,4 %	54,7 °C	<u>CACC</u> not in sequence
pStHT6_R1	TCTTCTCTACAAGTCAAGTTC	36,4 %	54,7 °C	
pMtST1_F1	CACCGACAATATCCACCAAC	50,0 %	56,5 °C	
pMtST1_R1	TTTTTCTGACCTCAGTAGCAAG	40,9 %	56,5 °C	
MST1atgNot_F1	<u>GCGGCCGC</u> ATGGGTAGCGTTATG (24 bp)	62,5 %	67,8 °C	with NotI restriction sites on the 5' ends
MST1endNot_R1	<u>GCGGCCGC</u> TCAAAGCTGCTCAAG (23 bp)	62,5 %	67,8 °C	
pEXTAMST1_F1	<u>CCATG</u> GGGAGCGTTTATGTATACGTATG (28 bp)	42,9 %	63,7 °C	with NcoI restriction sites on the 5' ends
pEXTAMST1_R1	<u>CCATG</u> GGAAGCTGCTTCAAGCTCC	56,5 %	64,2 °C	
pMST1_F1	AGACTCTAAAAGTTCTAAGATTATTAAC (27 bp)	25,9 %	55,9 °C	
pMST1_R1	TTCGGTAAATTTTATTATGGATAGTTG (27 bp)	25,9 %	55,9 °C	
Primers for DIG-Labelled Probes				
ProbeI-MST1_F1	AAGAGTTATTGCTGGCCTTG (20 bp)	45 %	55,3 °C	
ProbeI-MST1_R1	ACGCCCACGAATTTCTTTTG (20 bp)	45 %	55,3 °C	Amplicon 91 bp
ProbeI-MST2_F1	CTGTACAGAAGGAATACAC (19 bp)	42,1 %	52,4 °C	
ProbeI-MST2_R1	TTCCCAATAATACTCTTCTAC (21 bp)	33,3 %	52,0 °C	Amplicon 126 bp
ProbeI-pHT6_F1	CATGTTACATAAGTCAGAC (19 bp)	55,6 %	55,0 °C	
ProbeI-pHT6_R1	GACAATACCAACTGCCATTTC (21 bp)	42,9 %	55,9 °C	Amplicon 98 bp
ProbeII-pHT6_F1	AGATATATACAAAACCTCAACTGTC (25 bp)	32,0 %	56,4 °C	
ProbeII-pHT6_R1	CTAACCCAATTGTTCTAAACAATAG (25 bp)	32,0 %	56,4 °C	Amplicon 103 bp
ProbeI-pMST1_F1	CTGGTAAAATTCGTAAAAGGAATG (24 bp)	33,3 %	55,9 °C	
ProbeI-pMST1_R1	CAATCTACATTTATTCTCCAGATC (24 bp)	33,3 %	55,9 °C	Amplicon 165 bp
MST1situ_F1	CGTTGGTTAGTTGATCATGATC (22 bp)	40,9 %	56,5 °C	
MST1situ_R1	TTGCAGCAATTTCCCGCTC (19 bp)	52,6 %	56,7 °C	Amplicon 148 bp

Table A.4. Primers for TOPO T/A and TOPO ENTR Cloning® and the generation of DIG labelled probes for southern blotting and *in situ* hybridisation.

Appendix B

Sequences and Alignments

ATGGCAGTTGGTATTGTCCCAACAAGTGAGGGTTCCGCGGATTACAATGGAAGGATTACGTGGTTTGTGGTGTATCATCCATCG
TTGCAGCCACCGGAGGAATCATCTTTGGTTATGATATCGGAATTTTCAGGAGGAGTGATCTCTATGGCGCCGTTTCTGAAGAAATT
CTTCCCAGAAGTGTTCAC TAAGATGACACATGTAGCTGAAATAAGCAACTACTGTGTATTTGACAGCCA ACTACTGACCTCTTTC
ACTTCCTCTTTATACATTGCTGGTCTTATTGCTTCCTTCTGGCCTCACCAGTCACTCGTACATATGGTCGTA AACCATCAATTA
TAATCGGTGGAATAGCATTTCTCATCGGTTCTGCCCTTGGAGGTGCAGCATCCAATATCTACATGTTATTACTTGGTCGAATCCT
GCTAGGTGTAGGTGTGGTTTTGCAAATCAGGCAGTCCCTTTATACCTTTTCAGAAATGGCACCTGCTAAGTACAGGGGATCTTTC
AACATCGCGTTCCAATTATGTGTAGGAATTGGAGTACTATTTGCTAGCCTTCTTAACTACGGTGTCTAAAGATTAAAGGTGGTT
GGGGATGGAGAATTTCTTAGCAATGGCTGCAGCTCCTGCTACATTTCTAACAATAGGAGCATTTTTCTCCCAGAAACCGCAA
CAGCCTAATTCAAcATGGAATGATCATCAAAAAGCTAAGAAGATTCTACAACGTGTACGTGGTACAACCGATGTGCAAGCAGAA
CTAGACGATCTCATCAAAGCAAGTGACAAGTCAAAAGCCGTC AAGCATCCTTTTAAGCAAATCATTAACGGAAATACAGGCCAC
AACTTGCTATGTCAATATTAATACCATTCTTCCAACAGGTGACTGGGATCAACGTGATCTCCTTCTACGCTCCAATTCGTTTCA
AACAATAGGCCTAGGCGCGAGTGCATCACTTATGTCTGCTGTGGTGACAGGTGTGGTAGGCACCAGTGCAACTTCTTAGCATTG
TTGATAGTTGACAGGGTGGGGCGAAGGGCT**ATGTTCAGTTTTGGGGGAATC**CAAATGTTTGTATCGCAAATATTGATAGGGATAA
StHT6_F1
TAATGGCAGTTAAGTTAGGAGATCATGGGGTGTGAGCAAGGGGTATGGGCTATTGGTTTTGGTGTGATATGCATTTATGTTGC
StHT6_R1
AGGTTTTAGTTTGT CATGGG**GTCATTAGGATGGTTAGTTCC**CAAGTAAATATTTCCATTAGAAATAAGGTCAGCAGGACAAAGC
ATAACAGTGGCTGTGGGGTAAATATTCATTTTATAATGCTCAGACTTTCTTGGCTATGCTTTGCCATCTAAAATCAGGGATTT
TTTTTTTTTTGGGGCATGGGTGCAATCATGACTGTATTTGTCTACTTTTTCTTGCCAGAGACAAGGAATTTGCCAATTGAAAA
TATGGAAAGCATATGGAGGGATCATTGGTTTTGGAAGAGATTTGTTTTTGATGAGCAAGACTATGACAAAGGTGACACTACT**TAA**

Figure B.1. ORF of *StHT6* with location of qPCR primers StHT6_F1 and StHT6_R1 (shown in blue). Start and stop codon are highlighted in red.

Appendix B Sequences and Alignments

ATGCCCGGTGGAGATTTTCGACCTCCGGTAACGGAGAACGCATTTTCGAGGCTAAAATAACACCAATTGTTATCATTTCTTGTA
TTATGGCTGCTACTGGAGGACTCATGTTTGGTTATGATGTTGGAGTTTCTGGTGGTGTACATCGATGGATCCATTTTACAAAA
ATTCTTCCCAACGGTTTACAAGAGAACAAAGGAGCCAGGTTTAGACAGTAATTACTGCAAATACGATAATCAAGGCCTACAATTA
TTTACTTCATCTTTATATTTAGCCGGTTTAAACGGCGACGTTTTTCGCTTCTT**StHT2_F1**
T**ACACGACAAGAAA**CTTGGT**CGG**GAGATTAAC
TGTTAATCGCCGGTTGTTTTTCATCATCGGAGTTATACTAAATGCTGCTCAAGATTTAGCTATGCTTATTATTGGAAGAAT
StHT2_R1
TCTCCTTGGTTGTGGCGTT**GGTTTCGCCAATCAGGCAG**TTCCTACTATTTTTATCAGAAATAGCACCAACAAGAATTTCGTGGAGGA
CTTAACATTTTGTTCACCTAACGTAACATTTGGTATCTTTTTGCCAACCTCGTTAACTACGGAACAGCCAAAATTAGTGGAG
GATGGGGATGGAGATTATCATTAGGGTTAGCAGGATTTCCAGCAGTCTTGTGACTTTGGGTGCATTATTTGTTGTTGAAACCCC
AAACAGTTTGATTGAAAGAGGTTATTTAGAAGAAGGCAAAGAAGTACTTCGAAAAATCCGAGGTACCGACAACATTGAACCTGAA
TTCTTGGAACTTGTTGAGGCTAGTCGTGTTGCTAAAGAAGTCAAACACCCTTTCAGAAATTTACTCCAACGTAAAAATAGACCTC
AATTGATCATCTCTGTTGCCCTCCAGATATTCACAAATTCACAGGAATCAACGCTATATTTCTACGCGCCcGTTtTaTtTCAAaC
ACTAGGGTTCGGAAGCAGTGCAGCTCTTTACTCAGCCGTCATCACgGGAGCCGTC AACGTTCTCTCCACcGTAGTCTCGCTCTAC
TCCGTTGACAAGCTCGGACGACGAATCCTCCTCTAGAAAGCCGGGTTCAAATGTTACTATCCCAAATAATAATCGCTATAATCC
TCGGTATCAAAGTTACGGATACTTCAGACAACCTTAGCCACGGTTGGGGAATCTTCGTAGTAGTTTTGATCTGCACATATGTATC
GGCTTTCGCGTGGTCTGTTGGGCCACTAGGATGGTTAATTCCTAGCGAAACGTTCCCGTTGGAAACTCGTTCAGCCGGTCAAAGT
GTTACAGTGTGTTAACTTGCTCTTCACGTTTGTATGGCACAAAGCATTTCTCTCAATGCTTTGTCATTTCAGTATGGGATAT
TCTTGTCTTTTCGGGGTGGATTTTCGTTATGTCGTTGTTCTGTTTTCTTCTTGTGCTGAGACGAAGAATGTTCCCATTTGAGGA
GATGACGGAGAGGGTGTGGAAGCAACATTGGTTGTGGAAGAGGTTTATGGTTGATGAAGATGATGTTGATATTGTTAAAAAGAAT
GGACATGCTAACGGATATGATCCCCTTCTCGGTT**TAA**

Figure B.2. ORF of *StHT2* with location of qPCR primers StHT2_F1 and StHT2_R1 (shown in blue). Start and stop codon are highlighted in red.

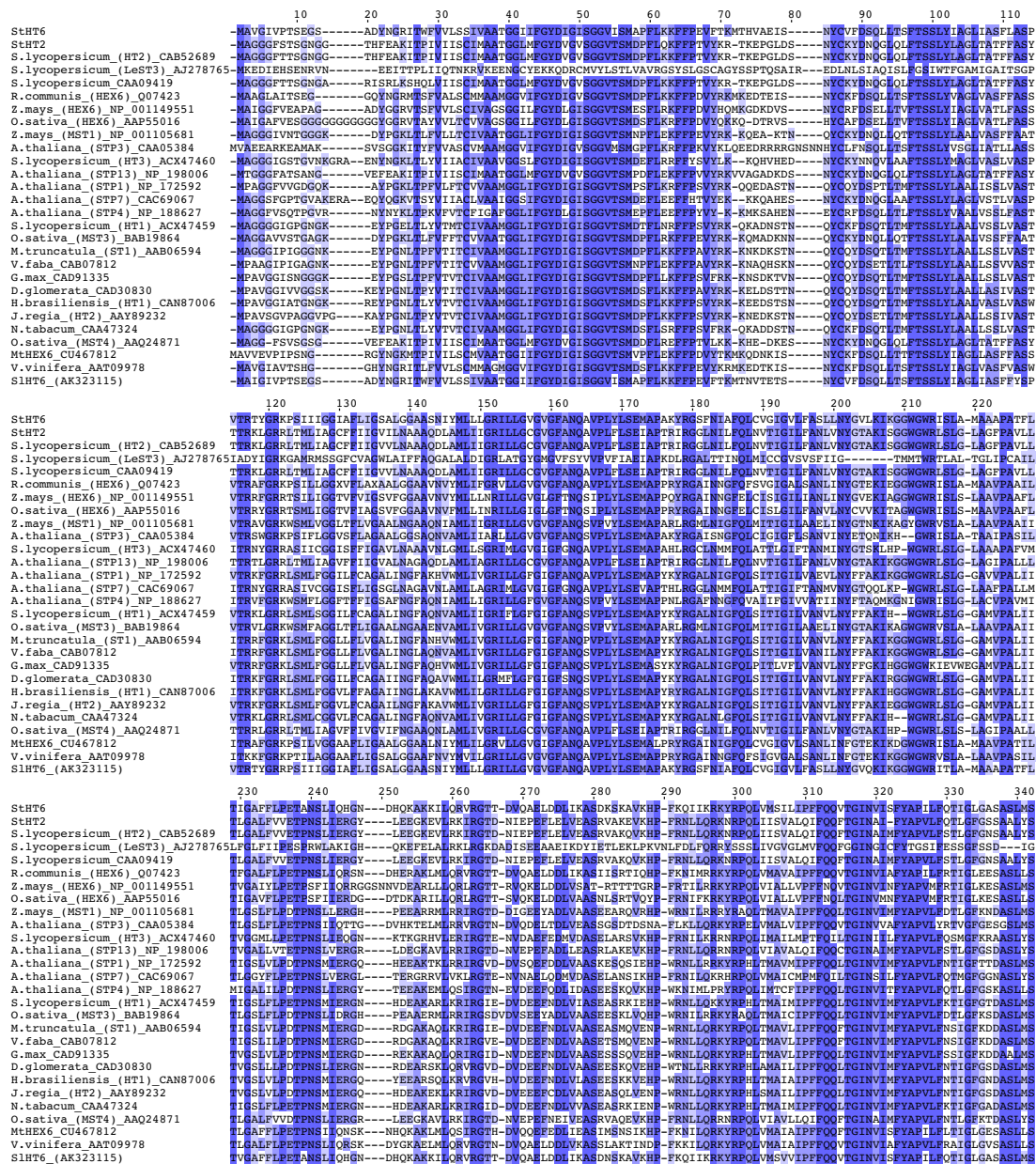


Figure B.3. ClustalW alignment of the deduced amino acid sequences of plant sugar transporters. Dark blue indicates high conserved amino acids in all sequences, blue indicates similar amino acids and light blue less similar amino acids. The red box highlights the conserved PETKG motif of MFS sugar transporters. Average length of the transporters are approximately 515 amino acids. (Part I)

pHT6_F1

TCCAATAATTTAACCACACCATCCATCAAATACATACACTAAAACATATATCACTTAAAGGGACATAAAGTGAATGCATTCAAC
TCAAACGAAATTTAGAACATACGATAAGGCTATTAATATTTGTGTCGAAGCTTTGACCTAAGACACTTTCTAGAAGTAAAATCCA
TGAAAATTTTTCATCATAAAATATAATAACCAAAACAATTTTTGTCTTGAAC TAGAGATGTTTTTTTTTAAAATAAAAAGCAAGA
ATAGAAAAGAGCAAAAATATTATCAAGAATGGAGGTTTTAACTAGATACTACAATGAAGAGATGAATGAAAGAGATGAGAGAGT
ATACGAGAGAGAAACATATGAGTCCAAAAAATAAGCACACTAATAAAAAAAAAAAGTGTATTGTCTTTAAATATTATATTTGT
AATTA AAAACTTAGTTTTGTAAATAAAAAATATATTTTACACTATAATTAAGCCTTTAAACACAATATCCTTATAATTTTCCT
AAAAGAAGTTATATAAGATGCAAATTAACTCTAAAATCTTAACTCTCAAACAATAAGAATCACAGTTTCTGAAATATATGACTA
TCACACATGCAATTTACTTCCCTAAAAGAAAAAATTTGATAAACTAGCTATTAGTATTATATATAATTA AACACTCATGAATA
AAAATAAAATACTTTCAAAGAACGAAATAATAAATAATAAATTTGTTTAGACATAGGATAAAAACATGATCAAGATCAGTGACA
AGTAAAATATAAAAATTTGGCTATGTATTTTAAAAAGAAATTAAGTGTATTGACCCCTCATTGCGTTCCAGCAATAATACGACT
TGCTATCAGAGTTATTTCTCAATTTTCTAATTTCTATATATGGATTTTTTAAAAACTACTTACTAAACATCTTAATTTATTA AAA
ATTAATTACGAAGATCAACAAAAGAGTAATAATGACACCAACATTTTGACAATGATCATGTAAAAGGCTAAGAGAAGGCTGCCAA
GAATCCAGGGAATAGAATATGTCAAAGTTATACATATATGACCTCATTAAATGAAATTCACGTCAAATAACACCTATTTAAAGATAT
TATACAAAACCTCAACTTGCTTGTAAATAGCAATCCAAAAC TAATTAATTTCCATGTAATAATTAATACTATTTGTTAGAA
CAATTTGGTTAGGTGATAGTGAGTGGTTATGGGAGTTGTTAGAGCTGATGCAATCTTTTTTCTCGTCATTACTATATATATTAT
AGACTGAGTCCGGCAGAGATTAATTAATTAATTAATTAATTAATTAATTAATTAATTAATTAATTAATTAATTAATTAATTAATTA
ATTAATAAAGGGACCATATGTGGTGTGACTGGGCTGAACAAGTGGTACAGTTTACCAGTTTTGATTGATCTTGATTTGCATTTA
CTTTGTTTGTCTGGGGTCCAGTACTGGCTTGCTAGTTACAAGTGAATAATCTACTTCAGAAGATTAGTCAACTGCTCAATATA
TGTATCGCAACGTGCTACAGGCATTTGTTTTTCTGTC CAATTGGTACCAAAGTCTGCATTGATCCGAGAAATGTAGATATTGT
CATGATCAATCAAGAATTGTATATTGATACGATGATTGACGAAATTA AACATGTAAACAAGAGAACATGTAACGTGAATCCAC
TTAATTAGGAGAAAATTGCCAAGACTAGCCATAATACAGGAAAGTGTGACAACAAGATAAGAAGCCAAAAATATGACTAGTTCA
ACTTATAATTAATTGTTATATATATGACCC TAAAGTCCAAATAATTAAGAGTAGTAGATACGCCATCCAATTGCAAGGCATTGA
CCAAATTAATTTATTTAGCCATGCTGATTTTGTAGCTGTGCATTAGTCATGATGTATAGCTTATTATATACTACTCCTATAAG
5' UTR
TTCATGTTACATAAGTCAGACCTTACAATTCATACTTGAATTTACACTCTACACAGTTTGAACCTGAGTGAAGAA
GSP2
ATGGCAGTTGGTATTGTCCCAACAAGT GAGGGTTCCGCGGATTACAATGGAAGGATTACGTTGGTTTGTGGTGTATCATCCATCG
GSP1
pHT6_R1
TTGCAGCCACCGGAGGAATCATCTTTGGTTATGATATCGGAATTTCA

Figure B.5. Full promoter sequence of StHT6 (shown in gray) with location of the primers pHT6_F1 and pHT6_R1 (lilac). Genome walker primers GSP1,2,1a and 2a are shown in blue. The start codon is highlighted in red. Putative TATA boxes are shown in green.

5' UTR
TCTCAACTATCCATAATAAAATTAACCGAAATAATGATGGGTAGCGTTTATGTATACGTATGTGGAGGCTATCTGCTATT
GGGGTCTACTTTTTGGATATGACATCGGTGTCATATCTGGAATTCCTACTATGCCTTATTTTCGTAAGGAATCCCTTC
TGGACCAGCAAAGAAGGATCAATGTGGCATCGCTTTTAGCAGGATGCTTTTTTGGCGCACTTGGCAGGATATTT
GCTGTAGATAATTGGTAGAAAGTACTCAGTCTTGTCTGGATCTGTGTATTTGTGTCGGTGGTATTTTGAAGCATCT
TCTACGACATTTGCTCAAAATGTATACGGGAAGAGTTATTGCTGGCCTTGCAGTTGGTGAACCTTCTATGATCGTACCCT
TGTATCAATCCGAGATCAGCCAAAAGAAATTCGTGGGCGTTTGGTATCTCTTCAACAGTGGTTCGATTACTATAGGGAT
TGCAATTTCAATTTGGATCGATTATGCCACACTTCAAATCGATTTCGCCTCAACAATGGAGAATCCATTATGGATTCAA
TTGTTCCAGCAATAATTCTTGTATAGGAACATTTTTCTCCCATTTTCAACACGTTGGTTCGATTACTATAGGGAT
GAAGAAGCAATAACAGTATTGGCAAAATTTACGATCCAAAGGAGATAGAAATGCAACAGTTGTACAAGAAGAATTTAGGG
AAATTAAGAACTGTTATATTTGAGCGGGAAATTCGCTGCAAAAAGTTATTGGGAATTGCTTAAAGTAGGACCTGAAAT
ATTCGTAGAAGAGTGTGTGGGAGTTTTTATTACAGGCTTTCAACAGTTGACCGGAATTAATGCTATTATGTACTACGC
ACCTCAAATTTTTAGTAATGCTGGACTTGGCGGATAATTCATCCAGACTTCTTGCAACAGGAGTTAATGGTCTTGTCAATA
TGTTAGCAACAATTCCTGCAATAATTTGGATAGATCGTTTGGGACGTAAACCTACTCTAATATCAGGAGGCTTATTAATG
GGCTCATCAATGATAATTATAGGATCTATATTAGCCACACATGGAAACAAAATATTTTGATGAATCGTTGGGAAAACATTTT
GTATATTTAGACAACAAGGAAGCTCCTATGCTGTTATTGTTTTATATATGTTTTTGTGGCTAGTTTTGCTTATTCTTGGG
GCCCAGCTGGATGGATTTATCCTGCTGAAATTTTTCCGTTACGCATTCGAGGTAAAGCTATGTAGTAAACAACAGCTT
GTAATTGGCTATTTAATTTGTTATTGGACTAGTTGTGCCAATTTTATTGGATAGTATTATATGGGTACATATTTAATCTTT
GGAATTTTTGTGTATTAATGGCAGCTGCAATATACATATTTTATCCAGAAAACAAAAGGTAATCATTAGAGGAGATGGA
CAATTTATTTGGCAACGTGCAAAAATCAAAAACCTGGAAAAAATGAAGGGGAGCTTGAAGCAGCTTGAAGCAACA
AAAATGATCGTAGAGAAACGGCTAAACGTTAAAAGTTATTATTACTATTATTACTAACTTTTCTTATCATTATTTTAAATAAT
ATGTATATTTATTTGTGTACCATTGTTTATAATATGGTGATACTGTAATACGTTAGTGATGGTCAAAATTTTATATATAA
AAAAAATTTGTCACATGTATGTATTTTAAATAAATTTATAATTGTAGCTTTGACTTAAAAGTTCCAAGCTAAATTTGGACA

Figure B.7. ORF of *GiMST1*. Real time primers (GiMST1Real_F1 and R1) are shown in red. Primers for the amplification of the *in situ* probe are shown in light blue (GiMST1situ_F1/R1). RACE primers are highlighted in blue (GiMST1down_F1/F2/F3/F4). Start and stop codon are shown in red, 3' and 5'UTR in yellow. The full sequence of *GiMST1* has been deposited at the EMBL databank with accession no. HM143864.

Appendix B Sequences and Alignments

```
GATTACTTTGCGAAGTTCCGAAGCAAATCTATGCAAAAAAGACTCTAAAGTTCTAAGATTATTAACGTTAATCCTACAACCTGC
TATGAAAGAAGTTAATGGATTATCATCGATAAAGTTTTTTGGACAATATCAAAATTAACAATACCTTAATTTTCCTTAAAAATAA
ATTATTGTACAATCCACATTGGATAATTAATTAATTAATATCTAATTAATATCTGTCAAGAATAATTATTCCTAAATTCGA
CTCTTAATTCTGTGAATCTTTAATCAATTAGTAAAAATCTAGTATTAGTTCCCACGCATCATTAAAATTAATTAAGTACTGTACT
ACAGTTCACAATATAAACACGCGGTACAGTATCACGTGTCAAGAATGACGCAAAATCGCGATTTAGAAGAAATTTGAATATCT
GAATCCGAATATCCAATATTTGTTTGATACCTGCCCTCTTGAAAAATAAAAAAGGTAATAATTAACAACATGATTTGTTTTAATAA
AATAAAAAATATGCGCTCTTGAAGTTATCAGCATAGACTTGTCAAACATGGAATAAGTTAATTTAGATATATAAAAGTAAATG
TAAAAAATGGCGTAAACGTAATCAAGGAAACAATTGTAGTGAGCGTTAATCTCATCTCGATTGCGACTTTTTGTGGAGATTCC
CAATATAGAATAATAAACAAAGAAACATATTGTGTATTGTGCCGGAAGAGTTAAAAATAAGTATGCTTAATAATGAGAATTA
TTAATTTATAAACTTTCAACTTGTCTTAACCTTGATGATTAAATGAAAAATCAGAAGAACTGATAGACATTTTAGATTTTCA
ATAACTTGTATTTTTTCCGTAATGCTATAAAAAGTTAATAAAGAAAAATGAGAAAAATTAATTTTTCCAAAGCTAGCAATTTA
AAACATATGTTGGTCATGTGTTATCTGGCGGATTTGACTCGCTTGATGATCGGAATGTCGATCATTTTGGCTAAAATTAACGTTA
ATTTTGCCAAAATGATCGACATTTCAAGGACACTGGCGCTGTATAAGTGAAGAAACCAACCAAATTTAGCGATTAAAGTACC
GGGAAAAGCGTTACGGCATTACCATTATCAGTCGCCATGAAGATTATGATCAACCAGCAGATGAAATTTAATGAATACAAA
CTAAGACGTGCTACGACAGGAAAACTTAATGTTATTTTTAAAGAAATTCGTGAACAAAAATCGTAAGTTTCTCTCCAAGTGAATT
TCAATCTGCTTTTTGTGTTTTTTGTAAGAAAAAGTTTTACTCATTAAATAATCCAAACGATAATCAAAGCCGTTTATAATAA
CTTTAATTTAAAATTCGTAAAAGGAATGTTACAAATTATAAAAAAGGATGCAATAATGTAAAACCGGAGAAAATCTTTAACCG
ATTAGGATTTCCGAAGTTTGTGGAAGTCCATAAAGTTATTTATGATGTGAGATGCAGATCTGGAGAATAAATGTAGATTG
TCCTATGATTTCTAAAAACTATTAGTAAATTTCTTGATAATGTGACTAATTCGGCAAGTTTCTTTTCGCACGATAATATCAGGA
MST1_GSP2
MST1_GSP1
TCAACAATAGTACTAGGGACTGACCACTAGTCCTAACCAAATTCGGATTATAACAAGAAAGAGAAAAATGTCCATTACCGTGAA
GTATATAAAGCATGTAGTTTTTTTTCTTATCCTCATTTTTTTTTTAAAAAATAATCTCAACTATCCATAATAAAATTAACCG
AAATAATG
```

Figure B.8. Promoter sequence of *GiMST1*. Genome walker primers are shown in blue. Start codon is shown in red.

5' UTR
GAAAATTTTTTGTCTTCTCCTTAATTTTTTCTTTCTTTTCACGATAACATCCATCGCGACTTTTTTCTTTGGAATTATTTTA

ATGATTTTATAACAAAATGAATGAAAGCAGTTATGTATATGTGTGCGGCGTTTTCTGCTATTGGTGGTTACTTTTTGGGTA
MST2_GSP2
TGATATCGGTGTCATATCCGGAACTTACTATGT**CTCACTTCCGCGAAAAGTTCCCTCTGG**ACCTGCAAAAAGAAGGATCAATT
GiMST2Real_F1
GTATCTTCGCTGTAGCAGGATGTTTTTTGGCGCACTTGTTTCAGGATATTTTCTGATAAAAATTGGTAGAAA**ATTCTCGATT**C
MST2_GSP1
TTGGTGCATCTATGGTGTTTAT**GTCGGTAGTGTTTTGCAAGCAACTGCTACG**ACTTTTATTCAATTGTATTTTGAA**GAGTCGTT**
GiMST2Real_R1
GCTGGCGTATCAATTGGATACTTCTATGATCGTACCTCTGTATCAATCTGAAATAAGTCCAAAAGAATTCGTGGTCTGTTAAT
ATCTTTTCAACAATGGTCAATTACTATAGGGTTTGCATTTTCATTTTGGATTAATTACGCTACAGAAAAATTTGATTATCTGCA
MST2_GSP1a
CAATGGAGGATTCATTATGGATACAAAATGTTCCAGCATTAATACTTGCCTTCGGGATGCCTTTCTTCCATTTCA**CCACGCT**
MST2_GSP2a
GGTTGGTACATTCCGATCGTGACGAAGAAGCAATAACAGTATTAGCAAAATAC**GAGCCGGTGGCGATAGAACTGCAGT**GCTGT
ACAGAAGGAATACCGGAAATCAAAGATAATGTGAGATTGCAACGAGAATTTGCTGCAAAAAATTTCTGAATTGGTTAAAAGA
GGGCCCGAAAATATTCGTAGAAGAGTATTATGGGAATCTTTATTCAGATTTTTCAACAATTGAATGGAATAAATGCTATTATGT
TTTATGCACCTCAAATTTATAATAATGCCGAATTGATCTTTCTACAGGAATTAACGCTACAATTCCTGCAATACTTTGGGTAGA
TCGTTGGGGACGTAGACCAACTTTAATATCGGGAAGCATAATAATGGGAGCATCAATGTTGGTCAATAGGAAGTATATTAGCAATA
AATGGAACAAAGTATTTTGTAGTTCCTAGGAAAAATTTTATAAAATAGATAATAAAGCAAGCTCCTTAGCTGTTATTATTT
TTATATATATTTTTGTGGCTGGTTTTGCTTATTCATGGGGTCCGACCAGATGGATTTATCTGCTGAAATCTATCCATTACGTAT
TCGAGGTAAGCAATGTCTATAACAACCTGCGTTTAAATGGTTATTTAATTTCTGTTCTGGACAAATGTACCGATTTTATTGAAT
AGTATTACATGGGTACATATATAAATTTTGAATATTTAGTATTATAATGGCAATATCTGTACACATATTTTACCCAGAAACAA
AGGGAAATTCATTAGAAGAAATGGATAGTATATTCCAGTAATATTCATCCAAATAATATTTCTATTTCAAGACAACATTATCCACC
3' UTR
ATCTCCACT**TAATAGT**GAAAGTATTAATATTGGTCAACAAAGAGAAAATTTTAGAGACCTGGAAAGTGGAAATACCCGAAGAAGAG
GAAAGAAGAGATTTATTTATCTACTTAACAAATATAATAAGACCTTTAAAAAAGATAGCTGATGAATTTGAACCAGTTATTGGTA
TTACATATTATCATTATAAATACTTTAATTAATCTTAGATTCAAGATTGTTACAATTATATATACTTGTTCACAAATATACATCA
AGATTGTATATTAAGGATATATTAGGTGATGGATTAAGAGCAGACAAATTATATATATATTGTAATTACATATATATATAA
AGTAATTTTTTTTAAACAATTTGT

Figure B.9. ORF of *GiMST2*. Real time primers (GiMST2Real_F1 and R1) are shown in red. RACE primers are highlighted in blue (MST2_GSP1/GSP2/GSP1a/GSP2a). Start and stop codon are shown in red, 3' and 5'UTR in yellow.

Appendix B Sequences and Alignments

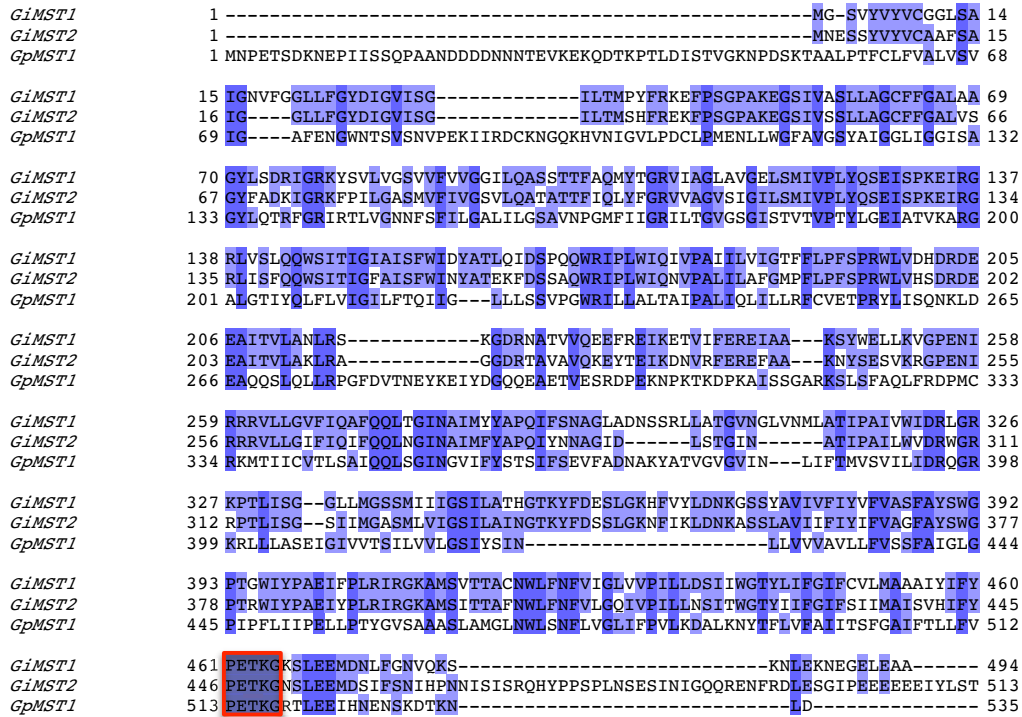


Figure B.10. ClustalW alignment of the deduced amino acid sequences of the glomeromytan sugar transporters GiMST1, GiMST2 and GpMST1. Dark blue indicates high conserved amino acids in all sequences, blue indicates similar amino acids and light blue less similar amino acids. The PETKG sequence highly conserved among sugar transporters is marked in red.

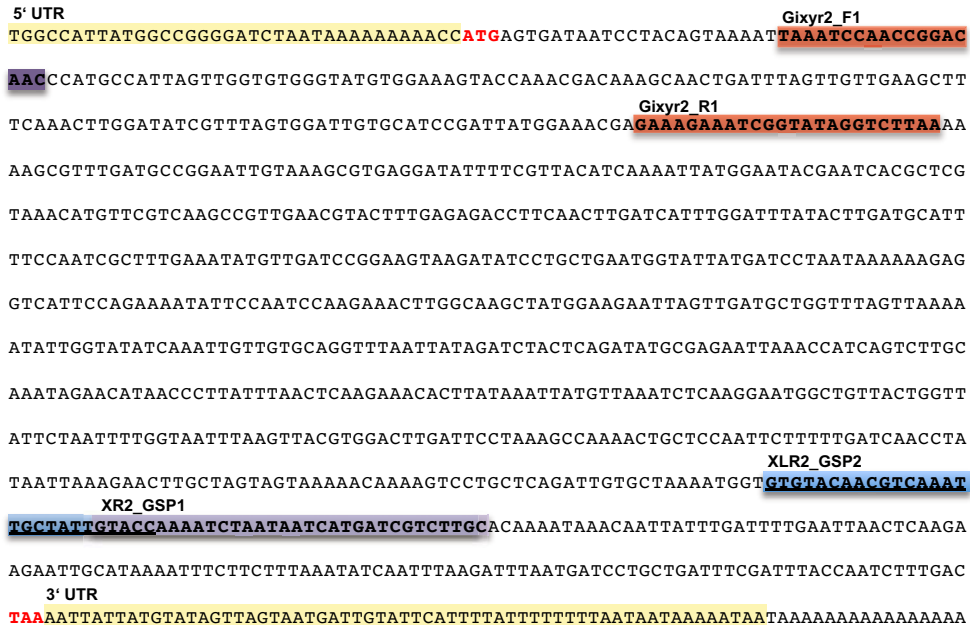


Figure B.11. ORF of *GiXR2* showing the location of the RACE PCR primer XR2up_R1 (lilac) and R2 (blue and black underlined) and the qPCR primer qXR2_F1 and R1 (red). 3' and 5' UTR are highlighted in yellow.

G1XR2 1 -----MSDNFTVKNLPTGQPMLVGVGVEMKRVPHDKATLDLVEEAFRLGYRLVCAASDYGNEKEIEI 61
 M.oryzae (CAI67591) 1 -----MSFTVKLKL-NELDMPQVGFGLKRVNSCBVTVNNAIKAGYRLFDGAGYDNGEVEE 59
 A.clavatus (XP_001269678) 1 -----MSFTVKLKL-SGYEMPLVGFGLKRVNNDPCADQVFAIKAGYRLFDGAGYDNGEVEE 59
 N.fischeri (XP_001265183) 1 -----MTTPTTKLKL-SGYDMLVGFGLKRVNNEFCADQVFAIKAGYRLFDGAGYDNGEVEE 59
 T.emersonii (ACR78268) 1 -----MATPTTKLKL-SGYDMLVGFGLKRVNNEFCADQVFAIKAGYRLFDGAGYDNGEVEE 59
 A.nidulans (CBF89516) 1 -----MSPPTVKLKL-SGYDMLVGFGLKRVNNDPCADQVFAIKAGYRLFDGAGYDNGEVEE 59
 T.stipitatus (XP_002484051) 1 -----MSSPTVKLKL-SGYDMLVGFGLKRVNNDPCADQVFAIKAGYRLFDGAGYDNGEVEE 59
 N.crassa (XP_963931) 1 -----MVAIKLKL-SGDFMPOVGFGLKRVNNDPCADQVFAIKAGYRLFDGAGYDNGEVEE 58
 C.dubliniensis (XP_002420572) 1 -----MSTTPTTKLKL-SGYEMPLVGFGLKRVNNAADQVFAIKAGYRLFDGAGYDNGEVEE 67
 A.fumigatus (XP_750231) 1 -----MTTPTTKLKL-SGYDMLVGFGLKRVNNEFCADQVFAIKAGYRLFDGAGYDNGEVEE 59
 C.albicans (EEO46327) 1 MLIKSNWYNCINIKRFLNLTQVRSVYASNSFSYFVYFKFKFCNKYSYSTMSTTPTTKLKL-SGHEHMLVGFGLKRVNNDPCADQVFAIKAGYRLFDGAGYDNGEVEE 110
 A.niger (XP_001388804) 1 -----MSTTPTTKLKL-SGYEMPLVGFGLKRVNNAADQVFAIKAGYRLFDGAGYDNGEVEE 59
 C.tropicalis (XP_002546500) 1 -----MFKFSTPTTIKRTSTFLFNYSGLFSLKSLITYYR-----TMSHTPTTKLKL-SGYEMPLVGFGLKRVNNEFCADQVFAIKAGYRLFDGAGYDNGEVEE 98
 C.parapsilosis (ABK32844) 1 -----MSIKLKL-SGHEHMLVGFGLKRVNNEFCADQVFAIKAGYRLFDGAGYDNGEVEE 56
 A.terreus (XP_001211802) 1 -----MATPTTKLKL-SGDFMPOVGFGLKRVNNDPCADQVFAIKAGYRLFDGAGYDNGEVEE 59
 P.stipitidis (XP_001385181) 1 -----MPSIKLKL-SGYDMLVGFGLKRVNNDPCADQVFAIKAGYRLFDGAGYDNGEVEE 57
 P.tritici-repentis (XP_001939973) 1 -----MAPNTPTVTLN-DGNKMPQVGFGLKRVNNAADQVFAIKAGYRLFDGAGYDNGEVEE 61
 P.marneffeii (XP_002150209) 1 -----MSSPVTVKLKL-SGYDMLVGFGLKRVNNEFCADQVFAIKAGYRLFDGAGYDNGEVEE 59
 C.cinerea (XP_001840096) 1 -----MVQVFKLKL-NGQELPQVGFGLKRVNNDPCADQVFAIKAGYRLFDGAGYDNGEVEE 59
 C.sheatae (ABK35120) 1 -----MSPFTFAFKLKL-NLEHETSIFGFCWMLKRSADQVFAIKAGYRLFDGAGYDNGEVEE 62
 P.guilliermondii (AAD09330) 1 -----MSIKLKL-SGYDMLVGFGLKRVNNDPCADQVFAIKAGYRLFDGAGYDNGEVEE 56
 C.glabrata (XP_447303) 1 -----MSSVVTLKL-NGLKMLVGLKRVNNDPCADQVFAIKAGYRLFDGAGYDNGEVEE 58

 G1XR2 62 LKKAFDAGIVKREDFIVTSKLNWNTNARKHVRQAVERTIRLQLDHLDLVLMHPIALKYVQPEVRYAEWYDPPK-----EVPENIPQIETWQAMELVDAGLVKNGI 169
 M.oryzae (CAI67591) 60 VKRALDEGLVKKREELFVSKLWNTPHDGERVEPIVKROLADWGIYDFDLYLHFPVAVLEVDPSVRYPPGWYDDADG-----EIRPSKASIQETWQAMELVDAGLVKNGI 167
 A.clavatus (XP_001269678) 60 VARAIKQEGIVKREELFVSKLWNSPHDGERVEPICRKROLADWGDVDFDLYIVHFPVAVLEVDPSVRYPPGWYDDADG-----EIRPSKASIQETWQAMELVDAGLVKNGI 165
 N.fischeri (XP_001265183) 60 VARAIKQEGIVKREELFVSKLWNSPHDGERVEPICRKROLADWGDVDFDLYIVHFPVAVLEVDPSVRYPPGWYDDADG-----EIRPSKASIQETWQAMELVDAGLVKNGI 165
 T.emersonii (ACR78268) 60 VARAIKQEGIVKREELFVSKLWNSPHDGERVEPICRKROLADWGDVDFDLYIVHFPVAVLEVDPSVRYPPGWYDDADG-----EIRPSKASIQETWQAMELVDAGLVKNGI 165
 A.nidulans (CBF89516) 60 VARAIKQEGIVKREELFVSKLWNSPHDGERVEPICRKROLADWGDVDFDLYIVHFPVAVLEVDPSVRYPPGWYDDADG-----EIRPSKASIQETWQAMELVDAGLVKNGI 165
 T.stipitatus (XP_002484051) 60 IARAIKQEGIVKREELFVSKLWNSPHDGERVEPICRKROLADWGDVDFDLYIVHFPVAVLEVDPSVRYPPGWYDDADG-----EIRPSKASIQETWQAMELVDAGLVKNGI 165
 N.crassa (XP_963931) 60 IARAIKQEGIVKREELFVSKLWNSPHDGERVEPICRKROLADWGDVDFDLYIVHFPVAVLEVDPSVRYPPGWYDDADG-----EIRPSKASIQETWQAMELVDAGLVKNGI 165
 C.dubliniensis (XP_002420572) 68 INRAIKQEGIVKREELFVSKLWNSPHDGERVEPICRKROLADWGDVDFDLYIVHFPVAVLEVDPSVRYPPGWYDDADG-----EIRPSKASIQETWQAMELVDAGLVKNGI 177
 A.fumigatus (XP_750231) 60 VARAIKQEGIVKREELFVSKLWNSPHDGERVEPICRKROLADWGDVDFDLYIVHFPVAVLEVDPSVRYPPGWYDDADG-----EIRPSKASIQETWQAMELVDAGLVKNGI 165
 C.albicans (EEO46327) 111 INRAIKQEGIVKREELFVSKLWNSPHDGERVEPICRKROLADWGDVDFDLYIVHFPVAVLEVDPSVRYPPGWYDDADG-----EIRPSKASIQETWQAMELVDAGLVKNGI 217
 A.niger (XP_001388804) 60 IARAIKQEGIVKREELFVSKLWNSPHDGERVEPICRKROLADWGDVDFDLYIVHFPVAVLEVDPSVRYPPGWYDDADG-----EIRPSKASIQETWQAMELVDAGLVKNGI 165
 C.tropicalis (XP_002546500) 99 INRAIKQEGIVKREELFVSKLWNSPHDGERVEPICRKROLADWGDVDFDLYIVHFPVAVLEVDPSVRYPPGWYDDADG-----EIRPSKASIQETWQAMELVDAGLVKNGI 205
 C.parapsilosis (ABK32844) 57 INRAIDEGIVKREELFVSKLWNSPHDGERVEPICRKROLADWGDVDFDLYIVHFPVAVLEVDPSVRYPPGWYDDADG-----EIRPSKASIQETWQAMELVDAGLVKNGI 163
 A.terreus (XP_001211802) 60 VARAIKQEGIVKREELFVSKLWNSPHDGERVEPICRKROLADWGDVDFDLYIVHFPVAVLEVDPSVRYPPGWYDDADG-----EIRPSKASIQETWQAMELVDAGLVKNGI 165
 P.stipitidis (XP_001385181) 58 VKKAIKQEGIVKREELFVSKLWNSPHDGERVEPICRKROLADWGDVDFDLYIVHFPVAVLEVDPSVRYPPGWYDDADG-----EIRPSKASIQETWQAMELVDAGLVKNGI 164
 P.tritici-repentis (XP_001939973) 62 VARAIKQEGIVKREELFVSKLWNSPHDGERVEPICRKROLADWGDVDFDLYIVHFPVAVLEVDPSVRYPPGWYDDADG-----EIRPSKASIQETWQAMELVDAGLVKNGI 168
 P.marneffeii (XP_002150209) 60 IARAIKQEGIVKREELFVSKLWNSPHDGERVEPICRKROLADWGDVDFDLYIVHFPVAVLEVDPSVRYPPGWYDDADG-----EIRPSKASIQETWQAMELVDAGLVKNGI 165
 C.cinerea (XP_001840096) 60 IARAIKQEGIVKREELFVSKLWNSPHDGERVEPICRKROLADWGDVDFDLYIVHFPVAVLEVDPSVRYPPGWYDDADG-----EIRPSKASIQETWQAMELVDAGLVKNGI 165
 C.sheatae (ABK35120) 63 VKRALDEGLVKKREELFVSKLWNSPHDGERVEPICRKROLADWGDVDFDLYIVHFPVAVLEVDPSVRYPPGWYDDADG-----EIRPSKASIQETWQAMELVDAGLVKNGI 169
 P.guilliermondii (AAD09330) 57 INRAIDEGIVKREELFVSKLWNSPHDGERVEPICRKROLADWGDVDFDLYIVHFPVAVLEVDPSVRYPPGWYDDADG-----EIRPSKASIQETWQAMELVDAGLVKNGI 163
 C.glabrata (XP_447303) 59 IRKAIKQEGIVKREELFVSKLWNSPHDGERVEPICRKROLADWGDVDFDLYIVHFPVAVLEVDPSVRYPPGWYDDADG-----EIRPSKASIQETWQAMELVDAGLVKNGI 169

 G1XR2 170 SNCCAGIIDLILRYARIRKPAVLOIEHHPYLQPRRIEFVQAGIATVAYSSGPGSFLSELEKSKALNDPTLPEHEITKSIADKHGKSPAQVLLRWATORGIAIIPKSNNDP 276
 M.oryzae (CAI67591) 168 SNFAQIIDLILRYARIRKPAVLOIEHHPYLQPRRIEFVQAGIATVAYSSGPGSFLSELEKSKALNDPTLPEHEITKSIADKHGKSPAQVLLRWATORGIAIIPKSNNDP 276
 A.clavatus (XP_001269678) 166 SNFAQIIDLILRYARIRKPAVLOIEHHPYLQPRRIEFVQAGIATVAYSSGPGSFLSELEKSKALNDPTLPEHEITKSIADKHGKSPAQVLLRWATORGIAIIPKSNNDP 276
 N.fischeri (XP_001265183) 166 SNFAQIIDLILRYARIRKPAVLOIEHHPYLQPRRIEFVQAGIATVAYSSGPGSFLSELEKSKALNDPTLPEHEITKSIADKHGKSPAQVLLRWATORGIAIIPKSNNDP 276
 T.emersonii (ACR78268) 166 SNFAQIIDLILRYARIRKPAVLOIEHHPYLQPRRIEFVQAGIATVAYSSGPGSFLSELEKSKALNDPTLPEHEITKSIADKHGKSPAQVLLRWATORGIAIIPKSNNDP 276
 A.nidulans (CBF89516) 166 SNFAQIIDLILRYARIRKPAVLOIEHHPYLQPRRIEFVQAGIATVAYSSGPGSFLSELEKSKALNDPTLPEHEITKSIADKHGKSPAQVLLRWATORGIAIIPKSNNDP 276
 T.stipitatus (XP_002484051) 166 SNFAQIIDLILRYARIRKPAVLOIEHHPYLQPRRIEFVQAGIATVAYSSGPGSFLSELEKSKALNDPTLPEHEITKSIADKHGKSPAQVLLRWATORGIAIIPKSNNDP 276
 N.crassa (XP_963931) 166 SNFAQIIDLILRYARIRKPAVLOIEHHPYLQPRRIEFVQAGIATVAYSSGPGSFLSELEKSKALNDPTLPEHEITKSIADKHGKSPAQVLLRWATORGIAIIPKSNNDP 276
 C.dubliniensis (XP_002420572) 166 SNFAQIIDLILRYARIRKPAVLOIEHHPYLQPRRIEFVQAGIATVAYSSGPGSFLSELEKSKALNDPTLPEHEITKSIADKHGKSPAQVLLRWATORGIAIIPKSNNDP 276
 A.fumigatus (XP_750231) 166 SNFAQIIDLILRYARIRKPAVLOIEHHPYLQPRRIEFVQAGIATVAYSSGPGSFLSELEKSKALNDPTLPEHEITKSIADKHGKSPAQVLLRWATORGIAIIPKSNNDP 276
 C.albicans (EEO46327) 166 SNFAQIIDLILRYARIRKPAVLOIEHHPYLQPRRIEFVQAGIATVAYSSGPGSFLSELEKSKALNDPTLPEHEITKSIADKHGKSPAQVLLRWATORGIAIIPKSNNDP 276
 A.niger (XP_001388804) 166 SNFAQIIDLILRYARIRKPAVLOIEHHPYLQPRRIEFVQAGIATVAYSSGPGSFLSELEKSKALNDPTLPEHEITKSIADKHGKSPAQVLLRWATORGIAIIPKSNNDP 276
 C.tropicalis (XP_002546500) 166 SNFAQIIDLILRYARIRKPAVLOIEHHPYLQPRRIEFVQAGIATVAYSSGPGSFLSELEKSKALNDPTLPEHEITKSIADKHGKSPAQVLLRWATORGIAIIPKSNNDP 276
 C.parapsilosis (ABK32844) 164 SNFAQIIDLILRYARIRKPAVLOIEHHPYLQPRRIEFVQAGIATVAYSSGPGSFLSELEKSKALNDPTLPEHEITKSIADKHGKSPAQVLLRWATORGIAIIPKSNNDP 316
 A.terreus (XP_001211802) 167 SNFAQIIDLILRYARIRKPAVLOIEHHPYLQPRRIEFVQAGIATVAYSSGPGSFLSELEKSKALNDPTLPEHEITKSIADKHGKSPAQVLLRWATORGIAIIPKSNNDP 277
 P.stipitidis (XP_001385181) 165 SNFAQIIDLILRYARIRKPAVLOIEHHPYLQPRRIEFVQAGIATVAYSSGPGSFLSELEKSKALNDPTLPEHEITKSIADKHGKSPAQVLLRWATORGIAIIPKSNNDP 276
 P.tritici-repentis (XP_001939973) 169 SNFAQIIDLILRYARIRKPAVLOIEHHPYLQPRRIEFVQAGIATVAYSSGPGSFLSELEKSKALNDPTLPEHEITKSIADKHGKSPAQVLLRWATORGIAIIPKSNNDP 276
 P.marneffeii (XP_002150209) 166 SNFAQIIDLILRYARIRKPAVLOIEHHPYLQPRRIEFVQAGIATVAYSSGPGSFLSELEKSKALNDPTLPEHEITKSIADKHGKSPAQVLLRWATORGIAIIPKSNNDP 276
 C.cinerea (XP_001840096) 166 SNFAQIIDLILRYARIRKPAVLOIEHHPYLQPRRIEFVQAGIATVAYSSGPGSFLSELEKSKALNDPTLPEHEITKSIADKHGKSPAQVLLRWATORGIAIIPKSNNDP 276
 C.sheatae (ABK35120) 164 SNFAQIIDLILRYARIRKPAVLOIEHHPYLQPRRIEFVQAGIATVAYSSGPGSFLSELEKSKALNDPTLPEHEITKSIADKHGKSPAQVLLRWATORGIAIIPKSNNDP 280
 P.guilliermondii (AAD09330) 175 SNFAQIIDLILRYARIRKPAVLOIEHHPYLQPRRIEFVQAGIATVAYSSGPGSFLSELEKSKALNDPTLPEHEITKSIADKHGKSPAQVLLRWATORGIAIIPKSNNDP 276
 C.glabrata (XP_447303) 170 SNFAQIIDLILRYARIRKPAVLOIEHHPYLQPRRIEFVQAGIATVAYSSGPGSFLSELEKSKALNDPTLPEHEITKSIADKHGKSPAQVLLRWATORGIAIIPKSNNDP 280

 G1XR2 280 RLAKNQLQFD-FELTOEELHKSISLNINRFRNDEADFDL-----FTPD----- 321
 M.oryzae (CAI67591) 279 TMSKNFEAVG-WMDESDIKTISALDGRFRNDEADFDL-----TDKLWIFG----- 324
 A.clavatus (XP_001269678) 277 RLAKNQLDVTG-FNLEEASETEIASALDRNFRNDEADFDL-----FVSLCAGYQGFYAPIF 330
 N.fischeri (XP_001265183) 277 RLAKNQLDVTG-WLEETSEIVSSINRNRNFRNDEADFDL-----LDFPDD----- 321
 T.emersonii (ACR78268) 277 RLAKNQLDVTG-WLEEPADIEALSALNKRNRNFRNDEADFDL-----YIPIFA----- 320
 A.nidulans (CBF89516) 277 RLAKNQLDVTG-FDLEDEGKALSDLDKGRFRNDEADFDL-----FTTTF----- 319
 T.stipitatus (XP_002484051) 277 RLAKNQLDVTG-WLEEQSDIDANGLDLGRFRNDEADFDL-----YIPIFA----- 320
 N.crassa (XP_963931) 277 TMSKNLNSLD-FDLESEEDIKTISGDRGRFRNDEADFDL-----AENLWIFG----- 322
 C.dubliniensis (XP_002420572) 289 RLAKNQLAVD-FDLTDEDLQATSKLDIGLGRFRNDEADFDL-----IPIFV----- 331
 A.fumigatus (XP_750231) 277 RLAKNQLDVTG-WLEEASETEIASALNRRNFRNDEADFDL-----V----- 315
 C.albicans (EEO46327) 329 RLAKNQLAVD-FDLTEEDLQATSKLDIGLGRFRNDEADFDL-----IPIFV----- 371
 A.niger (XP_001388804) 277 RLAKNQLDVTG-WLEEBEETIASALDGRGRFRNDEADFDL-----YAPIF----- 319
 C.tropicalis (XP_002546500) 317 RLAKNQLAVD-FDLTKDDLDLAKLDIGLGRFRNDEADFDL-----IPIFV----- 359
 C.parapsilosis (ABK32844) 275 RLAKNQLNSD-FELSKEDLERLNKLDKGRFRNDEADFDL-----IPIFV----- 317
 A.terreus (XP_001211802) 278 RLAKNQLVTVG-WLEEOSEIDALSALDGRFRNDEADFDL-----YVBTIF----- 320
 P.stipitidis (XP_001385181) 276 RLAKNQLDVTG-FDLDEQDFADLAKLDIGLGRFRNDEADFDL-----IPIFV----- 318
 P.tritici-repentis (XP_001939973) 280 RLAKNQLDVTG-FDLKDEEIKESLDLDRNFRNDEADFDL-----IPCYFA----- 323
 P.marneffeii (XP_002150209) 277 RLAKNQLDVTG-WLEEEATEIANGLDLGRFRNDEADFDL-----YIPIFA----- 320
 C.cinerea (XP_001840096) 277 RLAKNQLDVTG-FDLTEEBEIKQTSNDRNFRNDEADFDL-----TLYIFA----- 320
 C.sheatae (ABK35120) 281 RLAKNQLNSD-FELTKEDFEELSKLDIGLGRFRNDEADFDL-----IPIFV----- 323
 P.guilliermondii (AAD09330) 275 RLAKNQLNSD-FDLSDQDFEELSKLDIGLGRFRNDEADFDL-----IPIFV----- 317
 C.glabrata (XP_447303) 281 RLAKNQLNSD-FELTKEDFEELSKLDIGLGRFRNDEADFDL-----IPIFV----- 326

Figure B.12. ClustalW alignment of the deduced amino acid sequences of fungal glyoxylate reductases. Dark blue indicates high conserved amino acids in all sequences, blue indicates similar amino acids and light blue less similar amino acids.

Appendix C

Expression Data

Relative Expression of <i>StHT6</i> , <i>StHT2</i> and <i>StPT4</i> in Microdissected Potato Hairy Roots			
	- myc	+ myc	++ <i>myc</i>
<i>StHT6</i>	0.2291 (± 0.0122)	0.3785 (± 0.025)	1.0769 (± 0.0310)
<i>StHT2</i>	0.00054 (± 0.00012)	0.00061 (± 0.00007)	0.00050 (± 0.00012)
<i>StPT4</i>	-	31 (± 7)	126 (± 11)

Table C.1. Relative expression of *StHT6*, *StHT2* and *StPT4* in microdissected potato hairy roots. The expression was calculated relative to the transcriptional elongation factor alpha 1 (*StTEF*). (Errors are presented as s.d.)

Relative Expression of <i>StHT6</i> , <i>StHT2</i> and <i>StPT4</i> in Mycorrhized Potato Hairy Roots (Time Course)				
	3 dpi	11 dpi	14 dpi	32 dpi
<i>StHT6</i>	2.0993 (± 0.1085)	5.0533 (± 6.2655)	6.2655 (± 0.9390)	5.9155 (± 0.3916)
<i>StHT2</i>	0.00233 (± 0.00003)	0.00393 (± 0.00047)	0.00491 (± 0.0002)	0.00196 (± 0.00007)
<i>StPT4</i>	-	1.1266 (± 0.0621)	7.8486 (± 0.0665)	6.4434 (± 0.1833)

Table C.2. Relative expression of *StHT6*, *StHT2* and *StPT4* in a time course experiment with mycorrhized potato hairy roots. The expression was calculated relative to the transcriptional elongation factor alpha 1 (*StTEF*). dpi means days post infection. (Errors are presented as s.d.)

Appendix C Expression Data

Relative Expression of <i>MtST1</i> , <i>MtHT6</i> and <i>MtPT4</i> in Mycorrhized <i>M. truncatula</i> Hairy Roots			
	Sample I	Sample II	Sample III
<i>MtST1</i>	Myc: 0.0408 (± 0.0025) Non-myc: 0.0269 (± 0.0026)	Myc: 0.0751 (± 0.0042) Non-myc: 0.0299 (± 0.0039)	Myc: 0.0761 (± 0.004) Non-myc: 0.0344 (± 0.003)
<i>MtHT6</i>	Myc: 0.00037 (± 0.00003) Non-myc: 0.00049 (± 0.00008)	Myc: 0.0007 (± 0.00012) Non-myc: 0.00055 (± 0.00003)	Myc: 0.00047 (± 0.00006) Non-myc: 0.00056 (± 0.00006)
<i>MtPT4</i>	Myc: 0.5931 (± 0.0405)	Myc: 0.4706 (± 0.0289)	Myc: 0.4338 (± 0.0167)

Table C.3. Relative expression of *MtST1*, *MtHT6* and *MtPT4* in mycorrhized and non-mycorrhized *M. truncatula* hairy roots. The expression was calculated relative to the transcriptional factor alpha 1 (*MtTEF*). (Errors are presented as s.d.)

Relative Expression of <i>G. intraradices</i> Sugar Transporters and <i>StPT4</i> in Microdissected Potato Roots						
	<i>GiMST1</i>	<i>GiMST2</i>	<i>GiMST3</i>	<i>GiMST4</i>	<i>GiSUC1</i>	<i>StPT4</i>
Sample I	0.1046 (± 0.0032)	0.0155 (± 0.005)	0.0122 (± 0.0005)	0.0415 (± 0.0016)	0.0245 (± 0.0018)	30 (± 6)
Sample II	0.1705 (± 0.0103)	0.0142 (± 0.0009)	0.0038 (± 0.0004)	0.0197 (± 0.0009)	0.0104 (± 0.0007)	126 (± 11)

Table C.4. Relative expression of *G. intraradices* sugar transporters and the potato phosphate transporter *StPT4* in different samples of microdissected mycorrhized potato hairy roots. The expression was calculated relative to the transcriptional factor alpha 1 *GiTEF* for the fungal genes and *StTEF* for *StPT4*. (Errors are presented as s.d.)

Relative Expression of <i>GiMST1</i> and <i>StPT4</i> in a Time Course Experiment of Mycorrhized Potato Roots				
	3 dpi	11 dpi	14 dpi	32 dpi
<i>GiMST1</i>	0.0035 (± 0.0004)	0.0262 (± 0.0009)	0.1013 (± 0.0094)	0.0873 (± 0.0078)
<i>StPT4</i>	-	1.1266 (± 0.0621)	7.8486 (± 0.0665)	6.4434 (± 0.1833)

Table C.5. Relative expression of *GiMST1* and *StPT4* in a time course experiment of mycorrhized *M. truncatula* plants. The expression was calculated relative to the transcriptional factor alpha 1 *GiTEF* for the fungal genes and *StTEF* for *StPT4*. dpi means days post inoculation. (Errors are presented as s.d.)

Relative Expression of <i>GiMST1</i> and <i>MtPT4</i> in a Time Course of Mycorrhized <i>Medicago</i> Plants			
	1 dpi	12 dpi	25 dpi
<i>GiMST1</i>	0.0038 (±0.00008)	0.1311 (±0.0183)	0.1544 (±0.024)
<i>MtPT4</i>	0.00002 (±0.000001)	0.02005 (±0.00263)	0.07536 (±0.01014)

Table C.6. Relative expression of *GiMST1* and *MtPT4* in a time course experiment of mycorrhized potato hairy roots. The expression was calculated relative to the transcriptional factor alpha 1 *GiTEF* for the fungal genes and *MtTEF* for *MtPT4*. dpi means days post inoculation. (Errors are presented as s.d.)

Relative Expression of <i>G. intraradices</i> Xylose Utilisation Pathway Genes				
	<i>GiXR1</i>	<i>GiXR2</i>	<i>GiXDH1</i>	<i>GiXK1</i>
AEM	0.0606 (±0.004)	0.3354 (±0.0446)	0.0133 (±0.0023)	0.001 (±0.0002)
ERM	0.004 (±0.001)	0.0323 (±0.0076)	0.0147 (±0.0012)	0.0011 (±0.0001)
Spores	0.0106 (±0.0015)	0.0439 (±0.0033)	0.0169 (±0.0021)	0.0014 (±0.0001)

Table C.7. Relative expression of xylose utilisation pathway genes of *G. intraradices* in different fungal tissue. AEM means arbuscule enriched material. The expression was calculated relative to the *G. intraradices* transcription elongation factor alpha 1 (*GiTEF*). (Errors are presented as s.d.)

Relative Expression of <i>G. intraradices</i> XlnR Orthologues						
	<i>contig54</i>	<i>contig19</i>	<i>contig41</i>	<i>contig60</i>	<i>contig57</i>	<i>contig33</i>
AEM	0.0018 (±0.0006)	0.0125 (±0.0017)	0.0476 (±0.0061)	0.0348 (±0.008)	0.0006 (±0.0002)	0.0107 (±0.0018)
ERM	0.0123 (±0.0016)	0.0427 (±0.0042)	0.0067 (±0.0009)	0.1143 (±0.0101)	0.0001 (±0.00002)	0.0787 (±0.0103)
Spores	0.0177 (±0.0018)	0.0053 (±0.0007)	0.0096 (±0.0007)	0.0018 (±0.00009)	0.0001 (±0.00001)	0.1026 (±0.0142)

Table C.8. Relative expression of XlnR orthologues of *G. intraradices* in different fungal tissues. The expression was calculated relative to the *G. intraradices* transcription elongation factor alpha 1 (*GiTEF*). (Errors are calculated as s.d.)

Appendix C Expression Data

Relative Expression of <i>G. intraradices</i> Sugar Transporters in the ERM							
	control	Gluc	Man	Gal	GlucA	Xyl	Ara
<i>GiMST1</i>	0.0024 (±0.001)	0.0041 (±0.0004)	0.0047 (±0.0004)	0.0073 (±0.0001)	0.001 (±0.0001)	0.0679 (±0.0077)	0.003 (±0.0005)
<i>GiMST2</i>	0.00023 (±0.00011)	0.00049 (±0.00006)	0.00005 (±0.00008)	0.00036 (±0.00008)	0.00051 (±0.00003)	0.00106 (±0.00012)	0.00128 (±0.00029)
<i>GiMST3</i>	0.0127 (±0.0031)	0.0161 (±0.0016)	0.0137 (±0.001)	0.005 (±0.0007)	0.0055 (±0.00002)	0.0184 (±0.0034)	0.0122 (±0.0007)
<i>GiMST4</i>	0.0253 (±0.0025)	0.1755 (±0.0295)	0.0154 (±0.0032)	0.0095 (±0.0017)	0.0209 (±0.0011)	0.0884 (±0.0122)	0.031 (±0.0021)
<i>GiSUC1</i>	0.0197 (±0.0015)	0.0543 (±0.0111)	0.0366 (±0.0067)	0.0193 (±0.0027)	0.0133 (±0.004)	0.0204 (±0.0041)	0.0168 (±0.0015)

Table C.9. Relative expression of *G. intraradices* sugar transporters in the ERM. The ERM was exposed five days with 2% concentrations of different sugars or sugar derivatives. The expression was calculated relative to the *G. intraradices* transcription elongation factor alpha 1 (*GiTEF*). (Errors are calculated as s.d.)

Relative Expression of <i>G. intraradices</i> XUGs and XlnR Orthologues in the ERM										
	<i>GiXR1</i>	<i>GiXR2</i>	<i>GiXDHI</i>	<i>GiXK1</i>	contig54	contig19	contig41	contig60	contig57	contig33
Control	0.0054 ±0.0002	0.0153 ±0.0014	0.0251 ±0.0006	0.0018 ±0.0006	0.012 ±0.001	0.0244 ±0.0015	0.0028 ±0.0003	0.05 ±0.0013	0.00004 ±0.00001	0.0397 ±0.0017
Xyl	0.0029 ±0.0001	0.0179 ±0.0006	0.0075 ±0.0003	0.0008 ±0.0001	0.0043 ±0.0011	0.007 ±0.0002	0.0005 ±0.00001	0.0257 ±0.0003	0.000006 ±1.4x10 ⁻⁶	0.071 ±0.003

Table C.10. Relative expression of xylose utilisation pathway genes (XUGs) and XlnR orthologues of *G. intraradices* in the ERM incubated for five days in 2% xylose medium. The expression was calculated relative to the *G. intraradices* transcription elongation factor alpha 1 (*GiTEF*). (Errors are presented as s.d.)

Relative Expression of <i>G. intraradices</i> Sugar Transporters in Presence of Roots and Root Exudates						
	control roots	wt roots	<i>rmc</i> roots	control exudates	wt root exudates	<i>rmc</i> root exudates
<i>GiMST1</i>	0.00933 (±0.00042)	0.000239 (±0.00005)	1.09 (±0.48)	0.00126 (±0.0001)	0.000819 (±0.00006)	0.00082 (±0.00002)
<i>GiMST2</i>	0.001124 (±0.00003)	0.001427 (±0.00006)	0.34 (±0.015)	0.000313 (±0.00006)	0.000088 (±0.00001)	0.000083 (±0.000004)

Table C.11. Relative expression of the *G. intraradices* sugar transporters *GiMST1* and *GiMST2* in the ERM in the vicinity of wild type tomato roots, roots of the tomato mutant *rmc*, or in the presence of their root exudates. The ERM was exposed with roots or exudates for one week. The expression was calculated relative to the *G. intraradices* transcription elongation factor 1 (*GiTEF*). (Errors are presented as s.d.)

Effect of Increased Phosphate Concentrations						
	<i>GiMST1</i>	<i>StPT4</i>	<i>StHT6</i>	<i>GiXR2</i>	<i>contig41</i>	<i>StXTH1</i>
17.5 μM P	0.0351 (\pm 0.0073)	0.1788 (\pm 0.0679)	3.64 (\pm 1.24)	0.1476 (\pm 0.0572)	0.0326 (\pm 0.0277)	1.33 (\pm 0.59)
3.5 mM P	0.0081 (\pm 0.0037)	0.0052 (\pm 0.0039)	9.17 (\pm 0.65)	0.04 (\pm 0.0229)	0.0061 (\pm 0.0002)	2.62 (\pm 1.54)

Table C.12. Relative Expression of *GiMST1*, *StPT4*, *StHT6*, *GiXR2*, *contig41*, and *StXTH1* in mycorrhized potato hairy roots treated with different phosphate concentrations (17.5 μ M P, 3.5 mM P). The expression was calculated relative to the transcription elongation factor 1 of *G. intraradices* (*GiTEF*) or *S. tuberosum* (*StTEF*). (Errors are presented as s.d.)

Appendix D

Uptake Studies

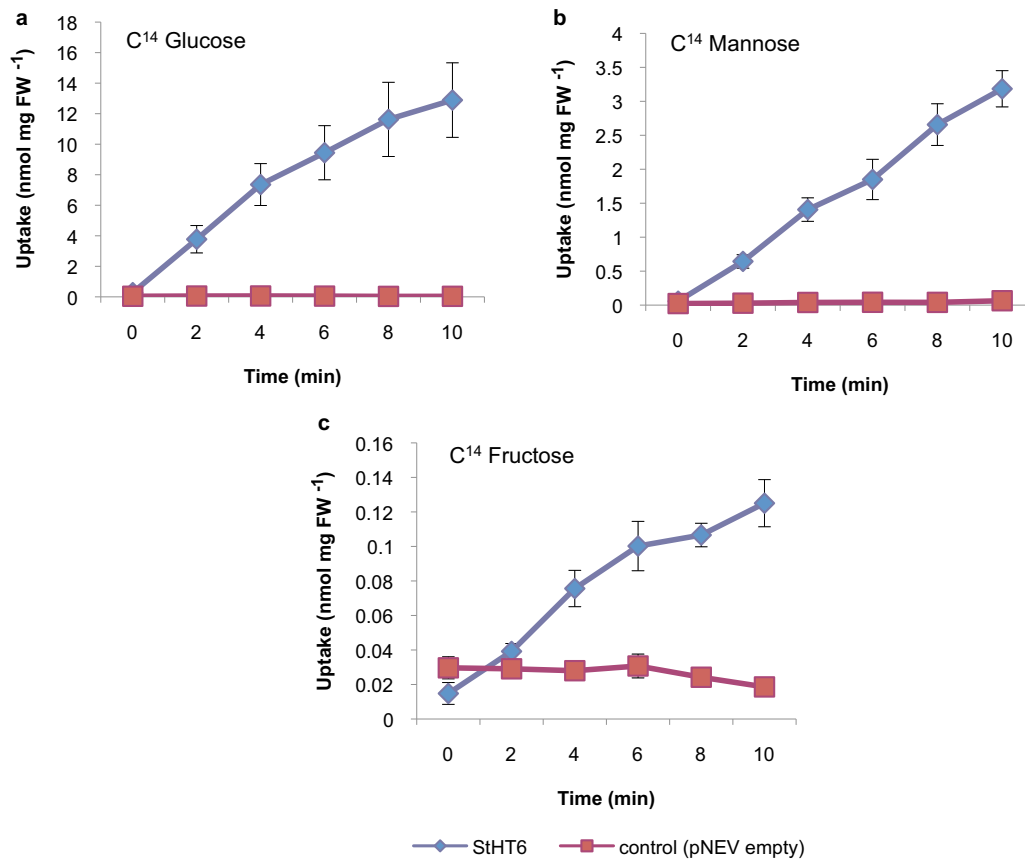


Figure D.1. Uptake of radio-labelled sugars in yeast cells expressing heterologously the *S. tuberosum* hexose transporter StHT6.

Bibliography

- Abelson PH. A potential phosphate crisis. *Science*, 283:2015, 1999.
- Akiyama K, Matsuzaki K, Hayashi H. Plant sesquiterpenes induce hyphal branching in arbuscular mycorrhizal fungi. *Nature*, 434:824–827, 2005.
- Aluri S, Büttner M. Identification and functional expression of the *Arabidopsis thaliana* vacuolar glucose transporter 1 and its role in seed germination and flowering. *Proc. Natl. Acad. Sci. USA*, 104:2537–2542, 2007.
- Andersen MR, Vongsangnak W, Panagiotou G, et al. A trispecies *Aspergillus* microarray: comparative transcriptomics of three *Aspergillus* species. *Proc. Natl. Acad. Sci. USA*, 105:4387–4392, 2008.
- Aoika K, Yano K, Suzuki A, Kawamura S, et al. Large-scale analysis of full-length cDNAs from the tomato (*Solanum lycopersicum*) cultivar Micro-Tom, a reference system for the *Solanaceae* genomics. *BMC Genom.*, 11:210, 2010.
- Atwell B, Kriedemann P, Turnbull C. *Plants in action: adaption in nature, performance in cultivation*. Macmillen publishers Australia PTY LTD, 1999.
- Auge G. Water relations, drought and vesicular-arbuscular mycorrhizal symbiosis. *Mycorrhiza*, 10:51–54, 2001.
- Ausubel FM, Brent R, Kingston RE, Moore DD. *Short protocols in molecular biology: a compendium of methods from current protocols in molecular biology*. John Wiley & Sons, 1999.
- Azcón-Aguilar C, Bago B. *Impact of arbuscular mycorrhizas on sustainable agriculture and natural ecosystems*. Birkhäuser, Basel, 1994.
- Bago B, Pfeffer PE, Abubaker J, et al. Carbon export from arbuscular mycorrhizal roots involves the translocation of carbohydrates as well as lipid. *Plant Physiol.*, 131:1496–1507, 1991.
- Bago B, Pfeffer PE, Abubaker J, et al. Carbon export from arbuscular mycorrhizal roots involves the translocation of carbohydrate as well as lipid. *Plant Physiol.*, 131: 1496–1507, 2003.
- Bago B, Pfeffer PE, Douds DD, Brouillette J, Bécard G, et al. Carbon metabolism in spores of the arbuscular mycorrhizal fungus *Glomus intraradices* as revealed by nuclear magnetic resonance spectroscopy. *Plant Physiol.*, 121:263–271, 1999.

Bibliography

- Bago B, Shachar-Hill Y, Pfeffer PE. Carbon metabolism and transport in arbuscular mycorrhizas. *Plant Physiol.*, 124:949—957, 2000.
- Bago B, Zipfel W, Williams RM, et al. Translocation and utilization of fungal storage lipid in the arbuscular mycorrhizal symbiosis. *Plant Physiol.*, 128:108–124, 2002.
- Balestrini R, Bonfante P. The interface compartment in arbuscular mycorrhizae: a special type of plant cell wall? *Plant Biosyst.*, 139:8–15, 2005.
- Barker SJ, Edmonds-Tibbett TL, Forsyth L, et al. Root infection of the reduced mycorrhizal colonization (rmc) mutant of tomato reveals genetic interaction between symbiosis and parasitism. *Physiol. Mol. Plant Pathol.*, 67:277–283, 2005.
- Barker SJ, Stummer B, Gao L, et al. A mutant in *Lycopersicon esculentum* Mill. with highly reduced VA mycorrhizal colonization: isolation and preliminary characterisation. *Plant J.*, 15:791–797, 1998.
- Benedetto A, Magurno F, Bonfante P, Lanfranco L. Expression profiles of a phosphate transporter gene (*GmosPT*) from the endomycorrhizal fungus *Glomus mosseae*. *Mycorrhiza*, 15:620–627, 2005.
- Besserer A, Puech-Pagès V, Kiefer P, et al. Strigolactones stimulate arbuscular mycorrhizal fungi by activating mitochondria. *PLoS Biology*, 4:1239–1247, 2006.
- Bever JD. Dynamics within mutualism and the maintenance of diversity: inference from a model of interguild frequency dependence. *Ecology Letters*, 2:52–62, 1999.
- Blee KA, Anderson AJ. Transcripts for genes encoding soluble acid invertase and sucrose synthase accumulate in root tip and cortical cells containing mycorrhizal arbuscules. *Plant Mol. Biol.*, 50:197—211, 2002.
- Boisson-Dernier A, Chabaud M, Garcia F, et al. Hairy roots of *Medicago truncatula* as tools for studying nitrogen-fixing and endomycorrhizal symbioses. *Mol. Plant-Microbe Interact.*, 14:693–700, 2001.
- Boles E, Hollenberg CP. The molecular genetics of hexose transporter in yeasts. *FEMS Microbiol. Rev.*, 21:85–111, 1997.
- Bonfante P, Perotto SS. Strategies of arbuscular mycorrhizal fungi when infecting host plants. *New Phytol.*, 130:3–21, 1995.
- Bruce A, Smith SE, Tester M. The development of mycorrhizal infection in cucumber: effects of P supply on root growth, formation of entry points and growth of infection units. *New Phytol.*, 127:507—514, 1994.
- Bryla DR, Eissenstat DM. *Respiratory costs of mycorrhizal associations*. Springer, 2005.
- Bécard G, Fortin J. Early events of vesicular-arbuscular mycorrhiza formation on Ri T-DNA transformed roots. *New Phytol.*, 108:211–218, 1988.

- Bécard G, Piché Y. New aspects of the acquisition of biotrophic status by a vesicular-arbuscular mycorrhizal fungus, *Gigaspora margarita*. *New Phytol.*, 112:77–83, 1989a.
- Bécard G, Piché Y. Fungal growth stimulation by CO₂ and root exudates in the vesicular-arbuscular mycorrhizal symbiosis. *Appl. Environ. Microbiol.*, 55:2320–2325, 1989b.
- Bücking H, Abubaker J, Govindarajulu M, et al. Root exudates stimulate the uptake and metabolism of organic carbon in germinating spores of *Glomus intraradices*. *New Phytol.*, 180:684–695, 2008.
- Bücking H, Pfeiffer PE, Shachar-Hill Y. Phosphate uptake, transport and transfer by the arbuscular mycorrhizal fungus *Glomus intraradices* is stimulated by increased carbohydrate availability. *New Phytol.*, 165:899–912, 2005.
- Büttner M, Sauer N. Monosaccharide transporters in plants: structure, function and physiology. *Biochim. Biophys. Acta.*, 1465:263–274, 2000.
- Callow JA, Capaccio LCM, Parish G, Tinker PB. Detection and estimation of polyphosphate in vesicular-arbuscular mycorrhizas. *New Phytol.*, 80:125–134., 1978.
- Cappellazzo G, Lanfranco L, Fitz M, Wipf D, Bonfante P. Characterization of an amino acid permease from the endomycorrhizal fungus *Glomus mosseae*. *Plant Physiol.*, 147:429–437, 2008.
- Carpita N, McCann M. *The cell wall*. In: *Biochemistry and molecular biology of plants*. 2000.
- Chenchik A, Zhu YY, Diatchenko L, Li R, Hill J and Siebert PD. *Gene cloning and analysis by RT-PCR*. BioTechniques Books, Natick, MA, 1998.
- Chomczynski P, Sacchi N. Single-step method of RNA isolation by acid guanidinium thiocyanate-phenol-chloroform extraction. *Anal. Biochem.*, 162:156–159, 1987.
- Cordier C, Pozo MJ, Barea JM, Gianinazzi S, Gianinazzi-Pearson V. Cell defense responses associated with localized and systemic resistance to *Phytophthora parasitica* induced in tomato by an arbuscular mycorrhizal fungus. *Mol. Plant-Microbe Interact.*, 11:1017–1028, 1998.
- Cosgrove DJ. Wall structure and wall loosening. A look backwards and forwards. *Plant Physiol.*, 125:131–134, 2001.
- Cruz C, Egsgaard H, Trujillo C, et al. Enzymatic evidence for the key role of arginine in nitrogen translocation by arbuscular mycorrhizal fungi. *Plant Physiol.*, 144:782–792, 2007.

Bibliography

- Davies FT, Porter JR, Linderman RG. Drought resistance of mycorrhizal pepper plants, independent of leaf phosphorus concentration, response in gas exchange, and water relations. *Physiol. Plant.*, 87:45–53, 1993.
- Dehne H, Schoenbeck F. The influence of endotrophic mycorrhiza on plant diseases. 1. Colonization of tomato plants by *Fusarium oxysporum* T. sp. *lycopersici*. *Phytopathol. Z.*, 95:105–110, 1979.
- Delrot D, Bonnemain JL. Involvement of protons as a substrate for the sucrose carrier during phloem loading in *Vicia faba* leaves. *Plant Physiol.*, 67:560–564, 1981.
- Denarie J, Maillet F, Poinso V, Bécard G, et al. Lipochito-Oligosaccharides stimulating arbuscular mycorrhizal symbiosis. *International Patent*, WO 2010/049817 A2.
- Dickson S, Smith S. Cross wall in arbuscular trunk hyphae form after loss of metabolic activity. *New Phytol.*, 151:735–742, 2001.
- Dufrense M, Perfect S, Pellier A-L, et al. A GAL4-like protein is involved in the switch between biotrophic and necrotrophic phases of the infection process of *Colletotrichum lindemuthianum* on common bean. *Plant Cell*, 12:1579–1589, 2000.
- Eckardt NA. Role of xyloglycan in primary cell walls. *Plant Cell*, 20:1421–1422, 2008.
- Ehness R, Ecker M, Godt DE, Roitsch T. Glucose and stress independently regulate source and sink metabolism and defense mechanisms via signal transduction pathways involving protein phosphorylation. *Plant Cell*, 9:1825–1841, 1997.
- Elias KS, Safir GR. Hyphal elongation of *Glomus fasciculatus* in response to root exudates. *Appl. Environ. Microbiol.*, 53:1928–1933, 1987.
- Ezawa T, Cavagnaro TR, Smith SE, Smith FA, Ohtomo R. Rapid accumulation of polyphosphate in extraradical hyphae of an arbuscular mycorrhizal fungus as revealed by histochemistry and a polyphosphate kinase/luciferase system. *New Phytol.*, 161:387–392, 2003.
- Fajardo Lopez M, Dietz S, Grunze N, et al. The sugar porter gene family of *Laccaria bicolor*: function in ectomycorrhizal symbiosis and soil-growing hyphae. *New Phytol.*, 180:365–378, 2008.
- Fehlberg V, Vieweg MF, Dohmann EMN, et al. The promoter of the leghaemoglobin gene Vflb29: functional analysis and identification of modules necessary for its activation in the infected cells of root nodule and in the arbuscule-containing cells of mycorrhizal roots. *J. Exp. Bot.*, 56:799–806, 2005.
- Ferrol N, Barea JM, Azcón-Aguilar C. The plasma membrane H(+)-ATPase gene family in the arbuscular mycorrhizal fungus *Glomus mosseae*. *Curr. Genet*, 37:112–118, 2000.

- Fitter AH. What is the link between carbon and phosphorus fluxes in arbuscular mycorrhizas? A null hypothesis for symbiotic function. *New Phytol.*, 172:3–6, 2006.
- Fotopoulos V, Gilbert MJ, Pittman JK, et al. The monosaccharide transporter gene, *AtSTP4*, and the cell-wall invertase, *Atβfruc1*, are induced in Arabidopsis during infection with the fungal biotroph *Erysiphe cichoracearum*. *Plant Physiol.*, 132:821–829, 2003.
- Francis R, Read DJ. Direct transfer of carbon between plants connected by vesicular-arbuscular mycorrhizal mycelium. *Nature*, 307:53–56, 1984.
- Frank AB. Über die auf Wurzelsymbiose beruhende Ernährung gewisser Bäume durch unterirdische Pilze. *Bericht der Deutschen Botanischen Gesellschaft*, 3:128–145, 1885.
- Frank B. On the nutritional dependence of certain trees on root symbiosis with belowground fungi (an English translation of A.B. Frank's classic paper of 1885). *Mycorrhiza*, 15:267–275, 2005.
- Franken P, Gianinazzi-Pearson V. Construction of genomic phage libraries of the arbuscular mycorrhizal fungi *Glomus mosseae* and *Scutellospora castanea* and isolation of ribosomal RNA genes. *Mycorrhiza*, 6:167–173, 1996.
- Franken P, Lapopin L, Meyer Gauen G, Gianinazzi-Pearson V. RNA accumulation and genes expressed in spores of the arbuscular mycorrhizal fungus, *Gigaspora rosea*. *Mycologia*, 89:293—297, 1997.
- Fry S. Primary cell wall metabolism: tracking the careers of wall polymers in living plant cells. *New Phytol.*, 161:641–675, 2004.
- Gallaud I. Etudes sur les mycorrhizes endotrophes. *Rév. Gen. Bot.*, 17:5–48, 1905.
- Gao L-L, Delp G, Smith SE. Colonization patterns in a mycorrhiza-defective mutant tomato vary with different arbuscular-mycorrhizal fungi. *New Phytol.*, 151:477–491, 2001.
- Garcia-Garrido JM, Ocampo JA. Regulation of the plant defence response in arbuscular mycorrhizal symbiosis. *J. Exp. Bot.*, 53:1377–1385, 2002.
- Garcia-Rodriguez S, Pozo MJ, Azcón-Aguilar C, Ferrol N. Expression of a tomato sugar transporter is increased in leaves of mycorrhizal of *Phytophthora parasitica*-infected plants. *Mycorrhiza*, 15:489–496, 2005.
- Garcia-Romera I, Garcia Garrido JM, Ocampo JA. Pectolytic enzymes in the vesicular-arbuscular mycorrhizal fungus *Glomus mosseae*. *FEMS Microbiol. Lett.*, 78:343–346, 1991.

Bibliography

- Gear ML, McPhillips ML, Patrick JW, McCurdy DW. Hexose transporters of tomato: molecular cloning, expression analysis and functional characterization. *Plant Mol. Biol.*, 44:687–697, 2000.
- Genre A, Chabous M, Timmers T, Bonfante P, Barker D. Arbuscular mycorrhizal fungi elicit a novel intracellular apparatus in *Medicago truncatula* root epidermal cells before infection. *Plant Cell*, 17:3489–3499, 2005.
- Gianinazzi-Pearson V, Arnould C, Oufattole M, Arango M, Gianinazzi S. Differential activation of H(+)-ATPase genes by an arbuscular mycorrhizal fungus in root cells of transgenic tobacco. *Planta*, 211:45–57, 2000.
- Gianinazzi-Person V, SMith SE, Gianinazzi S, Smith FA. Enzymatic studies on the metabolism of vesicular-arbuscular mycorrhizas. *New Phytol.*, 117:61–74, 1991.
- Gielkens MM, Dekkers E, Visser J, de Graaff LH. Two cellobiohydrolase-encoding genes from *Aspergillus niger* require D-xylose and the xylanolytic transcriptional activator XlnR for their expression. *Appl. Environ. Microbiol.*, 65:4340–4345, 1999.
- Giovannetti M, Sbrana C, Avio, L. Differential hyphal morphogenesis in arbuscular mycorrhizal fungi during preinfection stage. *New Phytol.*, 125:587–593, 1993.
- Glassop D, Godwin RMC, Smith SE, Smith FW. Rice phosphate transporters associated with phosphate uptake in rice roots colonised with arbuscular mycorrhizal fungi. *Can. J. Bot.*, 85:644–651, 2007.
- Glassop D, Smith S, Smith F. Cereal phosphate transporters associated with the mycorrhizal pathway of phosphate uptake into roots. *Planta*, 222:688–698, 2005.
- Glenn M, Chew F, Williams P. Hyphal penetration of *Brassica* (*Cruciferae*) roots by a vesicular-arbuscular mycorrhizal fungus. *New Phytol.*, 99:463–473, 1985.
- Gonzalez-Guerrero M, Azcón-Aguilar C, Mooney M, et al. Characterization of a *Glomus intraradices* gene encoding a putative Zn transporter of the cation diffusion facilitator family. *Fungal Genet. Biol.*, 42:130–140, 2005.
- Govindarajulu M, Pfeffer PE, Jin HR, et al. Nitrogen transfer in the arbuscular mycorrhizal symbiosis. *Nature*, 435:819–823, 2005.
- Graham JH. Effect of citrus root exudates on germination of chlamydospores of the vesicular-arbuscular mycorrhizal fungus, *Glomus epigaeum*. *Mycologia*, 74:831–835, 1982.
- Grierson C, Du JS, de Torres Zabala M, et al. Separate cis sequences and trans factors direct metabolic and developmental regulation of a potato tuber storage protein gene. *Plant J.*, 5:815–826, 1994.
- Guttenberger M. Arbuscules of vesicular-arbuscular mycorrhizal fungi inhabit an acidic compartment within plant roots. *Planta*, 211:299–304, 2000.

- Güimil S, Chang HS, Zhu T, et al. Comparative transcriptomics of rice reveals an ancient pattern of response to microbial colonization. *Proc. Natl. Acad. Sci. USA*, 102:8066–8070, 2005.
- Güther M, Neuhäuser B, Balestrini R, et al. A mycorrhizal-specific ammonium transporter from *Lotus japonicus* acquires nitrogen released by arbuscular mycorrhizal fungi. *Plant Physiol.*, 150:73–83, 2009.
- Harrier LA, Wright F, Hooker JE. Isolation of the 3-phosphoglycerate kinase gene of the arbuscular mycorrhizal fungus *Glomus mosseae* (Nicol. & Gerd.) Gerdemann & Trappe. *Curr. Genet.*, 34:386—392, 1998.
- Harrison MJ. A sugar transporter from *Medicago truncatula*: altered expression pattern in roots during vesicular–arbuscular (VA) mycorrhizal associations. *Plant J.*, 9:491–503, 1996.
- Harrison MJ, Dewbre GR, Liu JY. A phosphate transporter from *Medicago truncatula* involved in the acquisition of phosphate released by arbuscular mycorrhizal fungi. *Plant Cell*, 14:2413—2429, 2002.
- Harrison MJ, Van Buuren ML. A phosphate transporter from the mycorrhizal fungus *Glomus versiforme*. *Nature*, 378:626—629, 1995.
- Hasper AA, Dekker E, van Mil M, van de Vondervoort PJI, de Graaff LH. EglC, a new endoglucanase from *Aspergillus niger* with major activity towards xyloglucan. *Appl. Environ. Microbiol.*, 68:1556—1560, 2002.
- Hasper AA, Visser J, de Graaff LH. The *Aspergillus niger* transcriptional activator XlnR, which is involved in the degradation of the polysaccharides xylan and cellulose, also regulates D-xylose reductase gene expression. *Mol. Microbiol.*, 36:193–200, 2000.
- Hattori T, Nakagawa S, Nakamura K. High level expression of tuberous root storage protein genes of sweet potato in stems of plantlets grown in vitro on sucrose medium. *Plant Mol. Biol.*, 14:595–604, 1990.
- Hayes MA, Davies C, Dry IB. Isolation, functional characterization, and expression analysis of grapevine (*Vitis vinifera* L.) hexose transporters: differential roles in sink and source tissues. *J. Exp. Bot.*, 58:1985—1997, 2007.
- Hayman DS. Plant growth responses to vesicular arbuscular mycorrhiza. *New Phytol.*, 73:71–80, 1974.
- Helber N, Requena N. Expression of the fluorescence markers DsRed and GFP fused to a nuclear localization signal in the arbuscular mycorrhizal fungus *Glomus intraradices*. *New Phytol.*, 177:537–548, 2008.

Bibliography

- Herbers K, Meuwly P, Frommer WB, Metrauy J-P, Sonnewald U. Systemic acquired resistance mediated by the ectopic expression of invertase, possible hexose sensing in the secretory pathway. *Plant Cell*, 8:793–803, 1996.
- Hirrel MC, Gerdemann JW. Enhanced carbon transfer between onions infected with a vesicular-arbuscular mycorrhizal fungus. *New Phytol.*, 83:731–738, 1979.
- Hirrel MC, H Mehravaran H, Gerdemann J. Vesicular-arbuscular mycorrhizae in the *Chenopodiaceae* and *Cruciferae*: Do they occur? *Can. J. Bot.*, 56:2813–2817, 1978.
- Ho I, Trappe JM. Translocation of ^{14}C from *Festuca* plants to their endomycorrhizal fungi. *Nature*, 244:30–31, 1973.
- Ho NWY, Chen Z, Brainard AP. Genetically engineered *Saccharomyces* yeast capable of effective cofermentation of glucose and xylose. *Appl. Environ. Microbiol.*, 64:1852–1859, 1998.
- Hodge A, Campbell CD, Fitter AH. An arbuscular mycorrhizal fungus accelerates decomposition and acquires nitrogen directly from organic material. *Nature*, 413: 297–299, 2001.
- Hohnjec N, Perlick AM, Pühler A, Küster H. The *Medicago truncatula* sucrose synthase gene MtSucS1 is activated both in infected regions of root nodules and in the cortex of roots colonized by arbuscular mycorrhizal fungi. *Mol. Plant-Microbe Interact.*, 16: 903—915, 2003.
- Hosny M, de Barros J-PP, Gianinazzi-Pearson V, Dulieu H. Base composition of DNA from glomalean fungi: high amounts of methylated cytosine. *Fungal Genet. Biol.*, 41:422–428, 1998.
- Huang N, Sutliff TD, Litts JC, Rodriguez RL. Classification and characterization of the rice alpha-amylase multigene family. *Plant Mol. Biol.*, 14:655—668, 1990.
- Jakobsen I, Rosendahl S. Carbon flow into soil and external hyphae from roots of mycorrhizal cucumber plants. *New Phytol.*, 15:77–83, 1990.
- Javot H, Pumplin N, Harrison MJ. Phosphate in the arbuscular mycorrhizal symbiosis: transport properties and regulatory roles. *Plant Cell Environ.*, 30:310–322, 2007.
- Jin H, Pfeffer PE, Douds D, et al. The uptake, metabolism, transport and transfer of nitrogen in an arbuscular mycorrhizal symbiosis. *New Phytol.*, 168:687—696, 2005.
- Johnson NC, Graham JH, Smith FA. Functioning of mycorrhizal associations along the mutualism–parasitism continuum. *New Phytol.*, 137:575–589, 1997.
- Judge N. Plant protein inhibitors of cell wall degrading enzymes. *Trends Plant Sci.*, 7: 359–367, 2006.

- Juge C, Samson J, Bestien C, et al. Breaking dormancy in spores of the arbuscular mycorrhizal fungus *Glomus intraradices*: a critical cold-storage period. *Mycorrhiza*, 12:37–42, 2002.
- Karandashov V, Bucher M. Symbiotic phosphate transport in arbuscular mycorrhizas. *TRENDS Plant Sci.*, 10:23–29, 2005.
- Kuhn H, Küster H, Requena N. Membrane steroid-binding protein 1 induced by a diffusible fungal signal is critical for mycorrhization in *Medicago truncatula*. *New Phytol.*, 185:716–733, 2010.
- Kämper J, Kahmann R, Böler M, et al. Insights from the genome of the biotrophic fungal plant pathogen *Ustilago maydis*. *Nature*, 444:97–101, 2006.
- König J, Baumann S, Koepke J, et al. The fungal RNA-binding protein Rrm4 mediates long-distance transport of *ubi1* and *rho3* mRNAs. *EBMO*, 28:1855–1866, 1999.
- Lammers PJ, Jun J, Abubaker J, et al. The glyoxylate cycle in an arbuscular mycorrhizal fungus. Carbon flux and gene expression. *Plant Physiol.*, 127:1287–1298, 2001.
- Larkan NJ, Smith SE, Barker SJ. Position of the reduced mycorrhizal colonisation (Rmc) locus on the tomato genome map. *Mycorrhiza*, 17:311–318, 2007.
- Law CJ, Maloney PC, Wang D-N. Ins and outs of Major Facilitator Superfamily antiporters. *Annu. Rev. Microbiol.*, 62:289–305, 2008.
- Leigh J, Hodge A, Fitter AH. Arbuscular mycorrhizal fungi can transfer substantial amounts of nitrogen to their host plant from organic material. *New Phytol.*, 181:199–207, 2009.
- Liu A, Hamel C, Hamilton RI, Ma BL, Smith DL. Acquisition of Cu, Zn, Mn and Fe by mycorrhizal maize (*Zea mays* L.) grown in soil at different P and micronutrient levels. *Mycorrhiza*, 9:331–336, 2000.
- Livak KJ, Schmittgen TD. Analysis of relative gene expression data using real-time quantitative PCR and the 2- $\Delta\Delta$ CT method. *Methods*, 25:402–408, 2001.
- Loftus BJ, Fung E, Roncaglia P, et al. The genome of the basidiomycetous yeast and human pathogen *Cryptococcus neoformans*. *Science*, 307:1321–1324, 2005.
- Logi C, Sbrana C, Giovannetti M. Cellular events involved in survival of individual arbuscular mycorrhizal symbionts growing in the absence of the host. *Appl. Environ. Microbiol.*, 64:3473–3479, 1998.
- Long SR. Rhizobium symbiosis: nod factors in perspective. *Plant Cell*, 8:1885–1898, 1996.

Bibliography

- Lopez-Pedrosa A, Gonzalez-Guerrero M, Valderas A, Azcon-Aguilar C, Ferrol N. GintAMT1 encodes a functional high-affinity ammonium transporter that is expressed in the extraradical mycelium of *Glomus intraradices*. *Fungal Genet. Biol.*, 43:102–110, 2006.
- Lu CA, Lim EK, Yu SM. Sugar response sequence in the promoter of a rice alpha-amylase gene serves as a transcriptional enhancer. *J. Biol. Chem.*, 273:10120—10131, 1998.
- Lugtenberg BJ, Kavchenko LV, Simons M. Tomato seed and root exudate sugars: composition, utilization by *Pseudomonas* biocontrol strains and role in rhizosphere colonization. *Environ. Microbiol.*, 1:439–446, 1999.
- MacDonald RM, Lewis M. The occurrence of some acid phosphatases and dehydrogenases in the vesicular-arbuscular mycorrhizal fungus *Glomus mosseae*. *New Phytol.*, 80:134–141, 1978.
- Maeda D, Ashida K, Iguchi K, et al. Knockdown of an arbuscular mycorrhiza-inducible phosphate transporter gene of *Lotus japonicus* suppresses mutualistic symbiosis. *Plant Cell Physiol.*, 47:807—817, 2006.
- Maherali H, Klironomos JN. Influence of phylogeny on fungal community assembly and ecosystem functioning. *Science*, 316:1746–1748, 2007.
- Maldonado-Mendoza IE, Dewbre GR, Harrison MJ. A phosphate transporter gene from the extra-radical mycelium of an arbuscular mycorrhizal fungus *Glomus intraradices* is regulated in response to phosphate in the environment. *Mol. Plant-Microbe Interact.*, 14:1140—1148, 2001.
- Maldonado-Mendoza IE, Dewbre GR, Blaylock L, Harrison MJ. Expression of a xyloglucan endotransglucosylase/hydrolase gene, Mt-XTH1, from *Medicago truncatula* is induced systemically in mycorrhizal roots. *Gene*, 345:191–197, 2005.
- Matusova R, Rani K, Verstappen FWA, et al. The strigolactone germination stimulants of the plant-parasitic *Striga* and *Orobancha* spp. are derived from the carotenoid pathway. *Plant Physiol.*, 139:920–934, 2005.
- Menge JA, Johnson ELV, Platt RG. Mycorrhizal dependency of several citrus cultivars under three nutrient regimes. *New Phytol.*, 81:553–559, 1978.
- Mersereau M, Pazour GJ, Das A. Efficient transformation of *Agrobacterium tumefaciens* by electroporation. *Gene*, 90:149—151, 1990.
- Mosse B. Observations on the extramatrical mycelium of a vesicular-arbuscular endophyte. *Trans. Br. Mycol. Soc.*, 42:439—448, 1959.
- Mosse B. Some studies related to 'independent' growth of vesicular-arbuscular endophytes. *Can. J. Bot.*, 66:2533–2540, 1988.

- Mosse B, Hepper CM. Vesicular-arbuscular mycorrhizal infections in root organ cultures. *Physiol. Plant Pathol.*, 5:215–223, 1975.
- Mugnier J, Mosse B. Vesicular-arbuscular mycorrhizal infections in transformed Ri T-DNA roots grown axcenically. *Phytopathol.*, 11:1045–1050, 1987.
- Nagy R, Karandashov V, Chague V, et al. The characterization of novel mycorrhiza-specific phosphate transporters from *Lycopersicon esculentum* and *Solanum tuberosum* uncovers functional redundancy in symbiotic phosphate transport in solanaceous species. *Plant J.*, 42:236—250, 2005.
- Nehls U. *Carbohydrates and Nitrogen: Nutrients and Signals in Ectomycorrhizas*. In: *Plant Surface Microbiology*. Springer-Verlag (Berlin, Heidelberg), 2004.
- Nehls U, Wiese J, Guttenberger M, Hampp R. Carbon allocation in ectomycorrhizas: identification and expression analysis on an *Amanita muscaria* monosacchride transporter. *Mol. Plant-Microbe Interact.*, 11:167–176, 1998.
- Olsson PA, Hansson MC, Burleigh SH. Effect of P availability on temporal dynamics of carbon allocation and *Glomus intraradices* high-affinity P transporter gene induction in arbuscular mycorrhiza. *Appl. Environ. Microbiol.*, 72:4115—4120, 2006.
- Olsson PA, Rahm J, Aliasgharzad N. Carbon dynamics in mycorrhizal symbioses is linked to carbon costs and phosphorus benefits. *FEMS Microbiol. Ecol.*, 72:123—131, 2010.
- Pao SS, Paulsen IT, Milton HS Jr. Major Facilitator Superfamily. *Microbiol. Mol. Biol. Rev.*, 62:1–34, 1998.
- Parniske M. Arbuscular mycorrhiza: the mother of plant root endosymbiosis. *Nature Rev.*, 6:763–775, 2008.
- Paszkowski U, Kroken S, Roux C, Briggs SP. Rice phosphate transporters include an evolutionarily divergent gene specifically activated in arbuscular mycorrhizal symbiosis. *Proc. Natl. Acad. Sci. USA*, 99:13324—13329, 2002.
- Pauly M, Andersen LN, Kauppinen S, et al. A xyloglucan-specific endo- β -1,4-glucanase from *Asperillus aculateus*: expressing cloning in yeast, purification and characterization of the recombinant enzyme. *Glycobiol.*, 9:93–100, 1999.
- Peng S, Eissenstat DM, Craham JH, Williams K, Hodge NC. Growth depression in mycorrhizal citrus at high-phosphorus supply. *Plant Physiol.*, 101:1063–1071, 1993.
- Peretto R, Bettini V, Favaron F, Alghisi P, Bonfante P. Polygalacturonase activity and location in arbuscular mycorrhizal roots of *Allium porrum* L. *Mycorrhiza*, 5:157–163, 1995.
- Pfeffer PE, Douds DD, Bécard G, Shacchar-Hill Y. Carbon uptake and the metabolism and transport of lipids in an arbuscular mycorrhiza. *New Phytol.*, 150:543–553, 1999.

Bibliography

- Pirozynski KA, Malloch DW. The origin of land plants: a matter of mycotrophism. *Biosys.*, 6:153–64, 1975.
- Polidori E, Ceccaroli P, Saltarelli R, et al. Hexose uptake in the plant symbiotic ascomycete *Tuber borchii* Vittadini: biochemical features and expression pattern of the transporter TBHXT1. *Fungal Genet. Biol.*, 44:187—198, 2007.
- Pozo MJ, Slezack-Deschaumes S, Dumas-Gaudot E, Gianinazzi S, Azcón-Aguilar C. Plant defense responses induced by arbuscular mycorrhizal fungi. In: *Mycorrhizal technology in agriculture: from genes to bioproducts*. Birkhäuser, Basel, 2002.
- Quandt HJ, Pühler A, Broer I. Transgenic root nodules of *Vicia hirsuta*: a fast and efficient system for the study of gene expression in indeterminate-type nodules. *Mol. Plant-Microbe Interact.*, 6:699–706, 1993.
- Rausch C, Daram P, Brunner S, et al. A phosphate transporter expressed in arbuscule-containing cells in potato. *Nature*, 414:462—470, 2001.
- Ravnskov S, Wu Y, Graham JH. Arbuscular mycorrhizal fungi differentially affect expression of genes coding for sucrose synthases in maize roots. *New Phytol.*, 157: 539–545, 2003.
- Read DJ, Duckett JG, Francis R, Ligrone R, Russel A. Symbiotic fungal association in 'lower' land plants. *Philos. Trans. R. Soc. London*, 355:815–830, 2000.
- Reader J. *Potato: a history of the propitious esculent*. Yale Univ. Press, 2009.
- Rejon-Palomares A, Garcia-Garrido JM, Ocampo JA, Garcia-Romera I. Presence of xyloglucan-hydrolyzing glucanases (xyloglucanases) in arbuscular mycorrhizal symbiosis. *Symbiosis*, 21:249–261, 1996.
- Remy W, Taylor TN, Hass H, Kerp H. Four hundred-million-year-old vesicular arbuscular mycorrhiza. *Natl. Acad. Sci.*, 91:11841—11843, 1994.
- Rentsch R, Laloi M, Rouhara I, et al. NTR1 encodes a high affinity oligopeptide transporter in *Arabidopsis*. *FEBS Lett.*, 370:264–268, 1995.
- Requena N, Breuninger M, Franken P, Ocón-Garrido A. Symbiotic status, phosphate and sucrose regulate the expression of two plasma membrane H(+)-ATPase genes from the mycorrhizal fungus *Glomus mosseae*. *Plant Physiol.*, 132:1540–1549, 2003.
- Requena N, Serrano E, Ocon A, Breuninger M. Plant singals and fungal perception during arbuscular mycorrhiza establishment. *Phytochem.*, 68:33–40, 1997.
- Rose JKC, Braam J, Fry SC, Nishitani K. The XTH family of enzymes involved in xyloglucan endotrasglucosylation anf endohydrolysis: current perspecives and a new unifying nomenclature. *Plant Cell Physiol.*, 12:1421–1435, 2002.

- Saito M. Enzyme activities of the internal hyphae and germinated spores of an arbuscular mycorrhizal *Gigaspora margarita* Becker & Hall. *New Phytol.*, 129:425–431, 1995.
- Sambrook J, Fritsch EF, Maniatis T. *Molecular cloning: a laboratory manual*. Cold Spring Harbor, NY Cold Spring Harbor Laboratory Press, 1989.
- Sauer N, Stolz J. SUC1 and SUC2: two sucrose transporters from *Arabidopsis thaliana*; expression and characterization in baker's yeast and identification of the histidine-tagged protein. *Plant J.*, 6:67–77, 1994.
- Scarborough GA. Sugar transport in *Neurospora crassa*. A second glucose transport system. *J. Bio. Chem.*, 245:3985–3987, 1970.
- Schaarschmidt S, Roitsch T, Hause B. Arbuscular mycorrhiza induces gene expression of the apoplastic invertase LIN6 in tomato (*Lycopersicon esculentum*) roots. *J. Exp. Bot.*, 57:4015—4023, 2006.
- Schachtman D, Reid DJ, Ayling SM. Phosphorous uptake by plants: from soil to cell. *Plant Physiol.*, 116:447–453, 1998.
- Schenck NC, Smith GS. Additional new and unreported species of mycorrhizal fungi (*Endogonaceae*) from Florida. *Mycologia*, 74:77–92, 1982.
- Schubert A, Allara P, Morte A. Cleavage of sucrose in roots of soybean (*Glycine max*) colonized by an arbuscular mycorrhizal fungus. *New Phytol.*, 107:183–190, 2004.
- Schwab MS, Menge JA, Tinker PB. Regulation of nutrient transfer between host and fungus in vesicular—arbuscular mycorrhizas. *New Phytol.*, 117:387–398, 1991.
- Schüßler A, Martin H, Cohen D, Fitz M, Wipf D. Characterization of a carbohydrate transporter from symbiotic glomeromycotan fungi. *Nature*, 444:934–936, 2006.
- Schüßler A, Martin H, Cohen D, Fitz M, Wipf D. Studies on the *Geosiphon symbiosis* lead to the characterization of the first glomeromycotan sugar transporter. *Plant Signal. Behav.*, 2:431–434, 2007.
- Schüßler A, Schwarzott D, Walker C. A new fungal phylum, the *Glomeromycota*: phylogeny and evolution. *Mycol. Res.*, 105:1413–1421, 2001.
- Shachar-Hill Y, Pfeffer PE, Douds D, et al. Partitioning of intermediate carbon metabolism in VAM colonized leek. *Plant Physiol.*, 108:7–15, 1995a.
- Shachar-Hill Y, Pfeffer PE, Douds D, et al. Partitioning of intermediate carbon metabolism in vesicular–arbuscular leek. *Plant Physiol.*, 108:2979—2995, 1995b.
- Shachar-Hill Y, Pfeffer PE, Douds D, et al. Partitioning of intermediary carbon metabolism in vesicular-arbuscular mycorrhizal leek. *Plant Physiol.*, 108:7–15, 1995c.

Bibliography

- Silhavy T, Berman ML, Enquist LW. *Experiments with gene fusion*. New York, Cold Spring Harbor Laboratory Press, 1984.
- Smith FA, Smith SE. Mutualism and parasitism: biodiversity in function and structure in the 'arbuscular' (VA) mycorrhizal symbiosis. *Adv. Bot. Res.*, 22:1–43, 1996.
- Smith FW, Mudge SR, Rae AL, Glassop D. Phosphate transport in plants. *Plant Soil*, 248:71—83, 2003.
- Smith SE, Dickson S. Quantification of active vesicular-arbuscular mycorrhizal infection using image analysis and other techniques. *Aust. J. Plant Physiol.*, 18:637—648, 1991.
- Smith SE, Gianinazzi-Pearson V. Phosphate uptake and arbuscular activity in mycorrhizal *Allium cepa* L.: effects of photon irradiance and phosphate nutrition. *Aust. J. Plant Physiol.*, 17:177–188, 1990.
- Smith SE, Read DJ. *Mycorrhizal symbiosis*. Academic Press (London), 1997.
- Solaiman MZ, Ezawa T, Kojima T, Saito M. Polyphosphates in intraradical and extraradical hyphae of an arbuscular mycorrhizal fungus, *Gigaspora margarita*. *Appl. Environ. Microbiol.*, 65:5604–5606, 1999.
- Solaiman MZ, Saito M. Use of sugars by intraradical hyphae of arbuscular mycorrhizal fungi revealed by radiorespirometry. *New Phytol.*, 109:163–166, 1997.
- Son CL, Smith SE. Mycorrhizal growth responses: interactions between photon irradiance and phosphorus nutrition. *New Phytol.*, 108:305–314, 1988.
- Sparks DL. *Soil physical chemistry*. Crc Pr. Inc., 1998.
- St-Arnaud M, Hamel C, Vimard B, Caron M, Fortin J. Enhanced hyphal growth and spore production of the arbuscular mycorrhizal fungus *Glomus intraradices* in an in vitro system in the absence of host root. *Mycol. Res.*, 100:328–332, 1996.
- Staddon PL, Heinemeyer A, Fitter AH. Mycorrhizas and global environmental change: research at different scales. *Plant Soil*, 244:253–261, 2002.
- Subramanian KS, Charest C, Dwyer LM, Hamilton RI. Arbuscular mycorrhizas and water relations in maize under drought stress at tasselling. *New Phytol.*, 129:643–650, 1995.
- Terskikh A, Fredov A, Ermakova G, et al. 'Fluorescent Timer': protein that changes color with time. *Science*, 290:1585–1588, 2000.
- Tester M, Smith F, Smith S. Phosphate inflow into *Trifolium subterraneum* L.: Effects of photon irradiance and mycorrhizal infection. *Soil Biol. Biochem.*, 17:807—810, 1985.
- Thuring RW, Sanders JP, Borst P. Freeze-squeeze method for recovering long DNA from agarose gels. *Anal. Biochem.*, 66:213–220, 1975.

- Tisserant B, Gianinazzi-Pearson V, Gianinazzi S, Gallotte A. In planta histochemical staining of fungal alkaline phosphatase activity for analysis of efficient arbuscular mycorrhizal infections. *Mycol. Res.*, 97:245–250, 1993.
- Tommerup C. Spore dormancy in vesicular-arbuscular mycorrhizal fungi. *Trans. Br. Mycol. Soc.*, 81:37–45, 1983.
- Tsukaya H, Ohshima T, Naito S, Chino M, Komeda Y. Sugar-dependent expression of the CHS-A gene for chalcone synthase from petunia in transgenic *Arabidopsis*. *Plant Physiol.*, 97:1414—1421, 1991.
- van der Heijden MGA, Klironomos JN, Ursic M, et al. Mycorrhizal fungal diversity determines plant biodiversity, ecosystem variability and productivity. *Nature*, 32: 133–154, 1998.
- van Peij NNME, Gielkens MMC, de Vries RP, Visser J, de Graaff LH. The transcriptional activator XlnR regulates both xyylanolytic and endoglucanase gene expression in *Aspergillus niger*. *Appl. Environ. Microbiol.*, 64:3615—3619, 1998.
- Vance CP, Uhde-Stone C, Allan DL. Phosphorus acquisition and use: critical adaptations by plants for securing a non-renewable resource. *New Phytol.*, 157:423—447, 2003.
- Vierheilig H, Iseli B, Alt M, et al. Resistance of *Urtica dioica* to mycorrhizal colonization: a possible involvement of *Urtica dioica* agglutinin. *Plant Soil*, 183:131–136, 1996.
- Vieweg MF, Fruhling M, Quandt HJ. The promoter of the *Vicia faba* L. legemoglobin gene Vflb29 is specifically activated in the infected cells of root nodules and in the arbuscule-containing cells of mycorrhizal roots from different legume and non-legume plants. *Mol Plant-Microb Interact*, 220:757–766, 2004.
- Voegelé RT, Struck C, Hahn M, Mendgen K. The role of haustoria in sugar supply during infection of broad bean by the rust fungus *Uromyces fabae*. *PNAS*, 98:8133–8138, 2001.
- Wahl R, Wippel K, Goos S, et al. A novel high-affinity sucrose transporter is required for virulence of the plant pathogen *Ustilago maydis*. *PLoS Biology*, 8, 2010.
- Wainwright M. *Oligotrophic growth of fungi—stress or natural state*. In: *Stress Tolerance of Fungi*. Marcel Dekker, New York, 1993.
- Wang Y, Xiao Y, Zhang Y, et al. Molecular cloning, functional characterization and expression analysis of a novel monosaccharide transporter gene *OsMST6* from rice (*Oryza sativa* L.). *Planta*, 228:525–35, 2008.
- Waring RB, May GS, Morris NR. Characterization of an inducible expression system in *Aspergillus nidulans* using *ascA* and tubulin coding genes. *Gene*, 79:119–130, 1989.

Bibliography

- Wei H, Vienken K, Weber R, et al. A putative high affinity hexose transporter, hxtA, of *Aspergillus nidulans* is induced in vegetative hyphae upon starvation and in ascogenous hyphae during cleistothecium formation. *Fungal Genet. Biol.*, 41:148–156, 2004.
- Weig A, Franz J, Sauer N, Komor E. Isolation of a family of cDNA-clones from *Ricinus communis* L. with close homology to the hexose carriers. *J. Plant Physiol.*, 143:178–183, 1994.
- Wieczorke R, Krampe S, Weierstall T, et al. Concurrent knock-out of at least 20 transporter genes is required to block uptake of hexoses in *Saccharomyces cerevisiae*. *FEBS Lett.*, 464:123–128, 1999.
- Woods RA, Gietz RD. High-efficiency transformation of plasmid DNA into yeast. *Methods Mol. Biol.*, 177:85–97, 2001.
- Wright DP, Read DJ, Scholes JD. Mycorrhizal sink strength influences whole plant carbon balance of *Trifolium repens* L. *Plant Cell Environ.*, 21:881–891, 1998.
- Wright DP, Scholes JD, Read DJ, Rolfe SA. European and African maize cultivars differ in their physiological and molecular responses to mycorrhizal infection. *New Phytol.*, 167:881–896, 2005.
- Yaoi K, Mitsuishi Y. Purification, characterization, cDNA cloning, and expression of a xyloglucan endoglucanase from *Geotrichum* sp. M128. *FEBS Lett.*, 560:45–50, 2004.
- Yelton MM, Hamer JE, Timberlake WE. Transformation of *Aspergillus nidulans* by using a trpC plasmid. *Proc. Natl. Acad. Sci. USA*, 81:1470–1474, 1984.
- Zhu YG, Smith SE, Barritt AR, Smith FA. Phosphorus (P) efficiencies and mycorrhizal responsiveness of old and modern wheat cultivars. *Plant Soil*, 237:249–255, 2001.
- Özcan S, Johnston M. Function and regulation of yeast hexose transporters. *Microbiol. Mol. Biol. Rev.*, 63:554–569, 1999.

List of Abbreviations

aa	Amino acids
AM	Arbuscular mycorrhiza
AP	Adaptor-specific primer
BCIP	5-bromo-4-chloro-3-indolyl-phosphat
bp	Base pairs
BSA	Bovine serum albumine
CCCP	Carbonylcyanide m-chlorophenylhydrazone
cDNA	Complementary DNA
Ct	Threshold cycle
ddH₂O	Double distilled water
DEPC	Diethyl dicarbonate
DIG	Digoxigenin
DMF	N,N-dimethylmethanamid
DMSO	Dimethyl sulfoxide
DNA	Desriobnucleic acid
dNTP	Deoxyribonucleotide-triphosphate
dpi	Days post infection
dUTP	Deoxyuridine-triphosphate
EDTA	Ethylenedinitrilo-tetraacetic acid
ERM	Extraradical mycelium
EST	Expressed sequence tag
GSP	Gene-specific primer
GUS	β -glucuronidase
IRM	Intraradical mycelium
ITPG	β -D-1-thiogalactopyranoside
kb	Kilo base pair
kDa	Kilo Dalton
K_m	Michaelis Menten coefficient
LB	Luria Broth
LD PCR	Long distance PCR
Mb	Mega base pairs
MES	2-(N-morpholino)ethanesulfonic acid
MFS	Major facilitator superfamily
MOPS	3-(N-morpholino)propanesulfonic acid

Bibliography

NBT	Nitroblue-tetrazolium
OD	Optic density
ORF	Open reading frame
PAM	Periarbuscular membrane
PAS	Periarbuscular space
PBS	Phosphate buffered saline
PCR	Polymerase chain reaction
PEG	Poly ethylen glycol
Pi	Inorganic phosphate
PPP	Pentose phosphate pathway
u	Unit
UTR	Untranslated region
qPCR	Real-time PCR
RACE	Rapid amplification of cDNA ends
rnc	Reduced mycorrhizal colonisation
RNA	Ribonucleic acid
rpm	Rounds per minute
RT	Room temperature
s.d.	Standard deviation
SDS	Sodium dodecyl sulfate
s.e.m.	Standard error of mean
SMART	Switching mechanism at the 3' end
SSC	Saline-sodium citrate buffer
STE	Sodium-tris-EDTA buffer
TAE	Tris-acetate-EDTA
TAG	Triacylglycerol
TBS	Tris buffered saline
TE	Tris-EDTA buffer
T_m	Melting temperature
TMD	Transmembrane domain
TY	Tryptone-yeast
v/v	Volume/volume
wt	Wild type
w/v	Weight/volume
X-Gal	5-bromo-4-chloro-3-indolyl- β -D-galactopyranoside
X-Gluc	5-bromo-4-chloro-3-indolyl- β -D-glucuronid
YNB	Yeast-nitrogen base
YPD	Yeast-peptone-dextrose
YPDA	Yeast-peptone-dextrose-adenine

List of Figures

1.1	a , Life cycle of AM fungi. In the presymbiotic phase spores can germinate repeatedly in the absence of host roots. Colonisation of a root starts with the formation of an appressorium from which the fungus grows inter- and intracellularly through the root cortex forming arbuscules in the inner root cortex. The life cycle is fulfilled with the formation of an extraradical mycelium in the soil and the production of spores. b , Schema of an arbuscule. Plant and fungus are separated by the periarbuscular space. The periarbuscular membrane of the plant is involved in uptake of nutrients delivered by the fungus. c , Germinated spore. d , Colonised root (trypan blue stained). Fungal structures are shown in blue. e , Arbuscule stained with trypan blue. f , ERM with spores. (ERM: extraradical mycelium, IRM: intraradical mycelium, PAS: periarbuscular space, PAM: periarbuscular membrane)	7
1.2	Metabolic fluxes in the AM symbiosis after Bago et al. (2000) and Parniske (2008). Plant hexoses are taken up by the fungus by an unknown mechanism. Hexoses are incorporated in triacylglyceral (TAG) and glycogen (Glyc) for long distance transporter or metabolised via the oxidative pentose phosphate pathway (PPP). In the ERM hexoses are synthesised from lipids by gluconeogenesis and metabolised in the PPP. TAG and Glyc are used for synthesis of trehalose and chitin. Inorganic phosphate is taken up by the fungus from the soil and transferred as polyphosphate (PolyP) to intraradicular structures. Nitrogen in form of amino acids or ammonium are transferred as arginine putatively bound on PolyP to the arbuscules. Phosphate is released in the periarbuscular space and taken up by the plant cell via plant specific phosphate transporters like PT4. Nitrogen is released as urea from arginine and transferred to the plant as ammonium.	12
2.1	<i>In vitro</i> cultivation of <i>G. intraradices</i> . a , Cultivation of <i>G. intraradices</i> in a dual compartment system divided into a 'fungal compartment' (magnification showing hyphae and spores of <i>G. intraradices</i> grown on M medium without sucrose) and a 'root compartment' (magnification showing a <i>D. carota</i> root colonised with <i>G. intraradices</i> on M medium with sucrose). b , Dual compartment system for <i>G. intraradices</i> cultivation showing fungal hyphae grown in liquid M medium.	23
2.2	<i>In vitro</i> mycorrhization assay. a , Transgenic host root mycorrhized in the dual compartment <i>in vitro</i> system. b , Schema of a plate used for the mycorrhization assay. The new host root is placed between two cellophane sheets to increase contact sites with the fungal hyphae. c , Lateral view of a plate prepared for the mycorrhization assay. The medium in the 'fungal compartment' is poured diagonally to the compartment boarder (indicated by the dashed arrow).	25
2.3	Isolation of the partial promoter sequence of StHT6. a , Location of the gene-specific primers GSP1, GSP2 and the DIG-labelled probe I in the known sequence downstream of the promoter. b , EcoRI digested pPCRII-Topo clones. c , Positive clones identified by binding of the sequence-specific probe I.	32
2.4	Homologous recombination of a promoter sequence into the pPGFPPGUS-RR binary vector (Kuhn et al., 2010) via Gateway cloning. LB: left border sequence; RB: right border sequence; Km ^r : kanamycin resistance; Tnos: nopaline synthase terminator; Pubi: ubiquitin promoter; gus: β glucuronidase gene; gfp: green fluorescence protein; Sm/Sp ^r : streptomycin/spectinomycin resistance.	37

List of Figures

2.5	First strand cDNAs with primer binding sites and Digoxigenin labelled probe binding sites for RACE PCR of unknown 3' and 5' cDNA ends. a , cDNA created with the GeneRacer™ Kit (Invitrogen) and c , cDNA created with SMART cDNA library Kit (Clontech). b , Location of GeneRacer™ oligos in the GeneRacer™ RNA and Oligo dT sequence. GSP: gene specific primer.	38
2.6	Example of an adaptor-ligated blunt end fragment for genome walking produced with the GenomeWalker™ kit from Clontech (USA) showing position of the adaptor-specific primer binding sites (AP1 and AP2) and the gene-specific primer binding sites (GSP1_F1 and the nested primer GSP1_F2 for downstream amplification of unknown regions; GSP1_R1 and the nested primer GSP1_R2 for upstream amplifications). DIG labelled DNA-probes for southern blot screening are shown in red. The design of the GenomeWalker™ Adaptor is shown more in detail (highlighted in blue). The amine group at the 3' end of the lower strand prevents the 3' extension by the polymerase.	40
2.7	Localisation and promoter activity of StPT3 in mycorrhized roots. a , The mycorrhiza-upregulated plant phosphate transporter StPT3 from <i>S. tuberosum</i> is involved in the ATP dependant phosphate uptake from the periarbuscular spaces (PAS) into the plant cell. The protein localises in the plant plasma membrane surrounding the arbuscule. b-d , Fluorescent Timer protein expression under control of the StPT3 promoter in potato hairy roots mycorrhized with <i>G. intraradices</i> . Green fluorescence (b) indicates recent and red fluorescent (c) ceased promoter activity in arbusculated cells (arrows). d , Merged image of (b) and (c) shows yellow fluorescence indicating continuous promoter activity. e , Self-constructed micro-razor blade. Razor blade has a length of 3–5 mm.	42
2.8	a , LD-PCR of cDNA from arbusculated plant cells. Samples from different cycles are shown. The blue line indicates the increase of the cDNA length from cycle 18 to cycle 27. b , Two pooled samples of LD-amplified cDNAs from arbusculated potato cells. c , Same LD-PCR as in (b) after size-fractionation using the CHROMA SPIN Columns -400 (Clontech, USA). Arrows in (b) and (c) indicating shift in cDNA size after the remove of smaller nucleotides in the size-fractionated sample (c) compared to the untreated sample (b).	44
2.9	a , Plasmid card of the yeast expression vector pGADT7-Rec (Clontech, USA). b , Recombination cassette of pGADT7-Rec for homologous <i>in vivo</i> recombination of SMART created cDNA libraries in yeast. c , Plasmid card of the yeast expression vector pNH196.	46
2.10	One-Step cDNA library construction and screening. SMART generated double-strained (ds) cDNAs were co-transformed with the SmaI linearised yeast expression vector pNH196 in the hexose-uptake impaired yeast mutant EB.Y.VW4000. <i>In vivo</i> , ds cDNAs were integrated by homologous recombination in pNH196 over SMARTIII/CDSIII recombination sites. Putative hexose transporters were isolated by functional complementation of EB.Y.VW4000 on selective medium without uracil and with hexoses as only carbon source.	48
2.11	Preparation of sense and antisense probe for <i>GiMST1</i> . a , Cloning of the reverse transcribed <i>GiMST1</i> sequence in the pCRII-Topo vector. Location of T7 and Sp6 promoter sequences and XbaI and HindIII restriction sites are shown in the black box. b , Spot test of the first and second elution of the <i>GiMST1</i> sense and antisense probe. The RNA probes were spotted in a dilution series from 10 ng to 0.01 pg. The first elution of the probes showed a sufficient strength compared to the control RNA (Roche Diagnostics).	54
3.1	a , Example for less- (+myc) and heavily-mycorrhized (++) microdissected root regions observed under the fluorescent binocular. Arbuscule-containing cells are green fluorescent. The shape of the roots and of a single cell are indicated with a yellow dashed line. b , Integrity of the RNA isolated from microdissected potato roots proved by northern blotting. Quality of cDNA was tested by amplification of <i>StTEF</i> via qPCR. c , Fold change expression of <i>StPT4</i> in -myc, +myc and ++myc samples. <i>StPT4</i> expression was normalised to <i>StTEF</i> . (Bars represent s.d.)	59

- 3.2 **a**, BamHI and KpnI endonuclease restriction digestion of the isolated potato sugar transporters StHT6 and StHT2 in the yeast vector pNH196. **b**, Position of KpnI and BamHI restriction sites in pNH196-StHT6 and pNH196-StHT2. (UTR: untranslated region; PolyA: polyadenylated tail) 60
- 3.3 TMDs predicted by TMHMM program for the monosaccharide transporters StHT6 and StHT2. 60
- 3.4 Growth test of the hexose-uptake impaired yeast mutant EB.Y.VW4000, complemented with StHT6 and StHT2, in liquid medium. Overnight cultures of EB.Y.VW4000 expressing heterologously *StHT6* or *StHT2*, one negative control expressing the empty vector pNH196 and one positive control expressing the *S. cerevisiae* high-affinity sugar transporter *HXT2* were diluted to an OD₆₀₀ of 1 and used as inoculum for 2X YPDA (pH 6.5) with 2% hexose content. Cultures were incubated for 2 days at 37 °C and 200 rpm. 62
- 3.5 Growth test of the EB.Y.VW4000 yeast mutant complemented either with the *S. tuberosum* monosaccharide transporter *StHT6* and *StHT2* or the *S. cerevisiae* high-affinity sugar transporter *HXT2*. As negative control EB.Y.VW4000 was transformed with the empty vector pNH196. The yeast clones were spotted in a dilution series on YNB medium (pH 6.5) containing different hexoses as carbon source in two different concentrations (2% or 0.1%). The plates were incubated for 4 days at 37 °C. The sampling schema is shown in the upper right panel. 63
- 3.6 Phylogenetic tree of plant monosacchride transporters. The dendrogram was generated by MEGA 4.0 software using ClustalW for the alignment and the neighbour-joining method for the construction of the phylogeny. Bootstrap tests were performed using 1000 replicates. The branch lengths are proportional to the phylogenetic distance. The sequences of the yeast hexose transporters HXT1 and HXT2 were used as outgroup. Four groups were outlined with blue, green, orange and lilac boxes. StHT6 is marked in green. The putative orthologues of StHT6 and MtHT6 are outlined with green unfilled boxes. MtST1 is marked in blue, StHT2 in orange. 64
- 3.7 Effect of mycorrhization on *StHT6* and *StHT2* expression. **a**, Expression of *StHT6*, *StHT2* and *StPT4* in three microdissected root samples (non-mycorrhized, -myc; less-mycorrhized, +myc; full-mycorrhized, ++myc). **b**, Expression of *StHT6* and *StPT4* in a time course of potato hairy roots mycorrhized for 3, 11, 14 and 32 days post inoculation (dpi) with *G. intraradices*. (Bars represent s.d.) 66
- 3.8 Expression analysis of *MtST1*, *MtHT6* and *MtPT4* in non-mycorrhized (non-myc) and mycorrhized (myc) *M. truncatula* hairy roots. The roots were colonised in the two-compartment system with *G. intraradices* for 14 days. Three independent root samples were used for quantitative real-time PCR analysis (1, 2, 3). (Bars represent s.d.) 66
- 3.9 Schema of the promoter isolation of *StHT6* by genome walking. The first 900 bp were amplified from the DraI library using the primers HT6_GSP1 and GSP2. Additional ca. 1,200 bp were amplified from the StuI library with the primers HT6_GSP1a and GSP2a. The Probe I and Probe II were used for the identification of positive clones by southern blotting. The upper scale represents bp upstream or downstream of the ATG (+1). 67
- 3.10 GUS staining of non-mycorrhized *M. truncatula* roots transformed with promoter-reporter constructs for StHT6 and MtST1. **a-c**, Homologous expression of the *gus* gene under control of the MtST1 promoter in *M. truncatula*. **d-f**, Heterologous expression the *gus* gene under control of the StHT6 promoter in *M. truncatula*. **d-f**, Homologous expression the *gus* gene under control of the StHT6 promoter in *S. lycopersicum*. **i, j**, Heterologous expression of the *gus* gene under control of the MtST1 promoter in *S. lycopersicum*. Red arrows indicate GUS expression in old and new root tips. (Bars indicate 200 µm) 68
- 3.11 GUS and acid fuchsin counter staining of mycorrhized *M. truncatula* transformed with promoter-reporter constructs for StHT6 and MtST1. **a, c, e, g, i, k, m, o**, Blue GUS staining indicates promoter activity in arbusculated cells. **b, d, f, h, j, l, n, p**, Fuchsin stained fungal structures within roots under the fluorescent light. GUS and fuchsin staining are overlapping. Red arrows indicate exemplary arbuscule-containing cells. 69

List of Figures

3.12 Putative cis-regulatory elements in the promoter sequences of the sugar transporters StHT6 (pHT6: blue) and MtST1 (pST1: lilac). The lower scale represents base pairs upstream of the transcriptional start codon ATG (+1). (closed triangle: SURE1; open triangle: SURE2; open box; pentagon: SUCBOX3; closed circle: AMYBOX1; open circle: AMYBOX2; open box: OSE1ROOTNODULE; closed box: OSE2ROOTNODULE; C: CTTC-motif; T: TAAT-motif; red: elements on the +strand; black: elements on the -strand; E means end-of-sequence) 71

3.13 Putative MFS transporters found the *G. intraradices* genome database in this work. The outlined sections represent di- and monosaccharide transporters. (Disaccharide Transporters 1%; Monosaccharide Transporters 12%; Amino Acid Transporters 15%; Peptide Transporters 7%; Phosphate Transporters 22%; Nitrate/Ammonium Transporters 22%; UDP/GDP Sugar Transporters 18%; Multi Drug Transporters 3%) 72

3.14 Location of the partial amino acid sequences of *G. intraradices* sugar transporters compared to the *Uromyces cia-vabae* hexose transporter HXT1 (CAC41332) or the sucrose transporter of *Ajelomyces capsulatus* (EER44596). The location of the PETKG motif which is characteristic for hexose transporters is indicated at the C-terminus of HXT1. 73

3.15 Expression analysis of putative sugar transporters of *G. intraradices* in different fungal tissues by qPCR. The arbuscule-enriched material originates from the microdissection of potato hairy roots colonised with *G. intraradices*. Results are presented as relative expression to the *G. intraradices* transcription elongation factor alpha 1 (*GiTEF*). (Bars represent s.d.) 74

3.16 Schema of the RACE PCR for the isolation of *GiMST1*. In a first RACE PCR with the gene-specific primers MST1down_F1 and the nested primer MST1down_F2, 1 kb downstream of the ATG was isolated. The 3' end with 3'UTR (untranslated region) was amplified in a second RACE PCR with the gene-specific primers MST1down_F3 and the nested primer MST1down_F4. Specific probes in the known sequence regions were used for screening of the isolated clones. Scale bar represents base pairs downstream of the ATG (+1). 75

3.17 Phylogenetic tree of fungal monosaccharide transporter protein sequences. The dendrogram was generated by MEGA 4.0 software using ClustalW for the alignment and the neighbour-joining method for the construction of the phylogeny. Bootstrap tests were performed using 1000 replicates. The branch lengths are proportional to the phylogenetic distance. The sequence of the phosphate transporter GiPT from *G. intraradices* (AF359112) was used as outgroup. *GiMST1* is highlighted in green, clusters together with fungal xylose transporters are shown in red. A square delimits a group of putative xylose transporters. The *G. pyriformis* monosaccharide transporter, GpMST1, is marked with a blue circle. 76

3.18 Schema RACE PCR *GiMST2*. The 5' end with the 5' UTR (untranslated region) was amplified using the gene-specific primers MST2_GSP1 and GSP2. The 3' end with 3'UTR was amplified with the gene-specific primers MST2_GSP1a and GSP2a. Probe I was used to identify positive clones in the 2nd RACE PCR. Upper scale represents bp upstream or downstream of the ATG (+1). 77

3.19 Transmembrane domains of *GiMST1* and *GiMST2*. **a**, Protein alignment of *GiMST1* and *GiMST2*. Sites of TMDs for *GiMST1* predicted by the THMM program are shown as red bars. Sites of TMDs for *GiMST2* predicted by the THMM program are shown as green bars. The additional TMD assessed by TopPred is indicated in orange. Blue indicates homologous regions. **b**, Schema of *GiMST1* and *GiMST2* TMD locations predicted by THMM. Purple TMD of *GiMST2* represents TMD predicted by TopPred. 77

3.20	a , Relative Expression of the <i>G. intraradices</i> sugar transporters in +myc and ++myc samples of arbuscule-enriched material from mycorrhized potato hairy roots and the corresponding expression of the <i>S. tuberosum</i> phosphate transporter <i>StPT4</i> . b , Time course analysis of expression of <i>StPT4</i> and <i>GiMST1</i> in mycorrhized potato hairy roots after 3, 11, 14 and 32 days post inoculation (dpi). c , Time course analysis of expression of <i>MtPT4</i> and <i>GiMST1</i> in mycorrhized <i>M. truncatula</i> roots after 1, 12 and 25 days post inoculation (dpi). (Bars indicate s.d.)	78
3.21	<i>In situ</i> hybridisation of <i>M. truncatula</i> hairy roots mycorrhized with <i>G. intraradices</i> . a , Overview of a cross-sectioned mycorrhized <i>M. truncatula</i> root. b , Detail of a cross-sectioned mycorrhized root hybridised with the antisense probe for <i>GiMST1</i> . Positive purple staining at arbuscules and IRM indicates <i>GiMST1</i> expression. c , No staining is visible in samples of the same root hybridised with the <i>GiMST1</i> sense probe. (C: cortex, VB: vascular bundle, AR: arbuscule, IRM: intraradical mycelium)	79
3.22	a , Relative expression of <i>GiMST1</i> and <i>StHT6</i> which are heterologously expressed in the yeast mutant EBY.VW4000. b , Localisation of the GiMST1-GFP fusion protein in the plasma membrane of the yeast mutant EBY.VW4000. The EBY.VW4000 strain expressing the <i>Ustilago maydis</i> sugar transporter HXT1 fused to GFP was used as positive control (kindly provided by K. Wippel, FAU, Germany).	80
3.23	Growth test of the hexose-uptake impaired yeast mutant EBY.VW4000, complemented with the <i>G. intraradices</i> monosaccharide transporter GiMST1, on different sugars. Three clones expressing heterologously <i>GiMST1</i> , three yeast clones expressing the empty pNEV-N vector as negative controls and one positive control expressing the <i>S. cerevisiae</i> high-affinity sugar transporter HXT2 were spotted in a dilution series on YNB medium (pH 6.5) with different hexoses in two concentrations (2% or 0.1%). Plates were incubated for 11 days at 37 °C. Sampling schema is shown in the right upper panel.	81
3.24	Sugar uptake experiments with the EBY.VW4000 mutant transformed with pNEV-MST1. a , Uptake of different radio-labelled substrates (1 mM). (open circles, vector control; closed circles, D-glucose; closed squares, D-xylose; open triangles, D-mannose; closed triangles, D-fructose) b , Growth test of GiMST1 expressing yeasts on different sugar plates with a pH of 5.5. c , Michaelis-Menten kinetics of glucose uptake at pH 5. c , Uptake of glucose is optimal at acidic pH-values. e , Glucose transport is sensitive to the protonophore CCCP. f , Uptake of ¹⁴ C-glucose (0.1 mM) without competitor (w/o) or with potential substrates of GiMST1 (100-fold molar excess). (Error bars represent s.e.m.)	83
3.25	Evidence of the xylose utilisation pathway in <i>G. intraradices</i> . a , Schema of the xylose utilisation pathways in fungi and bacteria. (XR: xylose reductase, XDH: xylitol dehydrogenase, XK: xylulose kinase, XI: xylose isomerase, PPP: pentose phosphate pathway) b , Expression of genes involved in xylose utilisation in <i>G. intraradices</i> during different stages of the life cycle. (ERM: extraradical mycelium, error bars represent s.d.)	84
3.26	Phylogenetic tree of fungal xylose reductase protein sequences. The dendrogram was generated by MEGA 4.0 software using ClustalW for the alignment and the neighbour-joining method for the construction of the phylogeny (Tamura et al., 2007). Bootstrap tests were performed using 1000 replicates. The branch lengths are proportional to the phylogenetic distance. The sequences of the phosphate transporter GiPT from <i>G. intraradices</i> (AF359112) and of GiMST1 were used as outgroup. GiXR2, highlighted in green, clusters together with yeast xylose reductase (blue square). Full alignment of GiXR2 and other fungal xylose reductases is shown in Fig. B.12.	85
3.27	Increased expression of the xyloglucan endotransglucosylase/hydrolases <i>StXTH1</i> and <i>MtXTH-1</i> in mycorrhized potato and <i>Medicago</i> roots. Expression is represented as fold induction and normalised to StTEF or MtTEF, respectively. (Error bars represent s.d.) . . .	86
3.28	Expression of putative orthologues of the XlnR transcriptional activator in different developmental stages of <i>G. intraradices</i> . (Error bars represent s.d.)	88

List of Figures

- 3.29 Isolation of the *GiMST1* promoter sequence by genome walking. 358 bp upstream of the ATG were known from the *GiMST1* sequence found in the genome database. In a first PCR 840 bp upstream of the ATG could be isolated using the gene-specific primers MST1_GPS1 (-147 bp) and MST1_GPS2 (-187 bp). In a second PCR using MST1_GSP1a (-790 bp) and MST1_GSP2a (-816 bp) primers located within the sequence of the PvuII library clone at least 1.79 kb upstream of the ATG were isolated from the EcoRV library. Probe I was used to identify positive clones by southern blotting. Upper scale represents base pairs upstream of the ATG (+1). 88
- 3.30 Promoter analysis of *GiMST1*. **a**, Putative cis-regulative motifs in the promoter sequence of *GiMST1*. GAL4-like consensus sequences (TCCTC; TTATC; TTATATATC) and XlnR-like motif (GGCTAA). Scale represents base pairs upstream of the ATG (+1). (Red colour: design motifs on the positive strand; black colour: design motifs on the negative strand; E means end-of-sequence). **b**, Expression of PpMST1-DsRed-StuA in the *Aspergillus* strain GR5 in minimal medium with 2% xylose. DsRed signal is visible in the nucleus of the germling. **c**, Expression of pMST1-DsRed-StuA in the *Aspergillus* strain GR5 in minimal medium with 2% glycerol. No signal is visible in the nuclei. Bars indicate 10 μ m. 90
- 3.31 Expression analysis of sugar transporters and genes involved in xylose usage in the ERM. **a**, Expression of sugar transporters in the ERM exposed for five days with 2X M medium containing 2% sugar. As control, ERM was cultivated under standard conditions (2X M medium without sugar). (Gluc: glucose, Man: mannose, Gal: galactose, GlucA: glucuronic acid Xyl: xylose, Ara: arabinose) **b**, Expression of xylose utilisation genes in xylose and control treatment. (XR: xylose reductase, XDH: xylose dehydrogenase, XK: xylose kinase) **c**, Expression of XlnR orthologues in xylose and control treatment. (Error bars represent s.d.) 91
- 3.32 Expression of *GiMST1* and *GiMST1* in ERM **a**, in the vicinity of wild type (wt) tomato or *rnc* mutant hairy roots (ordinate is presented in logarithmic scale) or **b**, in the presence of their root exudates. The control was treated identical but was incubated either without roots or without root exudates. (Error bars represent s.d.) 93
- 3.33 Effect of elevated phosphate levels on the expression of **(a) *GiMST1***, **(b) *StPT4***, **(c) *StHT6***, in mycorrhizal potato hairy roots. The roots were treated after establishment of the AM symbiosis with a surplus of phosphate (3.5 mM P). Standard conditions are 17.5 mM of KH_2PO_4 . (Error bars represent s.d.) 94
- 4.1 'Carbon-for-phosphate' hypothesis. At low external phosphate (Pi) concentrations the fungus provides the plant with Pi which leads to a local increase of Pi concentrations in colonised root regions. This triggers the activation of the plant symbiotic phosphate transporter PT4. Furthermore, the carbon flow towards the fungus is stimulated which possibly triggers the expression of *GiMST1*. At high Pi concentrations in the surrounding, the plant can independently take up Pi from the soil. The symbiotic Pi-uptake pathway is shut-off leading to a decrease of *PT4* expression. The carbon flow towards the fungus is restricted possibly by increased uptake of glucose into the plant cells via plant sugar transporters like *StHT6*. This leads to the down-regulation of *GiMST1* and to reduced fungal growth and colonisation. 103

5.1	Carbon and phosphate flux in the AM symbiosis (after Bago et al., 2000; Parniske, 2008; this work). GiMST1 is involved in the symbiotic carbon uptake in arbuscules or intraradical hyphae. Mycorrhiza-inducible invertases cleave sucrose (Suc) into glucose (Gluc) and fructose (Fruc). Mainly glucose is taken up by the fungus via GiMST1 from the periarbuscular space (PAS). Cell wall sugars like xylose (Xyl) but possibly also mannose (Man), galactose (Gal), glucuronic and galacturonic acid (GlucA, GalA) can be taken up via GiMST1 and used as alternative carbon sources. Xylose and glucose are metabolised in the pentose phosphate pathway (PPP). Glucose is converted in triacylglycerol (TAG) or glycogen (Glyc) and transferred to the extraradical mycelium (ERM). There, glucose is synthesised via gluconeogenesis from TAG. TAG and Glyc are converted in chitin and trehalose. GiMST1 is also expressed in the ERM exposed to high levels of xylose, but its function there is not known. The plant sugar transporters StHT6 (<i>S. tuberosum</i>) and MtST1 (<i>M. truncatula</i>) compete with the fungus for glucose. In the opposite direction phosphate is transferred to the plant. Phosphate (Pi) is taken up by fungal phosphate transporters in the ERM, converted to polyphosphate (PolyP) and transported to the intraradical structures. <i>In planta</i> , Pi is released in the PAS and taken up by mycorrhiza-specific plant phosphate transporters like PT4.	109
B.1	ORF of <i>StHT6</i> with location of qPCR primers StHT6_F1 and StHT6_R1 (shown in blue). Start and stop codon are highlighted in red.	115
B.2	ORF of <i>StHT2</i> with location of qPCR primers StHT2_F1 and StHT2_R1 (shown in blue). Start and stop codon are highlighted in red.	116
B.3	ClustalW alignment of the deduced amino acid sequences of plant sugar transporters. Dark blue indicates high conserved amino acids in all sequences, blue indicates similar amino acids and light blue less similar amino acids. The red box highlights the conserved PETKG motif of MFS sugar transporters. Average length of the transporters is approximately 515 amino acids. (Part I)	117
B.4	ClustalW alignment of the deduced amino acid sequences of plant sugar transporters. (Part II)	118
B.5	Full promoter sequence of <i>StHT6</i> (shown in gray) with location of the primers pHT6_F1 and pHT6_R1 (lilac). Genome walker primers GSP1,2,1a and 2a are shown in blue. The start codon is highlighted in red. Putative TATA boxes are shown in green.	119
B.6	Full promoter sequence of <i>MtST1</i> (highlighted in grey) with location of the primers pST1_F1 and pST1_R1 (blue). ATG is highlighted in red. The putative TATA box is shown in green.	120
B.7	ORF of <i>GiMST1</i> . Real time primers (GiMST1Real_F1 and R1) are shown in red. Primers for the amplification of the <i>in situ</i> probe are shown in light blue (GiMST1situ_F1/R1). RACE primers are highlighted in blue (GiMST1down_F1/F2/F3/F4). Start and stop codon are shown in red, 3' and 5'UTR in yellow. The full sequence of <i>GiMST1</i> has been deposited at the EMBL databank with accession no. HM143864.	121
B.8	Promoter sequence of <i>GiMST1</i> . Genome walker primers are shown in blue. Start codon is shown in red.	122
B.9	ORF of <i>GiMST2</i> . Real time primers (GiMST2Real_F1 and R1) are shown in red. RACE primers are highlighted in blue (MST2_GSP1/GSP2/GSP1a/GSP2a). Start and stop codon are shown in red, 3' and 5'UTR in yellow.	123
B.10	ClustalW alignment of the deduced amino acid sequences of the glomeromytan sugar transporters GiMST1, GiMST2 and GpMST1. Dark blue indicates high conserved amino acids in all sequences, blue indicates similar amino acids and light blue less similar amino acids. The PETKG sequence highly conserved among sugar transporters is marked in red.	124
B.11	ORF of <i>GiXR2</i> showing the location of the RACE PCR primer XR2up_R1 (lilac) and R2 (blue and black underlined) and the qPCR primer qXLR2_F1 and R1 (red). 3' and 5' UTR are highlighted in yellow.	124

List of Figures

B.12 ClustalW alignment of the deduced amino acid sequences of fungal xylose reductases. Dark blue indicates high conserved amino acids in all sequences, blue indicates similar amino acids and light blue less similar amino acids. 125

D.1 Uptake of radio-labelled sugars in yeast cells expressing heterologously the *S. tuberosum* hexose transporter StHT6. 133

List of Tables

2.1	List of bacterial and fungal strains used for this work.	16
2.2	List of plant cultivars and hairy roots used for this work.	17
2.3	Antibiotics and their working concentrations used for bacterial media. Antibiotics were dissolved in dH ₂ O, filter sterilised and stored at -20 °C.	18
2.4	Amino acid concentrations used for YNB medium. The amino acids were prepared as stock solutions in dH ₂ O, filter sterilised and stored at 4 °C.	19
2.5	Carbohydrate sources and their concentrations used for different yeast media. The sugars were prepared as 20 or 40 % stock solutions in dH ₂ O, filter sterilised and stored at 4 °C.	20
2.6	M Medium composition after Bécard and Fortin (1988). All stock solutions were stored without autoclaving at 4 °C. The pH was adjusted to 5.5 and the media was solidified with 3 % phytigel.	22
2.7	List of bacterial and plant binary vectors used for this thesis.	27
2.8	List of yeast expression and <i>Aspergillus</i> vectors used for this thesis.	28
2.9	Cycling parameters for standard PCR reactions for Taq polymerase amplification of 1 kb PCR products. The annealing temperature of the primer pairs is variable.	36
2.10	Cycling parameters for Touchdown PCR. PCR starts with a high annealing temperature to accumulate specifically gene-specific cDNAs. Successive decrease of the annealing temperature to the T _m of the used GSP1 primer (*) should increase PCR efficiency. 1 min extension was used per 1 kb DNA.	39
2.11	Cycling parameters for Advantage 2 PCR. Depending on target size the extension was performed for 1 (< 1 kb) to 3 min (1-5 kb) (*). An additional 10 min extension at 70 °C was added to increase TOPO T/A Cloning® efficiency.	39
2.12	Cycling parameters for the primary GenomeWalker™ PCR with the AP1 and GSP1 primer pair.	41
2.13	Cycling parameters for the secondary GenomeWalker™ PCR with the AP2 and GSP2 primer pair.	41
2.14	Cycle parameters for qPCR.	51
2.15	Software and webservices used for sequence and data analysis.	56
3.1	List of clones isolated from cDNA libraries of arbuscule-enriched and spore material by complementation of the yeast mutant strain EBY.VW4000.	58
3.2	NCBI protein Blast results for the monosaccharide transporters StHT6 and StHT2.	61
3.3	Putative sugar transporters found in the <i>G. intraradices</i> genome database by Blast searches in this work.	73
3.4	Table of putative genes of the xylose utilisation pathway found in this work by Blast search in the <i>G. intraradices</i> genome database.	83
3.5	Putative orthologues of the transcriptional activator XlnR which were found in this work by Blast search in the <i>G. intraradices</i> genome database.	87
A.1	Primers used for quantitative real-time PCR (qPCR) of <i>S. tuberosum</i> and <i>M. truncatula</i> genes.	111
A.2	Primers used for quantitative real-time PCR (qPCR) of <i>G. intraradices</i> and <i>S. cerevisiae</i> genes.	112
A.3	Primers for RACE PCR and genome walking.	113
A.4	Primers for TOPO T/A and TOPO ENTR Cloning® and the generation of DIG labelled probes for southern blotting and <i>in situ</i> hybridisation.	114

List of Tables

C.1	Relative expression of <i>StHT6</i> , <i>StHT2</i> and <i>StPT4</i> in microdissected potato hairy roots. The expression was calculated relative to the transcriptional elongation factor alpha 1 (<i>StTEF</i>). (Errors are presented as s.d.)	127
C.2	Relative expression of <i>StHT6</i> , <i>StHT2</i> and <i>StPT4</i> in a time course experiment with mycorrhized potato hairy roots. The expression was calculated relative to the transcriptional elongation factor alpha 1 (<i>StTEF</i>). dpi means days post infection. (Errors are presented as s.d.)	127
C.3	Relative expression of <i>MtST1</i> , <i>MtHT6</i> and <i>MtPT4</i> in mycorrhized and non-mycorrhized <i>M. truncatula</i> hairy roots. The expression was calculated relative to the transcriptional factor alpha 1 (<i>MtTEF</i>). (Errors are presented as s.d.)	128
C.4	Relative expression of <i>G. intraradices</i> sugar transporters and the potato phosphate transporter <i>StPT4</i> in different samples of microdissected mycorrhized potato hairy roots. The expression was calculated relative to the transcriptional factor alpha 1 <i>GiTEF</i> for the fungal genes and <i>StTEF</i> for <i>StPT4</i> . (Errors are presented as s.d.)	128
C.5	Relative expression of <i>GiMST1</i> and <i>StPT4</i> in a time course experiment of mycorrhized <i>M. truncatula</i> plants. The expression was calculated relative to the transcriptional factor alpha 1 <i>GiTEF</i> for the fungal genes and <i>StTEF</i> for <i>StPT4</i> . dpi means days post inoculation. (Errors are presented as s.d.)	128
C.6	Relative expression of <i>GiMST1</i> and <i>MtPT4</i> in a time course experiment of mycorrhized potato hairy roots. The expression was calculated relative to the transcriptional factor alpha 1 <i>GiTEF</i> for the fungal genes and <i>MtTEF</i> for <i>MtPT4</i> . dpi means days post inoculation. (Errors are presented as s.d.)	129
C.7	Relative expression of xylose utilisation pathway genes of <i>G. intraradices</i> in different fungal tissue. AEM means arbuscule enriched material. The expression was calculated relative to the <i>G. intraradices</i> transcription elongation factor alpha 1 (<i>GiTEF</i>). (Errors are presented as s.d.)	129
C.8	Relative expression of XlnR orthologues of <i>G. intraradices</i> in different fungal tissues. The expression was calculated relative to the <i>G. intraradices</i> transcription elongation factor alpha 1 (<i>GiTEF</i>). (Errors are calculated as s.d.)	129
C.9	Relative expression of <i>G. intraradices</i> sugar transporters in the ERM. The ERM was exposed five days with 2% concentrations of different sugars or sugar derivatives. The expression was calculated relative to the <i>G. intraradices</i> transcription elongation factor alpha 1 (<i>GiTEF</i>). (Errors are calculated as s.d.)	130
C.10	Relative expression of xylose utilisation pathway genes (XUGs) and XlnR orthologues of <i>G. intraradices</i> in the ERM incubated for five days in 2% xylose medium. The expression was calculated relative to the <i>G. intraradices</i> transcription elongation factor alpha 1 (<i>GiTEF</i>). (Errors are presented as s.d.)	130
C.11	Relative expression of the <i>G. intraradices</i> sugar transporters <i>GiMST1</i> and <i>GiMST2</i> in the ERM in the vicinity of wild type tomato roots, roots of the tomato mutant <i>rmc</i> , or in the presence of their root exudates. The ERM was exposed with roots or exudates for one week. The expression was calculated relative to the <i>G. intraradices</i> transcription elongation factor 1 (<i>GiTEF</i>). (Errors are presented as s.d.)	130
C.12	Relative Expression of <i>GiMST1</i> , <i>StPT4</i> , <i>StHT6</i> , <i>GiXR2</i> , <i>contig41</i> , and <i>StXTH1</i> in mycorrhized potato hairy roots treated with different phosphate concentrations (17.5 μ M P, 3.5 mM P). The expression was calculated relative to the transcription elongation factor 1 of <i>G. intraradices</i> (<i>GiTEF</i>) or <i>S. tuberosum</i> (<i>StTEF</i>). (Errors are presented as s.d.)	131

Acknowledgments

I want to express my gratitude to everyone who made this thesis possible with their assistance and their support.

First, I want to thank Prof. Dr. Natalia Requena for giving me the opportunity to carry out this work. I am very grateful for her guidance, her invaluable ideas and comments. I also want to thank Prof. Dr. Peter Nick for acting as co-referee.

This work was financed by the Leibniz society within the Mycopact project. I want to thank all the members of the Mycopact consortium for the nice meetings and helpful ideas. A special thanks goes to Prof. Dr. Elke Neumann who initiated and organised this project.

I am grateful to Prof. Dr. Norbert Sauer for the opportunity to carry out the biochemical characterisation of GiMST1 in his institute and especially to Kathrin Wippel for her help during these experiments

I am sincerely thankful to Prof. Dr. Bettina Hause and especially to Dr. Sara Schaarschmidt for their advice and help for the *in situ* experiments. The time in Halle was really inspiring.

This work would not have been possible without the genome sequencing of *G. intraradices*. Therefore many thanks go to the Glomus Genome Consortium (Joint Genome Institute) and the National Institute for Agricultural Research (INRA) for the access to the GlomusDB database.

Of course, I want to thank all my colleagues of the Myclab group for the pleasant and inspiring working atmosphere.

I want to thank my parents for their love and support. Finally, I would like to thank Felix Werner for his critical reading, but mainly for his love and patience during the last years.

Nicole Helber

Dipl.-Biol.

Persönliche Daten

Geburtsdatum 24. 12. 1980
Geburtsort Vaihingen a. d. Enz
Nationalität deutsch

Bildungsweg

ab 2007 **Doktorarbeit**, *Karlsruher Institut für Technologie (KIT)*.
Institut für Botanik

2000–2006 **Diplom**, *Universität Karlsruhe (TH)*.
Studiengang: Biologie an der Fakultät für Chemie und Biowissenschaften
Hauptfächer: Mikrobiologie und Zoologie
Nebenfächer: Ingenieurbiologie und organische Chemie

1995–2000 **Abitur**, *Helene-Lange-Gymnasium*, Markgröningen.
Leistungskurse: Französisch und Bildende Kunst

Diplomarbeit

Thema Versuche zur Etablierung eines Transformationssystems für den arbuskulären Mykorrhiza Pilz *Glomus intraradices*

Institut Angewandte Biowissenschaften, *Universität Karlsruhe (TH)*

Abteilung Angewandte Mikrobiologie

Betreuung PD Dr. Requena

Korreferent Prof. Dr. Nick

Wissenschaftliche Veröffentlichungen

Helber N, Requena N. Expression of the fluorescence markers DsRed and GFP fused to a nuclear localization signal in the arbuscular mycorrhizal fungus *Glomus intraradices*. *New Phytol.*, 177:537–548, 2008.

Konferenzbeiträge

Poster Nicole Helber and Natalia Requena. Towards a transformation system for the arbuscular mycorrhizal fungus *G. intraradices*. Fungal Genetics Conference 2007, Asilomar (USA).

Poster Nicole Helber and Natalia Requena. Expression of the fluorescence markers GFP and DsRed in the arbuscular mycorrhizal fungus *G. intraradices*. VAAM Tagung 2007, Hamburg.

- Vortrag Molecular markers to assess mycorrhizal function. 1. Open Workshop Women in Plant and Soil Science Network (Mycopakt), 2008, Grossbeeren.
- Vortrag Sugar transporters in the AM symbiosis. 2. Open Workshop Women in Plant and Soil Science Network (Mycopakt), 2009, Berlin.
- Vortrag Molecular characterization of the AM functioning. Cost meeting 2009, Calella (Spanien).

Selbständigkeitserklärung

Hiermit versichere ich, die vorliegende Arbeit selbständig angefertigt und keine anderen als die angegebenen Quellen und Hilfsmittel benutzt sowie die wörtlich oder inhaltlich übernommenen Stellen als solche kenntlich gemacht und die Satzung des Karlsruher Institut für Technologie zur Sicherung guter wissenschaftlicher Praxis beachtet zu haben.

Karlsruhe, den 8. September 2010

Nicole Helber